

KIRINYAGA UNIVERSITY

AFRICAN JOURNAL OF SCIENCE, TECHNOLOGY AND ENGINEERING (AJSTE)

Volume 1, 2020

KIRINYAGA UNIVERSITY, KENYA KyU is ISO 9001:2015 Certified

AFRICAN JOURNAL SCIENCE, TECHNOLOGY AND ENGINEERING (AJSTE)

Chief Editor

Prof. Charles O. A. Omwandho

Assistant Editor

Dr. Jotham Wasike

Editorial Board

Dr. Jotham Wasike, Chairperson
Prof Laura Wangai, PhD
Dr. Samuel Mburu, PhD
Dr. Immaculate Marwa, PhD
Dr Irene Okello, PhD

Advisory Board

Prof. Mary Ndungu, PhD Prof. Charles Omwandho, PhD

Technical and Logistics

Caroline Mbuthia George Ngorobi Simon Gacheru Francis Kamau

© Copyright 2019, Kirinyaga University Copyright Statement

All rights reserved. Seek KyU's permission to reproduce, distribute, display or make derivative content or modification.

AFRICAN JOURNAL OF SCIENCE, TECHNOLOGY AND ENGINEERING (AJSTE)

Email: journals@kyu.ac.ke

ISSN 1356-6282

P.O Box 143- 10300

NAIROBI, KENYA

Preamble

African Journal of Science, Technology and Engineering (AJSTE) is an academic multidisciplinary peer-reviewed biannual publication that publishes original, innovative research and academic scholarship that contribute to growth of knowledge in Science, Technology and Engineering and related disciplines. Her key audiences are: Scientists and Engineers in academia and industry, researchers, students, government agencies/policymakers and citizens with a passion for "STEM".

This first edition contains the newest research, in contemporary transposition in Science, Technology and Engineering of global interests. It carries original and full-length articles that reflect the latest research and developments in both theoretical and practical aspects of global science. It promotes research awareness and compatibility platform through a concise and methodical interface to cater for all categories of scholars in science, while encouraging innovativeness and quality research.

The topical issues in this Journal include: Epithelial to mesenchymal transition (emt)in pathogenesis of endometriosi), management of chronic comorbid conditions, isolation and identification of heavy metal resistant bacteria risks and existing health services, deep neural networks for predictive sequence modeling, intelligent decision support (IDS) in software risk management, effect of the graphite dispersed titanium dioxide solid solar cell composition on the generated potential (v_{oc}) and optimal control for efficiency and reliability in the storage of perishable good, assessment of Forest Rehabilitation and Restocking Success along Mt. Kenya East Forest Reserve using Remote Sensing Data., Effect of Goat Manure-Based Vermicompost on Soil Chemical Properties Under Garlic Production in the Upper Eastern Region of Kenya, Intelligent 2D Outdoor Location Tracking System, Precision of 3-Configurations with Respective Sub-Configurations of 2-Ring Concentric Planar Array in Direction Finding, Synthesis and Characterization of Nanoparticles from Extracts of Fruits of Annona muricata: A green nanobiotechnology approach, Socioeconomic Determinants of Adoption of Eco-Friendly Farming Practices in Agroecosystems of Embu County, Kenya and Soil Concentration of Selected Heavy Metals in Chuka, Nakuru and Thika Municipal Dumpsites

The journal is produced in print and online versions.

Chief Editor

Table of Contents

Epithelial to Mesenchymal Transition (EMT) in the Pathogenesis of Endometriosis
 Ezekiel Mecha, Charles O.A. Omwandho, Jane Maoga, Cong
 Sui, Hans-Rudolf Tinneberg & Lutz Konrad
 1 – 12

2. Management of Chronic Comorbid Conditions Model: Context -Informed for Primary Health Care Settings in Kenya

Marwa N. Immaculate & Gloria N. Mtshali

13 - 33

3. Isolation and Identification of Heavy Metal Resistant Bacteria Producing Enzymes from Industrial, Laboratory and Dumping Sites Wastes in Mombasa County *Obiero, L.S, Msanzu J.B, Chimbevo M.L, Malala, J.B. & Gicharu, G.K*34 – 45

4. Risks and Existing Health Services for Men Having Sex with Men in Kilifi Town, Kenya

Eva Maina & Dennis Butto

46 - 58

5. Determination of Body Mass Index and Waist Circumference in Type II Diabetes Mellitus in Patients at Thika Level 5 Hospital

Kenny Kimani & Caroline Okumu

59 - 68

6. A Window-Based Approach to Training Deep Neural Networks for Predictive Sequence Modeling

Zachary Kirori & Jotham Wasike

69 - 81

7. Intelligent Decision Support (IDS) in Software Risk Management Based on Data Mining, Rough Sets and Decision Theory

Rose Mutheu & Jotham Wasike

82 - 96

8. Effect of the Graphite Dispersed Titanium Dioxide Solid Solar Cell Composition on the Generated Potential (Voc)

Njoroge D. Kimemia, Isaac K. Njoroge & Isaac W. Mwangi

97 - 112

African Journal of Science, Technology and Engineering Vol. 1, 2020

Page **i** of **232**

9. Assessment of Forest Rehabilitation and Restocking Success along Mt. Kenya East Forest Reserve using Remote Sensing Data.

Kibetu D. Kinoti& Mwangi J. Muthoni

113 - 126

10. Effect of Goat Manure-Based Vermicompost on Soil Chemical Properties Under Garlic Production in the Upper Eastern Region of Kenya

Vincent Makini Gichaba, Haggai Onyan'go Ndukhu & Moses Muraya 127 - 145

11. Intelligent 2D Outdoor Location Tracking System

Nelson M. Gachoki, Stanley Kamau, & Bernard Ikua

146 - 152

12. Synthesis and Characterization of Nanoparticles from Extracts of Fruits of *Annona muricata*: A green nanobiotechnology approach

Yahaya Gavamukulya, Esther N Maina, Hany A El-Shemy, Fred Wamunyokoli, & Gabriel Magoma 153 - 171

13. Precision of 3-Configurations with Respective Sub-Configurations of 2-Ring Concentric Planar Array in Direction Finding

David Musyoka Kinyili & Dominic Makaa Kitavi

172 - 190

14. Socioeconomic Determinants of Adoption of Eco-Friendly Farming Practices in Agroecosystems of Embu County, Kenya

Moses Kathuri Njeru

191 - 207

15. Soil Concentration of Selected Heavy Metals in Chuka, Nakuru and Thika Municipal Dumpsites

Joseph Maina Kariuki, Margaret Bates & Adiel Magana

197-225

Epithelial to Mesenchymal Transition (EMT) in the Pathogenesis of Endometriosis Mecha, Ezekiel^{1,2}, Omwandho, Charles O.A^{2,3}, Maoga, Jane², Sui, Cong¹, Tinneberg, Hans-Rudolf¹, Konrad, Lutz¹

¹Justus-Liebig University, Germany ²University of Nairobi, Kenya ³Kirinyaga University, Kenya

Correspondence: ezekiel_mecha@yahoo.com

Abstract

An epithelial-mesenchymal transition (EMT) is a biologic process that allows a polarized epithelial cell, which normally interacts with basement membrane via its basal surface, to undergo multiple biochemical changes that enable it to assume a mesenchymal cell phenotype, which includes enhanced migratory capacity, invasiveness, elevated resistance to apoptosis, and greatly increased production of ECM components. The aim of this study was to assess the epithelial phenotype in the pathogenesis of endometriosis by performing IHC studies with epithelial and mesenchymal markers. Researchers compared endometrium with and without endometriosis to peritoneal, ovarian and deep infiltrating endometriosis (DIE) with two structural (keratin-18, -19), one membrane-associated(mucin-1) and one mesenchymal protein (vimentin) to analyse the epithelial and mesenchymal phenotype of the endometrial glands and endometriotic lesions. Quantitation with the HSCORE showed no differences for keratin-18 (K18), keratin-19 (K19) and mucin-1 (MUC1) between endometrium with and without endometriosis. Also, K18 was not different between endometrium and endometriotic lesions. In contrast, K19 and MUC1 were significantly decreased in the endometriotic lesions compared to endometrium. However, all three proteins were found in almost every endometrial and endometriotic gland or cyst and in nearly all epithelial cells. The study also established that protein expression of vimentin was lower in the endometriotic lesions compared to the endometrium, especially in the ovary. The protein expression of the epithelial markers in nearly all glands as well as in nearly all epithelial cells in the endometrium endometriotic entities clearly indicates no loss of the epithelial cell phenotype. Additionally, the reduced expression of vimentin in the endometriotic lesions, suggests no shift of the epithelial phenotype to amesenchymal one. Thus, the study propose, that EMT is not a main factor in the pathogenesis of endometriosis.

Key words: Endometriosis, Mucin-!, EMT, Keratin – 18

Introduction

Endometriosis is a chronic gynecological disease affecting 10% of women in the reproductive age, characterized by occurrence of uterine endometrial tissue outside the uterus typically associated with pelvic pain and infertility (Deo et al., 2017). The exact cause is not known but it is generally believed that endometrial cells deposited in the pelvic region by retrograde menstruation can implant and develop into endometriomas. Endometrial-like tissue can be found in the myometrium (internal endometriosis), peritoneum, ovaries and other more distant loci (Clement, 2007). Retrograde menstruation followed by implantation of endometrial tissue on different surfaces in the pelvic or abdominal cavity is generally accepted as the main cause of endometriosis (Clement, 2007). However, despite the high rate of retrograde menstruation, only approximately 10% of the women in reproductive ages experience endometriosis, thus, alternative hypotheses such as the coelomic metaplasia theory, the embryonic rest theory, a fetal origin or dissemination via the hematogenous or lymphatic system have been suggested (Signorile et al., 1997) among other theories. Circulating stem cells originating from bone marrow or from the basal endometrial layer have also been associated with endometriosis (Bulun, 2009). Elsewhere, it has been hypothesized that peritoneal endometriosis, endometriomas and deep infiltrating endometriosis could represent three distinct entities, which do not share a common pathogenesis (Nisolle and Donnez., 1997). This hypothesis is seemingly supported by the observation that endometriotic cells were found to be different from those of the eutopic endometrium and that the eutopic endometrium was different in women with and without endometriosis with respect to cellular and gen/proteine expression patterns (Sampson, 1927). However, endometriotic glands almost always have an overtly endometrioid appearance and resemble histologically uterine endometrial glands (Koninckx et al., 1999). There is also evidence that most of the endometrial glands (Tanaka et al., 2003) and ovarian endometriotic cysts are mostly composed of monoclonal populations of epithelial cells (Jimbo et al., 1997, Wu et al., 2003). In contrast, peritoneal endometriosis was proposed to be multicellular in origin, although individual glands are derived from single precursor cells. However, in most of these studies the cell purity after isolation was not evaluated or only determined histologically (Nabeshima et al., 2003).

Although it is now well established that there is a different gene/protein expression profile in peritoneal, ovarian, and deep infiltrating endometriosis, there is also some evidence that eutopic endometrial glands as well as ectopic endometriotic lesions share a common basis and thus endometriotic foci most probably originate from the endometrium (Matsuzaki., 2011). In both studies, cytokeratins were used for immunohistochemical classification of endometrial and endometriotic glands (Kruitwagen *et al.*, 1991, Matsuzaki and Darcha., 2012). Cytokeratins exhibit characteristic expression patterns in human tissues and are important in tumor diagnosis particularly in precise classification and subtyping of tumor metastases (Moll *et al.*, 2008). Because endometriotic cells can be viewed as metastastic tumor cells, albeit with a benign phenotype, we used in this study a similar approach. We examined immunohistochemically endometrial glands with different tissue biomarkers and identified a number of proteins with a high sensitivity (~100%). Of these, expression of six distinct proteins in the epithelial cells of the endometriotic glands from peritoneal, ovarian, and deep infiltrating endometriosis was studied and similarity of protein expression between the endometrium and the three distinct entities quantified.

Methods

Patients

This study was approved by the Ethics Committee of the Medical Faculty of Justus-Liebig-University, Giessen, Germany (95/09). Participants gave written informed consent. Specimens were obtained by hysterectomy (uteri) or laparoscopy (endometriotic tissues) from patients mainly suffering from pain (~60%). Intraoperative findings were classified according to the rASRM and ENZIAN score in cases of DIE (Haas *et al.*, 2011). The first set of patients was used for screening of highly sensitive but less specific epithelial markers like cytokeratin-18 (K18, K19) and mucin-1 (MUC1). Patients with unknown phase were used to optimize the antibodies. A second set of patients including samples from provitro (Berlin, Germany) was used to screen highly endometrial-specific proteins as detailed elsewhere (Wilhelm *et al.*, 2014).

Specimens were fixed in Bouin's solution and partly in formaldehyde, embedded in paraffin wax, $5~\mu m$ sections stained with hematoxylin and eosin and histological evaluation performed.

Characteristics of the antibodies for quantification of endometrial and endometriotic glands

In this study, we used several antibodies for the detection of epithelial cells in endometrial and endometriotic glands. For general characterization of epithelial cells, we used K18, K19 and MUC1, but for a more specific classification, we evaluated 11 proteins and used in the end three proteins,

Immunohistochemistry and Quantitation

Only endometrium and endometriotic lesions with well-defined glands and stromal cells were used. Serial sections were cut to ensure that in most cases the same lesions were examined. Immunohistochemistry was performed as published previously (Stewart *et al.*, 2011). The Envision Plus System from DAKO (Hamburg, Germany) was used according to manufacturer's instructions. MUC1 (also known as CA15-3; diluted 1:200, DAKO cat-no M0613), K19 (diluted 1:300, Novus Biologicals, Herford, Germany cat-no NB100-687), PCK2 (diluted 1:100, Thermo Fisher, Schwerte, Germany cat-no PA5-30221). After incubation with the secondary antibody staining was visualized with diaminobenzidine. Counterstaining was performed with hematoxylin and after dehydration in ethanol, slides were mounted with Eukitt. Negative controls for immunohistochemistry were prepared by omitting primary antibody. Digital images were obtained with the inverted microscope FSX100 (Olympus) using the Olympus FSX-BSW software. Images were processed with Adobe Photoshop. Quantification was done by estimating the labelled epithelial cells and by counting stained and unstained glands.

Statistics

Values are given as either median or means ± SEM (standard error of the means). Comparison between two groups was done with Mann Whitney and between three and more groups was performed with the ANOVA followed by Kruskal Wallis with GraphPad Prism 6.01.

Results

To examine eutopic endometrial and ectopic endometriotic glands, we surveyed the literature for epithelial markers, and identified the following proteins: K5, K6, K7, K18, K19, E-Cadherin, c-kit, EpCam, and MUC1. Localization was analysed immunohistochemically in endometrial biopsies from patients with and without endometriosis (Table 1) and demonstrated only for three proteins, namely K18, K19 and MUC1, expressed in all endometrial glands and in nearly all epithelial cells (Fig. 1) irrespective of the cycle (data not shown). Based on these findings, we analysed localisation of the three proteins in deep infiltrating endometriotic lesions, and endometriotic lesions of the peritoneum and ovary (Table 1). In most cases serial sections were used.

Endometriotic glands and nearly all endometriotic epithelial cells demonstrated 100% positivity for K18, K19, and MUC1 in all peritoneal lesions (Fig. 2A-C), ovarian lesions (Fig. 2D-F) and deep infiltrating lesions (Fig. 2G-I). Although sensitivity in detecting endometriotic glands with K18, K19 and MUC1 was 100%, the three proteins were also identified in other cell types such as tubal epithelial cells and epithelial cells of endosalpingiosis (data not shown). However, marker expression together with histological classification of endometriosis never revealed any misclassification or missed cases of endometriosis.

Discussion

Using six different markers for epithelial cells, we performed an immunohistochemical study of eutopic endometrial and ectopic endometriotic glands in the endometrium, peritoneum, ovary and DIE. Our results demonstrated that nearly all epithelial cells in eutopic endometrial as well as ectopic endometriotic glands express K18, K19 and MUC1. Notably, a second screen with putative endometrial-specific proteins yielded several remarkable results. First, ten of eleven proteins showed 100% labelling of endometrial glands, suggesting a monoclonal origin of the glands (Wilhelm M *et al.*, 2014). However, ovarian endometriosis was clearly different from eutopic endometrium and the other endometriotic entities.

Keratin filaments comprise type I and type II intermediate filaments with at least 20 subtypes with keratins 7, 8, 18, and 19 expressed generally in simple epithelia such as the

human endometrium (Stewart et al., 2011). Keratin 19 is the smallest acidic keratin normally not paired with a basic keratin and was shown to be present in nearly all normal endometrial glands throughout the cycle (Bártek et al., 2011). However, K19 is also expressed by ovarian surface epithelial cells, mesothelial peritoneal cells, and epithelial cells of the fallopian tubes (Hattrup and Gendler, 2008). Kruitwagen et al., (1991) reported identical expression patterns of keratins K5, 7, 8, and 18 between eutopic endometrial and ectopic endometriotic glands but did not indicate how many glands or epithelial cells were stained. Since keratin expression varies considerably among different epithelia, they have been widely used to fingerprint various carcinomas, because keratin expression profiles usually remain constant even if an epithelium undergoes malignant transformation (Stewart et al., 2011). However, sometimes only evaluation of both, marker expression and histology can distinguish between different cell types. For example, endometrial adenocarcinomas and endometriotic foci are positive for K7 and negative for K20, but the tumor cells are clearly different histologically from the endometriotic cells. Thus, we hypothesized that keratins might also be useful in characterization of endometriotic lesions together with the histological evaluation (Stewart et al., 2011).

Mucin-1, which is normally expressed on polarised epithelial cells of normal glandular epithelia, is a member of the mucin family and is also a component of glandular secretions (Thathiah A and Carson D., 2004). Abnormal expression of MUC1 is observed in over 80% of some cancers and is associated with a poor prognosis (Thathiah and Carson, 2004). In the female genital tract, MUC1 is found on the endometrial cell surface (Hey *et al.*, 1995, Budiu *et al.*, 2009) and is also expressed in epithelial cells of the fallopian tubes and ovarian endometriosis (Deo Sujata *et al.*, 2017).

Remarkably, we found a highly consistent K18, K19, and MUC1 protein expression in nearly all epithelial cells of the endometrium and in all glands or cysts of peritoneal, ovarian and deep infiltrating endometriosis. Similarly, two other reports also showed a very high similarity between endometrial and endometriotic glands by using keratins, MUC1, E-cadherin or S100A4. Although these markers are highly sensitive, they lack specificity without a thorough histological examination. However, as demonstrated in our study, histological examination together with the immunohistochemical analysis yielded a 100% specificity, which is much better compared to metastasis detection (Stewart *et al.*, 2011).

Page 6 of 232

To date, differences in endometriotic tissues compared to endometrial tissues have been found, thus, peritoneal, ovarian and deep infiltrating endometriosis are often regarded as distinct entities of the disease (Nisolle and Donnez., 1997). However, histological resemblance between endometriotic tissue and uterine endometrium is well known and endometriotic glands almost always have an overtly endometrioid appearance suggesting that endometrial epithelial cells do not lose their epithelial phenotype (Clement, 2007). We suppose that our results of a 100% identity between endometrial and endometriotic epithelial cells with the three epithelial cell markers K18, K19 and MUC1 might reflect this histological observation.

Taken together, we suggest that the basic epithelial marker profile of endometrial as well as endometriotic epithelial cells is nearly 100% identical in the endometrium and the three distinct endometriotic entities as shown in this study and by previous reports. Furthermore, the protein expression profile suggests a monoclonal origin of the endometrial glands as well. However, there are some slight to modest differences of protein expression profile between epithelial cells of the endometrium compared to the three different endometriotic entities which are possibly attributable to the different microenvironments. This suggests a possible partial involvement of EMT in pathogenesis of endometriosis.

Conflicts of Interest

Researchers declare no conflicts of interest.

References

Bártek J, Bártková J, Taylor-Papadimitriou J, *et al.* Differential expression of keratin 19 in normal human epithelial tissues revealed by monospecific monoclonal antibodies. Histochem J 1986; 18:565-575.

Budiu R, Diaconu I, Chrissluis R, *et al.* A conditional mouse model for human MUC1-positive endometriosis shows the presence of anti-MUC1 antibodies and Foxp3+ regulatory T cells. Dis Model Mech 2009; 2:593-603.

Bulun SE. Endometriosis. N Engl J Med 2009; 360:268-279.

Clement PB. The pathology of endometriosis: a survey of the many faces of a common disease emphasizing diagnostic pitfalls and unusual and newly appreciated aspects. Adv Anat Pathol 2007; 14:241-260.

Deo Sujata, Jaiswar S P, Shankhwar PL, Iqbal Bushra,

ManishaJhirwar (2017). Peripheral

Haas D, Chvatal R, Habelsberger A, *et al.* Comparison of revised American Fertility Society and ENZIAN staging: a critical evaluation of classifications of endometriosis on the basis of our patient population. Fertil Steril 2011;95:1574-1578.

Hattrup CL, Gendler SJ. Structure and function of the cell surface (tethered) mucins. Annu Rev Physiol 2008; 70:431-457.

Hey NA, Li TC, Devine PL, et al. MUC1 in secretory phase endometrium: expression in precisely dated biopsies and flushings from normal and recurrent patients. Hum Reprod 1995; 10:2655-2662.

Jimbo H, Hitomi Y, Yoshikawa H, *et al*. Evidence for monoclonal expansion of epithelial cells in ovarian endometrial cysts. Am J Pathol 1997; 150:1173-1178.

Koninckx PR, Barlow D, Kennedy S. Implantation versus infiltration: the Sampson versus the endometriotic disease theory. Gynecol Obstet Invest 1999; 47: Suppl. 1:3-9; discussion 9-10.

Kruitwagen RF, Poels LG, Willemsen WN, *et al.* Immunocytochemical marker profile of endometriotic epithelial, endometrial epithelial, and mesothelial cells: a comparative study. Eur J Obstet Gynecol Reprod Biol 1991; 41:215-223.

Matsuzaki S, Darcha C. Epithelial to mesenchymal transition-like and mesenchymal to epithelial transition-like processes might be involved in the pathogenesis of pelvic endometriosis. Hum Reprod 2012; 27:712-721.

Matsuzaki S. DNA microarray analysis in endometriosis for development of more effective targeted therapies. Front Biosci (Elite Ed) 2011; 3:1139-1153.

Moll R, Divo M, Langbein L. The human keratins: biology and pathology. Histochem Cell Biol 2008; 129:705-733.

Nabeshima H, Murakami T, Yoshinaga K, *et al.* Analysis of the clonality of ectopic glands in peritoneal endometriosis using laser microdissection. Fertil Steril 2003; 80:1144-1150.

Nisolle M, Donnez J. Peritoneal endometriosis, ovarian endometriosis, and adenomyotic nodules of the rectovaginal septum are three different entities. Fertil Steril 1997; 68:585-595.

Sampson JA. Peritoneal endometriosis due to menstrual dissemination of endometrial tissue into the peritoneal cavity. Am J Obstet Gynecol 1927; 14:422-469.

Signorile PG, Baldi A. Endometriosis: New concepts in the pathogenesis. Int J Biochem Cell Biol 2010; 42:778-780.

Stewart CJ, Crook ML, Lacey J, et al. Cytokeratin 19 expression in normal endometrium and in low-grade endometrioid adenocarcinoma of the endometrium. Int J Gynecol Pathol 2011; 30:484-491.

Tanaka M, Kyo S, Kanaya T, Yatabe N, *et al*. Evidence of the monoclonal composition of human endometrial epithelial glands and mosaic pattern of clonal distribution in luminal epithelium. Am J Pathol 2003; 163:295-301.

Thathiah A, Carson DD. MT1-MMP mediates MUC1 shedding independent of TACE/ADAM17. Biochem J 2004; 382:363-373.

Wilhelm M, Schlegl J, Hahne H, *et al.* Mass-spectrometry-based draft of the human proteome. Nature 2014; 509:582-587.

Page 9 of 232

Wu Y, Basir Z, Kajdacsy-Balla A, *et al.* Resolution of clonal origins for endometriotic lesions using laser capture microdissection and the human androgen receptor (HUMARA) assay. Fertil Steril 2003; 79 Suppl1:710-717.

Table 1: Overview of the tissue samples used for K18, K19 and MUC1

	Endometrium	Ovarian	Peritoneal	DIE
		Endometriosis	Endometriosis	
All samples	n=39	28 (n=26)	43 (n=26)	17
(Age, median)	(45)	(34)	(34.5)	(n=14)
				(33)
Secretory	n=14			
(Age, median)	(43.5)			
Proliferative	n=14			
(Age, median)	(46)			
Unknown phase	n=11			
(Age, median)	(46)			
Leiomyoma	n=10			
Uterine fibroids	n=8			
Adenomyosis	n=12			
Bladder			n=15	n=1
Uterosacral ligament			n=4	n=7
Ovarian fossa			n=6	n=1
Pouch of Douglas			n=4	11 1
Round ligament of			n=3	
uterus			n=3	
Peritoneum			n=2	
Infundibulo pelvic			n=3	
ligament			n=1	
Pelvic wall				n=1
Mesogastrium			n=1	n=3
Rectum				n=1
Rectovaginal septum				n=1
Paraurethral			n=1	
Rectosigmoid				n=2
Fallopian tubes				
Sigma				

e.g. 28 (n=26) means 28 lesions from 26 patients; DIE, deep infiltrating endometriosis

Page 10 of 232

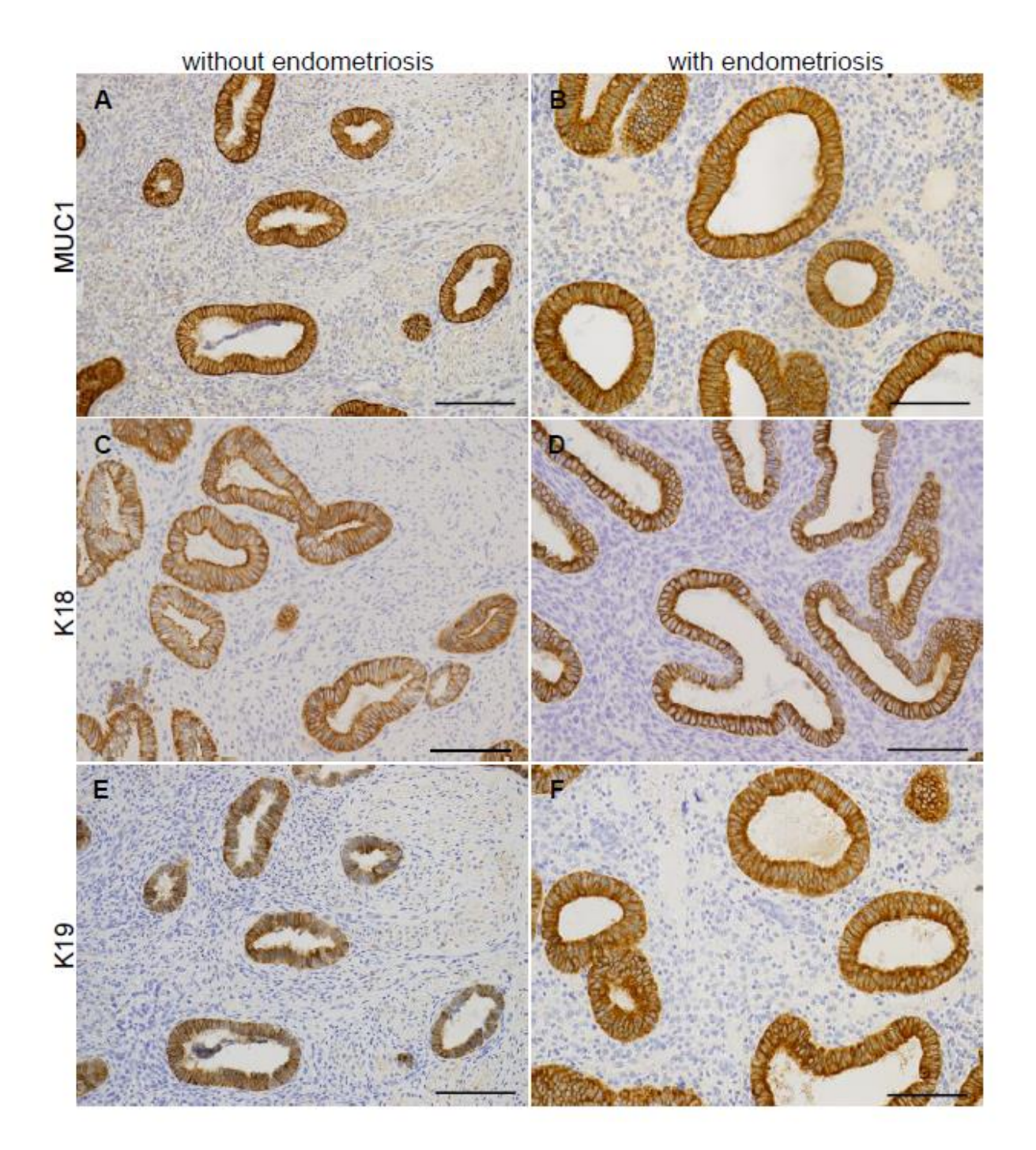


Figure 1: Immunohistochemical detection of MUC1 (A, B), K18 (C, D) and K19 (E, F) in the endometrium of patients without endometriosis (A, C, E) or with endometriosis (B, D, F). One patient (B) with a normal endometrium showed ovarian and rectovaginal endometriosis. One patient (D) also had adenomyosis. One patient (F) showed besides adenomyosis also endometriosis in the fallopian tubes. Counterstaining was performed with hematoxylin; Magnification A-F 17x

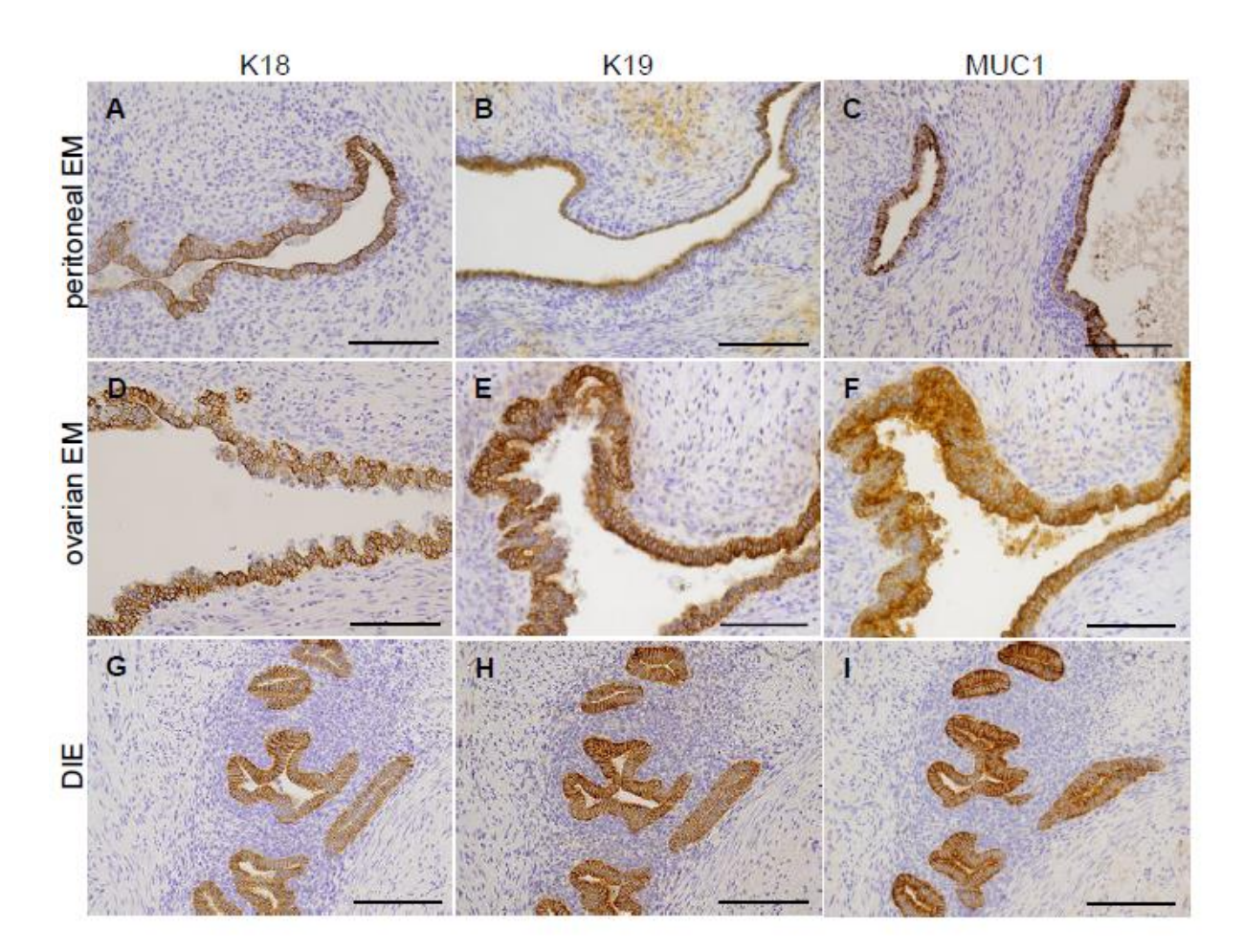


Figure 2: Immunohistochemical detection of K18 (A, D, G), K19 (B, E, H), and MUC1 (C, F, I) in peritoneal endometriosis (A-C, ovarian fossa), ovarian endometriosis (D-F), and DIE (G-I, rectovaginal septum). Counterstaining was performed with hematoxylin; Magnification A-F 17x

Management of Chronic Comorbid Conditions Model: Context -Informed for Primary Health Care Settings in Kenya.

Marwa, N. Immaculate¹, Mtshali, N. Gloria²

¹Kirinyaga University, Kenya

²University of KwaZulu Natal, South Africa

Correspondence: imarwa@kyu.ac.ke

Abstract

Comorbidity of non communicable diseases, posses a new global challenge to health systems. Management of chronic conditions require a comprehensive care provision to both at risk and affected by the coexisting conditions. Management process has to be cognizant of cultural differences, attitude, beliefs and practices of the community, patients and health care providers. The objective of this study was to explore and analyze current approaches to management of chronic comorbid diabetes and hypertension among adults in selected Primary Health Care settings in Kenya and further develop context informed model to guide management of chronic comorbid conditions in primary care settings. The study adopted a constructivist, qualitative approach and a combination of focused ethnography and grounded theory research designs towards the development of context informed model. Ethnography design was to collect data: participant observation; structured interviews, document analysis and focus group discussion. The study used constant comparative method in the field to ensure rich data collection. The study sites comprised; seven health facilities and 40 informants who were purposively selected. Data was analyzed using Open, axial and selective coding as presented in Strauss and Corbin substantive model.

Management of chronic comorbid conditions model was developed and, which is presented as: concepts of the model; the context, political commitment; integrated health service delivery; guiding principles and expected outcomes. Several basic assumptions to management of chronic comorbid conditions emerged. The model adds new literature on the management of chronic comorbid conditions, particularly in Primary care settings, and in-corporates a devolved health system into quality health care service provision, leading to improved quality of life and informed patients.

Keywords: Diabetes, Hypertension, Management, Comorbidity, Model, Culture Sensitive, Continuity.

Introduction

Non- Communicable Diseases (NCDs) emerge as a global burden, despite the efforts being put in place by World Health Organization (WHO) and other health related organizations (WHO, 2010). Evidence based studies have shown that people with type 2 diabetes usually have more than one co-existing chronic conditions among them, hypertension yet healthcare systems lack adequate information on management of chronic comorbid conditions, among (diabetes and hypertension) which is context specific to suit primary health care settings (Long and Dagogo-Jack, 2011, Islam et al., 2014, Piette and Kerr, 2006).

Global statistics indicate an increasing trend of NCDs concern despite the efforts by WHO to integrate prevention and control of NCDs into PHC, the efforts and the pace continually remain slow (WHO, 2010). According to WHO (2008), world statistics, it was projected that NCDs will cause 59 percent of annual deaths and lead to 46 per cent of the global disease burden by the end of 2030. WHO, (2013) report highlights the global concern of diabetes and hypertension being high risk factors for cardiovascular diseases, which coexist in patients commonly seen in PHC settings (Mohan et al., 2013, WHO, 2013). The International diabetes Federation (IDF) estimates that the number of adults (between 20 and 79 years of age) with diabetes in the world will increase by 54 percent from the current 371 million globally to 438.4 million by 2030, with sub-Saharan African region projected to experience an increase of 98 per cent from the current 12.1 million to 23.9 million by 2030, with 81.2 per cent being undiagnosed (International Diabetes Federation [IDF], 2012). The high prevalence of NCDs is attributed to globalization, adoption of westernized lifestyles and urbanization. Most mortality cases are reported in low and middle income countries and affect the most productive age groups in the community thus, propelling poverty further (Mathenge et al., 2010, Buowari, 2013, WHO, 2013). Most of the NCDs have similar risk factors, hence common management strategies, commencing with health promotion and illness prevention among at risk and unaffected groups (Mohan et al., 2013).

In Kenya like all other sub-Saharan African Countries, the prevalence of comorbidity of diabetes and hypertension is high and poses medical management challenges. It is evident

Page **14** of **232**

that 65 per cent of patients with comorbid diabetes and hypertension are poorly controlled; despite being on treatment and follow up care(Otieno et al., 2005). Unfortunately most health care systems in developing countries are ill equipped with strategies to manage chronic comorbid conditions in PHC settings (Mendis et al., 2012) hence the need to analyze the current approaches into management of comorbid conditions with the view to developing, context-informed interventional models to aid the management of chronic comorbid conditions in PHC settings.

Despite the availability of intervention models from developed countries on chronic care, developing countries' have not put them to practice. Lack of resources, policies, infrastructure and political interferences in the health sector. Furthermore interventional models developed outside the operational context have variations based on the levels of development and preparedness in chronic care management in other socio-economic contexts (Ploubidis et al., 2013, Olmen et al., 2012). For instance the Chronic Care Model (CCM) which is internationally recognized, puts more emphasises on clinical and selfmanagement strategies for chronic care, especially diabetes (Pilleron et al., 2014, Si et al., 2008). The Collaborative Care Model (CCM) uses different cadres of health professionals to manage patients through use of Managers for patients who need comprehensive chronic care (Unützer et al., 2013). Notably, most health facilities in Kenya do not practice coordinated or collaborated care to manage patients with chronic conditions. Thus all clinical guidelines in use single condition oriented; leaving out people with comorbid conditions and the same applies to available chronic care intervention models (Fortin et al., 2013). Implementation of health strategies therefore becomes a challenge for most Primary health care systems, especially in devolved health care settings (Turin, 2010).

These challenges in primary healthcare create the urgency to develop interventions which are context -specific, based on available resources and skills to suit patients' needs at community level, for effective management of comorbid diabetes and hypertension as well as other NCDs.

This study sought to explore and analyze management of chronic comorbid diabetes and hypertension among adults in selected PHC settings in Kenya with the view to developing a context informed model to be used as a guide in the management of chronic comorbid diabetes and hypertension in Nandi County.

Methodology

The study used a qualitative focused ethnography to collect within the community and grounded theory method was used for data analysis using Strauss and Corbin Paradigm model(Corbin and Strauss, 2008). The study was philosophically underpinned by interpretivism commonly referred to as constructivism. Interpretivism views the world that knowledge is constructed through interaction between research and informants within the environment. Reality is subjective and is usually based on what people think; see in their daily activities, where they live, and work through continuously interacting among themselves. (Crotty, 1998, Lincoln et al., 2011).

Study Settings

The study was conducted in Nandi County in North Rift Valley region of Kenya. The County covers an area of 2.884.4 KM². The county is subdivided into six political and developmental constituencies, and has a population of 813,803 people (Kenya National Bureau of Statistics, 2010). Nandi County has a total of 129 health facilities; among them the county referral hospital, which is the hub of primary health care in the county. The county is classified as rural because only 37% of the total population reside in urban areas.

Ethical Consideration

Ethical clearance for this study was granted by the University of KwaZulu Natal Bioethics Committee (BE231/2014). Institutional clearance in Kenya was obtained from University of Eastern Africa, Baraton and National Commission of Science and Technology and innovation Kenya (NACOSTI/P/14/14551/3239) and research conducted as permitted by the Kenya legal system.

Sampling and Sample Size

Study participants were purposely selected based on their experience and knowledge on the area of interest to the researcher or being members of the culture under investigation. A total of 40 informants took part in the study namely: six patients with comorbid diabetes and hypertension, five caregivers, 12 health care providers and two community health volunteers. Additional data was collected from two focused groups and other relevant documents were reviewed.

Data Collection and Analysis

Data was collected mainly through observations, where the researcher was the main instrument for data collection (Higginbottom et al., 2013). All informants gave their consent both written and verbal. Other data collection techniques included interviews, document analysis and focus group discussion. Data collection in the field took a period of 10 months of episodic emersion in the culture of the community of study. Data analysis was done concurrently with data collection and continued through the period to allow emergence of new themes and questions for further data collection. Interviews were tape recorded and transcribed verbatim, those collected in the Swahili translated to English and back to Swahili for quality checks. Data coding was done manually and adhered to coding sequences of open, axial and selective coding and data followed paradigm model for model or theory development (Corbin and Strauss, 2008). Data was continuously analysed usually taking a cyclic format through data collection and coding. (Hammersley and Atkinson, 2007).

Results

This study presents the third phase of selective coding for the development of substantive theory or model of management of chronic comorbid conditions in Kenya based on the paradigm model as ascribed in Grounded theory analytical procedures (Strauss and Corbin, 1998).

In this study a descriptive explanatory model was developed. The model goes beyond description of a phenomenon to include relationship with other concepts, gives rationale for the relation and makes predictions about their exact relationship and addresses changes

occurring in the phenomenon (Chinn and Kramer, 2008). This paper presents a conceptual model of management of chronic comorbid conditions in a simplified format for easy comprehension by all concerned personnel.

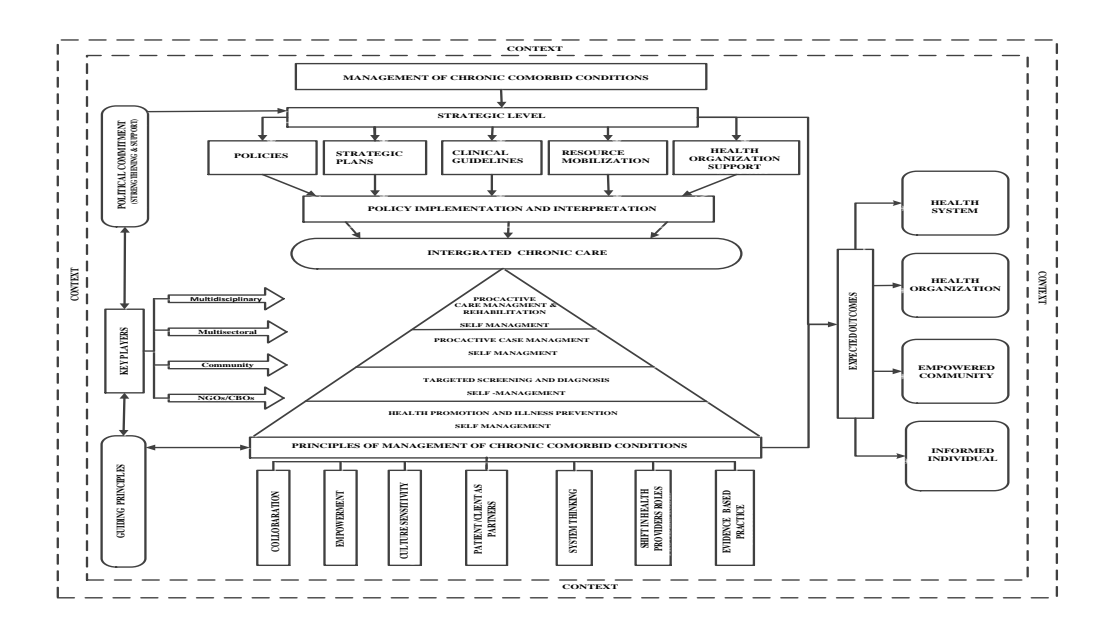
This model will be used in the next phase of this research to:

- Provide guidelines to multidisciplinary healthcare providers in management of chronic comorbid diabetes and hypertension among other conditions in PHC settings
- Provide a framework for policy review and implementation on management of chronic comorbid conditions in PHC settings and
- Guide nurses and other healthcare professionals on management of chronic comorbid conditions at PHC level.

Models or theories are made of core concept that has major concepts attached to it, followed by sub-concepts which make reference to the core concept as the phenomenon of study. Directly attached to the core concept are the major concepts which have a direct influence on the management of chronic comorbid diabetes and hypertension.

The relevant sub-concepts to each major concept are explained immediately under the concept as structurally represented in figure 1 below.

Figure 1: Structural Presentation of Middle Range Theory of Management of Chronic Comorbid Conditions (MCCC MODEL).



Definition of Concepts in the Conceptual Model

i) Management of Chronic Comorbid Conditions(MCCC)

The core concept "management of chronic comorbid condition" is defined through its characteristics which emerged from the findings of the study. It is defined as the process of comprehensive care provision to people at risk of developing chronic conditions and those affected with comorbid chronic conditions. It was defined in relation to the nature of collaboration among multidisciplinary teams and patients to provide care and support to patients and their families. The collaboration between different sectors with the Ministry of health, defined the nature of concerted efforts to prevent, treat and control chronic comorbid conditions. Further it was viewed as the incorporation of the community to take responsibility to prevent risk factors through behaviour change, providing support to the sick and sharing available resources.

Management of chronic comorbid conditions was defined in terms of provision of culturally sensitive care that is cognizant of individual patient's strongly held beliefs, expectation and practices, which are socially acceptable to them and their families culturally embedded and determined gender roles and interpretations of signs and symptoms, presented enhancers or barriers to management of comorbid conditions, communication with health providers and to some extent adherence to treatment plans.

Management of chronic comorbid conditions was characterized by the continuum of care, which was portrayed in the form of timely accessibility and affordability of health care services across care settings. Central to management of chronic comorbid conditions process was the ability of patients to provide self-care or being assisted by family members in consultation with healthcare providers. The success and utilization of self –management skills were influenced by health determinants such as age, level of functionality, literacy and health literacy levels to acquire skills, the ability to set personal goals and make efforts to achieve them through shared decision making.

ii) The Context

Management of chronic comorbid conditions is influenced by the context under which health care service provision takes place, the system of operations and the community under which patients live and work. Context represents health policies, social and environmental contexts, which determine health service delivery within the healthcare system. These include related activities which have direct and indirect influence to management of chronic comorbid conditions in PHC. The following are sub-concepts of the context in the management of chronic comorbid conditions:

The Kenyan Constitution: accessibility of health care services to citizen is influenced by the right to health for all which applies to all stages of life cycle of all Kenyans. The right to health allows all patients to have access to free medical services in primary care services and community health services.

The health policy framework: the framework gives direction on the chronic care provision in the Kenyan health system, with emphasis is on the health promotion and diseases prevention. The health policy determines re-organization of healthcare to allow chronic care service delivery. The influence of health policy in chronic care is evidenced by the available strategic plans for chronic conditions across different levels of care in support of evidence based practices.

Developmental agenda for Kenya Vision 2030: One of the factors that have an impact on the health system is the government development agenda, which aims to propel Kenya from a low income country into a middle income country by 2030. Decentralization of chronic care services and advocacy to create awareness enhances possibility of improving health accessibility, reducing morality rates and health expenditure.

International initiatives and partnership: management of chronic comorbid conditions in a resource constrained environment is influenced by presence of international developmental partners. This is achieved through provision of training and capacity building in management of chronic comorbid conditions in primary health care. In the context of this study, initiatives and partnership are relevant to communities working in partnership with NGOs and international bodies, with the government in support of health promotion and lifestyle modification.

iii) Political Commitment

In this model, government commitment is a major concept on management of chronic comorbid conditions in primary health care. The commitment of both governments at the national and county at the strategic levels of management involved:

Development of policies and legislations: At the strategic level in this model under the Ministry of Health at the national government, legal health policies and frameworks are conceptualized, developed and reviewed, which affect healthcare services across the health systems, based on specific areas involved. For instance the Chronic Care Model, health system provides support to health organizations involved in chronic care through information and clinical support (Glasgow et al., 2001).

Clinical guidelines and protocols: management of chronic comorbid conditions require evidence based guidelines to give directions on how comorbid conditions should be managed, as co-existing conditions compared to single occurring conditions. Clinical guidelines provide statements and recommendations for health promotion and prevention,

diagnosis, management, and treatment of comorbid conditions and the referral process to be followed to allow continuity of care and improved health outcomes.

Specific strategic plans: the strategic plans guided by the health policy framework forms the vehicle for implementation of the health policy in a systematic and responsive manner. These plans provide guidance on how to operationalized health services and give specific targets and indicators for monitoring and evaluation of health care services, risk factors and surveillance of those at risk.

Resources mobilization: In this model, resource mobilization at the strategic level cuts across the national and county governments. At the national level, financial planning for the ministry and the respective ministry in the county government takes place. The national government is responsible for mobilization of health human resources, both for clinical and preventive health through capacity building and trainings on chronic comorbid conditions.

Health organizational support: In this model, the organization represents those activities which are targeting an improved service delivery at the operational level within the health system. It involves strengthening service delivery to patients with chronic comorbid conditions, through empowerment of both the health provider and patients as partners. For further information consult ICDM of South Africa and also reflected in the Kenya Essential Package of Health (KEPH), which are essential for health care service delivery across settings (Asmall and Mohamed, 2013, KMOH, 2006).

Regular essential medicine supply: in this model supply of essential medicine forms an essential aspect of health organizational support, which supports the integrated chronic health care interventions across the continuum of care.

iv) Policy Implementation and Interpretation

Health system in decentralized government requires that policies made at national level be implemented and interpreted or operationalized to suit the context of the specific counties and the population needs. Implementation is done at the community level through community committees, SCHMTs and CHMTs, who have direct influence on how integrated health care services are offered within the county.

v) Integrated Chronic Care Approach

Integration of chronic care guides the way health-care services are organized and managed to allow individuals to have access to the service whenever they need it and the way they require it delivered in order to meet the value they pay for. Asmall and Mohamed (2013), defined integration of chronic care as provision of all health services in terms of prevention, diagnosis, treatment and chronic care entailing long term follow-up and monitoring. Integration may be seen as a solution to health care fragmentation in a resource constrained health care system and increased health care costs for patients who cannot afford the costs (Lorig and Holman, 2003, Unützer et al., 2013).

Primary prevention and illness prevention: integrated health services delivery in the context of this study is presented in the form of a pyramid of the public health approach with health promotion taking the base of the pyramid as the primary preventions.

Secondary prevention and targeted screening level: in integrated health services the next of the lower bases of the pyramid is the targeted screening and early detection of chronic conditions and those at risk of developing comorbid conditions.

Proactive case management of chronic comorbid conditions: closely linked to the secondary prevention is the proactive case management of individuals who are confirmed to have comorbid conditions, but with no identified complications. Proactive case management involves initiation of patients on combined therapy of both behaviour change and medications which could be multiple or single, injectable or oral medicines.

Tertiary prevention and proactive care management: tertiary level is characterized with appropriate referral of the high risk and complicated patients to specialized health care providers in the next level of management, where patients may benefit from. This can be achieved through preventive rehabilitation and physical rehabilitation services.

Page 23 of 232

Self-management focused care. Self-management guided by the social ecological perspectives allow patients to acquire the expert role in self-assessment, monitoring and self-drug administration, which enable individual patients to cope living with comorbid conditions rather than learning to manage the conditions only (Greenhalgh, 2009).

vi) Key Players

Key players are the main stakeholders with direct influence on management of chronic comorbid conditions in PHC settings. The following formed the key players in the context of this study:

Multidisciplinary teams: a team of health care providers from different cadres and training, responsible for health care service provision to patients with chronic comorbid condition. They include nurses, doctors, clinical officers, nutritionists and public health officers among others.

Multisectoral policy makers: these are leaders and representatives from different government sectors affiliated to health who directly or indirectly contribute to health care service provision. This may be through funding of health care services, provision of nutritional advice and self-help projects, procurement and distribution of healthcare supplies.

The community: is the general population among which individual household and patients with chronic comorbid conditions belong, either as clients, healthy people at risk of developing chronic conditions.

Community based organizations/NGOs/Advocacy groups: these include development partners and key stakeholders who provide support to the integrated health service delivery.

vii) Guiding Principles of Chronic Comorbid Conditions Management

In this model, the following principles provide the foundation to base management of chronic comorbid:

Collaboration: involves working together of different people from various fields of healthcare sector, health professionals, community, households and patients with an aim of improving health outcomes through active participation in decision-making and setting clinical goals.

Culture sensitivity: for patients to receive holistic care which is person-centred as compared to condition-centred, care must be sensitive to the cultural beliefs, norms, practices and expectations of the patient and their immediate family members.

Empowerment: Empowerment is a social action process through which individual, communities and organizations gain mastery over their lives or practices in the context of social political environment to bring about equity and quality of life.

Patient /client as partners: Patients are embodied as partners in chronic care performing a greater portion of their own care at home and in consultation with health care provider. Patients take active roles in learning practices, assessment practices and adaptation practices for improved competence (Pomey et al., 2015).

Systems thinking: it is the combination of patients' needs and diverse aspects of care to offer holistic care instead of fragmented care. System thinking is cardinal to problem solving which require actors from multileveled systems to provide solutions (Greenhalgh, 2009).

Shifting health provider roles: the role of patients and their families in direct care provision necessitates the shift from the monopoly of care provision of health care providers, where they make all the decisions, neglecting patients and their families.

Evidence-based practices: effective management of chronic comorbid conditions in PHC should be based on the health care professional clinical expertise integrated with best acceptable clinical evidence, patients' values to make sound decisions during the management process of patients.

viii) Expected Health Outcomes

These are consequences arising from management of chronic comorbid conditions in primary health care settings, directly influenced by the empowerment process and interactional activities at the health systems. The outcomes are based on the social cognitive theory which makes assumption that interactions between personal, physical and environmental factors have an effect on behaviour change of an individual's, community and organizations. The expected outcomes in this model are grouped into four levels namely: Individual/household outcomes, community-based outcomes, health organizations outcomes and health systems outcomes.

Individual/household outcomes: these are outcomes which are directly experienced by a patient with chronic comorbid conditions and their immediate family members. These are activities which ameliorate the conditions and improve quality of life.

Community-based outcomes: these are health-related outcomes directed at the community and the available health resources. Collaborations require active participation and involvement of community members in decision-making on health-related issues, which directly affects the targeted community.

Health organizations outcomes: health organizations provide an environment where health care providers interact patients, other health care providers to provide essential health services for the management of chronic comorbid conditions. With adequate training of health care providers, supply of essential medicines and equipment across care settings.

The health systems outcomes: these are proceedings of management of chronic comorbid conditions, which directly affect the health systems, in terms of strategic planning and resource distribution. The expected outcomes to health systems include increased awareness of health policy makers, development of relevant health policies for comorbid conditions, training and curricula development for health professionals and CHWs on chronic comorbid conditions.

A Basic Assumptions of the Conceptual Model

The following assumptions resulted from management of chronic comorbid model in primary health care settings:

Management of chronic comorbid conditions is socially constructed and interpreted: Management of chronic comorbid conditions is a socially constructed phenomenon, as it is mainly determined by the social process of knowing how people's attitudes, knowledge and skills determine their behaviour change either positively or negatively. Conrad and Barker (2010) assert that chronic illnesses are socially constructed, based on how meaning is attached to diagnosis, assuming of the sick roles and the social interactions within the community. Similarly, Martin and Peterson (2009) observed that health care reforms, need to have a an understanding on how chronicity is explained socially to guide redesigning of health care systems and services to chronically ill patients and families in the community. Similar views have led to the modification of the ICCC model to suit multi-morbidity in countries undergoing transition(Oni et al., 2014).

Management of chronic comorbid conditions is politically controlled: Management of chronic comorbid conditions in the health care system is politically influenced, and health services provision is heavily dependent on governance and style of governance being practiced in the country. Political reforms influence decentralization of health services and delivery especially to marginalized groups (Jadad et al., 2010). Political stability and governance influences health funding, budgetary allocation, accountability, equality and equity of health resources (Hogerzeil et al., 2013, Muchomba, 2015).

Management of chronic comorbid conditions is embedded in active participation in decision making: Patients active participation is determined by health determinants (Longtin et al., 2010) and the role they play in the whole process of care, especially in planning and goal settings lead to improved adherence to treatment plan, lifestyle modification and self monitoring (Epstein and Street, 2011, Roumie et al., 2011).

Self-management for patients with chronic comorbid conditions may be conflicting if skills and information is delivered separately for each condition: to avoid giving conflicting information to patients and care givers, multidisciplinary teams need to work together to improve patients care outcomes and improve quality of life through supported self-care and management. There exists evidence on the need for concerted effort in provision of self-management to patients with comorbid condition in PHC (Gilbert, 1997, Tapp et al., 2012, Thorogood et al., 2007).

Management of chronic comorbid conditions is based on community involvement and participation in health issues: that community provides the perfect environment of chronic care provision. Involvement of the community and participation in program development, budgeting and implementation of health promotion and disease prevention programs increases sustainability of the programs and adherence to long term risk control initiatives(Jadad et al., 2010, Greenhalgh, 2009).

Management of chronic comorbid conditions requires timely and well-coordinated across care settings: patients with comorbid conditions or at risk of developing comorbid conditions require timely, planned and coordinated care across care settings. Thus time is a central factor in measuring continuity of care in terms of duration and experiences of the patient on the conditions and the number of times patients can access the health facility for chronic condition care services (Haggerty et al., 2012).

Conclusion

The model adds to new literature and knowledge on management of chronic comorbid conditions especially diabetes and hypertension, particularly in PHC settings. Management of chronic comorbid conditions need to be all comprehensive, incorporating culture sensitive services, collaboration with other health related sectors and emphasizing self-management focused care across levels of service delivery.

The model also serves as an eye opener to policy makers to consult with health care providers and patients' experts during review and development of health policies and guideline and or strategies in the health sector.

This study was conducted with substantive influence of the professionalism of nursing. Nurses form the bulk of health care providers in primary health care services. Given the opportunity to implement outcomes of this study within the devolved health sector, the model will improve nursing services at the outpatient level, and open further areas of study with special references to nurse, CHWs and nutritionists who take the active roles in nutritional aspect of care and follow-up of patients with comorbid diabetes and hypertension.

References

- Asmall, S. & Mohamed, O. H. (2013). *The Integrated Chronic Disease Management Manual. In:* Health, N. D. O. (ed.). Pretoria: Government of South Africa.
- Buowari, O. Y. (2013). Diabetes Mellitus in Developing Countries and Case Series. *Diabetes Mellitus–Insights And Perspectives*. Intech Open Access Publishers.
- Chinn, P. L. & Kramer, M. K. (2008). *Integrated Theory and Knowledge Development in Nursing*, St. Louis, Elsevier Mosby.
- Conrad, P. & Barker, K. K. (2010). The Social Construction of Illness Key Insights and Policy Implications. *Journal of Health and Social Behavior*, 51, S67-S79.
- Corbin, J. & Strauss, A. (2008). Basics of Qualitative Research: Techniques and Procedures for Developing Grounded Theory, London, Sage.
- Crotty, M. (1998). The Foundations of Social Research Meaning and Perspective in the Research Process, London, Sage Publication.
- Epstein, R. M. & Street, R. L. (2011). The Values and Value of Patient-Centered Care. *The Annals of Family Medicine*, 9, 100-103.
- Fortin, M., Chouinard, M.-C., Bouhali, T., Dubois, M.-F., Gagnon, C. & Belanger, M. 2013. Evaluating the Integration of Chronic Disease Prevention and Management Services into Primary Health Care. *Bmc Health Services Research*, 13.
- Gilbert, L. (1997). Pharmacist and Nurse: A Team Approach Towards Primary Health Care or a Convenient "Therapeutic Alliance"? *International Journal of Nursing Studies*, 34, 367-374.

- Glasgow, R. E., Orleans, C. T., Wagner, E. H., Curry, S. J. & Solberg, L. I. (2001). Does the Chronic Care Model Serve also as a Template for Improving Prevention? *The Milbank Quarterly*, 79, 579.
- Greenhalgh, T. (2009). Chronic Illness: Beyond the Expert Patient. *Bmj: British Medical Journal*, 338, 629-631.
- Haggerty, J. L., Roberge, D., Freeman, G. K., Beaulieu, C. & Bréton, M. (2012). Validation of a Generic Measure of Continuity of Care: When Patients Encounter Several Clinicians. *The Annals of Family Medicine*, 10, 443-451.
- Hammersley, M. & Atkinson, P. (2007). *Ethnography: Principles in Practic.*, London: Taylor And Francis -Routledge.
- Higginbottom, G., Pillay, J. J. & Boadu, N. Y. (2013). Guidance on Performing focused Ethnographies with an Emphasis on Healthcare Research. *Qualitative Report*, 18, 1-17.
- Hogerzeil, H. V., Liberman, J., Wirtz, V. J., Kishore, S. P., Selvaraj, S., Kiddell-Monroe, R., Mwangi-Powell, F. N. & Von Schoen-Angerer, T. (2013). Promotion of Access to Essential Medicines for Non-Communicable Diseases: Practical Implications of the Un Political Declaration. *The Lancet*, 381, 680-689.
- International Diabetes Federation[IDF] (2012). *IDF Diabetes Atlas*. 5th ed. United Kingdom: International Diabetes Federation.
- Islam, M. M., Valderas, J. M., Yen, L., Dawda, P., Jowsey, T. & Mcrae, I. S. (2014). Multimorbidity and Comorbidity of Chronic Diseases among the Senior Australians: Prevalence and Patterns. *Plos One*, 9, 1-11.
- Jadad, A., Cabrera, A., Martos, F., Smith, R. & Lyons, R. (2010). When People Live with Multiple Chronic Diseases: A Collaborative Approach to an Emerging Global Challenge [Online]. Available:http://www.opimec.org/equipos/when-people-live-with-multiple-chronic-diseases/ [Accessed 25 Feb 2016.
- Kenya National Bureau of Statistics (2010). *Kenya Demographic Health Survey* 2008-2009 *Report*. Nairobi: Kenya National Bureau of Statistics.
- KMOH (2006). Taking the Kenya Essential Package for Health to the Community a Strategy for the Delivery of Level one Services. Nairobi: Republic of Kenya.

- Lincoln, Y. S., Lynham, S. A. & Guba, E. G. (2011). Paradigmatic Controversies, Contradictions, and Emerging Confluences, Revisited. *In:* Denzin, N. & Lincoln, Y. (Eds.) *The Sage Handbook of Qualitative Research*. Thousand Oaks Ca: Sage Publications.
- Long, A. N. & Dagogo-Jack, S. (2011). Comorbidities of Diabetes and Hypertension: Mechanism and Approaches to Target Organ Protection. *Journal of Clinical Hypertension*, 13, 244-251.
- Longtin, Y., Sax, H., Leape, L. L., Sheridan, S. E., Donaldson, L. & Pittet, D. (2010). Patient Participation: Current Knowledge and Applicability to Patient Safety. *Mayo Clinic Proceedings*, Elsevier, 53-62.
- Lorig, K. R. & Holman, H. R. (2003). Self-Management Education: History, Definition, Outcomes, and Mechanisms. *Annals of Behavioral Medicine*, 26, 1-7.
- Martin, C. M. & Peterson, C. (2009). The Social Construction of Chronicity–a Key to Understanding Chronic Care Transformations. *Journal of Evaluation in Clinical Practice*, 15, 578-585.
- Mathenge, W., Foster, A. & Kuper, H. 2010. Urbanization, Ethnicity And Cardiovascular Risk in a Population in Transition in Nakuru, Kenya: a Population-Based Survey. *Bmc Public Health*, 10, 569-575.
- Mendis, S., Al Bashir, I., Dissanayake, L., Varghese, C., Fadhil, I., Marhe, E., Sambo, B., Mehta, F., Elsayad, H., Sow, I., Algoe, M., Tennakoon, H., Lai Die, T., Le Thi Tuyet, L., Huiuinato, D., Hewageegana, N., Fahal, N. A. W., Mebrhatu, G., Tshering, G. & Chestnov, O. (2012). Gaps In Capacity In Primary Care In Low-Resource Settings for Implementation of Essential Noncommunicable Disease Interventions. *International Journal of Hypertension*, 1-7.
- Mohan, V., Seedat, Y. K. & Pradeepa, R. (2013). The Rising Burden of Diabetes and Hypertension in Southeast Asian and African Regions: Need for Effective Strategies for Prevention and Control in Primary Health Care Settings. *International Journal of Hypertension*, 14.
- Muchomba , F. G. (2015). Influence of Devolved Governance and Performace of the Health Sector in Kenya. *Strategic Journal of Business & Change Management*, **2**, 68-105.

- Olmen, J. V., Schellevis, F., Damme, W. V., Kegels, G. & Rasschaert, F. (2012). Management of Chronic Diseases in Sub-Saharan Africa: Cross-Fertilisation Between Hiv/Aids and Diabetes Care. *Journal of Tropical Medicine*, 1-11.
- Oni, T., Mcgrath, N., Belue, R., Roderick, P., Colaggiuri, S., May, C. R. & Levitt, N. (2014). Chronic Diseases And Multi-Morbidity A Conceptual Modification to the Who Iccc Model for Countries in Health Transition. *Bio Med Central Public Health* 14, 575-582.
- Otieno, C., Vaghela, V., Mwendwa, F., Kayima, J. & Ogola, E. (2005). Cardiovascular Risk Factorsi in Patients With Type 2 Diabetes Mellitus in Kenya: Levels of Control Attained at the Outpatient Diabetic Clinic of Kenyatta National Hospital, Nairobi. *East African Medical Journal*, 82, 1-8.
- Piette, J. D. & Kerr, E. A. (2006). The Impact of Comorbid Chronic Conditions on Diabetes Care. *Diabetes Care*, 29, 725-731.
- Pilleron, S., Pasquier, E., Boyoze-Nolasco, I., Villafuerte, J. J., Olchini, D. & Fontbonne, A. (2014). Participative Decentralization of Diabetes Carei in Davao City (Philippines) According to the Chronic Care Model: A Program Evaluation. *Diabetes Research and Clinical Practice*, 104, 189-195.
- Ploubidis, B. G., Mathenge, W., De Stavola, B., Grundy, E., Foster, A. & Kuper, H. (2013). Sociaoeconomic Position and Later Life Prevalences of Hypertension, Diabetes and Visual Impairment in Nakuru, Kenya. *International Journal for Public Health*, 58, 133-141.
- Pomey, M.-P., Ghadiri, D. P., Karazivan, P., Fernandez, N. & Clavel, N. 2015. Patients as Partners: a Qualitative Study of Patients' Engagement in their Health Care. *Plos One*, 10, E0122499.
- Roumie, C., Greevy, R., Wallston, K., Elasy, T., Kaltenbach, L., Kotter, K., Dittus, R. & Speroff, T.(2011). Patient Centered Primary Care Is Associated With Patient Hypertension Medication Adherence. *Journal Of Behavioral Medicine*, 34, 244-253.
- Si, D., Bailie, R., Cunningham, J., Robinson, G., Dowden, M., Stewart, A., Connors, C. & Weeramanthri, T. (2008). Describing and Analysing Primary Health Care System Support for Chronic Illness Care In Indigenous Communities in Australia's Northern Territory Use of The Chronic Care Model. *Bmc Health Services Research*, 8, 1-14.

- Strauss, A. & Corbin, J. (1998). *Basics of Qualitative Research: Techniques and Procedures for Developing Grounded Theory,* Thousand Oaks, Ca, Sage Publications.
- Tapp, H., Phillips, S. E., Waxman, D., Alexander, M., Brown, R. & Hall, M. (2012). Multidisciplinary Team Approach to Improved Chronic Care Management for Diabetic Patients in an Urban Safety Net Ambulatory Care Clinic. *The Journal of the American Board of Family Medicine*, 25, 245-246.
- Thorogood, M., Connor, M. D., Hundt, G. L. & Tollman, S. M. (2007). Understanding and Managing Hypertension in an African Sub-District: A Multidisciplinary Approach. *Scandinavian Journal of Public Health*, 35, 52-59.
- Turin, D. R.(2010). Health Care Utilization in the Kenyan Health System: Challenges and Opportunities. *Student Pulse*, 2, 1-3.
- Unützer, J., Harbin, H., Schoenbaum, M. & Druss, B. (2013). The Collaborative Care Model: An Approach For Integrating Physical And Mental Health Care In Medicaid Health Homes. *Health Home, Information Resource Center*, 1-13.
- WHO (2008). *The Global Burden of Disease:* (2004) *Update.* Geneva, Switzerland: World Health Organization; 2008.
- WHO (2010). Package of Essential Noncommunicable (PEN) Disease Interventions for Primary Health Care in Low-Resource Settings. . Geneva.
- WHO (2013) . Global Action Plan for the Prevention and Control of Noncommunicable Disease 2013-2020 [Online]. Geneva Swirtzerland: World Health Organization. Available: www. apps.who.int/iris/bitstream/10665/94384/1/9789241506236_eng.pdf [Accessed September 20th 2014].

Isolation and Identification of Heavy Metal Resistant Bacteria Producing Enzymes from Industrial, Laboratory and Dumping Sites Wastes in Mombasa County

¹Obiero, L.S., ¹Msanzu, J.B, ²Chimbevo, M.L., ³Malala, J.B, ¹Gicharu, G.K.

¹Technical University of Mombasa, Kenya ²Kirinyaga University, Kenya ³Mount Kenya University, Kenya

Correspondence: lchimbevo@kyu.ac.ke

Abstract

Industrial, laboratory and dumping sites wastes are sources of heavy metal introducing health risks to humans. However, bacterial strains living in such environments have capacity for wider industrial applications, including, productions of enzymes for detergent industry. The focus of the study was to screen and isolate enzymes produced by heavy metal-resistant bacteria. Wastewaters were collected from industrial discharge points at Tudor creek (TD) and laboratory effluent (TUL) at Technical University of Mombasa. Soil samples were collected from damping site in Kongowea 1 (KG1), Kongowea 2 (KG2), Tudor ground (TG) and Tudor district hospital (TH) in Mombasa County. Bacteria strains were isolated using nutrient agar media and further sub-cultured to obtain pure colonies. Pure strains were screened for production of protease and amylase using lytic activity. Heavy metal tolerance test was used to screen for copper and mercury resistance to isolated bacteria. Microscopic and biochemical characteristics were used to identify bacteria with ability to grow in heavy metals and actively produce viable enzymes. Positive growth was realized in all sample collected from the six sites in varying concentration with copper plates recording the highest counts. Activity of microbial protease and amylase ranged from 0.1080±0.0025 in KG1 to 0.3703±0.0014 in TUL and 0.200±0.0745 in TUL 0.3613±0.0014 in TH respectively at a concentration of 2.5 mg/L of copper. At a concentration of 2.5 mg/L of mercury, activity of microbial protease and amylase ranged from 0.0113 ± 0.0014 in TD to 0.2047 ± 0.0014 in TH. There was no significant difference (p < 0.05) in microbial community and enzyme activity from the six sampling points. In all the sampling points, S. aureus, N. Veillonella, B. licheniformis, B. azotoformans, Streptococcus, Peptostreptococcus, Enterococcus and Acinetobacter/Moraxella were identified. The sites studied contained bacteria adapted to heavy metal pollution that can be natured to produce enzymes for situations demanding resistant enzymes such as detergent industries.

Keyword: Heavy Metal Resistance, Enzymes; Industrial Wastes, Dumping Sites.

Background Information

In view of science, life involves catabolism and anabolism. Catabolism results in breakdown of complex molecules, a process that involves enzymes such as α-amylases, which are glycoside hydrolases acting on α-1, 4-glycosidic bonds (Alyer, 2005). These enzymes are produced by a wide range of living organisms, from bacteria to plants and humans. Enzymes have wide range of applications, from brewing to food industries, detergent industries and pharmaceutical industries, as well as textile industries. Enzymes producing microorganisms include *Bacillus subtilis*, *Bacillus licheniformis*, *Bacillus steriothermophilus*, *Bacillus megaterium*, *Lactobacillus*, *Escherichia*, *Proteus*, *Strepotmyces sp.*, and *Pseudomonas spp.*, among others (Parmar et al., 2012).

Use of microorganisms for production of industrial enzymes is due to cost effectiveness, consistency, less time and space required for production (Sindu et al., 1997). Further, microorganisms have ability to produce enzymes in bulk and they can easily be manipulated for production of desired products. Replacement of chemicals with microbial enzymes in industrial hydrolysis, pharmaceutical and fine chemical industries (Rao et al., 1998), has led to its increased use. This has placed greater stress on increasing indigenous enzyme production and search for more efficient processes for their production (Lonsanc, 1990). Owing to introduction of biotechnology, use of enzymes has widened in today's world to various fields.

Human activity has had a direct influence in the natural process of these microbial communities in their natural environment. This impact is felt in their natural metabolic process that involve enzyme production. For instance, pollution of soil and waste waters with heavy metal from industrial and laboratory processes is a common significant environmental problem (Cheng, 2003). It hampers production of enzymes for application in industrial products, both consumable and economically important. Release of wastewater from industries and sewage sludge has permanent toxic effects to humans and the environment (Rehman et al., 2008).

Thus byproducts of industrial and laboratory processes pose considerable health risks to human beings, as well as being a big challenge the microbial community in the soil and wastewaters. Existence of heavy metals in the microbial environment hinders use of microorganisms in production of industrial enzymes and its application in food,

Page **35** of **232**

pharmaceutical, textile and detergent industries. There is therefore need to enforce measures to monitor presence and concentration of heavy metals in wastewaters before discharging them into the environment, as mandated by the various environmental protection agencies. This study sought to screen and isolate enzymes produced by bacteria species living in selected industrial waste discharge ports of Mombasa County.

Materials and Methodology

Target Site

The research was conducted in Mombasa County in the coastal region of Kenya within coordinates of 4.0500°S, 39.6667°E. The county has a population of approximately one million according to Kenya population census records of 2009. The major economic activity in this region is tourism. This county has had a challenge of dumping garbage for quite some time till recently when the county government devised improved mechanism managing the garbage.

Sampling Techniques

Waste water samples were collected from industrial discharge points to the ocean (Tudor beach) and at a laboratory at Technical University of Mombasa. Soil samples were collected from three garbage points (Kongowea 1, Kongowea 2 and Tudor garbage) and one from hospital damping site (Tudor district hospital). Using a sterile spatula and transferred to sterile disposable plastic tubes in aseptic conditions. Discharged waste water sample was collected in sterile plastic containers. Samples were transferred to the Department of Pure and Applied Sciences laboratories at Technical University of Mombasa for analysis and at the Kenya bureau of standards Laboratories in Mombasa.

1) Isolation of Bacterial Strains from Waste Water and Soil Samples

Bacteria strains from waste water and soil samples were isolated as described by Yavuz, (2003). Briefly, 1 ml of waste water and 1g of soil sample were used. Each sample was mixed with 9 ml of sterilized distilled water and serially diluted up to 10⁻⁵. The serial dilutions was introduced into a sterile petri plates using the pour plate method into nutrient agar media fortified with 2% starch, lipid, and protein in different petri dishes. Plates were incubated at

Page **36** of **232**

37°C for 24 hrs and bacterial isolates further sub-cultured to obtain pure colonies. Pure colonies on respective agar slants were maintained at 4°C.

2) Screening for Enzyme Producing Bacteria

Isolated pure strains were screened for production of extracellular enzymes using amyl lytic activity. Microbial isolates were streaked on starch agar plate (amylase), agar plates containing skim milk as substrate (protease) and tributyrin agar (lipase), and incubated at 37°C for 48 hours. For amylase, 1% iodine solution was flooded with a dropper for 30 seconds on starch agar plate. The isolates that produced a clear zones of hydrolysis were considered as amylase producers (Gupta et al., 2003), were subjected to further analysis. For protease, micro-organisms that produced a zone of clearance on the culture media were subjected to further studies.

3) Isolation and Assay for Amylase Activity

A suitable volume of isolated culture broth incubated for 48 hrs was centrifuged at 5000 rpm for 20 min at 4°C and supernatant collected. Amylase activity was determined by spectrophotometric method. 1 ml crude enzyme and 1 ml 1% soluble starch in sodium phosphate buffer (pH 7) were mixed in test tubes covered and incubate at 35°C for 10 min. 2 ml DNS reagent was added in each tube to stop the reaction and incubated further for 10 minutes in boiling water bath. After cooling to room temperature, the final volume was made to 10 ml with distilled water and absorbance will be read at 540 nm by spectrophotometer (Kim et al., 1995). A control containing all the reagents with exception of the crude enzyme was run. Absorbance obtained from the control was subtracted from the ones read from respective sample tubes to obtain corrected absorbance which was tabulated as shown in tables 1 and 2 below.

4) Isolation and Assay for Protease Assay

Proteolytic activity was carried out according to Casein-Pholine method (Boethling, 1975). Culture media was centrifuged at 7200 rpm for 10 min. and supernatant used as enzyme source. However, 1% casein (in 0.1 M phosphate buffer pH 7.0) was used as substrate. 1 ml each of enzyme and substrate were incubated at 50°C for 60 min. The reaction was

Page 37 of 232

terminated by adding 3 ml of Trichloroacetic acid (TCA). Centrifuged at 5000 rpm for 15 minutes. From this, 0.5 ml of supernatant was taken, and 2.5 ml of 0.5M sodium carbonate was added, mixed and incubated for 20 minutes, added to 0.5 ml of folin phenol reagent and absorbance read at 660 nm using Spectrophotometer. A control was ran with all the reagent except the supernatant for enzyme source. Absorbance from control was used to calculate for corrected absorbance.

5) Heavy Metal Resistance Screening

Heavy metal tolerance test was used to screen for heavy metal resistance of isolated strains of bacteria. Cells of overnight grown cultures of bacteria that expressed ability to produce enzymes were inoculated on nutrient agar plates supplemented with different concentrations (0.5, 1.0, 1.5 and 2.5 mM) of different salts of heavy metals (Mercuric II chloride and Copper II sulphate). Cultures were incubated at 37°C for 24 hours and cell growth observed. Concentrations were dispensed from 0.5 to 2.5ml

6) Identification and Characterization of the Soil and Waste Water Bacteria

Colonies that expressed ability to grow in this condition and actively produce viable enzyme were considered for identification. Isolates were observed under a microscope to obtain their colony morphology (color, shape, size, nature of colony and pigmentation (Dipali et al., 2003). The following biochemical tests were used for oxidase and catalase activity tests: Voges-Proskauer (VP) test, methyl red-Voges-Proskauer (MR-VP) test, starch hydrolysis and gelatin hydrolysis, motility, indole production and citrate utilization, growth at 7%, 8%, 10% concentration of NaCl, Gram staining and growth at 55°C as described in Bergey's Manual of Systematic Bacteriology (Claus and Berkeley, 1986) and identified by means of taxonomic schemes and descriptions (Buchenan et al., 1974).

Result

Colonies on each plate were counted using a colony counter and the average count for each set calculated and results tabulated in the table 1 below. The growth proved positive for the entire plate sample and a cross the concentration.

Table 1: The Average Score of Viable Colonies Counted on the Three Sets of Each Sample Plates

Plate Count Results

	Mercury Plates			Copper Plates						
	0.5	1.0	1.5	2.0	2.5	0.5	1.0	1.5	2.0	2.5
TH	103	72	61	43	35	>200	107	109	74	63
KG1	32	37	31	26	21	73	61	71	57	45
KG2	67	54	56	47	32	81	34	51	21	19
TG	71	74	70	41	36	67	61	72	62	47
TD	61	60	43	31	21	67	66	64	59	29
TUL	41	42	33	27	23	107	94	61	57	47

Copper plates had the highest plate count, mercury the lowest plate count. There was a general growth decrease in all plates with high hits being recorded in samples obtained from Tudor hospital. This might be due to the plasmid that confers antibiotic resistance.

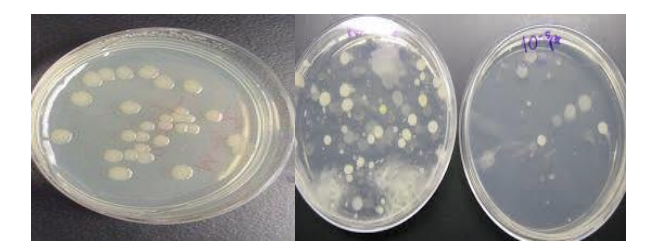


Figure 1: Microbes on Copper Plate Showing High Count and Low Count Plates in Mercury Plate

Table 2: Activity of Microbial Protease Produced Under Different Concentration of Copper (Mean±SEM)

Sample	Concentration of Copper (mg/L)				
	0.5	1.0	1.5	2.0	2.5
TH	0.4313±0.0014	0.3913±0.0014	0.3903±0.0014	0.2940±0.000	0.2047±0.0014
KG1	0.3187±0.0014	0.2967±0.0014	0.2713±0.0014	0.098±0.0014	0.0200±0.0025
KG2	0.2907±0.0087	0.1923±0.0014	0.1213±0.0014	0.1017±0.0029	0.0213±0.0025
TG	0.2073±0.0014	0.2073±0.0014	0.2057±0.0014	0.1760±0.000	0.0713±0.0014
TD	0.1923±0.0014	0.013±0.0014	0.1217±0.0029	0.0453±0.0014	0.0113±0.0014
TUL	0.3517±0.0029	0.2967±0.0014	0.2083±0.0014	0.1973±0.0014	0.0980±0.0025

Concentration of the Essayed Heavy Metals in the Test Samples

Crude enzymes were used to digest respective substrates and activity measured photo spectrometer. Along this a control was ran that contained all the reagents accept the crude enzyme. This was used to calculate for corrected absorbance. The obtained corrected absorbance were fed into excel and its Mean±SEM calculated for each set which was conducted in triplicate. Results of corrected absorbance are represented on tables 3 and 4 below.

Sample	Concentration of copper (mg/L)				
	0.5	1.0	1.5	2.0	2.5
TH	0.3907±0.00140	0.3927±0.0014	0.4033±0.0143	0.3673±0.1040	0.2010±0.000
KG1	0.3800±0.0025	0.3973±0.0014	0.391±0.000	0.2133±0.0143	0.1080±0.0025
KG2	0.394±0.000	0.3973±0.00014	0.3980±0.0025	0.3037±0.0137	0.2763±0.0014
TG	0.2963±0.0014	0.2970±0.0025	0.2987±0.0014	0.2917±0.0014	0.2817±0.0029
TD	0.03967±0.0014	0.3983±0.0014	0.3907±0.0014	0.3807±0.0014	0.3010±0.0025
TUL	0.3707±0.0014	0.3613±0.0052	0.3713±0.0029	0.3713±0.0014	0.3703±0.0014

Table 3: Activity of Microbial Amylase Produced Under Different Concentration of Copper (Mean±SEM)

SAMPLE	Concentration of Copper (mg/l)				
	0.5	1.0	1.5	2.0	2.5
TH	0.3947±0.0014	0.4013±0.0014	0.4190±0.000	0.3717±0.0014	0.3613±0.0014
KG1	0.3863±0.00014	0.3867±0.0014	0.3910±0.000	0.3183±0.0029	0.2803±0.0014
KG2	0.3673±0.0014	0.3553±0.0014	0.3680±0.000	0.3610±0.0025	0.3110±0.0025
TG	0.3753±0.0014	0.3780±0.0025	0.3770±0.00	0.2913±0.0014	002007±0.0014
TD	0.3907±0.0014	0.3980±0.0025	0.4013±0.0014	0.3203±0.0014	0.2933±0.0143
TUL	0.3907±0.0014	0.3914±0.0014	0.4027±0.0160	0.2810±0.0025	0.200±0.0745

Table 4: Activity of Microbial Protease Produced Under Different Concentration of Mercury (Mean±SEM)

Page **41** of **232**

Table 5: Activity of Microbial Amylase Produced Under Different Concentration of Mercury (Mean±SEM)

B. Sample	C. Concentration of Copper (mg/L)				
	D. 0.5	E. 1.0	F. 1.5	G. 2.0	Н. 2.5
I. TH	J. 0.4083±0.0180	K. 0.3917±0.0014	L. 0.3817±0.0038	M. 0.3013±0.0014	N. 0.2940±0.0151
O. KG1	P. 0.2907±0.0014	Q. 0.2907±0.0014	R. 0.2810±0.0050	S. 0.1023±0.0014	T. 0.0300±0.0025
U. KG2	V. 0.2940±0.000	W. 0.2003±0.0014	X. 0.2770±0.0043	Y. 0.0973±0.0014	Z. 0.0013±0.0014
AA. TG	BB. 0.2027±0.0038	CC. 0.2003±0.0029	DD. 0.2007±0.0014	EE. 0.0117±0.0014	FF. 0.0900±0.0248
GG. TD	HH. 0.3960±0.000	II. 0.2713±0.0029	JJ. 0.1633±0.0143	KK. 0.0407±0.0014	LL. 0.0214±0.0016
MM. TUL	NN. 0.3410±0.000	OO. 0.2917±0.0014	PP. 0.3010±0.0025	QQ. 0.1917±0.0014	RR. 0.0642±0.2058

Identification of the Microbes

Using the bar, the following microorganisms were able to be identified. The group (Streptococcus/Peptostreptococcus/Enterococcus) was the most dominant, *B. licheniformis* and *B. azotoformans* recoding the least dominant.

The following colonies were successfully characterizing

		Sample				
Microbes	Th	Kg1	Kg2	Tg	Td	Tul
Staphylococcus aureus	+	+	+	-	-	+
Acinetobacter/Moraxella	-	-	+	+	+	+
Neisseria Veillonella	+	-	+	+	-	-
B. licheniformis	+	-	-	+	-	-
Streptococcus/Peptostreptococcus/ Enterococcus	+	+	+	+	+	+
B. azotoformans	-	-	+	+	-	-

Table 6: Spread of Identified Microbes in the Respective Samples Discussion, Conclusion and Recommendations

Discussion

Microorganisms exposed to heavy metal stress are vulnerable to toxic conditions caused by reactive oxygen species. The aim of this study was to investigate the tolerance of stressed bacteria and detect the ability of some resistant bacterial strains to produce antioxidant enzymes under heavy metal stress. The activities of antioxidant enzymes produced in the resistant bacterial strains were measured using a spectrophotometer. Results showed that of the two metals used, Hg was more toxic from plate count to enzymatic activity. Antioxidant enzymes can be used to biologically monitor heavy metal pollution. This is well explained from the results obtained from analysis of the samples for heavy metal. It shows that most of the samples obtained contain microorganisms adapted more to copper compared to mercury.

Analysis of results further revealed a gradual increase in enzymatic activity from concentration 0.5 to 1.0 or 1.5 then a drop as concentration rises through 2.0 to 2.5. This show that these microbes can tolerate certain concentration of heavy metal before the later turns to toxic concentration and hinder normal microbial physiological activity. These metals play an important role in the microbial activity probably by acting as co-factors.

An interesting outcome was experienced with the sample TH. This sample showed high degree of activity on both metals. Activity of enzyme isolated from microbes of this sample, had high tolerance to high concentration of metal. Considering the plate count results, there was relatively high growth in plates containing this sample in comparison to the other plates.

This is might be linked to the point that bacterial resistance to heavy metals is determined by plasmids, which in many instances also encode resistance to antibiotics (Izaki, 1977). The plasmid-determined nature of resistance to heavy metal compounds was established by deter mining the ability for cotransduction (with other plasmid- encoded determinants) and high frequency of conjugal transfer of the Hg determinant (Summers et al. 1978). Isolation of covalently closed circular DNA from the Hg strains and its ability to transform Hgs recipients to the Hgr phenotype provided further evidence that the Hgr determinant is

plasmid encoded, as did curing Hg strains with agents such as ethyl methanesulfonate (Nakahara et al., 1977). The relationship between resistance to mercury and other heavy metals and antibiotics in the hospital environment has been explored in numerous studies. There thus appears to be a strong correlation between antibiotic resistance and resistance to mercury and several other metals (Novick, et al., 1968). In most instances, the frequency of heavy-metal resistance is the same as or higher than that of antibiotic resistance (Kondo et al., 1974.).

From the anova analysis, the p values were less than 0.5. This implies that there were no statistically significant differences between group means as determined by one-way ANOVA. The activity of microbes obtained from the six sampling points is relatively the same. This serves two sets of information; thus there is equal distribution of industrial microorganism across the sampling points and there is relatively equal rate of pollution among the six sampling points.

Conclusion

Result of this study show that the immediate environment contains industrial microorganisms that are well adapted to functioning in environment polluted with heavy metal. These environs may be important source for microorganisms that can be natured to produce enzymes that function well in situations demanding heavy metal resistant enzymes such as detergent industries.

Recommendations

Feature studies should focus on shading light on the composition and stability of these microorganisms. As well studies focusing on purification and titre increment of the enzyme produced by these microorganisms should be conducted in order to facilitate full scale implementation of the project. On the other hand, regular studies into rate of pollution into the environment should be monitored to guarantee the public safety.

References

Aiyer, P. V., (2005). Amylases and their Application. Afr. J. Biotechnology., 4(13), 1525-1529.

Buchanan, R.M, & Gibbons, N.E. (1974). *Bergey's Manual of Determinative Bacteriology*, 8th ed. Baltimore: The Williams and Wilkins Company

Gupta, G. P. (2003). Microbial-amylases: A Biotechnological perspective. *Process Biochem*; 38, 1599-1616.

Izaki, K. (1977). Enzymatic Reduction of Mercurous ions in Escherichia Coli Bearing R Factor. J. Bacteriol. 131:696-698.

Kondo, I., T. Ishikawa, and H. Nakahara. (1974). Mercury an Cadmium Resistances Mediated by the Penicillinase Plasmid in Staphylococcus Aureus. *J. Bacteriol*. 117:1-7.

Kim, T.U. (1995). Purification and Characterization of Maltotetraose forming Alkaline Alpha Amylase from an Alkalophilic Bacillus Strain, GM 8901. *Appl. Environ. Microbiol.*, 61: 3105-12

Lonsane, M.V. (1990). Advances in Appl. Microbiology., 35: 54-56.

Nakahara, H., Ishikawa, Y, Sarai, I, Kozukue, H & Mitsuhashi. S (1977). MercuryResistance and R Plasmids in Escherichia Coli Isolated from Clinical Lesions in Japan. Antimicrob. *Agents Chemother*. 11:999-1003.

Novick, R. P., and C. Roth. (1968). Plasmid-linked Resistance Inorganic Salts in Staphylococcus Aureus. *J. Bacteriol*.95:1335-1342.

Parmar, A.P., (2012), Characterization of Amylase Producing Bacterial Isolates, *Bulletin of Environment, Pharmacology and Life Sciences*.; Vol. 1 [6] May: 42 -47

Rao, A. T. (1998) Microbiol. Mol. Biol. Rev., 62, 597-634.

Sindhu, B.S., (1997) T Prased. Int. Phytopathol., 34, 269-271.

Yavuz. M. (2003). MSc. thesis, İzmir Institute of Technology İzmir, Turkey.

Risks and Existing Health Services for Men Having Sex with Men in Kilifi Town, Kenya.

Maina, Evah & Butto, Dennis

Kirinyaga University, Kenya

Correspondence: emaina@kyu.ac.ke

Abstract

Homosexuels and especially men who have sex with men, face numerous health risks and limited options for health services due to associated stigma and discrimination from the general population. Understanding these risks is important in designing health promotion and behavior change interventions for this key population group. The objective of this study was to determine health risks among homosexuals and to establish health promotion and management services for Men having Sex Men (MSM) in Kilifi Town, Kenya. It was a descriptive cross-sectional study and snowballing sampling technique was used to reach MSM. The study revealed that 69.4% of respondents did not use condoms during their last sexual act. There was high prevalence of multiple sexual partners and drug abuse among the study participants. There was limited access to health services with government facilites catering for 87% of respondents. 63.9%, of respondents had experienced some form of discrimination when they last sought health services. This study recommends policy formulation; health services partnerships and advocacy for homosexuals' sexual reproductive health to improve health status of men who have sex with men in Kilifi town

Keywords: Bisexuality, Heterosexuality, Lesbian, Men having Sex with Men

Introduction

Homosexuality is the term used to refer to people who are sexually attracted to members of the same sex. Homosexuality also refers to the individual sense of personal and social identity based on these attractions, behaviors that express them and membership to a community of individuals that share the beliefs and sexual orientations. Scientists have no consensus as to why people develop certain sexual orientations but biological based theories have been favored by experts who relate this to genetic predisposition and early uterine development. The common terms for homosexuals are Lesbian for females who have sex with females and gay for men who have sex with men. Many men who have sex with men are in committed same sex relationships with few being bisexual. The number of people who

identify themselves as homosexuals is difficult to determine since not many declare this openly, especially in the African set up due to homophobia and heterosexist discrimination.

According to Men who have sex with men (MSM) was a term coined in 1992 in an attempt to capture a range of male- male sexual behaviors and avoid characterization of men engaging in these behavior by sexual orientation (homosexual, heterosexual, bisexual or gay) or gender identity (male, female, transgender, queer). MSM includes gay- identified men, heterosexually identified men who have sex with men, bisexual men, male sex workers who can have any orientation, men engaging in these behaviors in all male settings, such as prisons, and the rich and wide array of traditional identities and terms for these men across cultures and subcultures. Transgender people born male share some biological risks with MSM, especially receptive anal intercourse, but their female gender identity places them in a different category from MSM; hence not included as subgroup in MSM

Human Immunodeficiency Virus and Acquired Immune Deficiency Syndrome (HIV/AIDS) was originally referred to as "gay disease" due to the high incidence among homosexuals. Understanding the sexual behaviors of populations who are vulnerable to HIV is an important component in the fight against HIV/AIDS. In Kenya, male homosexuality is criminalized under the penal code and there is wide spread stigma and discrimination against homosexuals. This environment has made it difficult for these people to access health services thereby increasing their vulnerability to negative health outcomes including HIV/AIDS, STI's and other health consequences. The Kenya National Aids and STI program has reported prevalence of HIV to be 18.2% among MSM in Nairobi and 11.1% among MSM in Kisumu. The Kenya modes of transmission study (2008) had previously estimated that nationally, 15% of new infections occur among MSM and prisoners. Although homosexuality is illegal, HIV pandemic among MSM has started being addressed by government institutions.

In Kenya the incidence of HIV among MSM is as high as 35% compared to 6% in bisexual men. Prevalence of HIV among MSM equals or exceeds that seen in the general population in most sub-Saharan countries.

According to a study by Bowers et al 2012 the medical dangers of homosexuality are under emphasized. Homosexuality is associated with higher rates of sexually transmitted diseases,

substance abuse and mental illnesses. While in U.S homosexual men represent about 2% of the population, they have the highest burden of hepatitis B infection, about 44% of new HIV infections annually and contract syphilis at a rate 3-4 times higher than heterosexual men. Anal intercourse causes hemorrhoids, anal rectal trauma, anal fissures, retained foreign bodies and high risk for anal rectal cancer. Among homosexuals engaging in oral to anal contact, high rates of parasitic and other intestinal infections and high mortality rates. A Canadian medical centre predicted that nearly half of today's gay and bisexual men 20 years old would not reach 65th birthday.

Materials and Methods

Study Design

This was a cross sectional descriptive study.

Study Site

The study was carried out in Kilifi town on Kilifi Greek approximately about 60km north of Mombasa, Kenya. The township has a population of 122, 899 according to Kenya census (2009) with HIV/AIDS prevalence at Kilifi county stands at 7% according to Kenya Aids Indicator Survey. The communities living here include Mijikenda, Swahili, Bajuni, Indians, Arabs, Europeans as well as other native Kenyan communities who migrated during colonial times. This town council was chosen because it presents a semi-rural urban set up in the coastal region which has the highest prevalence of MSM in Kenya.

Study Population

The study population was men who have sex with men in Kilifi town. This included all MSM above 18 years, of all ethnicities and socio economic background.

Sampling

Non probability, snowballing sampling technique was used. The initial subjects were sought at MSM friendly health services and MSM self-identified groups. After observing the initial subject, we asked for a referral from the subject to help identify people with a similar trait of interest. All available and consenting homosexuals were sampled.

The study used questionnaires, focused discussion guide and key informant structured interviews pretested in a similar population in Mtwapa town council. Ten MSM and two key informants were used.

This study used both primary and secondary data to investigate the objectives. Primary data was collected by self-administered open and closed ended structured questionnaires given to MSM, two focused group discussion with 6 MSM each and structured key informant interviews with key people who included a health worker at Kilifi District hospital, CASCO (County Aids and STI control officer),non-Governmental Organization officer, MSM representative and law enforcer as well as research assistants who were trained in data collection. Data from FGD and key informant interviews were audio recorded. Secondary data was obtained from the related literature.

Descriptive statistics was analyzed and presented in tables, graphs and charts. Qualitative data was analyzed according to emerging themes. Frequency distribution tables was used to analyze the various variables while correlation and chi –square test were utilized to assess the relationships between selected variables. Regression analyses were performed to show the strength of association between selected variable and health risks among homosexuals.

The study was conducted through voluntary participation, informed consent, ensuring privacy and confidentiality of the respondents. Institutional ethical reviews, scientific honesty and competency were also considered

Study Results

Demographic Characteristics of study population are presented on table 1 below

Table 1: Demographic characteristics of study population

Age of the Respondent	Frequency n=72	Percentage %
20 years and below	4	5.6
21-30 years	52	72.2
31-40years	14	19.4
51-60 years	2	2.8
Sexual Orientation		
Homosexual	52	72.2
Bisexual	20	27.8

Marital Status					
Married	20	27.8			
Single	46	63.9			
Divorced	6	8.3			
Age in which the Respondents Were First Attracted to Other Me					
Below 10 years	12	17			
11-20 years	58	80			
21-30	2	3			
Level of education					
Primary	23	31.9			
Secondary	21	29.2			
Tertiary education	28	38.9			
Average Income of the	he Respondents				
<10,000 ksh	38	52.8			
11,000-40,000	24	33.3			
41,000-90,000	10	13.9			
Religion					
Christianity	32	44.4			
Islam	28	38.9			
Atheist	12	167			

In this study, majority of the respondents, 72.2% were aged between 21-30 years. 72.2% of the respondents indicated that they were homosexual compared to 27.8% who were bisexual. 63.9% indicated they were single, 27% were married and 8.3% divorced at the time of study.

80.6% of the respondents revealed that they started being attracted to other men when they were between 11-20 years and a further 17 % developed attraction even before the age of 10 years. 38.9% of the respondents had attained tertiary education, 29.2% had secondary school education while 31.9% were educated up to primary school level.

53% of respondents earned less than 10,000 Kenya shillings per month. 34% between Kshs 11,000-40,000 and 13.9% were earning Ksh 41,000-90,000. Majority of respondents 45. % were Christians, 38.9% were Muslim and only 16.7% were atheists.

Table 2: Type of Health Facility from Where the Homosexuals Received Health Services.

Type of Health		
Facility	Frequency	Percent
Government owned	58	80.6
Both government and privately owned	12	16.7
Privately owned	2	2.7
Total	72	100

58(80.6%) of the respondents indicated that they had access to government health facilities, 12(16.7%) access both government and private hospitals. These findings revealed that all the respondents do seek health services with government facilities serving more clients. These findings are confirmed by FGD...." We go to KEMRI for free STI screening and treatment, picking lubricants and condoms –prevention package, for HIV testing. Not all staff in KEMRI are friendly. (there is only one good nurse at Kilifi County Hospital's CCC that always treats us immediately without allowing you to wait in the queue. Others think you have gone to snatch them their husbands...Mnarani dispensary we also get health services" ... (FGD, KILifi town council.

(b) Access to Lubricants and Condoms

Table 3: Source of Condoms and Lubricants

Attribute	Frequency	Percent
Government facilities	50	69.4
Chemists and pharmacies	4	5.6
NGO	15	20.8
Others	2	2.8
Government and NGOs	1	1.4
Total	72	100.0

Majority 50(69.4%) of the respondents indicated that they access lubricants and condoms from government facilities,15(20.8%) from NGOs, 4(5.6%) from chemists, 1(1.4%) from both NGOs and government facilities and 2(2.8%) from others sources. This was affirmed by FGD.". KEMRI for free STI screening and treatment, picking lubricants and condoms – prevention package, for HIV testing" (FGD, Kilifi town council). The NGO representative from APHIA Plus Nairobi/Coast further emphasizes." We support the government in providing technical structural dimensions. You know the combination prevention therapy is divided into behavioral and structural. Behavioral is what we are doing with peer education, condom promotion, intervention to gender violence, biomedical is where they are provided with clinical services STI treatment and screening and provision of condoms. Structural is where we are dealing with the community now both the government and relevant institutions......we are building their capacity..." (NGO Officer, APHIA Plus Kilifi).

(c) Discrimination in Health Care Provision

Table 4: Report on Respondents' Discriminated

Face Discrimination	Frequency	Percent
Yes	46	63.9
No	26	36.1
Total	72	100.0

46, (63.9%) of respondents indicated that they were discriminated while seeking health service upon. These findings were confirmed by FGD." we face discrimination in and out of hospitals; If you are abused you cannot go to report. Many times we report and there is no action from police or you go to report and you are chased or locked in yourself unlawfully". And further by FGD." Waiting too long in the queue to be served until other patients start calling us names-angalia shoga, huyo ni shoga...Some health care providers start preaching to us to stop same sex...Sometimes health care workers whisper or call on each other to come and see MSM whenever we go to health facilities for services" (FGD, Kilifi town council). The area officer commanding police station ascertains "...these people are beaten up by people known or unknown to them because of their sexual orientation, mannerisms, clients who refuse to pay after services or failed sex advances" (OCS, Kilifi). This could indicate that some homosexuals may be in the practice for commercial purposes.

(d) Health Risks among Homosexuals Awareness of HIV Status

Table 5. Respondents' Knowledge of HIV Status

Know status	Frequency	Percent
Yes	56	77.8
No	16	22.2
Total	72	100.0

Majority 56 (77.8%) of the respondents indicated that they knew their HIV status while 16(22.2%) do not. The fact that majority of the respondents knew their HIV status could imply that they know the health risks associated with the practice

(f) Having Multiple Sexual Partners Concurrently Over the Last 12 Months

Table 6. Declaration of Multiple Sexual Partners

Multiple			
sexual partners	Frequency	Percent	
Yes	60	83.3	
No	12	16.7	
Total	72	100.0	

83.3% of respondents indicated that they had more than one sexual partner concurrently over the last one year while 16.7% had one sex partner.

(j) Condom Use by the Respondents

Table 7. Distribution of the Respondents by Frequency of Condom Use

Condom Use	Frequency	Percent
All the time	22	30.6
Sometimes	42	58.3
Never	8	11.1
Total	72	100.0

Table 7 above shows that 30.6% of homosexuals use condom for every sexual encounter, 58.3% use condom sometimes, meaning other times they don't use condom during sexual

intercourse while 11.1% never used condom at all. These findings are confirmed by FGD.." Sometimes you find a mum and you feel like doing sex without any protection, you don't want to use a condom or anything because you want it without a condom (FGD,Kilifi Town Council)

(k) Use Lubricants by the Respondents

Table 8. Report on Respondents Use of Anal Lubricants

Use of			
Lubricants	Frequency	Percent	
Yes	44	61.1	
No	28	38.9	
Total	72	100.0	

44(61.1%) of the respondents indicated that they used lubricants at the time while 28(38.9%) did not.

Other Diseases Respondents Suffered from in the Past 12 Months

Table 9. Distribution of Respondents by Diseases they Have Suffered from in the Past 12 Months

Infection suffered	Frequency	Percent
HIV/AIDS	22	30.6
Hemorrhoids	6	8.3
STI	32	44.4
Anal fissures	4	5.6
More than one	8	11.1
Total	72	100.0

Majority 32(44.4%) of the respondents indicated that they had contracted STI, 22(30.6%) HIV/AIDS, 6(8.3%) suffer hemorrhoids 4(5.6%) suffer anal fissures and 8(11.1%) suffered STI, AIDS and fissures. These findings were confirmed in FGD.." At times you know your HIV status and you meet with a person and you look at him and decide this one is whole and I would give him without a condom only to realize he is HIV positive and not on ARVs,

it is much better the one that is on ARVs....Being gay alone increases your chances of being infected with HIV" (FGD, Kilifi Town Council).

Discussion

Existing Health Promotion and Management Services for Homosexuals

Most of the homosexuals access health care services from government facilities at 58%. The facilities that provide gay friendly services are few though, with Kilifi county Hospital taking the lead. USAID funded NGO's like APHIA Plus and KEMRI support the government to provide comprehensive care to homosexuals, capacity building of staff and provision of lubricants and condoms to the MSM. As affirmed by County Aids and STIs Control Officer (CASCO) "...Mtwapa, Kilifi County Hospital, Vipingo it does not have to be written somewhere that facilities are offering gay friendly services. Health care workers in Mtwapa, Matsangoni, Vipingo, Kilifi County hospital have been trained on MSM friendly services.." (CASCO, Kilifi County). He further noted the role of these NGO's in MSM care."

There is a local CBO that deals with MSMs and is registered and works with diverse NGOs that are USAID funded to provide gay friendly services. KEMRI is also commonly having diverse programs to work with the government. They do research on MSMS and provide them with condoms and lubricants. They offer Comprehensive Care Clinic services to those MSM that turn to be HIV positive. They support them to come out and train health care providers through online training forum s to equip them with skills on handling MSM. There was a time they were helping them to come up with income generating activities and provision of shelter to those rejected by their family members..." (CASCO, Kilifi County).

It was noted that although training has been done on gay friendly services, most health care workers attitude towards homosexuals needed to change. They need to take them as clients and detach from their own personal, moral and religious values when offering care to this group. CASCO notes" Stigma among health care providers and the community at large need to change. The group likes isolating themselves and the lack of special space in health facilities for attending to them is a barrier.." (CASCO,Kilifi County). The FGD affirms "Sometimes health care workers whisper or call on each other to come and see MSM whenever we go to health facilities for services.... other times some lecture you for being a homosexual as they treat you...there was a time I was given wrong medication by a doctor

for being a homosexual and he abused me....sometimes you fear going to hospital and buy drugs from chemist or use herbs..." (FGD, Kilifi town council).

The health services at the government facilities are free of charge and they are accessible to MSM, the challenge is that some supplies like lubricants are not available all the time." They can come here for STI and we screen them. Condoms they collect from here. Lubricants are the only thing we are lacking. Treatment they are able to access it for free.." (gay friendly nurse, Kilifi District Hospital) and the CASCO further notes." Lack of adequate resources for training health care workers on gay friendly services and purchase of equipment for anal health services is a real challenge." (CASCO, Kilifi County"

Health Risks among Homosexuals

Homosexuals are among the key populations that are exposed to more health risks as a result of the nature of "un natural sex" acts they engage in. They also face social and physical health risks because they engage in unnatural sexual activities that are punishable under the Kenyan Law. 77.8% of homosexuals know their HIV status but majority took their tests more than three months earlier making those results questionable given their high risk of exposure. From the study, majority of the homosexuals suffer or have suffered from STI's and HIV/AIDS

44.4% and 30.6% respectively. These findings agree with those of Kenya Aids Indicator survey, which showed incidence of HIV/AIDs to be greatest among homosexuals at 35%. The fact that majority of them have multiple sexual partners or have had multiple sexual partners (83.3%) further puts them at more risk, this echoes findings of Valle et al, (2004) who reported that MSM have 1.3 times the number of sexual partners. In other words, MSM compared to their exclusively heterosexual counterparts have more opportunities to engage in risky sexual behaviors due to their greater number of sexual partners.

Bisexuality among this group is at 27.8%, meaning that these are married men, probably with families, married to women, yet they have same sex partners secretly. This puts these men together with their partners at higher risk for HIV/AIDS and other STI's.

Majority of the homosexuals (69.4%), do not use condom all the time or not at all when engaging in sexual activities, putting them at a higher risk for STI's and HIV/AIDS. These findings concur with those of Valle et al(2004)who noted that no sexual behavior is more

risky than unprotected anal sex, and evidence indicates that percentages of MSM who engage in this behavior remain high. Furthermore, another reason for non-condom use as cited in the FGD was commercial sex, where male sex workers get more money from clients not willing to use condoms..."Sometimes you find a client and it is difficult to negotiate for condom use. You may be told "with a condom I would pay Kshs 5000, without a condom I would pay Kshs 50,000. What would you opt when you alone you have never held Kshs 50,000 since you were born. At times you know your HIV status and you meet with a person and you look at him and decide this one is whole and I would give him without a condom only to realize he is HIV positive and not on ARVs, it is much better the one that is on ARVs...." (FGD. Kilifi town council...".

One of the major reasons cited for non-condom use was the influence of drug and alcohol. It was noted that 47.2% of respondents who use condoms do not use them consistently and were also abusing drugs. Steuve et al, (2002) in their study conducted in over 3,000 MSM reported that nearly one third of their sample "reported being high on drugs or alcohol the last time they had sex with a non-main partner, and that men who were high were over 60 percent likely to have engaged in unprotected receptive anal intercourse. Substance abuse was associated with other factors, including having multiple sexual partners, trading sex and succumbing to peer norms discouraging condom use that increase risk of MSM contracting HIV.

That majority of homosexuals at abuse substances and other drugs and are likely to engage in risky sexual behavior.

Conclusion

Homosexuals in Kilifi are exposed to many health risks including increased chances of contracting HIV/AIDs, STI's, anal fissures and anal incontinence among others. The inconsistency in condom use, drug and substance abuse and sex for pay are some of the factors fueling these risks. Although the health services are free, access is hampered by lack of essential supplies for the gays coupled with discrimination from the service providers and the community in general.

Recommendations

Policy planning and implementation on homosexual friendly sexual and reproductive health services, even though homosexuality is illegal in Kenya, gay people should not be denied health care as a basic human right because they are affected by adverse health outcomes due to nature of their sexual activities. Provision of supplies, drugs and equipment for provision of sexual and reproductive health services to homosexuals with emphasis on reproductive health education especially prevention of risky sexy behaviors will go a long way in improving the health status of homosexuals in Kilifi town, Kenya.

References

Bowers, J. R., Branson, C. M., Fletcher, J. B.& Reback, C. J. (2012). Predictors of HIV Sexual Risk Behavior among Men Who Have Sex with Men, Men Who Have Sex with Men and Women, and Transgender Women. *International Journal of Sexual Health*, 24(4), 290-302

National AIDS and STI Control Programme (NASCOP) (2003). *Kenya AIDS Indicator Survey* 2012: *Preliminary Report*. Nairobi, Kenya: NASCOP

Steuve. A., O'Donnell, L., Duran, R., and Geier, J. (2002). Being High and Taking Sexual Risks: Findings from Multisite Survey of Men Who Have Sex with Men. *AIDS Education and Prevention Journal*. 14 Pp 482- 495.

Valle, S. D., Evangelista, A. M., Velasco, M. C., Kribs-Zaleta, C. M., and Schmitz, S. H. (2004). Effects of Education, Vaccination and Treatment on HIV Transmission in Homosexuals with Genetic Heterogeneity. *Mathematicalbiosciences*, 187(2), 111-133

Zietsch, B.P., Verweij, K.J., Bailey, J.M., Wright, M.J. and Martin, N.G., (2011). Sexual Orientation and Psychiatric Vulnerability: *A Twin Study of Neuroticism and Psychoticism*. *Archives of Sexual Behavior*, 40(1), Pp.133-142.

Determination of Body Mass Index and Waist Circumference in Type II Diabetes Mellitus in

Patients at Thika Level 5 Hospital

Kimani, Kenny1, Okumu, Caroline2.

¹Kirinyaga University, Kenya, ²Nairobi Hospital, Kenya.

Correspondence:Kimani.kenny@gmail.com

Abstract

Diabetes mellitus is a universal health problem due to its chronic nature severity of complications

mobility and mortality. BMI provides a simple numeric measure of a person's body mass for a given

height using Waist Circumference to assess abdominal fat. A high waist circumference or a greater

level of abdominal fat is associated with increased risk for chronic diseases like Type II diabetes, high

blood pressure and heart disease. The purpose of this study was to determine the body mass index and

waist circumference in Type II diabetes mellitus patients attending Thika Level 5 hospital in relation

to age, gender and social economic status. A descriptive cross sectional study design was employed.

The study targeted patients' age 36-60 years, with a study sample of 117 diabetic patients. Weight

and height were measured using a weighing machine and height meter respectively and BMI

calculated. A tape measure was used to take the waist circumference. There was no strong relationship

between the body mass index and waist circumference in patients with type II diabetes mellitus. We

recommend that new ways of evading sedentary lifestyle and exercising should be embraced.

Keywords: BMI, WC, Type II Diabetes Mellitus

Overview

Diabetes mellitus is a group of metabolic diseases characterized by hyperglycaemia resulting

from defects in insulin secretion, insulin action or both. The chronic hyperglycaemiain

diabetics is associated with long-term damage, dysfunction and failure of various organs,

especially the eyes, kidneys, nerves, heart and blood vessels. Several pathophysiological

processes are involved in the development of diabetes mellitus. These range from

autoimmune destruction of the beta-cells of the pancreas (Robertson and Harmon, 2006)

with consequent insulin deficiency to abnormalities that result in resistance to insulin action.

Deficiency and insufficient action of insulin on target tissues leads to carbohydrates, fats and

proteins metabolism abnormalities.

For families in USA with a child who has diabetes, the corresponding figure is 10% (WHO, 2002). Studies in India estimate that for a low- income Indian family with a diabetic adult, as much as 25% of the family income may be devoted to diabetes care. Thus diabetes is a costly disease not only for affected individuals and their families but also for the health systems in sub- Saharan Africa, diabetes mellitus distribution was estimated to be 0.01% in 2000 and is projected to rise to 0.12% by the year 2025(ADA, 2002).

In Kenya, it was estimated to be 1.06% in 2000 and would possibly rise to 1.32% by the year 2025(Hillary et al, 1998). In the study area it has been estimated to be 8.3 % Kenya National Diabetes Fact Sheet (Jan. 26, 2011).

The body mass index (BMI), or Quetelet index, is a measure for human body shape based on an individual's mass and height and is defined as the individual's body mass divided by the square of their height. Although BMI is not actually a measure of body fat, it connects well with body fat and has become the medical standard for assessing the degree of body fatness (Lori et al, 2002).

A study published in JAMA in 2005 showed that overweight people had a similar relative risk of mortality to normal weight people as defined by BMI, while underweight and obese people had a higher death rate. High BMI is associated with Type II diabetes only in persons with high serum gamma- glutamyltranspetidase. In an analysis of 40 studies involving 250,000 people, patients with coronary artery disease with normal BMI were at higher risk of death from cardiovascular disease than people whose BMIs are in the overweight range (BMI 25-29.9). In the overweight, or intermediate range of BMI (BMI 25-29.9), BMI failed to discriminate between body fat percentage and lean mass. (Lori and Mary, 2002). The study concluded that accuracy of BMI in diagnosis of obesity is limited, particularly for individuals in the intermediate BMI ranges in men and in the elderly. These results may help to explain the unexpected better survival in overweight or mild obese patients (Romero- Corral et al, 2008).

Waist circumference (WC) is a measure of the distance around the abdomen. It is one of the most practical tools to assess abdominal fat for chronic disease risk and during weight loss treatment. A high waist circumference or a greater level of abdominal fat is associated with an increased risk for type II diabetes, high cholesterol, high blood pressure and heart disease

when the BMI is between 25 and 34.9 (BMI greater than 25 is considered overweight and a BMI greater than 30 is considered obese) (McKinley, 2011).

Overweight individuals with apple-shaped body types deposit fat in the abdominal region and are at greater risk of developing heart disease and diabetes. The overweight individuals with pear- shaped body types deposit fat in the hips and thighs where it is primarily subcutaneous. (Lori, 2002)

The number of people with diabetes mellitus is increasing due to population growth, aging, urbanization, and increase in obesity and physical inactivity (Hillary, 2004). Available data indicate a range of 1 case per 1,350 children at 5 years to 1 case in 360 children at 16 years as having type 1 diabetes mellitus. The distribution of diabetes for all age groups worldwide was estimated to be 2.8 % in 2000 and 4.4% in 2030. The number of people with diabetes is projected to rise to 171 million in 2000 to 366 million in 2030 (WHO, 2002)

The major factors identified for developing diabetes are inheritance (genetic predisposition) and environmental factors such as nutrition resulting to increased body mass, waist circumference and chemical toxins (WHO,2000)The world prevalence of diabetes among adults (aged 36-60 years) will be 6.4%, affecting 285 million adults by 2030. Between 2010 and 2030, there will be a 69% increase in number of adults with diabetes in developing countries and a 20% increase in developing countries like Kenya (WHO, 2010 Atlas) people realize this once the disease has already developed and therefore awareness at the community level should be advocated for purposes of disease prevention.

In developing countries, those most frequently affected by type II diabetes mellitus are in the middle productive years of their lives, aged between 36 and 60 (WHO, 2002). Thika being a developing town faces the threat of its citizens who are in the working bracket being affected by type II diabetes mellitus. By determining body mass index, waist circumference in type II diabetes mellitus, the results will help the middle aged Kenyans manage their eating habits and exercise to cut down their body weight that would predispose them to type II diabetes mellitus. Study area was at Thika level 5 hospital. The hospital is located within Kiambu County in Kenya. A descriptive cross sectional study was done on 201 patients attending Thika level 5 hospitals diabetic clinic.

Inclusion Criteria: Diabetic patients between the ages of 36 -60 years attending Thika level 5 hospital diabetic clinic. Exclusion Criteria: All diabetic patients that were pregnant, diabetic patients below 36 years and above 60 years. Glucose oxidase method glucose only was used. A glucometer was placed on a flat firm bench. The patient sat comfortably and middle finger disinfected using spirit swab, allowed to dry and pricked on the side of the figure tip. The first drop of blood was wiped with a dry cotton wool and the subsequent drop put on the test area of the test strip that was already inserted in a test glucometer. The results displayed on the glucometer screen were read and recorded on the lab request from the R₁ filled in the data collection sheet. Patients were thereafter instructed to step on the weighing machine placed on a leveled ground and weight recorded on the data collection sheet in kilograms. The patient was instructed to stand straight on the height meter and face forward at the angle of 90° and height measurement recorded in centimeters and later converted to meters. The top hipbone was located and tape measure placed evenly around the bare abdomen at the level of the hip bone and the readings recorded in centimeters.

Ethical Consideration: Approval for this study was granted by the ethical consideration committee at Mount Kenya University and the letter submitted to relevant authority at Thika Level 5 Hospital. Consent was sort from patients/guardians and confidentiality of patient observed.

Data Analysis: Data was collected from 201 individuals, entered in Microsoft Excel, exported to SPSS version 20, analyzed by SPSS and chi-square test and presented on tables, bar graphs and pie charts.

FBS level was used as the dependent variable and BMI, WC, Gender and Age as predictors. Descriptive statistics on predictor mean, and Standard deviations based on Gender was also sought.

Descriptive

Comparison of Variables Based on Gender

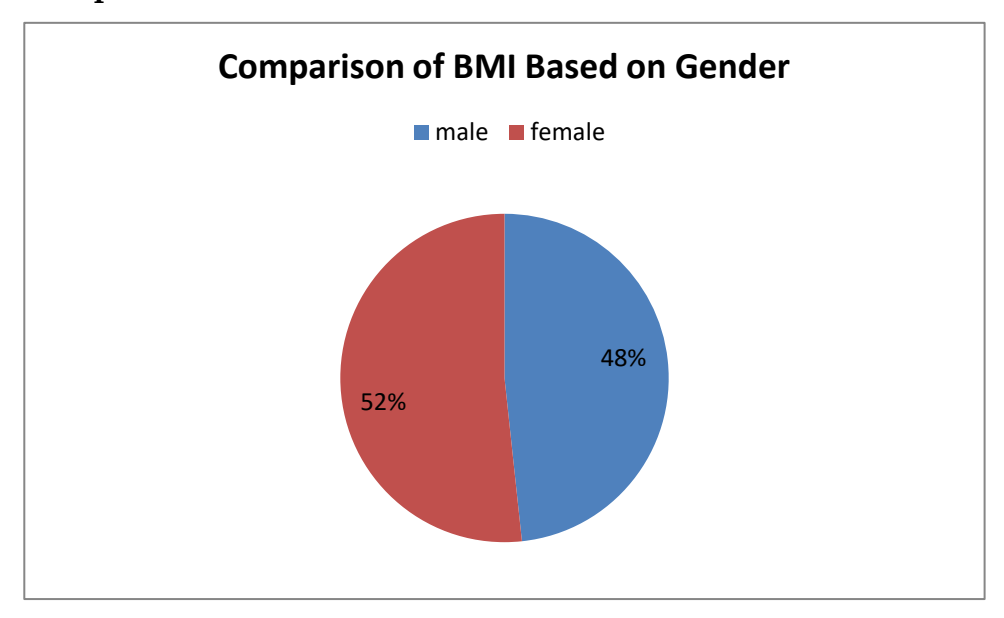


Figure 1: Comparison of BMI Based on Gender

The mean BMI of females was (27.29kg/m^2) while that of males was (25.50kg/m^2) .

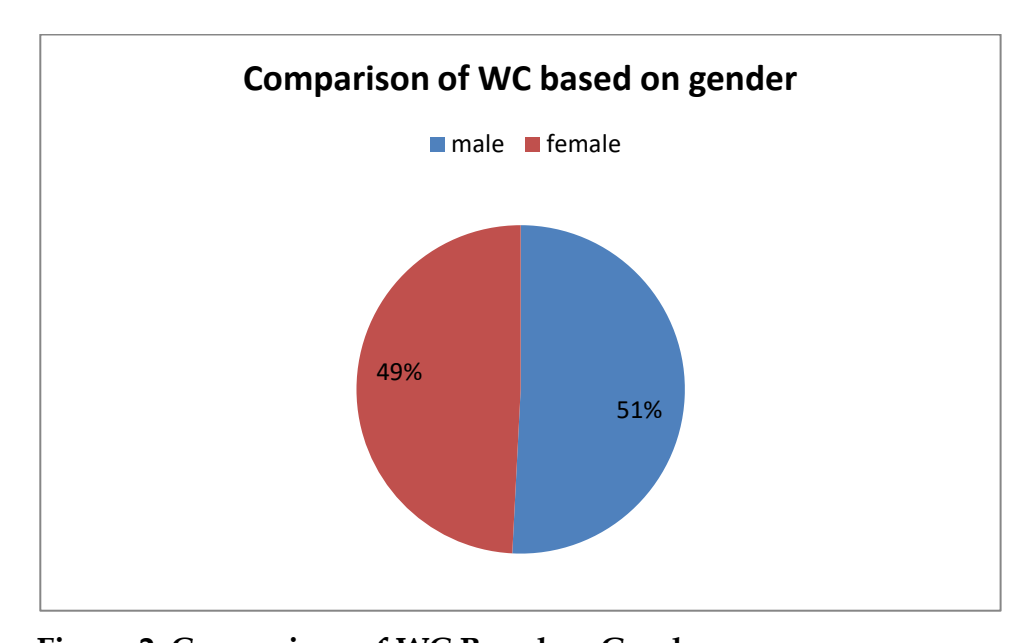


Figure 2: Comparison of WC Based on Gender.

The mean WC for males was 89.54 cm and that of females was 86.67cm.

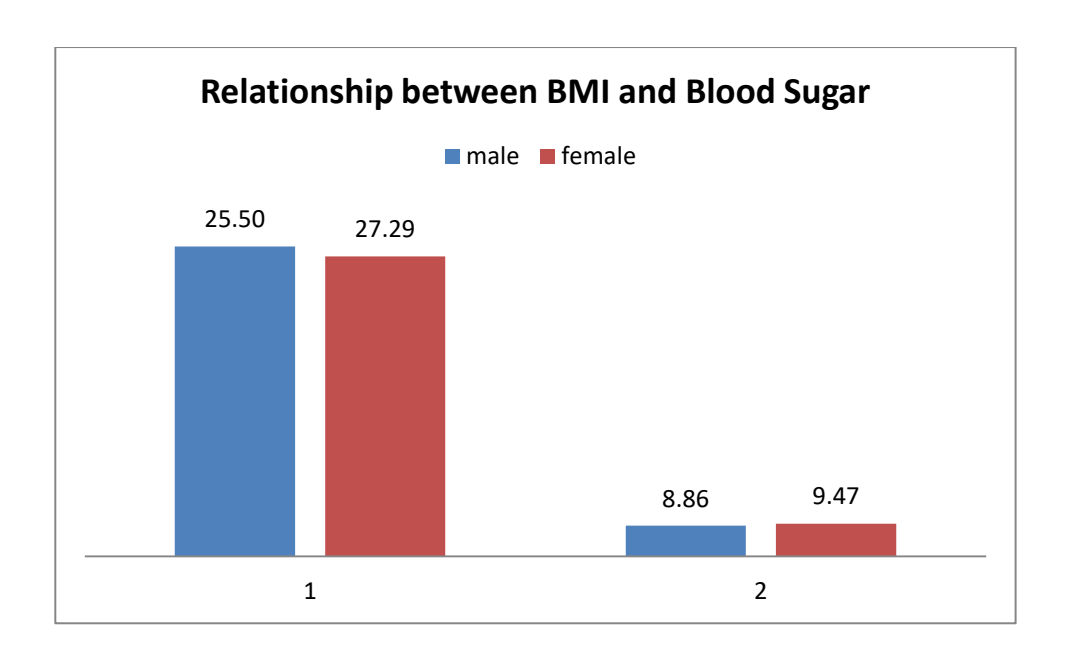


Figure 3: Relationship between BMI and Blood Sugar

The mean BMI of males was 25.5kg/m2 with a FBS of 8.86mmol/l while that of females was 27.29kg/m2 with a FBS of 9.47mmol/l.

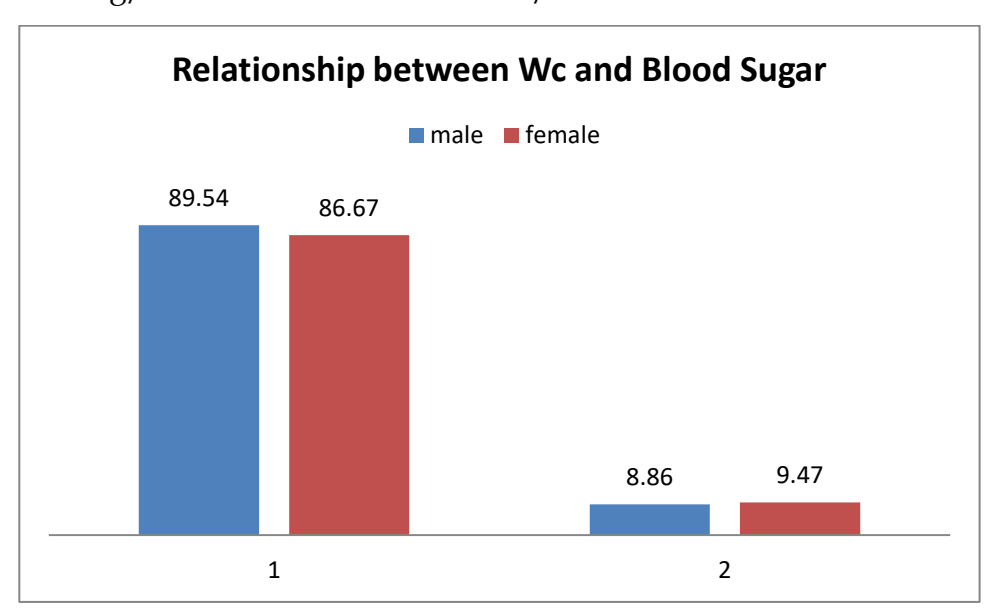


Figure 4: Relationship between WC and Blood Sugar

The mean WC for males was 89.54cm with a FBS of 8.86mmol/l while that of females was 86.67cm with a FBS of 9.47mmol/l.

Table 1: Comparison of Mean BMI of Both Genders within Various Age Groups

The table below shows the comparison between the mean BMI in kg/m2 between both genders distributed in the same age groups.

Age	Mean BMI of	Mean BMI of
Group(yrs)	Men(kg/m2)	Female(kg/m2)
40-45	25.25	27.6
46-51	25.65	27.32
52-57	25.82	27.35
58-63	24.73	26.63

Discussion

The purpose of this study was to establish whether there's a relationship between body mass indices, waist circumference and type II diabetes mellitus. This study aims to get the Descriptive Statistics, compare the means of stipulated variables with respect to gender. The purpose of this study was also to compare BMI and FBS against their respective reference values and come to a conclusion. The study relied on the independent samples student t-test to compare the means of the variables. Under the null hypothesis, the t-statistic has a student's T-distribution with n1 + n2 - 2 degrees of freedom.

Comparison of BMI and WC of People with Type II Diabetes Mellitus Based on Gender

From the results obtained it clearly indicates that the study sample subjects were all overweight having a BMI greater than 25kg/m2 compared to the non-diabetic control group according to WHO whose BMI was between 18.5 to 25kg/m2.WHO regards BMI of below 18.5kg/m2 as underweight and might attribute it to malnutrition while one of above 25kg/m2 is overweight.

The populations mean BMI of 26.7kg/m2 was just over the normal weight. From the crosstabs analysis, 41.3% had normal weight (18.5kg/m2 to 25kg/m2) of whom 26.9% were females and 14.4% males while 58.7% of the population was overweight (over 25) of whom 42.8% were females and 15.9% males. Comparison of the BMI based on gender showed no

significant difference statistically. There was that there's no strong evidence of gender associated difference in the mean BMI.

Comparison of WC based on gender also gave no significant difference statistically; the non –diabetic control sample as presented by WHO showed that males have WC of 102 cm while females 88cm, diabetic males and females had 89.54cm and 86.67cm respectively. Thus there was no strong evidence of gender associated difference in the mean WC.

Comparison of BMI, WC and Type II Diabetes Mellitus

Comparison of BMI and FBS showed that; both genders were overweight with increased FBS levels. According to WHO a non –diabetic individual has FBS level of less than 7.0 mmol/l. This result therefore shows a relationship between BMI and FBS.

Comparison of WC and FBS indicated that both males and females had normal WC of 89.54cm and 86.67cm respectively as compared to a control group which had 88cm for females and 102cm for males. The FBS were still high despite the normal WC results. Thus there was no relationship between the two variables.

Comparison of the BMI and WC within Various Age Groups of Diabetic Patients

Comparison of BMI for both genders within the various age groups indicated that, all age groups are equally overweight. Thus Age and WC are not, while BMI is a significant predictor of Type II Diabetes Mellitus.

Conclusion

Results of this study support the thesis that males and females had identical distributions patterns for type II diabetes mellitus. The mean BMI for the sampled population was 26.7. The crosstabs indicated that more than 58% of the population is in the range of overweight to obese and were therefore at risk of contracting type II diabetes mellitus. No underweights were recorded in the population.

Additionally, 70.1% of the population with 7.8mmol/1 FBS concentration were at a high risk of contracting type II Diabetes Mellitus.

Regression analysis indicated that BMI was a better prediction of Type II diabetes mellitus than age and WC since variation in BMI was highly associated with variation of blood sugar levels. Thus very high and low BMI impacted blood sugar levels adversely and can potentially cause type II diabetes mellitus. Age was found to be second in relative

importance to variations in blood sugar levels. The implication is that susceptibility to high blood sugar levels increased with increase in age.

Recommendations

- 1. There is need for stakeholders in the health sector to pursue further research to establish why the average FBS levels among patients in Thika Hospital level V are higher than the nationwide average.
- 2. Deliberate efforts should be made to educate the people on the need to avoid sedentary lifestyles and unhealthy feeding habits. A low carbohydrate diet plan for the age group would go a long way in combating this menace.
- 3. Efficient Insulin distribution and administering by the ministry to public hospitals be encouraged.
- 4. The government and stakeholders should embark on facilitation for the affected to attain improved individual care and metabolic control.
- 5. Further research should be carried out to assess the outcomes of the interventions.

References

American Dietetic Association(1997). Position of the American Dietetic Association: Weight Management, Pg 71 -74

David, W & Vincent, M. (1994). Scientific Foundations of Biochemistry in Clinical Practice, 2nded, Pg. 103-108

Harmon, J. S. (2006). Regulation of the insulin gene by glucose and fatty acids. *The Journal of nutrition*, 136(4), 873–876. https://doi.org/10.1093/jn/136.4.873

Hillary et al, (2004) Integrating Type 2 Diabetes Mellitus and Depression Treatment among African Americans. *Sage Journals*. https://doi.org/10.1177/0145721709356115

Lori, A.S & Mary, B. G. (2002). Nutrition; Science and Application, 3rded. Pgs 106-107, 210-213

Mc Kinley et al (2011). Diabetes and Hypertension: Evaluation and Management. *Humana press*.

Ministry of public health and sanitation (2010). Kenya National diabetes strategy 2010-2015.

Poitout, V., Hagman, D., Stein, R., Artner, I., Robertson, R. P., &

World Health Organization (2002). Inhibition of Protein Kinase C Beta Prevents Impaired E2ndothelium-Dependent Vasodilation caused by Hyperglycaemia in Humans. *Circulation Research* 90, 107–111

A Window-Based Approach to Training Deep Neural Networks for Predictive Sequence

Modeling

Kirori, Zachary & Wasike, Jotham

Kirinyaga University, Kenya

Correspondence: *zkirori@kyu.ac.ke*

Abstract

Deep machine learning potentially holds the key to unlocking the door to modern applied

computational intelligence. Presently, it is becoming progressively possible to process great

amounts of data whether static or arriving in streams of varying velocities using deep learning

models. Applications are innumerably many ranging from time series data modeling, signal

processing, image analysis, natural language processing to object recognition among others. The

critical area of predictive data modeling requires efficient and carefully selected algorithms and

models for effective and accurate predictions. In this paper, we present a novel deep machine

learning Neural Network for predictive tasks based on a fixed size window of time steps, tested on

a well-known dataset on customer arrivals to an airline. At the core of the architecture is a Multi-

Layer Perceptron – a classical deep learning Neural Network optimized on a number of dimensions

that include the training algorithm, batch size, number of iterations, and the loss function among

others. We present experimental results and conclude that, upon tuning and optimization, classical

deep learning neural networks such as the Multi -Layer Perceptron (MLP) have comparable

predictive abilities compared to advanced neural networks such as the Recurrent Neural Networks

(RNN) and Convolution Neural Network (CNN).

Keywords: Deep Learning, Predictive Sequence Modeling, Time Series Data Analysis,

Multi-Layer Perceptron, Deep Learning Optimization, Fixed Window Method

Introduction

The sub-field of Deep Machine Learning (DML) in the larger field of Artificial Intelligence

(AI) undoubtedly holds the key to solving some of the classical computational problems in

natural language understanding, image analysis, signal processing, computer vision,

navigation; tasks that traditionally have been considered difficult. It has been made

progressively possible to train larger and larger computational models within short times,

with ease and using minimal computational resources of memory and bandwidth (Bengio, 2012).

Rooted in computational statistics and relying heavily on the efficiency of numerical algorithms and Deep Neural Networks (DNNs), DML techniques capitalize on the world's increasingly powerful computing platforms and the availability of datasets of immense size to analyze and give solutions to problems where recommendation approaches fail (Schmidhuber, 2015; LeCun, et al, 2015).

DML is primarily an optimization procedure which, in this context, involves numerical computation of parameters for a system designed to make optimal decisions based on yet unseen data by choosing parameters that exhibit the best values with respect to a given learning problem. (Bergstra and Bengio Y., 2012; Bottou, et el, 2017; Vankadara, 2015)

Typically, these tasks are characterized by large amounts of training data, high dimensionality, ill-conditioning that require extensively many cycles of computing power (Chaudhuri & Ghosh, 2016).

Literature Review

Most work using ANN to manipulate Time-Series data focus on modeling and forecasting. This section reports on a selected number especially in regression modeling of time series data to rightfully place this work in context.

(a) Regression with Time Steps

Some sequence problems may have a varied number of time steps per sample. For example, we may have measurements of a physical machine leading up to a point of failure or a point of surge (Venkatraman, 2017; Patel, Chaudhary & Garg, 2016). Each incident would be a sample and the observations that lead up to the event would be the time steps, while the variables observed would be the features (Gamboa John. 2017).

Time steps provide one way to phrase time series problems. Instead of phrasing the past observations as separate input features, we can use them as time steps of the one input feature. This technique is especially required by most stateful Neural Networks such as the

Recurrent Neural Network (CNN), the Long Short Term Memory (LSTM) and the Gated Recurrent Unit (GRU) (Olof M., 2016).

(b) Regression with Memory between Batches

The stateful networks have memory, giving them ability to remember across long sequences. Typically, the state within the network is reset after each training batch when fitting the model, as well as during prediction and evaluation. This means that the network can build state over the entire training sequence and even maintain that state if needed to make predictions providing us with finer control over the internal state (Talagala, Hyndman & Athanasopoulos, 2018).

One of the requirements for this approach is that the training data should not be shuffled when fitting the network. It also requires explicit resetting of the network state after each exposure to the training data (epoch). Finally, when the network layer is constructed, the stateful parameter must be set true and instead of specifying the input dimensions, we must hard code the number of samples in a batch, number of time steps in a sample and number of features in a time step by setting the batch input shape parameter (Bao, et el, 2017).

(c) Window Method

In the window method, a time series problem is framed so that a selected number of recent time steps are used to make the prediction for the next time step. In this case the size of the window is a parameter that is often tuned for each problem (Busseti, Osband & Wong, 2012; Bontempi, 2013).

For instance, given the current time (t) we may desire to predict the value at the next time in the sequence i.e. (t + 1), by relying on the current time (t) as well as a selected number previous time steps, say (t-1, t-2, ...,t-N) for an N-size window. Phrased as a regression problem the input variables would be t-N,.., t-2, t-1, t and the output variable would be t+1. (Chaudhuri, Ghosh, 2016).

(d) Optimization for Regression Modeling

Optimization problems in machine learning arise through the definition of prediction and loss of functions that appear in measures of expected and empirical risk that one aims to minimize. There are two varieties of optimization problems that arise in machine learning: the first involves convex optimization problems, derived from use of logistic regression or support vector machines, while the second typically involves highly complex and problems with non-convex error functions, derived from use of deep neural networks. Deep Neural Networks are trained using the Back propagation especially the Back Propagation Through Time (BPTT) which is numerically formulated as a highly non-convex optimization problem in a very high dimensional feature space. Algorithm (Ngiam, Coates, Lahiri, Prochnow, Le Q., & Ng, 2011, Bottou, Curtis, & Nocedal, 2017).

However, the training process requires extreme skill and care. For instance, it is crucial to initialize the optimization process with a good starting point through parameter tuning and to monitor its progress while correcting conditioning issues as they appear (Bergstra. & Bengio, 2012). A great deal of these successes lie in the choice, regularization of the training algorithm as well as the domain of application.

Unfortunately, attempts to optimize these models such as increasing model size and training data - which is necessary for good prediction accuracy on complex tasks, requires significant amount of computing cycles proportional to the product of model size and training data volume. Due to the computational requirements of deep learning almost all deep models are trained on Graphic Processing Units (GPUs) (Nikhil₇ et el, 2016). According to Schmidhuber, (2015), the tremendous success of Deep Neural Networks (DNNs), in a wide range of practically relevant applications has triggered a race to build larger and larger DNNs (Simonyan & Zisserman, 2014), which need to be trained with more and more data, to solve learning problems in fast extending fields of applications.

Optimization methods for machine learning fall into two broad categories namely First Order (1st Order) and Second Order (2nd Order). Of the 1st Order methods, the stochastic and batch techniques are key. The prototypical stochastic optimization method is the Stochastic Gradient Method (SGD) where the target value is chosen randomly from a set of target values [1..N] in a positive step-size (Parker, 2012; Lee, et el, 2011; Josh, et al. 2016).

Each iteration of this method is thus very cheap, involving only the computation of the gradient corresponding to one sample. Similarly, due to the sum structure of the empirical risk, a batch method can easily benefit from parallelization since the bulk of the computation lies in evaluations of empirical risk and its gradient. Further, calculations of these quantities can even be done in a distributed manner.

Use of the Multi-Layer Perceptron

The experiments were conducted using a fully connected Multi Layer Percentron (MLP) of three (3) input layers optimized using dropout at each layer's input to improve the generalization capability and its potential non-linearity addressed by the rectified linear activation unit (ReLU). The latter has the effect of preventing saturation of the gradient when the network becomes very deep. (Raudys, Mockus, 1999) The last layer of the network uses a softmax function whose basic layer block is formalized as

$$x' = fdropout.p(x)$$

$$y = W.x'+b$$

$$h = ReLU(y)$$

ReLU helps to stack the networks deeper and dropout largely prevent the co-adaption of the neurons to help the model generalize well especially on some small datasets. However, if the network is too deep, most neuron will hibernate as the ReLU totally halve the negative part. The dropout rates at the input layer, hidden layers and the softmax layer were varied as {0.1, 0.2, 0.3}, respectively as seen in figure 1 below

Experiment & Results

In this section we present the experimental setup that includes the problem definition, the dataset, the DML platform of choice, the results as well as their comparative analysis.

(a) Problem Definition

The DML problem selected for this study is a typical regression scenario of time series data representing the number of airline passengers arriving at an international airport. This is a prediction problem where given a year and a month, the task is to predict the number of international airline passengers in units of 1,000 collected over a period of 144 months.

The time series prediction is phrased as a regression problem where given the number of passengers (in units of thousands) this month, last month and previous months, what is the number of passengers next month.

The initial pre-processing step is to convert the given dataset into the required window of several months in the past. For purposes of the experiment, a window of three (3) months was selected as it was found to optimize the results. In this regard, the first column contains two months' (t-3) passenger count before the current month. Subsequently, t-2, t-1 and t represent the remaining window period up to the present month. The next month's (t+1) passenger count, is the target prediction.

(b) Dataset

The dataset is available for free from the Data Market webpage as a .CSV downloadable file with the filename "international-airline-passengers.csv".

(c) Deep Learning Platform

the selected development platform consisted of a set of Python DML libraries and frameworks available for the experiment under the permissive MIT license namely: Keras and Tensor flow. Tensor flow is one of the two numerical backend platforms in Python that provide the basis for Deep Learning research and development.

Keras runs on Python 2.7 or 3.5 and can seamlessly execute on GPUs and CPUs based on available hardware the underlying frameworks.

Experiment

The time series problem was phrased as a regression problem with a window size of three (3) recent time steps that were used to make the prediction for the next time step given the

current time step. In this case the input variables are t-3, t-2, t-1, t and the output variable is t+1.

The code below was used import all of the functions and classes used to model this problem in the Science Python (SciPy) environment within the Keras deep learning library.

Multilayer Perceptron to Predict International Airline Passengers (t+1, given t, t-1, t-2)
import numpy
import matplotlib.pyplot as plt import matplotlib.pyplot as plt1
import matplotlib.pyplot as plt2 import matplotlib.pyplot as plt4
import pandas
import math
from keras.models import Sequential

from keras.layers import Dense #Default MLP Neural Network

With time series data, the sequence of values is important. The method that was used for purposes of stratified cross validation was to split the ordered dataset into train and test datasets. This was necessary in order get an idea of the skill of the model on new unseen data. The code below was used to calculate the index of the split point and separates the data into the training dataset with two thirds (2/3) or roughly 67% of the available observations used to train the model, leaving the remaining a third (1/3) or roughly 33% for testing the model.

```
# split into train and test sets size_Train = int(len(dataset) * 0.67) size_Test
= len(dataset) - size_Train
train_Set, test_Set = dataset[0:size_Train,:], dataset[size_Train:len(dataset),:]
```

Next a function to create a new dataset was defined in accordance with the window size as described above. The function takes two arguments, the dataset which is a Python Number array that we want to convert into a dataset and the look back which is the number of previous time steps to use as input variables to predict the next time period.

This has the role to create a dataset where X is the number of passengers at a given time (t) and Y is the number of passengers at the next time (t + 1). The value of the look back argument was set to three (3) to conform to the selected window size.

A sample of the dataset with this formulation looks as follows:

```
# convert an array of values into a dataset matrix
def create_dataset(dataset, look_back=1): inputX, OutputY = [], []
    for i in range(len(dataset)-look_back-1): a = dataset[i:(i+look_back), 0]
    inputX.append(a) OutputY.append(dataset[i + look_back, 0])
return numpy.array(inputX), numpy.array(OutputY)
```

This function was applied to reshape the datasets by overriding the default look back value with the window size as below.

```
# reshape dataset
look_back = 3
trainX, trainY = create_dataset(train_Set, look_back)
testX, testY = create_dataset(test_Set, look_back)
```

The effect of this function on the first few rows of the dataset are seen in table 1 below.

Table 1: Reshaped Dataset

S/N	Х3	X2	X1	Χ	Y
o					
1	112	118	132	129	121
2	118	132	129	121	135
3	132	129	121	135	148
4	129	121	135	148	148

Source: (Authors)

Comparing these first 4 rows to the original dataset sample listed in the previous section, the X=t and Y=t+1 pattern in the numbers is clearly visible.

The parameters that were found to optimize the network capacity are a hidden layer of 14 neurons, a second hidden layer of 8 neurons, 1 output layer of neurons, 300 epochs, a batch size of size 2.

```
# create and fit Multilayer Perceptron model
model = Sequential()
```

```
model.add(Dense(8, input_dim=look_back, activation='relu'))
model.add(Dense(1)) model.compile(loss='mean_squared_error', optimizer='adam')
model.fit(trainX, trainY, epochs=300, batch_size=2, verbose=2)
```

Once the model is fitted, the subsequent activity is to estimate its performance on the train and test datasets. The role of this is to provide a point of reference when comparing new models. The technique applied was the Mean Squared Error (MSE) and the Root Mean Squared Error (RMSE) as illustrated in the code below.

```
# Estimate model performance
```

```
trainScore = model.evaluate(trainX, trainY, verbose=0)

percTr = (1000.0-(math.sqrt(trainScore)))/10 print('Train Score: %.2f MSE (%.2f RMSE) Accuracy %.2f %%' % (trainScore, math.sqrt(trainScore), percTr))
```

Finally, predictions were generated using the model for both the train and test datasets to get a visual indication of the skill of the model. Once prepared, the results were plotted, showing the original dataset in figure 2, predictions on training and test sets in figure 3 and figure 4 respectively. Subsequently the combined data is shown in figure 5 below. The code that produces these statistical results is shown below

```
testScore = model.evaluate(testX, testY, verbose=0) percTs = (1000.0-
(math.sqrt(testScore)))/10 print('Test Score: %.2f MSE (%.2f RMSE) Accuracy %.2f %%'%(testScore, math.sqrt(testScore), percTs))
```

```
# generate predictions for training trainPredict = model.predict(trainX)
testPredict = model.predict(testX)
```

```
# shift train predictions for plotting trainPredictPlot =
numpy.empty_like(dataset) trainPredictPlot[:, :] = numpy.nan
trainPredictPlot[look_back:len(trainPredict)+look_b ack, :] = trainPredict
```

```
# shift test predictions for plotting testPredictPlot = numpy.empty_like(dataset)
testPredictPlot[:, :] = numpy.nan
testPredictPlot[len(trainPredict)+(look_back*2)+1:l en(dataset)-1, :] = testPredict
```

plot Combined Graphs

```
plt4.plot(dataset, color="green",
label="dataset") plt4.plot(trainPredictPlot, color="blue", label="train")
plt4.plot(testPredictPlot, label="test", color="red")
plt4.title("Combined Graphs", color="magenta") plt4.xlabel("months", color="blue")
plt4.ylabel("passengers in '000s",
color="green") plt4.legend()
plt4.show()
```

Results and Analysis

The extract of five rows of summary statistics based on the 300 epochs as well as the MSE and RMSE values are indicated below:

```
Epoch 296/300

92/92 [======- 0s 544us/step - loss:
500.0288 Epoch 297/300

92/92 [=====- 0s 544us/step - loss: 533.4240 Epoch 298/300

92/92 [====== 0s 544us/step - loss: 504.7706 Epoch 299/300

92/92 [====== 0s 489us/step - loss: 505.2075 Epoch 300/300

92/92 [====== 0s 544us/step - loss: 498.6430
```

Train Score: 487.92 MSE (22.09 RMSE) Acc: 97.79 % Test Score: 2135.39 MSE (46.21 RMSE) Acc: 95.38 %

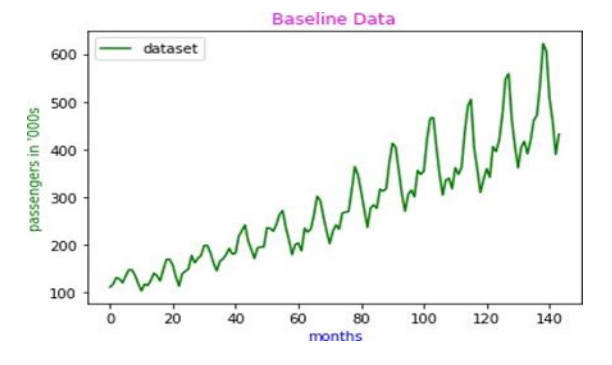


Figure 2: Baseline Data (Source: Author)

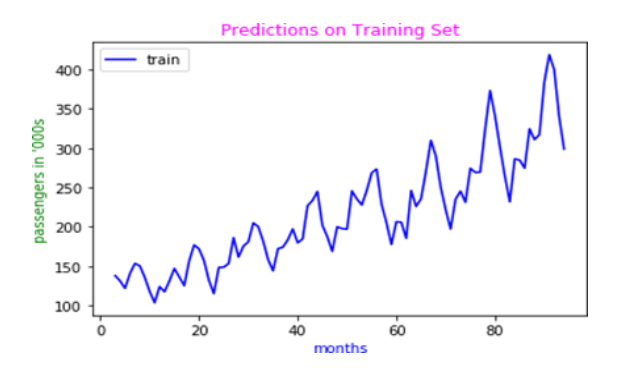


Figure 3: Training Set Predictions (Source: Author)

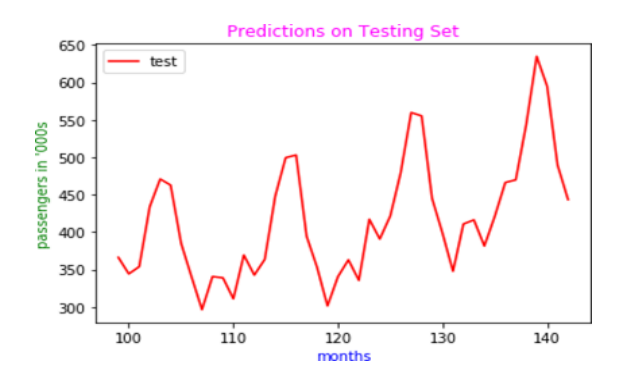


Figure 4: Testing Set Prediction (Source: Author)

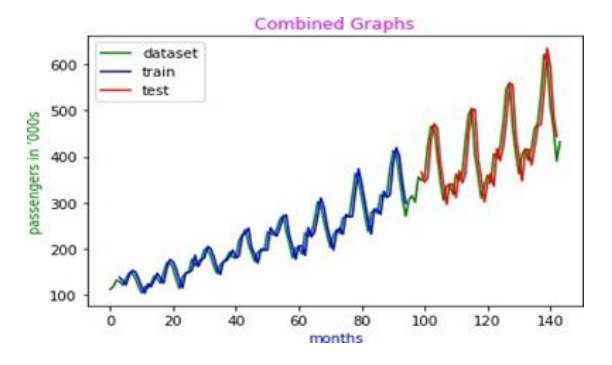


Figure 5: Combined Predictions (Source: Author)

Conclusion

In this research, the study has demonstrated the applicability of a typical neural network with parameter tuning to the problem of sequence data modeling. It is clear from the results above that it performs well on both the training and the testing datasets with minimal error rates. It is therefore imperative to conclude that basic neural networks such as MLP can perform equally as well as advanced neural networks such as RNNs, CNNs, Boltzman Machines among others with careful fine tuning, optimization, parameter search and pre- processing steps.

Recommendations

This study may be improved by 1) comparative analysis with other neural models 2) experimentation with different training algorithms beyond adaptive moment (ADAM) 3) automatic hyper-parameter search using grid search procedures 4) experimentation with different window sizes and 5) considering additional tests on varied time variant data sets.

References

Bao, W, Yue, J, & Rao, Y. (2017). A Deep Learning Framework for Financial Time Series Using Stacked Autoencoders and Long- Short Term Memory. *PLoS ONE* 12(7): e0180944. htts://doi.org/10.1371/journal.pone.0180944

Bengio, Y., (2012). Practical Recommendations for Gradient-Based Training of Deep Architectures, arXiv:1206.5533v2

Bergstra, J. & Bengio, Y. (2012). Random Search for Hyper- Parameter Optimization, *Journal of Machine Learning Research*, pp. 281-305

Bottou, L., Curtis, F. E., & Nocedal, J. (2017). Optimization Methods for Large-Scale Machine Learning, arXiv:1606.04838v2 [stat.ML]

Cristian, J & Gamboa, B.(2017). Deep Learning for Time-Series Analysis. ArXiv 2017

Lee, V. C., Ngiam, J., Coates, A. & Lahiri, A. (2011). On Optimization Methods for Deep Learning, In *Proceedings of the 28th International Conference on Machine Learning*, Bellevue, WA, USA.

Le, Q, Ngiam, J, Coates, A, Lahiri, A., Prochnow, B, & Ng A. (2011). On optimization methods for deep learning. ICML Conference. CVPR Conference

Minal, P, Sanjay, C, & Sanjay, G. (2016). Machine Learning Based Statistical Prediction Model for Improving Performance of Live Virtual Machine Migration. Hindawi Publishing Corporation. *Journal of Engineering*. Volume 2016. Available

at: https://doi.org/10.1155/2016/3061674

- Nikhil, J., Abhinav, B., Sam, W., Todd G., & Laxmikant, V. K., (2016). Evaluating HPC Networks via Simulation of Parallel Workloads
- Olof, M. (2016). C-RNN-GAN: Continuous Recurrent Neural Networks with Adversarial Training, Xiv:1611.09904v1[cs.AI]
- Parker, C., (2012). Unexpected Challenges in Large Scale Machine Learning, In the Proceedings of 1st International Workshop on Big Data, Streams and Heterogeneous Source Mining, Algorithms, Systems, Programming Models and Applications
- Patterson, J. & Gibson, A. (2016). Deep Learning: A Practitioner's Approach: Gravenstein Highway: O'Reilly Media
- Schmidhuber, J. (2015). Deep Learning in Neural Networks: An Overview, *Neural Networks*, Vol 61 pp. 85–117
- Simonyan, K. & Zisserman, A. (2014). Very Deep Convolutional Networks for Large-Scale Image Recognition. Arxiv Preprint Arxiv:1409.1556
- Thiyanga, S, Talagala, R. Hyndman J, & George, A. (2018). Meta-Learning How to Forecast Time Series. Working paper. Available at: http://business.monash.edu/econometrics-and-businessstatistics/research/publication
- Zhiguang, W, & Weizhong, Y. (2016). Time Series Classification from Scratch with Deep Neural Networks: A Strong Baseline.

Intelligent Decision Support (IDS) in Software Risk Management Based on Data Mining,

Rough Sets and Decision Theory

Mutheu, Rose and Wasike, Jotham

Kirinyaga University, Kenya.

Correspondence: rmunyao@kyu.ac.ke

Abstract

Risks are intrinsic to any project and risk-taking is a necessary component of any process of decision making. High risks from software projects threaten healthy development of any Nation because of the complex nature of projects. For sustainable development, we should focus on risk assessment and risk decision. Assessment of risks in most of the software projects has been done qualitatively ignoring the risk decision. Attempts at risk decisions have been based on individuals' rational opinions hence subjective. Previous reports have shown limited evidence on successful use of DSSs in practice. To address this anomaly, this study proposes intelligent decision support that provides more objective, repeatable, and observable decision – making support for software risk management. Software risk managers will be supported in gathering and analyzing evidence, identifying and diagnosing problems, proposing possible courses of action and evaluating such proposed actions. IDS is based on

data mining, rough sets and decision theories which improve decision making in uncertain conditions. Risks will be looked at as identifiable and quantifiable possible events or factors from which negative

or positive consequences may occur. The main sources of data will be a set of secondary data collected

over time and knowledge of domain expert (s). The techniques used in this paper will provide efficient

algorithms for finding hidden patterns in software risks and generate sets of decision rules to support

decisions in software risks management.

Keywords: Software Risks, Risk Decision-Making, Data Mining, Rough Set Theory, Decision

Theory, Intelligent Decision Support.

Introduction and Background

A software risk management study by Kumar & Yadar, 2015 showed that industry-wide, only 16.2% of software projects are on time and budget, 52.7% delivered with reduced functionality and 31.1% cancelled before completion. The main reason for this large amount of less quality software and failure of software projects is the lack of proper software risk management and decision making. Software projects management entails keeping a balance between requirements, expectations, perceptions, opportunities and risks (Cunha, et al, 2016).

Software products are flexible and uncertain hence general approaches of project management are not appropriately applicable. Thus, "The success of software projects depends on how the managers deal with the problem and make decisions", Cunha et' al 2016. According to the project management institute (PMI), poor decisions contribute to 47% of unsuccessful projects. Since decision making is a complex process which affects projects negatively if poorly done, there is dire need for researchers to establish support in decision making in project management. Such decision can be rational or otherwise, be based on explicit or tacit knowledge and beliefs and can yield optimal or less satisfactory solutions. Because software development lifecycle, generates of bulk streaming data which calls for application of big data analytics technologies in data collection and analysis, and many decisions have to be made concerning people, resources, processes, tools and techniques involved. These decisions can be less successful or otherwise subject to the various factors that affect the process.

Subjective analysis or expert judgment has been generally used in project risk management based on the experience of an expert which is not readily shared among different teams within an organization. It is thus critical to develop perfect modeling techniques that can provide more objective, repeatable, and observable decision – making support for risk management. This is achievable through use of an intelligent decision support system which should behave like a human consultant to support decision makers by gathering and analyzing evidence, identifying and diagnosing problems, proposing possible courses of action and evaluating proposed actions.

Decision making process is mainly geared at finding an optimal solution to a given problem by analyzing a finite set of alternatives, ranking these alternatives in terms of how attractive they are to the decision-maker and finding the best alternative for maximum expected utility. Since Artificial Intelligence has a greater computational information processing capacity and analytical approach, it plays a crucial role in extending humans' cognition when addressing complexity in organizational decision making. The aim of the Artificial Intelligence (AI) techniques embedded in an intelligent decision support system is to enable these tasks to be performed by a computer, while emulating human capabilities as closely as possible. Accuracy and consistency can be comparable to (or even exceed) that of human

experts when the decision parameters are well known. These techniques focus on enabling systems to respond to uncertainty in more flexible ways.

Problem Statement

The outcome of any project is greatly affected by the decisions made at any stage of the project. Since decision making is a complex process, researchers should establish support in decision making in software development projects. Most Decisions are made through subjective methods hence they are unreliable. It would benefit more with an objective, repeatable, and observable decision – making support for risk management. In other cases, there is lack of clarity on how teams make and evaluate decisions from software inception to product delivery and refinement. The team of software developers who may be colocated or dispersed members adopt a discussion based approach thereby lacking a structured way of decision-making. In such teams there is rare usage of dedicated software tools for decision-making. The decisions made are thus affected by groupthink and divergence.

Literature Review

This section seeks to summarize existing knowledge into coherent systems in order to give the new study direction and impetus. Any relevant theory to the area under study is considered. These theories could be from a single or multiple disciplines. This review is useful because it helps the researcher identify what is known about the research study and the type of knowledge available and helps establishing the theories that best guide the research work. This review determines if the research study is theory proven and how existing theories and findings are applicable in practice.

Risk Management in Software Projects

Risks are uncertain meaning that they may or may not occur. If they occur, they cause undesired outcomes thus affecting the success of the project. This therefore calls for continuous management of the risks. Risk Management depends on the perception and recognition of sources of risk in all phases of a project. Managing risk in multiple project environments is important to enrich and qualify the information for project manager's decision-making (Wanderley, etal, 2015). Risk management comprises identifying, analyzing, planning and controlling events that threaten project environment so as to

avoid or reduce the damage of these events should they occur. Risk Management, on its own does not guarantee the success of projects, but increase the probability of project success by ensuring deadlines are adhered to, the project is inside the planned budget and the project goals are met. Software Risk Management is a cyclical and continuous process which involves the following phases:

- a) Risk Management Plan. In this phase, decisions are made on how to plan the project's risk management activities, resource allocations, teamwork, and documentation standards.
- b) **Risk Identification.** In this phase, risks that might affect the project are determined and their characteristics documented. Many techniques to collect risk are employed.
- c) **Risk Analysis.** All project activities conditions are analyzed qualitatively to determine and prioritize their impact on project objectives. Quantitative Analysis is done involving determining the probability and risk sequences in order to estimate their impact on the project objectives.
- d) **Risk Response Plan.** Though Risks are always involved with loss, the possibility that the outcome of certain risks might be a gain is considered. This activity determines how to enhance opportunities and minimize loss.
- e) **Risk Monitoring.** This entails checking all risks identified and looking forward to new risks in the environment.
 - d) **Risk Control.** The effectiveness of risk response plans is executed and evaluated. The success in this phase calls for well-defined schedules.
 - e) **Risk Communication.** For successful accomplishment of risk management, there is need for communication.

Bayesian Network

This paper will treat risks in software development projects as conditional risks since they depend on other factors like schedule slips, cost overruns, project scope and software quality. The probability of risks in software development project is therefore a conditional probability. The conditional probability of an event B, in relation to event A, is the probability that event B will occur given the knowledge that an event A has already occurred. According to Bayes rule, $P(A/B) = \frac{P(B/A)P(B)}{P(A)}$

P ($A \mid B1...Bn$) has to be attached to each variable A with parents B1, ...,Bn. Conditional probability will thus determine the probability of a software project failing given the

evidence that there has been a risk (s) in the management of software project's time, cost, scope and quality. For this to be reliable, the causal relationship between software projects failure and the causal factors is established using Bayesian network.

P (SW project failure / Schedule slips, Budget overruns, poor scope, poor quality) is calculated by applying

Bayes' rule, which states that: P (SW project failure, Schedule slips, Budget overruns, poor scope, poor quality) = P (SW project failure / Schedule slips, Budget overruns, poor scope, poor quality) *P (Schedule slips, Budget overruns, poor scope, poor quality). This equation will further be simplified as: P (SW project failure, Schedule slips, Budget overruns, poor scope, poor quality) =P (SW project failure / Schedule slips, Budget overruns, poor scope, poor quality) *P (Schedule slips) *P (Budget overruns) *P (poor scope) *(poor quality).

Since the variables Schedule slips, Budget overruns, poor scope, poor quality are independent their prior probability is calculated from experiment and experience. The Bayesian Belief Network (BBN) is useful in representing and reasoning with uncertainties. The Bayesian networks (belief network, probabilistic network, causal network, and knowledge map) captures uncertain knowledge in a natural and efficient way in order to determine the causal factor that directly affects project outcomes by giving the correlations between risk factors and project outcomes. A BBN consists of two parts which include;1) Qualitative part which represents the relationships among variables by the way of a directed acyclic graph, and, 2) Quantitative part which specifies the probability distributions associated with every node of the model.

BBN handles the situations where some data entries are missing or unavailable and can be used to model causal relationships. The update is easy whenever new knowledge is available. BBN are based on a set of conditional probabilities, and as evidence becomes available the expected probabilities of disruption occurrence are updated. The interrelationship among risk events is made explicit, allowing the user to trace the propagation of risks from one event to the next and ultimately across life-cycle phases. The BBN approach has proven to be a powerful tool when uncertainty is an important factor and allows easy visualization of the network through its graphical nature. This makes it easy to localize a problem or identify vulnerable areas in the network. Though powerful, BBN-based risk analysis is limited by its inability to handle feedback relationships. Due to

linear propagation of conditional relationships in BBNs, the reinforcing and balancing feedback relationships may not be fully captured.

Decision Theory

Decision theory is a model designed to describe how individuals actually make decisions (behavioral decision theory) or how they should make decisions (normative decision theory). The normative decision theory begins with a set of mathematical axioms which formalize the logical and rational preferences. These Axioms classify accepted truths to ensure there is consistency and the chosen alternatives are independent of any other available alternatives. They capture the minimum requirements for rational decision making. Representation theorem allows the decision maker to quantify their preferences using utility function. The expected utility theory is prominent in making decisions under uncertainty. This is because such decisions based on expected utility theory are logical and self-consistent. However, they are not easily deployed in systems' engineering organization. Axioms are stated in terms of preferences in uncertain events. These axioms are stated below-:

- a) Completeness axiom; establishes that the decision maker can always decide between two alternatives otherwise the decision method suffer indeterminacy.
- b) Transitivity axiom; asserts that preferences must be linear. That is if A ➤ B and B ➤ C then A ➤ C
- c) Continuity axiom; implies that there are no infinite preferences
- d) Independence axiom; postulates that one alternative between two alternatives should not be impacted by availability of other alternatives

A rational decision maker should select the alternative with maximum expected utility where there are more than one options.

Big Data Analytics

Big data deals with huge data which are unstructured. Using analytics tools, it can be chunked down and analyzed to provide valuable solutions. Big data analytics is widely used in all areas which deal with analyzing data especially unstructured data. Analysis of such data are difficult and can be implemented by use of different platforms and tools. Big data analytics has wide applications in software project risk management and can be used to predict the risk encountered in software project and provide objective recommendation,

Usually Big data is referred to in terms of its V's characteristics which have evolved over time. To date there are 7 V's characteristics of big data namely Volume, Velocity, Variety, Veracity, Variability, Value and Visualization (Rekha & Parvathi, 2015). The volume is the measurement of the amount of data generated in a day, velocity the speed with which the data is generated, and variety the type of data generated which can be structured or unstructured data though big data deals with unstructured data mostly. Veracity of data provides accurate data for processing both quality and understandability while variability of data deals with different data types. Visualizations is the representation of data in so many variables and parameters that makes the findings clear. Value of the data is how meaningful the data is and plays a big role in big data analytics because according to big data evangelists, if you can't put meaningful of data you can hardly put a monetary value on big data. Figure 1 below shows the 7 V's characteristics of Big Data

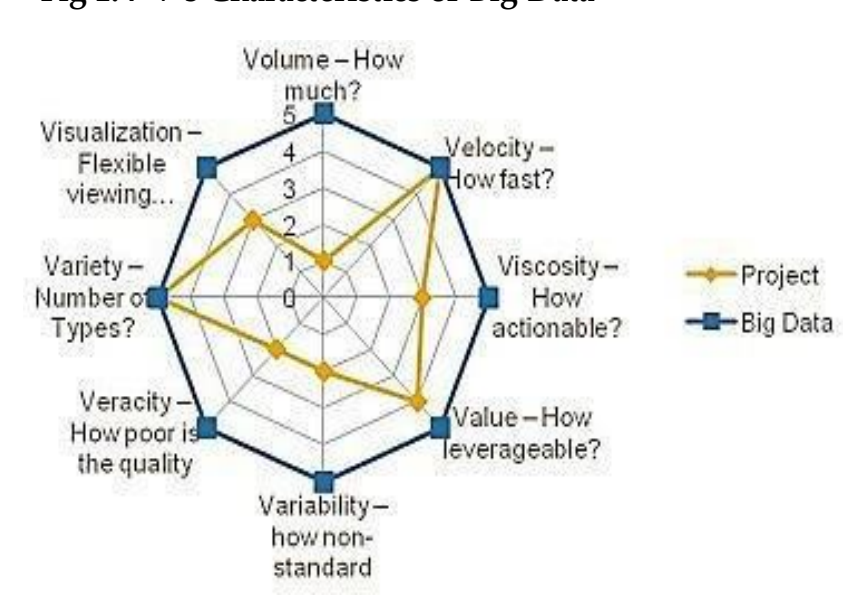


Fig 1: 7 V's Characteristics of Big Data

For Data mining to be highly effective, it should employ one or more of the data mining techniques which include the following

- i. **Tracking patterns;** This entails recognizing patterns in a data sets. Some deviations in the data which is happening at regular intervals or an instability of a certain variable over time are established.
- ii. **Classification;** This technique seeks to collect various attributes together into distinct categories, which you can be used to draw further conclusions, or serve some function.
- iii. **Association**; Association is related to tracking patterns, but is more specific to dependently linked variables. It entails looking for specific events or attributes that are highly correlated with another event or attribute.
- iv. **Outlier detection;** This helps to identify anomalies, or outliers in the data.
- v. **Clustering**; Clustering is similar to classification, but involves grouping chunks of data together based on extent of their similarities.
- vi. **Regression;** Regression is used as a form of planning and modeling to identify the likelihood of a certain variable, given the presence of other variables. Regression focuses on helping uncover the exact relationship between two (or more) variables in a given data set.
- vii. **Prediction**; Prediction is one of the most valuable data mining techniques. It's used to project the types of data you'll see in the future. In many cases, just recognizing and understanding historical trends is enough to chart a somewhat accurate prediction of what will happen in the future.

Research Methodology

The study was exploratory based on the objectives of the study. According to Kothari (2004) Exploratory Study mainly seeks to formulate a problem for more precise investigation or for developing the working hypotheses from an operational point of view. The study will emphasize on the discovery of ideas and insights.

This study is applied research based on the application of the study, designed to solve practical problems of the modern world, rather than to acquire knowledge for knowledge's sake. The goal of the applied study is to improve the human condition Kothari (2004) Considering the type of Information sought, this is a Quantitative Research involving quantitative generation of data and analysis of the data.

This study was based on Secondary data whose sources included the following

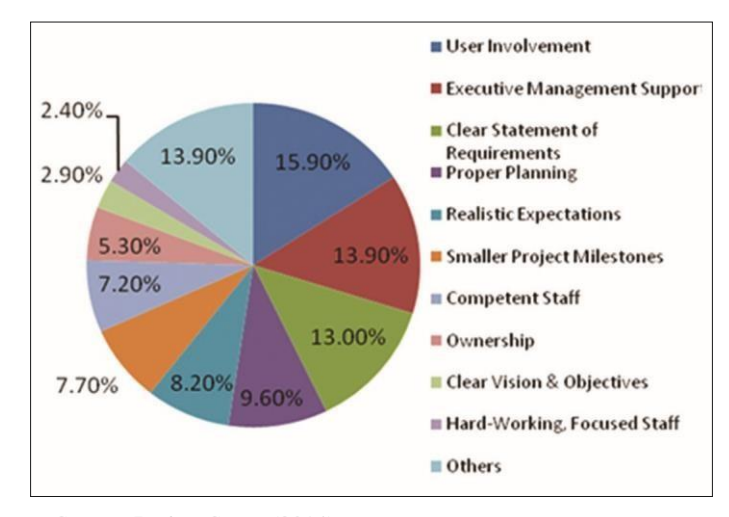
- i) Open source software companies and communities
- ii) Survey of related literature in scientific publication for software development
- iii) Experience survey of domain experts
- iv) Analysis of Case Studies in Large software development

Data Processing and Analysis

Software projects fail when they do not meet the criteria for success. Most of the IT projects run over budget or are terminated prematurely and those that reach completion often fall far short of meeting user expectations and business performance goals (Kaur et al, 2011). The three major key factor of project success are delivered on time, on or under budget, the system works as needed. However, the ability of the system to meet the user requirements is the basis for the success of software projects since success or failure of the project depends on how the software requirements process was carried out. The cost or the risks involved in a poorly engineered requirements process are great and sometimes irreparable (Hussain et al , 2016)

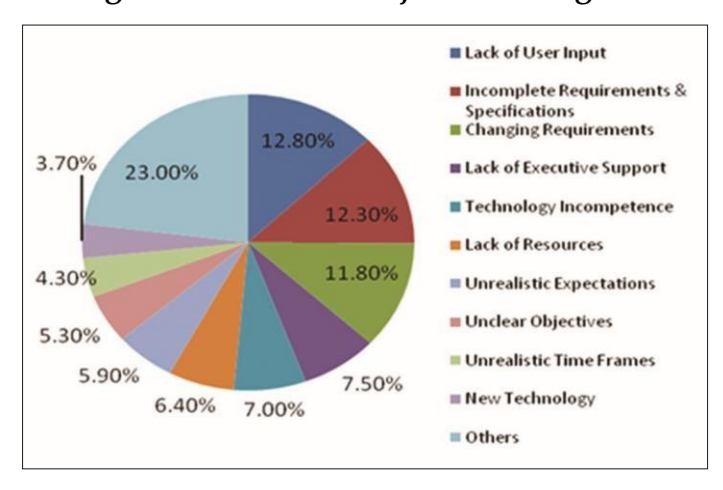
Statistics of why projects are impaired and ultimately cancelled shows that incomplete requirements and lack of user involvement contribute more (Project Smart, 2014) as illustrated in figures 2-4 below.

Figure 2: Software Project Success Factors



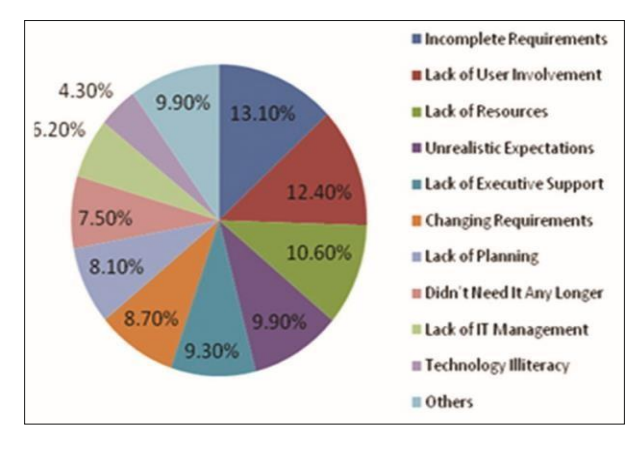
Source: Project Smart (2014)

Figure 3: Software Project Challenge factors



Source: Project Smart (2014)

Figure 4: Software Project Failure Factors



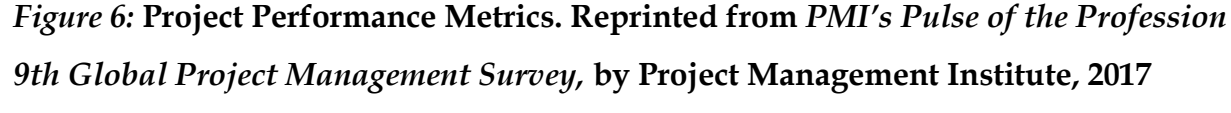
Source: Project Smart (2014)

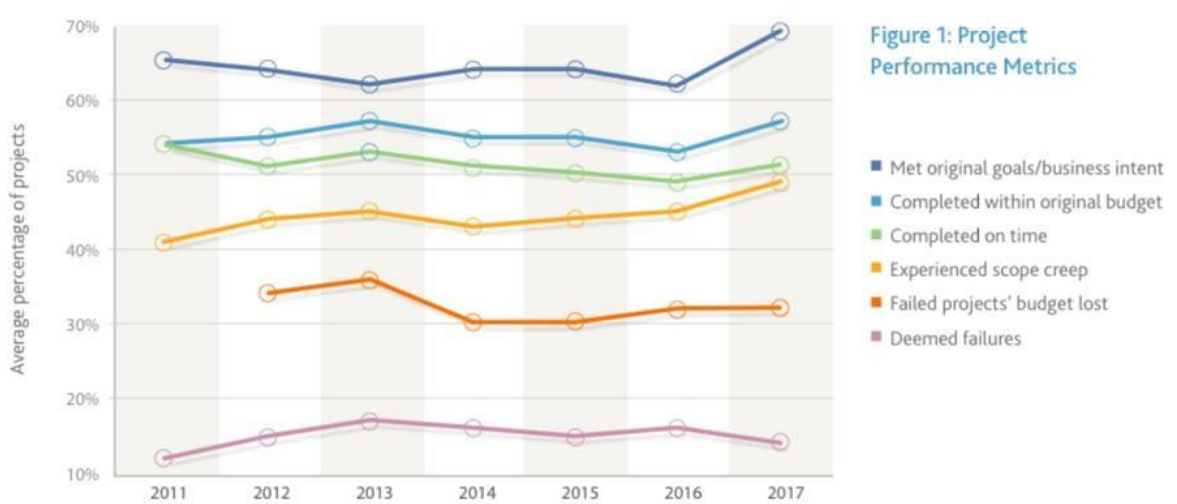
The 2018 Project Success Survey carried out by PwC Belgium ("Project Success Survey 2018 Driving project success in Belgium," 2018) shows that there are Twelve Elements of Project Success.



Figure 5: ("Project Success Survey 2018 Driving Project Success in Belgium," 2018)

The chart below shows the project performance metrics between 2011 and 2017 as per a survey carried out by the PMI in 2017.





The CHAOS Report by The Standish Group, 2015 from the software development industry, confirm that a larger project is harder to complete successfully than a smaller project. This is because larger projects have more resources and broader scope hence increased.

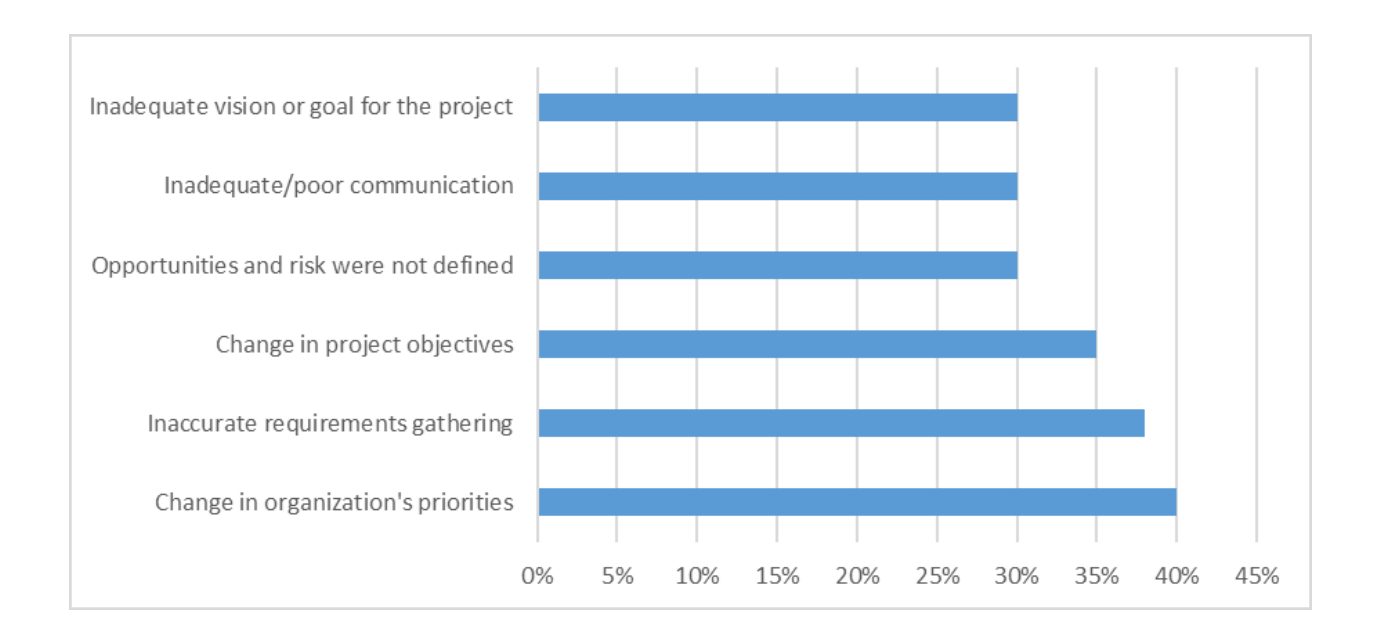
Table 1: Agile Vs. Waterfall. Adapted from 2015 Chaos Report, By The Standish Group, 2015

SIZE	METHOD	SUCCESSFUL	CHALLENGED	FAILED
All Size	Agile	39%	52%	9%
All Size	Waterfall	11%	60%	29%
Large Size	Agile	18%	59%	23%
Projects	Waterfall	3%	55%	42%
Medium Size	Agile	27%	62%	11%
Projects	Waterfall	7%	68%	25%
Small Size	Agile	58%	38%	4%
Projects	Waterfall	44%	45%	11%

Task complexity and durations (Rosato, 2018).

PMI Survey results in the annual "Pulse of the Profession" 2018 report shows the top six reasons why project fail as deduced from the response of 3,000 different individuals in various industries.

Figure 8: Reprinted from PMI's Pulse of the Profession 9th Global Project Management Survey, by Project Management Institute, 2017.



Conclusion and Recommendations

This paper points out that risks are inevitable in all software development projects hence risk management and decision making is vital. The review of existing literature establishes that risk assessment has been done qualitatively hence it is subjective. The paper points out that a more objective, repeatable, and observable risk assessment and decision-making support for risk management is necessary. Quantitative risk assessment analyzes the effect of those risk events by assigning a numerical rating to the risks. Decisions are based on established rules and utility function. Bayesian belief network (BBN) determines the causal factor that directly affect project outcomes by giving the correlations between risk factors and project outcomes. Normative Decision Theory model describes how individuals should make decisions. Expected utility theory optimizes decisions making under uncertainty. The rough set theory provides efficient algorithms for finding hidden patterns in data and generate sets of decision rules from data. Decision rules derived from a decision table links conditions to particular actions, preferences or decisions. Decision networks which is an extension of a Bayesian networks represents a decision problem. Evaluation of the decision networks based on an algorithm returns the action with the highest utility.

References

Chaos Manifesto (2013). Chaos Manifesto, Act Small. *Chaos Manifesto*, 2,52. Retrieved From Http://Www.Versionone.Com/Assets/Img/Files/Chaosmanifesto 2013.Pdf

Cunha, J. A. O. G., Da Silva, F. Q. B., De Moura, H. P., & Vasconcellos, F. J. S. (2016). Decision-Making In Software Project Management. In *Proceedings Of The 9th International Workshop On Cooperative And Human Aspects Of Software Engineering - CHASE '16* (Pp. 26–32). New York, New York, USA: ACM Press. Https://Doi.Org/10.1145/2897586.2897598

Hussain, A., Mkpojiogu, E. O. C., & Kamal, F. M. (2016). International Review of Management and Marketing the Role of Requirements in the Success or Failure of Software Projects. *International Review of Management and Marketing*, 6(S7), 11–13. Retrieved From Http:Www.Econjournals.Com

Kaur, R., & Sengupta, J. Ork (2011). Software Process Models and Analysis on Failure of Software Development Projects. *International Journal of Scientific & Engineering Research*, 2(2), 1–4. Retrieved From Http://Arxiv.Org/Abs/1306.1068

Kothari, C.R. (2004) Research Methodology: Methods and Techniques. 2nd Edition, *New Age International Publishers, New Delhi*.

Kumar, C., & Yadav, D. K. (2015). A Probabilistic Software Risk Assessment and Estimation Model for Software Projects. *Procedia* Computer Science, 54, 353–361. Https://Doi.Org/10.1016/J.Procs.2015.06.041

PMI (2016). The High Cost of Low Performance. Pulse of the Profession (Pp. 1–20).

Project Smart (2014) . Exploring trends and developments in project management today https://www.projectsmart.co.uk/why-software-projects-fail.php

Project Success Survey (2018) Driving project success in Belgium, 2018 www.ambysoft.com/surveys/success2018.html

Rekha, J. H., & Parvathi, R. (2015). Survey on Software Project Risks and Big Data Analytics. *Procedia Computer Science*, *50*, 295–300. Https://Doi.Org/10.1016/J.Procs.2015.04.045

Rosato, M. (2018). Go Small for Project Success 1, VII(V), 1–10.

Wanderley, M., Menezes, J., Gusmão, C., & Lima, F. (2015). Proposal of Risk Management Metrics for Multiple Project Software Development. *Procedia Computer Science*, 64, 1001–1009. Https://Doi.Org/10.1016/J.Procs.2015.08.619.

Effect of the Graphite Dispersed Titanium Dioxide Solid Solar Cell Composition on the Generated Potential ($V_{\rm OC}$)

Kimemia, D. Njoroge¹, Njoroge, K. Walter², Mwangi, W. Isaac²

¹Murang`a University of Technology; ²Kenyatta University, Kenya

Correspondence: kimemianjoroge@gmail.com

Abstract

Energy is globally recognized as one of the most fundamental inputs for social and economic development. Most energy sources are serious environmental pollutants. To overcome this challenge, presence of abundant sunshine was exploited through use of photovoltaic cells. However most photovoltaic cells are silicon based hence expensive. This study reports on the fabrication of a cost effective and environment friendly solar cell by use of TiO_2 and I_2 / KI (dispersed in graphite-Cx) layers in their solid form to provide an alternative source of clean energy. TiO_2 has a high photo generation ability when excited with radiation and is chemically inert over a wide pH range. The photo generated electrons were replenished by iodine complex and graphite facilitated their migration. The mixtures at varying ratios were made into pellets and their electrical properties investigated. The optimum electricity generation was observed at the ratio of TiO_2 / C_x : I_2 : KI as 0.4: 0.3: 0.17: 0.01 g respectively. The optimal thicknesses of the photo active layer and that of the electronegative layer were found to be 2.00 and 1.00 mm respectively. An open circuit voltage (Voc) of 0.979V and a short circuit current density (I_1) of 12.037 I_2 A was observed, giving efficiency (I_1) of 0.006% and a Fill factor (I_1) of 0.64. The cell did not suffer from corrosion effects as it was used in a dry solid state making it suitable for photovoltaic application.

Keywords: Graphite Dispersed Titanium Dioxide, Solid Solar Cell Composition, Generated Potential.

Introduction

Energy is recognized universally as one of the most fundamental inputs for social and economic development. Modern consumption patterns and energy production contribute significantly to climate change and air pollution. Substantive emissions reductions over the next few decades can reduce climate risks in the 21st century and increase prospects for effective adaptation, reduce the costs and challenges of mitigation in the longer term for sustainable development and reduced threats to human and environmental health across the world (IPCC, 2014). In the recent past, use of renewable energy as an alternative source of energy has increased considerably. The feasibility of photovoltaic solar energy as an

alternative source of energy has become real. However, solar PV systems are still compounded with low efficiencies and their dependency on weather conditions still offer room for improvement of the technology to extract higher outputs for different environmental conditions. Therefore, the current study proposes a low cost method of fabricating a renewable source of energy void of greenhouse gas emissions.

Air pollution and climate change influence each other through complex interactions in the atmosphere. High levels of GHGs alter the energy balance between the atmosphere and the Earth's surface, which lead to temperature changes that change the chemical composition of the atmosphere. These changes in temperature result in reduced water reservoir on the earth surface which in turn leads to reduced amount of hydro electric energy generated. There are technological solutions which address concerns of switching off from fossil fuels to renewable forms of energy that cuts down on air pollution emissions (Monasterolo & Raberto, 2018). This study sought to develop a photo cell which will reduce use of fossil fuels and in turn reduce on air pollution and climate change.

Literature Review

Titanium dioxide is a non-toxic inorganic chemical of industrial importance widely used aswhite pigments because of its brightness and high refractive index (Wang et al., 2017). Sellappan (2013) noted that TiO₂ generate electrons and holes when illuminated with UV radiation of wavelength domain 10nm to 400nm. Similar observations have been reported by Liu et al. (2018). A study by Hecht (2018) reported that with a suitable conductor, the discharged electrons have the ability to migrate in a specified direction leading to some conductivity. The conductivity can be improved by adding (doping) traces of elements that effectively add or remove electrons from the light illuminated titanium dioxide (Adler, 2011). This photo activity of TiO₂ makes it a preferred semiconductor material which is stable and chemically inert over a wide pH range under irradiation, and its relatively favourable deposition of band edges (Wang et al.,2017). Hebling (2010) reported that titanium dioxide has been utilized in photo cells in a wet chemical process. However, that application is associated with a lot of corrosion.

Similar studies used transparent single crystals or thin films which have a high refractive index as a conductor in contact with the TiO_2 material in multi-layers composition to monitor optical and electrical characteristics of the resulting cell (Colin, 2011). Other applications of the electron hole splitting enabled by TiO_2 are widely used for photo

catalysis such as water treatment by oxidation (Kanakaraju, et al, 2014). The TiO₂ photo active material used in electro chromic devices and dye-sensitized solar cells show promising results but it is affected by corrosion (Caitian *et al.*, 2014). Since exposure of TiO₂ to solar radiation generates electricity, this study explored options of developing a solar cell using this material. The solar cell fabricated was based on the use of TiO₂ in its solid form and graphite (C_X) which was used as a medium of electron migration. This was done by fabricating layer structured cells with external conductors which enables electrons to migrate and fill the deficient holes that exist upon illumination. The fabricated involved two layered solar cell of TiO₂ and I₂/ KI dispersed in graphite.

TiO₂ particles have nanocrystalline electronic junctions network, which are interconnected to allow for electronic conduction to take place and they present comparable band gap values and conduction band position as well as higher electron mobility (Chergui *et al.*, 2011). Tse et *al.* (2018) reported thatTiO₂ has a higher dielectric constant which provides effective capacitance that can be obtained with thicker layers of other materials and therefore used to provide high dielectric constant for storage of potential. According to Hussein *et al.* (2018),TiO₂ has been used as passivation layers on other cells and as photo-anode in solar cells in its solid state. When the energy band gap of TiO₂ particles are reduced, lower energy photons are absorbed by the TiO₂ catalyst and the photo activity of the catalyst are increased proportionally to the increase in the absorbed solar radiation (Ola & Maroto-valer, 2015).

Statement of the Problem

Hydro-electric source of lighting have been affected by the changing weather patterns resulting to reduced precipitation hence diminishing water levels due to global warming. This has reduced the amount of electricity generated. The use of fossil fuel has contributed to pollution of environment which has disastrous health effects (Perera, 2018). Domestic lighting is essential in many homesteads particularly in rural Kenya as most of them are not connected to the national grid (Ahmad &Mohammad, 2010). Their source of lighting comprises ordinary tin lamps to other form of lamps that use paraffin. Upon combustion of that fuel, toxic fumes result to respiratory ailments. That being the case, alternative sources of energy is required and solar power offers such alternative. The use of doped titanium dioxide activated by ordinary radiation and graphite as the conduit for the migration of electrons are suitable materials for making a solar cell (Ahmad &Mohammad, 2010). Due to the rising cost of energy, alternative options of generation of electricity necessitated this

study to be carried out. The study at hand endeavoured to fabricate a solid solar cell using titanium dioxide (TiO_2), and iodine (I_2) with potassium iodide (KI/I_2) dispersed in graphite (C_X) for solar cell application. This was intended to be an alternative green source of energy which is renewable and not easily degraded.

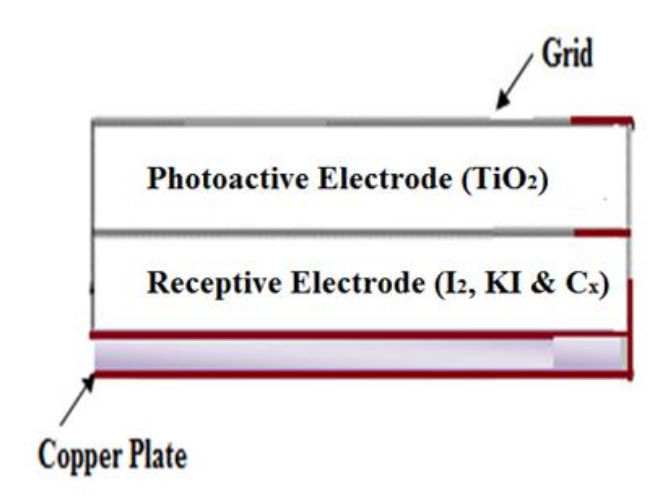
Materials and Methods

The study adopted an experimental research design to investigate the performance of the fabricated solar cell. It was done by first obtaining the optimal values of the parameters under investigation. The best parameters were obtained by establishing the optimal values of each material constituent of the cell. These were TiO₂, which was the photoactive material, the graphite which was the conducting medium and the Iodine/Iodide mixture which replenished the electrons conducted away after photo excitation. This process employed varying the weights of the component parts, and finally characterization of the fabricated solar cells under constant radiation intensity in clear day light.

The following assumptions were made; that solar radiation was constant at 100 mW/cm² irradiance (Hagfeldt *et al.*, 2010); the solar density on the solar cell was assumed to be uniform, and the voltage drop in the digital meter leads was assumed to be negligible. All reagents were of analytical grade and were sourced from Sigma Aldrich. The titanium dioxide (TiO₂), iodine (I₂), potassium iodide (KI) and graphite (C_X) in their powder form were used.

To fabricate the solar cell, different mass ratios of graphite (C_X) powder, titanium dioxide (TiO_2) powder, potassium iodide (KI) and iodine (I_2) were mixed and compressed to form a Solar Cell. Figure 1 below shows the schematic presentation of the fabricated cell.

Figure 1: Schematic Presentation of the Fabricated Solar Cell.



To provide the required dimensions, a copper plate was cut into 2.5 cm by 2.5 cm by the use of metal plate shears. An active cell of \emptyset 1.3 cm (A=1.327 cm²) was prepared, laid on the copper plate and covered with a transparent raisin as a copper conductor in contact with the upper electrode was drawn through the raisin for external connection.

The first cell electrode was made by placing the photo active measured sample separately in a circular dice and compressed thoroughly. The second electrode was made by disposing the mixtures of mass ratios of (graphite: iodine: I₂/KI) over the initial layer and the pressing procedure followed. The resultanting circular pellet served as the photo active cell. I-V characteristics of each of the resulting cells were monitored. The photo active (cathode) was prepared by varying masses of powdered TiO₂ ranging from (0.2-1) g. These masses were inserted in a molding dice and pressed into a disc form with a diameter of 1.3 cm to form a circular pellet.

The receptive layer (anode) was prepared by varying masses of finely divided mixtures of mass ratios (graphite: I₂: I₂/KI) ranging from (0.1: 0.1: 0.01) g to (0.6: 0.3: 0.01) g. These mixtures of mass ratios were then inserted in a molding dice and pressed into a disc form with a diameter of 1.3 cm to form a circular pellet similar in size to the photoactive layer. The receptive layer (anode) was then placed on the photo active (cathode) and pressed further to form a complete assembly of the solar cell. External conductors were then connected to the cell for I-V characterization. Figure 2 shows the schematic cell presentation of the solar cell.

Figure 2: Photo Voltaic Cell Scheme

The optimum I-V characteristics were established using the circuit diagram of Figure 3.

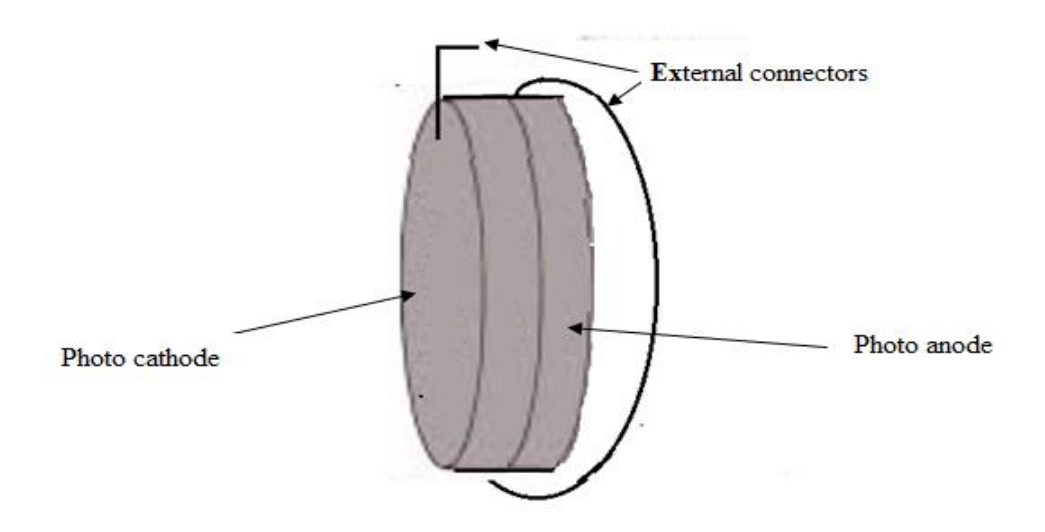
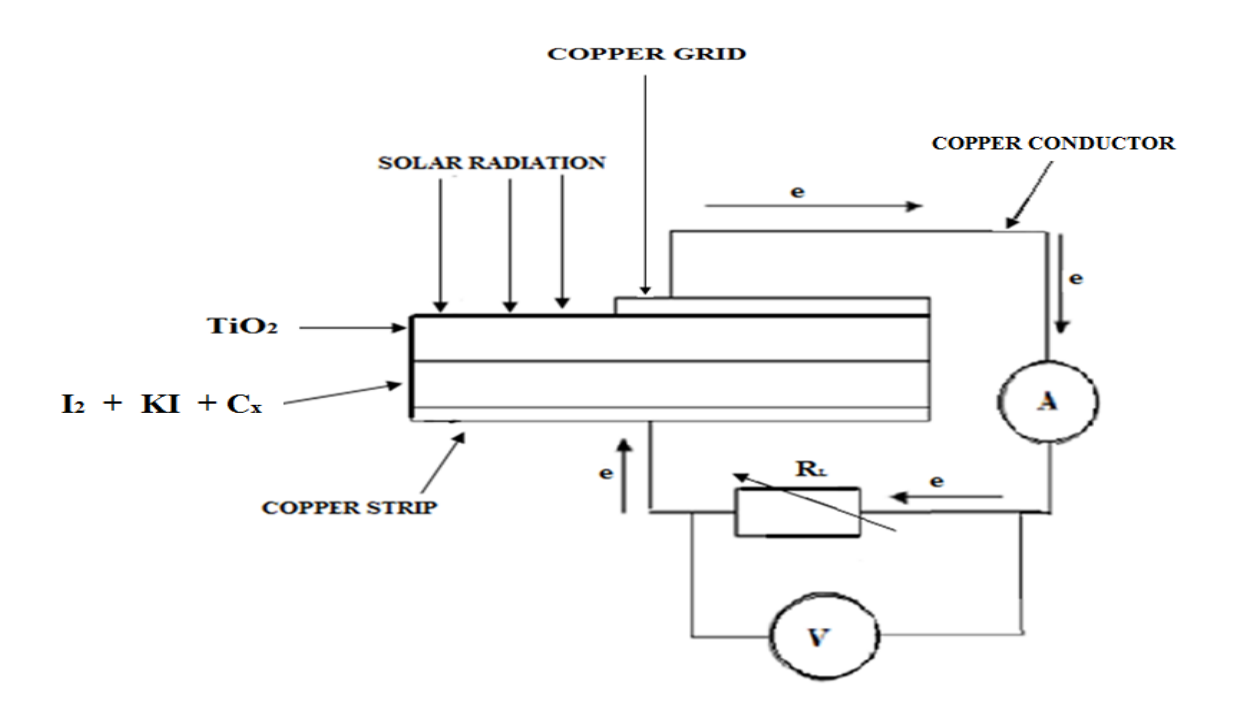


Figure 3: Assembly of the Circuit Diagram for the I-V Characterization



A high resolution micro-Ammeter (0 - 100 μ A) was connected in series with the fabricated Solar cell to measure the current density output (J_{MP}) resulting from the generated charge carriers which migrated from the photo active cathode layer of the cell through external conductors and back to the cell through the anode. A high resolution galvanometer (0 -250 mV) was connected in parallel with the arrangement of the \varnothing 1.3 cm (A=1.327 cm²) active

solar cell and the micro-Ammeter (0 - 100 μA) to measure the resulting open circuit voltage (V_{OC}) at the output terminals.

A high resolution graduated variable resistor (Ohmmeter) (0 -34 Ω) was connected in series with the micro-Ammeter (μ A) and in parallel with the galvanometer (0 - 250 mV). The variable resistor served the purpose of an external load and the ratio of the generated potential (V_{MP})to the measured resistance at any particular instant, confirmed the amount of the current density (J_{MP}) through the external circuit and this was recorded to determine the maximum power (P_{MAX}) of the solar cell. The short circuit current density (J_{SC}/cm^2) values were determined at zero applied voltage and the open circuit voltage (V_{OC}) values were determined at zero current under solar radiation. The current generated against their corresponding potential for various cells were collected and tabulated. The voltage output for maximum power output (P_{MAX}) were taken at 5 minutes intervals and tabulated for analysis.

The fabricated solar cell parameters were calculated using equations as applied by Adegbenro, (2016) while calculating parameters of different shapes and states of solar cells. In his study, the cells were in 1cm^2 squared blocks while the cell in this study had a diameter of (\emptyset) 1.3 cm giving an area (A) of 1.327 cm²;

$$V_{MP} = \frac{V_{MAX}}{A} (mV cm^{-2})$$
 (1)

$$J_{MP} = \frac{I_{MAX}}{\Delta} (\mu A cm^{-2})$$
 (2)

$$P_{MAX} = V_{MP} \times J_{MAX} \tag{3}$$

$$J_{SC} = \frac{I_{SC}}{A} (\mu A cm^{-2})$$
 (4)

$$V_{\rm OC}/cm^2 = \frac{V_{\rm OC}}{A} (mV/cm^2)$$
 (5)

$$P_{T} = V_{OC}/cm^{2} \times J_{SC}/cm^{2}$$
(6)

$$Fill Factor(FF) = \frac{J_{MP} V_{MP}}{J_{SC} V_{OC}}$$
 (7)

Shunt Resistance(R_{SH}) =
$$\frac{\Delta Y}{\Delta X}$$
 (8)

Series Resistance (R_S) =
$$\frac{\Delta X}{\Delta Y}$$
 (9)

Efficiency
$$\eta = \frac{J_{SC} \times FF \times V_{OC}}{p_{in} \times A}$$
(10)

'A' is the photoactive area of the cell; $A= 1.327 \text{ cm}^2$

In the study at hand, the parameters were obtained by adopting expression 1-10 as applied by Adegbenro (2016) when he characterized different shapes and states of solar cells to obtain their parameter values.

Nikhil (2013) defined the open circuit voltage (V_{OC}) as the voltage delivered by the solar cell when the electrodes are isolated and no current is sourced under infinite load resistance. This voltage represents the maximum potential energy stored to initiate the flow of electrons which are yet to be dissipated. Nikhil (2013) further noted that the voltage of a unit area (V_{OC}/cm^2) delivered by a solar cell when the electrodes are isolated represents the maximum potential energy stored to initiate the flow of electrons which are yet to be dissipated.

Results and Discussion

Effect of Varying Iodine-Iodide Complex on (Voc)

Variation of the electron replenishing source was investigated by varying the amount of iodine at a constant mass of TiO_2 (0.6 g) and graphite $-C_X$ (0.25 g) as presented in Table 1.

Table 1: Effect of variation of iodine masses of cells A, B and C on Voc

Cell		Mass (g)			Voc (V)		
	TiO ₂	KI C _X		I_2	V _{OC}		
A	0.6	0.01	0.25	0.12	0.496		
В	0.6	0.01	0.25	0.18	0.278		
C	0.6	0.01	0.25	0.24	0.243		

From the information recorded in Table 1 above, a graphical presentation of potential (Voc) against the masses of iodine was made as shown in Figure 4.

Figure 4: Variation of Iodine Mass against Potential of Cells A, B and C

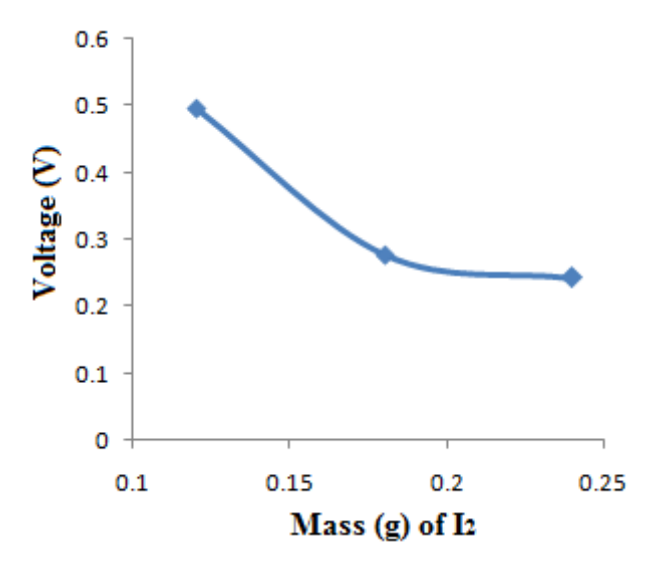


Figure 4 shows a general profile of decrease in potential as the mass of I₂ increases. The composition of TiO₂: graphite: I₂ of cells A, B and C were varied in the mass ratios (0.6: 0.25: 0.12), (0.6: 0.25: 0.18) and (0.6: 0.25: 0.24), respectively.

It is observed that between the mass of (0.18 and 0.24) g the generated voltage was almost constant. This can be explained by the fact that when the iodine ions surpassed the number of the electrons released from the photo active material, there was an increase in resistance which restricted the migration of the photo excited electrons on the photo active electrode to the external circuit (Jessica, 2018). Increasing the mass of I₂ beyond 0.24 g would decrease the potential difference because extra I₂ ions inhibited migration of the generated photo excited electrons.

The mass of TiO_2 and graphite (C_X) was then increased to (0.7 and 0.28) g respectively and a similar procedure was followed to characterize the resulting cells. The change in potential against the mass of iodine was monitored and the results were recorded as shown in Table 2.

Table 2: Effect of Variation of Iodine Masses of Cells D, E and F at Constant TiO₂ on V_{OC}

V) Current Density (μA cm-²) Cell TiO₂ KI Cx I₂ Voc Jsc D 0.7 0.01 0.28 0.15 0.956 6.474 E 0.7 0.01 0.28 0.2 0.295 2.000 F 0.7 0.01 0.28 0.28 0.2 1.353		Mass (g)					Short CCT
Cell TiO2 KI Cx I2 Voc Jsc D 0.7 0.01 0.28 0.15 0.956 6.474 E 0.7 0.01 0.28 0.2 0.295 2.000						V)	Current Density
D 0.7 0.01 0.28 0.15 0.956 6.474 E 0.7 0.01 0.28 0.2 0.295 2.000							(μA cm ⁻²)
E 0.7 0.01 0.28 0.2 0.295 2.000	Cell	TiO ₂	KI	Cx	I_2	V _{OC}	Jsc
	D	0.7	0.01	0.28	0.15	0.956	6.474
F 0.7 0.01 0.28 0.28 0.2 1.353	E	0.7	0.01	0.28	0.2	0.295	2.000
	F	0.7	0.01	0.28	0.28	0.2	1.353

From the information recorded in Table 4, a graphical presentation of potential (Voc) against the masses of iodine was made as shown in Figure 5.

Figure 5: Variation of Iodine Mass Against Potential of Cells D, E and F

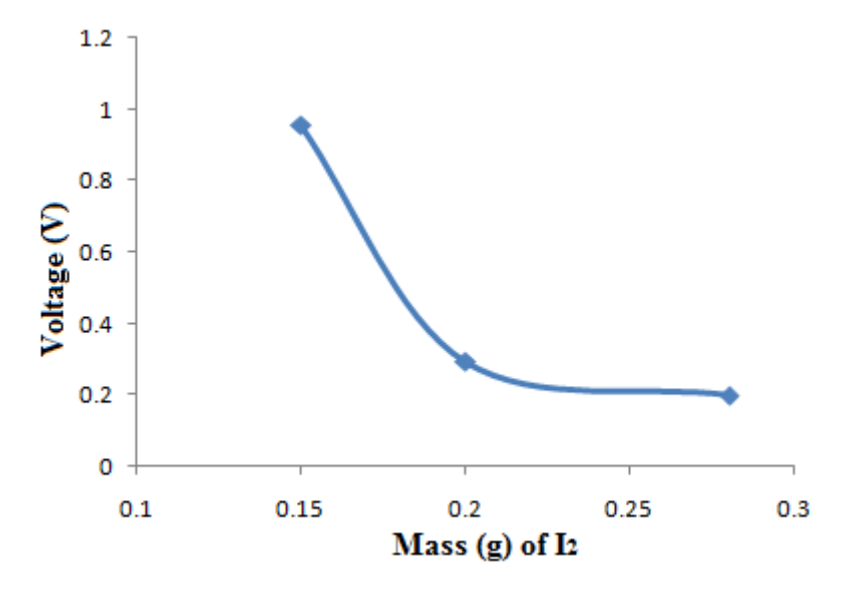


Figure 5 shows a general profile of a decrease in potential as the mass of I₂ was increased. However, the values of the potential generated were higher as compared to those found in Figure 4. This could be attributed to the ratios of iodine ions nearing the optimization value with respect to the other cell constituents which in turn increased the rate at which the iodine ions replenished the electron deficient holes (Khan, 2013).

Another set of cells were made with the mass of TiO₂ held constant at 0.8 g and that of iodine was varied from (0.15 to 0.30) g. The change in the potential against the mass of iodine at constant radiation was monitored and recorded as shown in Table 3.

Table 3: Effect of Variation of Iodine Masses of Cells G, H, I & J on V_{OC}

Cell		Mas	Potential (V)		
	TiO ₂	KI	Cx	I ₂	Voc
G	0.8	0.01	0.32	0.15	0.24
Н	0.8	0.01	0.32	0.2	0.304
I	0.8	0.01	0.32	0.25	0.284
J	0.8	0.01	0.32	0.30	0.248

A graphical presentation of potential (Voc) against the masses of iodine was made as shown in Figure 3. The mass of the composition of TiO_2 : graphite (C_X): I_2 were varied in the ratio of (0.8: 0.32: 0.15), (0.8: 0.32: 0.2), (0.8: 0.32: 0.25) and (0.8: 0.32: 0.30), respectively.

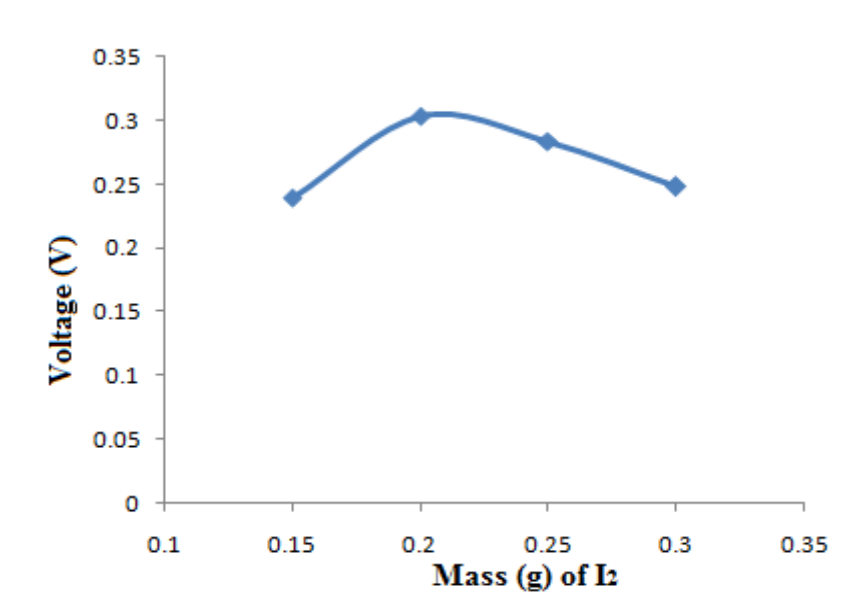


Figure 6: Variation of G, H, I Iodine Mass Against Potential of Cells and J

The result shown on Figure 6 is a general profile with increase in potential up to 0.304 V at a mass of 0.2 g. The voltage then decreased uniformly to 0.248 V when the iodine content was varied to 0.3 g. This showed that these ratios were nearing the optimum values of ratios which almost produced a uniform plateau with very small deviations. From the profile of figure 4.3, the resistance of the cell seems to have reduced drastically to indicate that the constituent ratio of the cell components enabled the migration of the charged species to generate almost a uniform open circuit voltage.

These results shows that there is an increase in potential with increase in the mass of iodine up to 0.2 g after which there was a drop in potential with further increase in the mass of iodine. Higher amounts of photo active material increase the charge density of TiO₂ which in turn increased the rate at which the electrons reached a recombination site (Martin, 2012). This observation was attributed to the increased quantity of TiO₂ which on irradiation, a higher number of charge carriers were generated and migrated through the external circuit. Further investigations were done on cells K, L and M made with mass cells ratios of iodine (I₂) varied as presented in Table 4. The mass ratios of the photo active material (TiO₂) and graphite-C_X were held constant at (0.9 g) and (0.36 g) respectively, as the composition of

 TiO_2 : graphite (C_X): I₂ of the cells were varied in the mass ratios of (0.9: 0.36: 0.1), (0.9: 0.36: 0.2) and (0.9: 0.36: 0.3), respectively.

Table 4: Effect of Variation of Iodine Masses of Cells K, L and M on Voc

Cell		Mass	(g)		Voltage
					(V)
•	TiO ₂	KI C _X		I_2	V _{OC}
K	0.9	0.01	0.36	0.1	0.2
L	0.9	0.01	0.36	0.2	0.6
M	0.9	0.01	0.36	0.3	0.3

From the information recorded in Table 4 a graphical presentation of potentials (Voc) against the masses of iodine was made as shown in Figure 7.

Figure 7: Variation of Iodine Mass Against Potential of Cells K, L and M

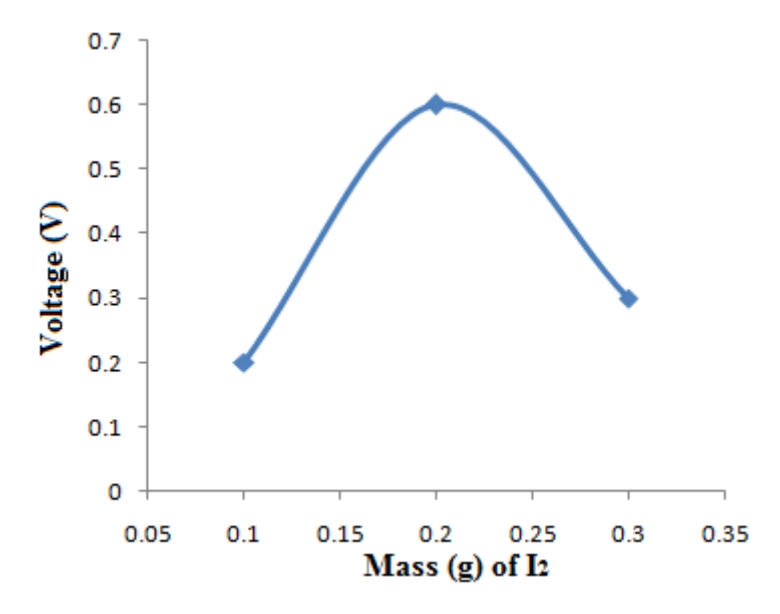


Figure 7 shows a gradual increase in potential with the mass of iodine varied from 0.1g to 0.2g producing the highest open circuit voltage of 0.6 V. The voltage then decreased gradually to 0.3V when the iodine content was varied to a mass of 0.3 g. The mass ratio (0.9: 0.36: 0.2) of TiO₂: graphite: I₂ was thought to exert impact on the conduction band edge (CB) of the TiO₂ and also on the electron recombination, therefore resulting in a higher photovoltaic.

Yordanov (2012) reported that higher iodine concentration leads to extra electron recombination between the injected photoelectron with the I³- ion. This ion replenishes the electrons lost upon absorption of radiation (Yordanov, 2012). However, excess of the I₃- ion contribute to losses of the photovoltaic performance in the iodine based photocell particularly on the short-circuit photo current density (Gorlov & Mikhil, 2010). Our conclusion based on the results, was that the highest optimization ratios of TiO₂: graphite: iodine which yielded the highest voltage was between (0.7: 0.28: 0.15) with a V_{oc} = 0.956 V to (0.9: 0.36: 0.2) with V_{oc} = 0.6 V. With higher mass ratios of iodine, limitation is less significant, while lower iodine concentration is favorable. The mass ratio of TiO₂: graphite: I₂ (0.8: 0.36: 0.2) generated a potential of 0.304 V. This implies that a mass ratio (0.7: 0.28: 0.15) of TiO₂: graphite: iodine gives a reasonably high output.

Conclusion and Recommendations

A solar cell was successfully fabricated using TiO_2 which is a non-toxic, chemically inert and stable material. The resulting cell was characterized in clear day light. The variation of current generated against its corresponding potential for the various cells was collected and the results obtained indicated that there is potential in the development of the photocell using TiO_2 graphite and I_2 materials in the mass ratios (0.4: 0.3: 0.17) for application at the point of use. These ratios yielded the best results of (V_{OC} = 0.979V, and J_{SC} = 12.037 μ Acm⁻², P_{MAX} = 7.55 μ W, fill factor (FF) = 0.64 and efficiency (η) = 0.006%). The general trend observed was that increase in the ratio of the photo active material generated higher potential which drastically reduced after the optimized ratio was reached, and the generation of potential reduced considerably. Considerable potential was generated with some ratio of iodine-iodide complex indicating that its presence contributed to generation and subsequent increase in voltage. The highest potential (V_{OC}) of 0.956V was generated with I_2 mass of 0.15 g. There is need to investigate the use of transparent conducting oxide (T_{CO}) as the cathode electrode.

References

- Adegbenro, A. (2016). *Comparison of Novel and State of the Art Solar Cells*. University of Kessel, Germany.
- Adler, E. (2011). Semi-Conductor Photocells and Rectifiers; A New Cuprous Ocide Photocell (Msc Thesis). Columbia University, New York.
- Ahmad, G., & Mohamad, M. (2010). Use Photovoltaic Systems in Remote Car Filling Stations. *Energy Conversion and Management*, 41, 1293-1301
- Caitian, Xiaodong, Xupeng, Lulu, Zemin, Youqing, Huigao, Zhenxing, Erqing, (2014).

 Branched hierarchical photo anode of titanium dioxide nanoneedles on tin dioxide nano fiber network for high performance dye-sensitized solar cells.

 Alloys and Compounds 10.1016. Lanzhou University, China
- Chergui, Y., Nehaoua, N., & Mekki, D. E. (2011). Comparative Study Of Dye-Sensitized Solar Cell Based on Zno and Tio2 Nanostructures, Solar Cells Dye-Sensitized Devices, Retrieved February 25,2017 From Http://Www.Intechopen.Com/Books/Solar-Cells-Dye-Sensitizeddevices
- Colin, X. (2011). Advanced Materials for Thermal Management of Electronic Packaging. New York: Springer-Verlag
- Gorlov, Mikhil (2010). 10620 Investigation of Iodine Concentration Effects in Electrolytes for Dye-Sensitized Solar Cells. 114, 10612-10620
- Hagfeldt, A. G., Boschloo, L. S., Kloo, L., & Pettersson, H. (2010). Dye-Sensitized Solar Cells. *Catalysis*, 110, 6595-6663.
- Hebling, G. (2010). Photovoltaic Materials. *Material Science Engineering*, 94(1):40–47.
- Hecht, J. (2018). Photonic Frontiers. *Journal of Thin Film Photovoltaics*, 34(40), 51-64.

- Hussein, A. M., Iefanova, A. V, Koodali, R. T., Logue, B. A., & Shende, R. V. (2018). Interconnected Zro 2 Doped Zno / Tio 2 Network Photoanode For Dye-Sensitized Solar Cells,4, 56–64. Https://Doi.Org/10.1016/J.Egyr.2018.01.007
- Jessica, C. L. (2018). *The Use of Nanostructured Calcium Silicate in Solar Cells*. Victoria University Of Wellington USA.
- Kanakaraju, D., Glass, B. D., & Oelgemo, M. (2014). Titanium Dioxide Photocatalysis for Pharmaceutical Wastewater Treatment Titanium Dioxide Photocatalysis for Pharmaceutical Wastewater Treatment. RSC Advances, (April). Https://Doi.Org/10.1007/S10311-013-0428-0
- Khan, M. (2013). A Study on the Optimization of Dye-Sensitized Solar Cells (PhD Thesis). University of South Florida.
- Khan, M., Gul, S. R., Li, J., Zeng, Y., & Chen, J. (2017). Pt / N Co-Doped Titanium Dioxide Visible-Light- Active Photo-Catalyst: Preparation And Characterization Pt / N Co-Doped Titanium Dioxide Visible-Light-Active Photo- Catalyst: Preparation and Characterization.
- Liu, L., Li, Y., Tao, E., Jiang, Z., Yang, S., Xu, J., & Qian, J. (2018). Surfactant-Assisted Titanium Dioxide / Graphene Composite for Enhanced Conductivity Zeta (Mv), 217(March), 365–370. Https://Doi.Org/10.1016/J.Matchemphys.2018.05.075
- Martin, K. (2012) Material Development For Solid State Dye-Sensitized Solar Cells. Uppsala University.
- Monasterolo, I., & Raberto, M. (2018). The Impact of Phasing Out Fossil Fuel Subsidies on the Low-Carbon Transition. *Energy Policy*, 124(June 2018), 355–370. Https://Doi.Org/10.1016/J.Enpol.2018.08.051
- Nikhil, J. (2013). Design of iii-V multifunction solar cells on silicon substrate: Cell Design & Modeling Epitaxial Growth & Fabrication.

- Ola, O., & Maroto-Valer, M. M. (2015). Applied Catalysis A: General Transition Metal Oxide Based Tio 2 Nanoparticles for Visible Light Induced CO 2 Photoreduction. "Applied Catalysis A, General,"502, 114–121. Https://Doi.Org/10.1016/J.Apcata.2015.06.007
- Perera, F. (2018). Pollution from Fossil-Fuel Combustion is the Leading Environmental

 Threat to Global Pediatric Health and Equity: Solutions Exist. *International Journal of Environmental Research and Public Health*, 15(16).

 Https://Doi.Org/Doi:10.3390/Ijerph15010016
- Sellappan, R. (2013). *Mechanisms of Enhanced Activity of Model Tio2/Carbon and Tio2/Metal Nanocomposite Photocatalysts*. University of Technology.
- Tse, M., Wei, X., Wong, C., & Huang, L. (2018). Enhanced Dielectric Properties of Colossal Permittivity Co-Doped Tio2/Polymer Composite Films. *RSC Advances*, 32972–32978. Https://Doi.Org/10.1039/C8ra07401a
- Wang, X., Chen, Z., Li, K., Wei, X., Chen, Z., & Ruso, J. M. (2017). The Study of Titanium Dioxide Modification by Glutaraldehyde and its Application of Immobilized Penicillin Acylase. *Colloids And Surfaces*, 560(October 2018), 298–305. Https://Doi.Org/10.1016/J.Colsurfa.2018.10.001
- Yordanov, G. H. (2012). Characterization and Analysis of Photovoltaic Modules and the Solar Resource Based on In-Situ Measurements. Norwegian University Southern Norway.

Assessment of Forest Rehabilitation and Restocking Along Mt. Kenya East Forest Reserve

Using Remote Sensing Data

Kibetu, D. Kinoti¹, Mwangi, J. Muthoni²

¹Chuka University, ²Galaxy Geo Consultancy Services, Kenya.

Correspondence: *kinotikibetu@yahoo.com*

Abstract

The nationwide ban on harvesting of forest products in 1999 was aimed at promoting regeneration of

forest resources in Kenya after years of uncontrolled intensive logging. This was followed by massive

tree planting programs spearheaded by the Kenya Forest Services (KFS) and other stakeholders. It is

estimated that millions of tree seedlings were availed to support the program. One of the heavily

affected forests was Mount Kenya Forest Reserve gazetted in 1932. The diverse tree species and its

proximity to human settlements has made this important national water tower vulnerable to

deforestation and illegal logging. Despite development of a ten year Mt. Kenya ecosystem

management plan (2010-2020) to address threats to Mount Kenya's natural resources, comprehensive

mapping of degraded areas to inform rehabilitation program has not been carried out along the

perceived forest-human activity transition zone. This study sought to assess effectiveness of

rehabilitation efforts moreso restocking after the 10-year ban. This will ascertain success or failure of

such an ambitious program and inform probable causes and if possible advise on the way forward.

Geospatial approaches and tools were integrated in data collection, analysis and presentation. Such

tools especially remote sensing and GIS have been applied in forest cover spatial extent mapping as

well as forest change detection analysis.

Key words: Remote Sensing, Mt. Kenya, Ban, Restocking, KFS.

Overview and Background Information

Globally, forests are an important natural resource providing safe habitats for biodiversity,

food for humanity as well as livelihood to many people. As such management, protection

and restoration of forests is crucial for continuation of social, ecological and economic

benefits sundry (FAO, 2015; Gamfeldt et al., 2013). Internationally, excessive exploitation of

forest resources has resulted to loss of global forest cover with an estimated 129 million

hectares cleared between 1990 and 2015 (FAO, 2016). This points to the alarming rate of

deforestation calling for more attention on management and development of forests.

Although there exist international treaties and directives on forest management, locally forests continue to face threats from population pressure related outcome and climate change risks. This calls for re-evaluation of forests conservation and associated land use management practices at locally to understand spatial and temporal dynamics of forest management approaches across the many forest blocks in the country.

Kenya has diverse forest types ranging from the lowland tropical rainforest, montaine forests to coastal mangrove types existing in different altitudes. Assessment of the different forest conservation approaches across the country will inform good management practices for sustainable development of national forest resources. Given the high rates of deforestation in 1990s, a nationwide ban on harvesting of forest resources was realized in 1999 coming into effect in the year 2000. This move aimed at promoting regeneration of forests in the country after years of uncontrolled logging. Massive tree planting programs were then initiated by the Kenya Forest Services and sector specific stakeholders with millions of tree plants species availed across the country for restocking and rehabilitation to date. For effective management of these diverse forest clusters, information on their spatial extents, altitudinal location and regions of degradation is important. Recently constituted taskforce using aerial surveys to assess status of National forests pointed out wanton destruction of the forest cover through illegal logging and excision rights allotment. Their findings are consistent with many studies done in the region and country (Soini, 2002; Nkako et al, 2005).

Locally most studies in forest change analysis have focused on monitoring forest cover change through deforestation using optical remote sensing imageries (Baldyga et al, 2007; Ochego, 2003). Satellite remote sensing technologies have gained popularity in the field of forest studies due to its synoptic and continuous earth observation. These characteristics make remote sensing less costly and effective in monitoring and assessment of forest dynamics on a temporal scale. For instance, remote sensing data has been used widely in forest mapping (Wagner et al., 2003; Dwyer et al., 2000) and Forest Change Detection (Ahmed et al, 2018; Gimeno et al., 2002) among others. Understanding changes in forest cover is important for operational forest management especially those aimed at assessing success of forest rehabilitation and restocking programs (Dostálová, et al, 2016; Johannes, et al, 2017). In most instances, forest cover dynamics arise from fires, diseases and illegal

logging all which interplay to influence deforestation and regeneration of forests globally. These activities are reportedly common along forest border zones in all Kenyan forest complexes. The Mount Kenya Forest Reserve gazetted in 1932 is under the jurisdiction of Kenya Forest Service to especially ensure establishment of plantations in areas where harvesting of indigenous stands have occurred. Despite development of a ten year Mt. Kenya ecosystem management plan (2010-2020) to address threats impacting on Mount Kenya's natural resources, comprehensive mapping of degraded areas to inform rehabilitation program has not been carried out along the perceived forest-human activity zones. One of the action plan envisaged in the ten year management plan is to carry out assessment of forest degraded areas to inform the type of enrichment plantation. Effective reforestation requires assessment of target enrichment areas to identify forest dynamics such as tree density on a spatial-temporal dimension.

There have been no extra terrestrial based assessments of Mt. Kenya forest dynamics after the ban especially along the degraded Eastern and South Eastern forest border zones. This has limited effective monitoring of the success rate of forest tree establishment after years of expansive tree cover restoration process. Every year national, regional and local tree planting activities are carried out by institutions, corporate and individuals around Mt. Kenya Forest Reserve. Although some successes have been achieved to this end, it is not known which areas of the forest have regenerated after restocking and the effects of these strategies on the overall forest rehabilitation generally. Despite Mt.Kenya forest reserve being a protected area, management of this forest is faced with threats of illegal logging and forest resource depletion along the populated low elevation areas of the forest reserve.

Previous studies done on Mt.Kenya forest using Landsat imageries have shown consistent patterns of increased forest loss over time. According to Yi-Hua, 2011, between 1980 and 2000, Mt. Kenya forest cover decreased to about 12.7 %, while Ngigi &Tateishi in 2004 observed a 2 % drop in forest cover between 1987 and 2000. A study by Ndegwa, (2005) indicated that about 17.5 % of the Montaine forest was destroyed between 1978 and 2002. These findings confirm the fact that Mt. Kenya forest is under threat from urbanisation and agricultural land use practices. The greatest limitation towards effective monitoring of forests in the country is the over dependence on snap shoot field data and the focus on forest degradation as though it were the only major threat to local forest development. This clearly

shows a gap and need to re-shift attention from forest degradation and it drivers to matters of forest restocking, rehabilitation and regeneration. Integration of remote sensing imageries with field data will provide approaches essential for quantification of forest areas under regeneration and rehabilitation as indicated in this study.

This study seeks to assess the effectiveness of plantation establishment activities in the degraded areas under the forest resource management program within Mt.Kenya ecosystem management plan. Most studies carried out in the Mt.Kenya region have applied optical remote sensing imageries to map the extent of forest cover loss between 1978 and 2002. Use of optical sensors in the acquisition of high quality cloud-free imageries is hampered by presence of frequent cloudy conditions in the area. This leads to misclassification of land cover and land use features (Asner, 2001; Yi-Hua, 2011). Due to these challenges, this study will use Landsat 8 OLI Low Cloud Cover Data (LCCD) to derive forest area under target enrichment based on the initially identified low tree density patches. Although SAR data are not affected by cloud coverage, weather or light condition, they have not been widely used in tropical forest mapping though they are effective in forest biomass estimation; forest cover mapping and discriminating forests from other land cover (Hamdan et al, 2017). In particular, the new Synthetic Aperture Radar sentinel 1A satellite data from European Space Agency has gained popularity of use in forestry studies especially derivation of forest area (Dostálová et al, 2016) and forest change detection analysis (Olesk et al., 2015) in Europe. However, although SAR data is promising compared to optical ones, their use is pegged on having knowledge on Radar nomenclature and availability of specifically designed tools to handle radar data image processing as well as analysis.

Study Area

Mount Kenya Forest reserve, also gazetted in 2000 as a national reserve co-managed by Kenya wildlife service and Kenya Forest service respectively. It is a protected area for its biodiversity and water catchment values. This study was carried out along the Eastern and South Eastern Forest Border zone(Fig.1). This belt has minimal potential for tourism development and comprises of community lands and forest resource dependent population. The zone is often threatened by human activities of illegal logging and charcoal burning owing to its proximity to permitted settlement areas. It contains Nyayo Tea plantation Zones and is often a target for farm forestry activities.

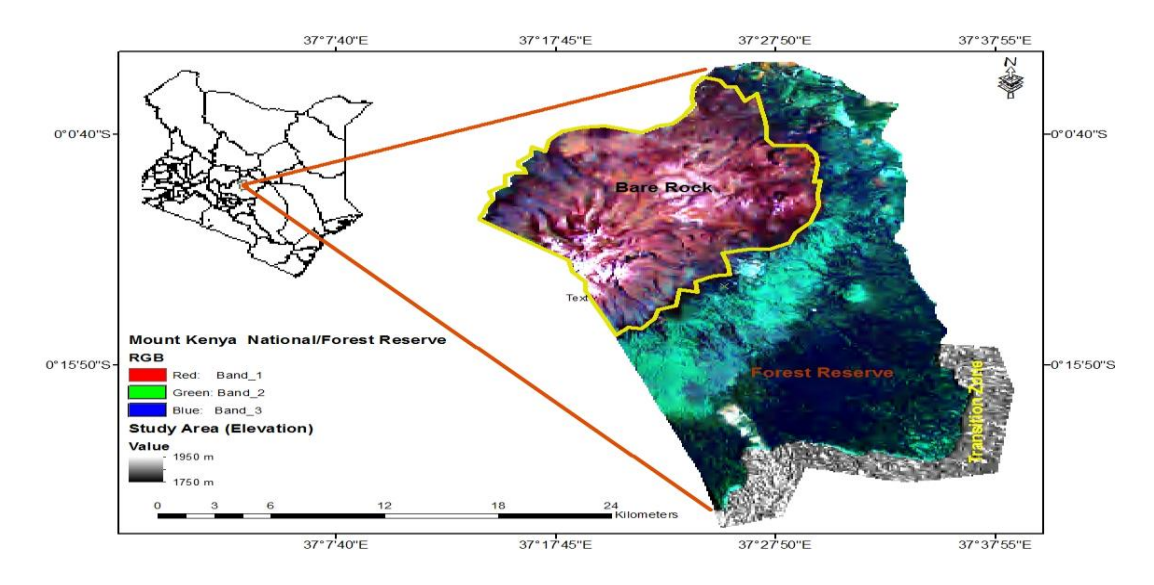


Figure 1: Location of the Study

Data, Materials and Methods

Data and Materials

Multispectral Landsat 5 TM and Landsat 7 ETM+ Path 168 and Row 60 for the study area were downloaded from US geological Survey official website (http: www.earthexplorer.usgs.gov). Images for 2011, 2015 and 2018 with less than 6 % cloud cover were selected, downloaded and used in this study. All images were acquired during January a dry month inorder to reduce reflectance attenuation associated with seasonal variation. Visible and Near-infrared wavelength bands were used to map the greennes of forest (Table.1). A 30m ASTER digital elevation model of the area was used to extract slope and elevation. Roads and towns data used was obtained from Kenya Open data portal as shapefiles. Satellite image processing was done using Idrisi Kilimanjaro and GIS analysis was carried in QGIS version 2.14.1 Essen. Land use/ land cover validation data was collected from both field visits and high resolution google earth images.

Table1: Landsat images and their bands used in calculating Normalised Digital Vegetation Index

Image	Wavelength(micrometers)	Date	Resolution
Landsat 7 ETM+		21st January 2018	30m
Band3:	Red (0.63-0.69)		
Band4:	NIR (0.77-0.90)		
Landsat 7ETM+		29thJanuary 2015	30m
Band3:	Red (0.63-0.69)		
Band4:	NIR (0.77-0.90)		
Landsat 5 TM		10 th January 2011	30m
Band3:	Red(0.63-0.69)		
Band4:	NIR(0.76-0.90)		

Methods

Extraction of Study Area

Area of interest comprised of the Eastern and SouthEastern blocks of Mount.Kenya forest. The area consist of the expansive montaine forest across Meru,Tharaka Nithi and Embu counties. Images of 2011, 2015 and 2018 were then subsetted to get the desired study area. ASTER digital elevation model image of 2018 was clipped to the study area to give the forest altitudinal height.

Image Processing and NDVI Calculation

The 3 pairs of subset Landsat images were pre processed to correct for atmosphere errors using cost(t) atmopsheric correction model in Idrisi Kilimanjaro image processing software. Band 3 for red and band 4 for Near infrared were used to discriminate the forest vegetation from non vegetation land use/cover. The study used Normalised Difference Vegetation Index(NDVI) to quantify forest vegetation abudance by measuring greeness. Although there are other vegetation discrimination indexes for mapping vegetation, NDVI was used because it is easier and straight forward to use compared to others and that is has been

applied widely in discriminating vegetation from other landuses/cover (Pettorelli et al., 2005; Mancino et al., 2014; Slimani et al., 2017).

Vegetation Cover Density Classification

NDVI values for the resultant image derived maps of 2011, 2015 and 2018 ranged from 0.28 to 0.70. An appropriate NDVI threshold value to classify forest vegetation cover density was selected based on calculated NDVI values and visual interpretation of the high resolution Google earth images.

To classify the forest cover, NDVI values were categorised where the intensity of greenness was used to reclassify the vegetation types in the AOI.

Validation and Accuracy Assessment

Effective interpretation of the resultant NDVI images was based on integrated field data, google earth images, roads, towns and population data. These data helped to understand attributing causes of the observed forest vegetation changes especially along the permited settlement/forest areas

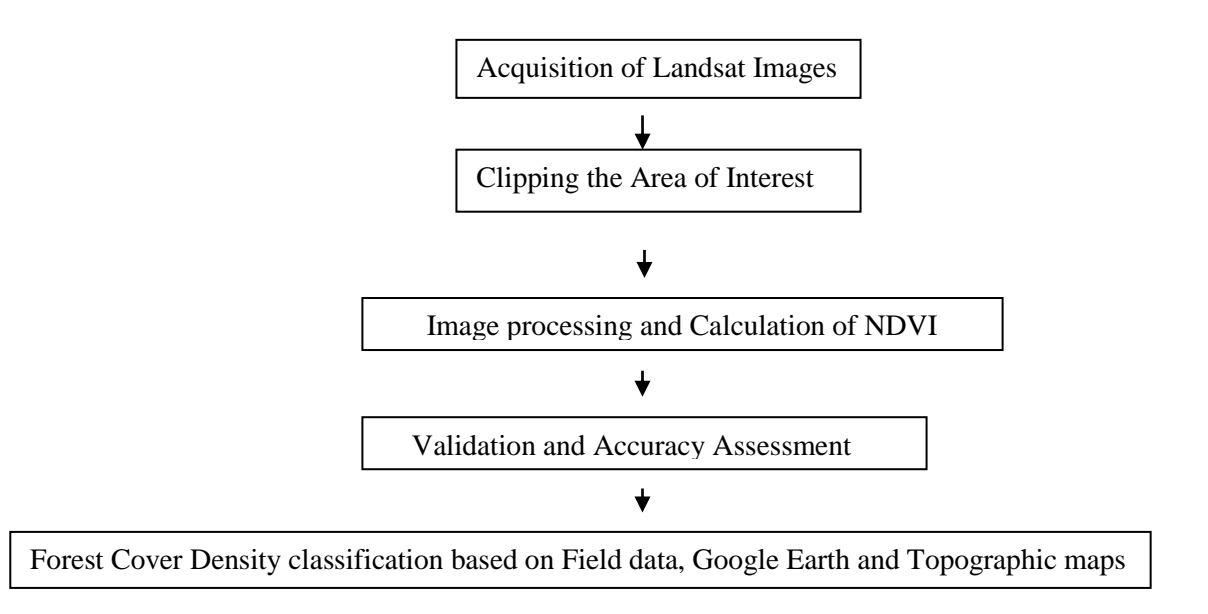


Figure 2: A Schema of the Image Processing and Spatial Data Analysis

Results and Discussion

Dynamics of Forest Density Cover

Forest cover density for 2011, 2015 and 2018 was classified as Non-vegetation(NDVI<0.31), Scanty vegetation(0.31<NDVI< 0.46) and dense vegetation(0.36<NDVI<0.69) based on the NDVI values. Analysis of the spatial distribution for vegetation cover along forest border showed that areas of high density were concentrated about 1000m from the border. The quantity of cover was not symmetrical across the three years under review. In 2011, 10250.73 ha of assorted shrubs—were mapped compared to 8947.17 ha of the same in 2015. This represents 12.72 % decrease in low and medium—dense vegetation. Similarly proportion of high dense vegetation showed a decline from 56639.25 ha(2011) to 50841.90ha (2015) and a total of 48796.74 ha in 2018(Table.2) This trend—show a consistent decline of—woody vegetation cover at a rate of 13.85% for the 7 year period (2011-2018). A look at the resultant NDVI maps of 2011, 2015 and 2018 shows a consistent loss of high valued forest woody species at least 2500 meters from the permitted forest border(Fig.3). This means illegal and selective harvesting of trees is still happening deep into the forest away from the forester watch stations along the south eastern and eastern Mt. Kenya forest blocks.

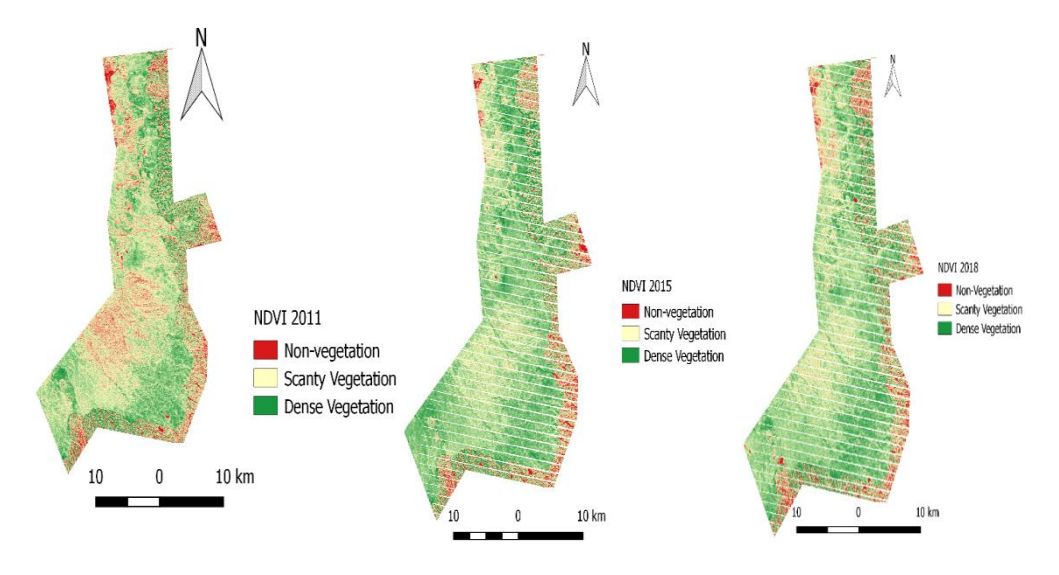


Figure 3: Maps of the Resultant NDVI values for 2011, 2015 and 2018

Table 2: Temporal Variation in Forest Density Area Cover in Hectares for 2011, 2015 and 2018.

Forest Cover	2011	2015	2018
	(ha)	(ha)	(ha)
Non Vegetation	4862538.81	4949868.42	4968897.93
Scanty Vegetation	10250.73	8947.17	10676.43
Dense Vegetation	56639.25	50841.90	48796.74

Cause Factors

Observed variations in forest cover show interesting patterns with scanty vegetation decreasing between 2011 and 2015 and later increasing. Dense forest vegetation cover showed a decrease across the seven year period (2018-2011). This can be attributed to encroached population and related human activities along the forest border zones. As can be seen there has been increase in population around the forest border areas between 2010 and 2015 (figure.4). This increase is attributed to births and localised migrations of population to work in Nyayo tea zones and private tea farms overlooking the forest.

Low elevation, upgraded roads and close proximity of the forest blocks to towns and roadnetworks has contributed substantially to the observed variations along Embu, Chuka, Chogoria and Imenti forest blocks of Mt. Kenya ecosytstem (Figure.5). Woody trees which form the dense vegetation are found on gentle slopes. It is thence important to note that altitude and slope have contributed to the spatial distribution of the forest cover density variations identified in this study. This explains why restocking has been persistently done along the forest edges and at low elevation as these comprise hot spots areas mostly encroached by the communities neighbouring forests.

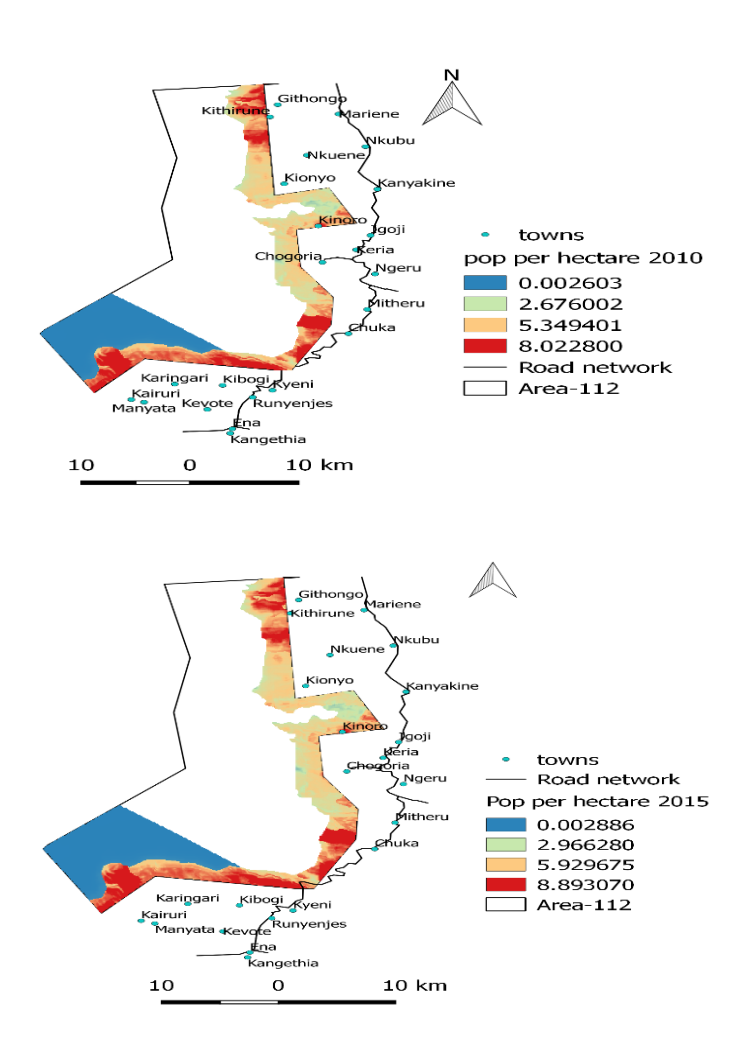


Figure 4: Increased Population Across the Forest Border Zones Between 2010 and 2015

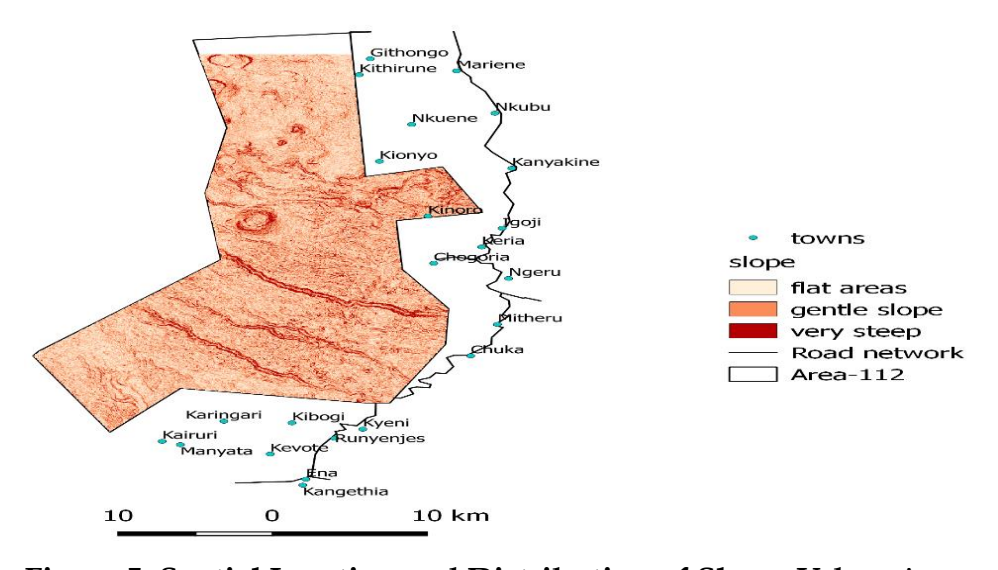


Figure 5: Spatial Location and Distribution of Slope, Urban Areas and Roads

Accuracy Assessment

Analysis of the spectral signature for forest vegetation types proved difficult to discriminate individual trees species. Mixing up of pixels due to problem of spectral similarity lead to development of general forest cover classes used during classification.

Overall accuracy for the three NDVI maps as assessed using Kappa Index of Agreement (KIA) was 0.7892 (2011), 0.8512% (2015) and 0.7638 (2018). These accuracies were deemed good given that a critical value of 0.759(KIA) is considered acceptable. Producers accuracies of 0.77, 0.86 and 0.78 were recorded for the Non vegetation, Scanty vegetation and Dense vegetation cover classes while Users accuracy varied between 0.85 to 0.90 respectively. It is therefore advisable to use high resolution images more so radar imageries and the doing of adequate field surveys to assist in development of effective training sites.

Conclusion

The findings of this study showed an increase in shrubs and other low to medium density forest vegetation between 2011 and 2018. The increase realised was about 4.15% for the seven year period especially exotic trees planted in the patches within forest stands. The fact that dense forest tree cover has been reducing as revealed by this study especially those deep into the forest, highlights limitations of the current ground based forest beats and surveys. These approaches restrict forest managers to known areas and only to those served by access routes. Generally, results of this study have shown the importance of integrating aerial and space born platform data in assessing and understanding dynamics of the evolving Mt.Kenya montaine forest cover. The study reveal mixed stories of success and failed reforestation cum restocking as shown by the processed, classified and analysed Landsat imageries. Some of the limitations with findings of this study are attributed to the season when the images were captured, image spatial resolutin and lack of adequate current ground truth information. The study proposes other studies to look at forest dynamics during wet seasons to help account for the greenness variation across dry and wet seasons.

References

Ahmed, B., Rida, K., Aafaf, J., Fatima, T & Samir, N (2018). Monitoring of Forest Cover Dynamics in Eastern Area of Béni-Mellal Province Using ASTER and Sentinel-2A Multispectral Data, *Geology, Ecology, and Landscapes*, 2(3), 203-215.

Asner, G.P. (2001). Cloud Cover in Landsat Observations of the Brazilian Amazon. *International Journal of Remote Sensing*, 22:3855–3862.

Baldyga, T. J., Miller, S. N., Driese, K. L. & Gichaba, C. M. (2007). Assessing Land Cover Change in Kenya's Mau Forest Region Using Remotely Sensed Data. *African Journal of Ecology*, 46: 46-54.

Dostálová, A., Hollaus, M., Milenković, M. & Wagner, W. (2016). ISPRS Annals of the Photogrammetry, *Remote Sensing and Spatial Information Sciences*, Volume III-7, 2016 XXIII ISPRS Congress, 12–19 July 2016, Prague, Czech Republic.

Dostálová, A., Hollaus, M., Milenković, M. & Wagner, W.(2016). Forest Area Derivation from Sentinel-1 Data. *ISPRS Annals of the Photogrammetry, Remote Sensing and Spatial Information Sciences*, Volume III-7: 227-233.

Dwyer, E., Monaco, S. & Pasquali, P. (2000). An Operational Forest Mapping Tool Using Spaceborne SAR Data. In: *ERS-ENVISAT Symposium*, Göteborg, Sweden.

FAO (2015). Global Forest Resources Assessment 2015-How Are the World's Forests Changing? (Food and Agriculture Organization of the United Nations). Retrieved from: http://www.Fao.Org/Resources/Infographics/Infographicsdetails/En/C/32583 On 23rd January 2018

FAO (2016). State of the World's Forests and Agriculture: Land-Use Challenges and Opportunities. Rome, Italy: Food Agriculture Organisation.

Gamfeldt, L., Snäll, T., Bagchi, R., Jonsson, M., Gustafsson, L., & Kjellander, P. (2013). Higher Levels of Multiple Ecosystem Services are Found in Forests with More Tree Species. *Nature Communications*, 4:13-40.

Gimeno, M., San-Miguel, J., Barbosa, P. & Schmuck, G. (2002). Using ERS-SAR Images for Burnt Area Mapping in Mediterranean Landscapes. *Forest Fire Research & Wildland Fire Safety*, 14.

Hamdan, O., Muhammad. M. & Abd, R. K. (2017). Synergetic of PALSAR-2 and Sentinel-1A SAR Polarimetry for Retrieving Aboveground Biomass in Dipterocarp Forest of Malaysia. *Applied Sciences*, PP 1-20.

Johannes, S., Fabian, E., Michael, F & Sebastian, S.(2017). Synergetic Use of Sentinel-1 and Sentinel-2 for Assessments of Heath Land Conservation Status. *Remote Sensing in Ecology and Conservation*, Pp 1-15.

Mancino, G., Nolè, A., Ripullone, F., & Ferrara, A. (2014). Landsat TM Imagery and NDVI Differencing to Detect Vegetation Change: Assessing Natural Forest Expansion in Basilicata, Southern Italy. *Forest - Biogeosciences and Forestry*, 7, 75.

Ndegwa, L. W. (2005). *Monitoring the Status of Mt. Kenya Forest Using Multi-Temporal Landsat Data.* Department of Geography. Miami University Oxford, Ohio, USA.

Ngigi, T. G. & Tateishi, R. (2004). Monitoring Deforestation in Kenya. *International Journal of Environmental Studies* 61: 281 – 291.

Nkako. M., Lambrechts, C., Gachanja, M. & Woodley, B. (2005). *Maasai Mau Forest Status Report 2005*. Ewaso Ngiro South Development Authority, Narok, Kenya.

Ochego, H. (2003). Application of Remote Sensing in Deforestation Monitoring: A Case Study of the Aberdares (Kenya). 2nd FIG Regional Conference. Marrakech, Morocco.

Olesk, A., Voormansik, K., Pohjala, M. &Noorma, M. (2015). Forest Change Detection from Sentinel-1 and ALOS-2 Satellite Images, Synthetic Aperture Radar (APSAR), IEEE 5th Asiapacific Conference, 1-4 Sept. 2015, Pp. 522-527.

Pettorelli, N., Vik, J.O., Mysterud, A., Gaillard, J.M., Tucker, C.J., & Stenseth, N.C. (2005). Using the Satellite-Derived Normalized Difference Vegetation Index (NDVI) to Assess Ecological Effects of Environmental Change. *Trends in Ecology & Evolution*, 20, 503–510.

Slimani, M.A., El Aboudi, A., Rahimi, A., & Khalil, Z. (2017). Use of GIS and Satellite Imagery in the Study of the Spatial Distribution of Vegetation in the Entifa Forest (High Atlas Central, Morocco). *Euro-Mediterranean Conference for Environmental Integration*.

Soini, E. (2002). Changing Landscapes on the Southern Slopes of Mt. Kilimanjaro, Tanzania: An Aerial Photo Interpretation between 1961 and 2000. *Working Paper* World Agro Forestry Centre (ICRAF) US Geological Survey Web Site Accessed on 16th June 2018 from: Http:// *Www.Earthexplorer.Gov*.

Wagner, W., Luckman, A., Vietmeier, J., Tansey, K., Balzter, H., Schmullius, C., Davidson, M., Gaveau, D., Gluck, M., Toan, T.L., Quegan, S., Shvidenko, A., Wiesmann, A. & Yu, J.(2003). Large-Scale Mapping of Boreal Forest in SIBERIA Using ERS Tandem Coherence and JERS Backscatter Data. *Remote Sensing of Environment*, 85:125-144.

Yi-Hua, W. (2011). *Investigation of Deforestation in East Africa on Regional Scales*. Unpublished Master's Thesis, University of Stockholm, Sweden.

Effect of Goat Manure-Based Vermicompost on Soil Chemical Properties under Garlic Production in the Upper Eastern Region of Kenya

Gichaba, Vincent Makini, Ndukhu, Haggai Onyan'go & Muraya, Moses Chuka University, Kenya

Correspondence: vincent.gichaba@gmail.com

Abstract

Majority of farmers in upper Eastern region of Kenya mainly apply chemical fertilizers to boost crop yields. Continuous use of chemical fertilizers causes several adverse effects such as P-fixation, volatilization of essential nutrients and leaching that affect safety of groundwater and agricultural environment. The effects of goat manure-based vermicompost on soil chemical properties under garlic were evaluated in Chuka University farm, Meru South sub-county and KALRO Embu horticultural field, Manyatta sub-county; from December 2018 to March 2019. The experiment was laid out in a randomized complete block design and replicated thrice. Treatments were; goat manure-based vermicompost applied at five quantities (0, 5, 10, 20 and 30 t ha⁻¹), NPK 17-17-17 at 200 Kg ha⁻¹ and goat manure (30 t ha⁻¹). The treatments were randomly assigned to experimental plots. Soil sampling and analysis were done before planting and after harvesting of garlic on each experimental unit. Results showed that application of goat manure-based vermicompost had statistically significant difference ($p \le 0.05$) on soil chemical properties. Application of 30 tha-1 goat manure-based vermicompost showed significantly ($p \le 0.05$) higher soil pH (8.00), total N (0.606%), available P (21.933 ppm) and exchangeable K (0.863 Cmol Kg⁻¹) than control treatment that had pH (6.59), total N (0.043%), available P (4.67 ppm) and exchangeable K (0.456 Cmol Kg^{-1}) at Chuka. A similar trend was observed in Embu where vermicompost gave significantly higher soil pH (7.91), total N (0.563%), available P (21.053 ppm) and exchangeable K (0.71 Cmol Kg⁻¹) compared to control which had pH (6.54), total N (0.03%), available P (4.6 ppm) and exchangeable K (0.34 Cmol Kg⁻¹). Results of this experiment revealed that addition of goat manure-based vermicompost enhanced soil chemical properties leading to improved garlic productivity.

Keywords: Garlic, Goat Manure-Based Vermicompost, Soil Chemical Properties

Introduction

Agriculture sector is the mainstay in the Kenyan economy contributing 30 percent of the gross domestic product and accounting for 80 percent of the employment (Horticultural Crops Development Authority [HCDA], 2016). Vegetables are a recognized source of

essential nutrients that lacks in many diets and their production is becoming a source of selfemployment and income generation in rural areas leading to rural development and a source of foreign exchange in the country (Kioko *et al.*, 2017). However, soil fertility decline contributes to low and unsustained crop yields in Kenya (Mucheru-Muna *et al.*, 2013). But in particular, the major nutrients, Nitrogen (N) and phosphorous (P), are commonly deficient in the soils (Okalebo *et al.*, 2006).

Garlic (*Allium sativum* L.) is gaining prominence as a high value horticultural crop in the onion family in Kenya. Farmers in upper eastern Kenya are getting interested in growing garlic due to its high returns and the readily available local market (HCDA, 2016). It is cultivated mostly under rain fed conditions in Kenya. Successful commercial cultivation of this crop greatly relies on many factors such as climate, soil fertility, irrigation, fertilizer management, spacing and growing season (Nainwal *et al.*, 2014). Depletion of macro and micro- nutrients from the soil, use of low yielding varieties and poor management practices are major causes of low yields (Tadesse, 2015).

Hence, farmers mainly use mineral fertilizers such as di-ammonium phosphate (DAP), urea and NPK to increase and sustain crop yields. The nutrients in these fertilizers are poorly utilized due to environmental and soil related factors such as P-fixation, leaching and volatilization of NO₃ and N₂O, respectively (Rop *et al.*, 2019). Application of required nutrients through chemical fertilizers alone can have a negative effect on soil health due to high levels of chemical residues in the soil and this can lead to unsustainable yields (Mbithi *et al.*, 2015). Continuous application of mineral nitrogenous fertilizers reduces soil pH, microbial populations and activities, organic matter content, buffering capacity and cation exchange capacity of the soils (Olomilua *et al.*, 2007). Use of chemical fertilizers in garlic production also increases the cost of production, cause environmental pollution and associated health problems (Uwah and Eyo, 2014).

A major constraint to fertilizer use and profitable farming has been high production cost, a function of a number of variables such as high transport cost, fertilizer unavailability, lack of credit and markets, devaluation of domestic currencies, weak extension services and skewed agricultural policies that favour industrialists but not the farmers (Rop *et al.*, 2019). Thus, indigenously available organic sources of nutrients have enhanced the efficiency of crop performance and reduced the requirements for chemical fertilizers (Bhat *et al.*, 2007). Use of

organic manures and bio fertilizers to maintain soil health and soil productivity is essential in production of garlic (Bhandari *et al.*, 2012). Thus, renewable and low cost sources of plant nutrients for supplementing chemical fertilizers and that are affordable to the majority of farming community need to be used (Kokobe *et al.*, 2013). The desire for low cost agricultural production using optimum concentrations of vermicompost is of great importance to farmers today (Moghadam *et al.*, 2012).

Vermicompost is a nutrient rich, microbiologically active organic amendment which results from interactions between earthworms and micro-organisms during the breakdown of organic matter (Lazcano and Dominguez, 2010). Vermicompost applied soils have high porosity, aeration, drainage, water-holding capacity, enhances cation exchange capacity (CEC) and large surface area, providing a strong capacity to hold and retain plant available nutrients such as nitrates, exchangeable phosphorus, soluble potassium, calcium and magnesium (Chaudhuri *et al.*, 2000). The organic carbon in vermicompost releases the nutrients slowly and steadily into the soil and enables the plant to absorb the available nutrients (Lalitha *et al.*, 2000).

The application of goat manure significantly increases soil pH, organic matter (OM) content, total N, available P, exchangeable K, calcium, magnesium and the cation exchange capacity (CEC) status of the soil (Uwah and Eyo, 2014). Goat manure is readily available on most farms in Meru south area and Manyatta sub-county. However, its use has received little research attention and hence not effectively used in sustainable agriculture. Driven by the desire to improve productivity while maintaining low cost in garlic production, this study was undertaken to evaluate the utilization of goat manure-based vermicompost in organic production of garlic in Meru south sub-county and Manyatta sub-county of upper eastern Kenya.

Materials and Methods

Study Site

The study was conducted on Chuka university farm, Meru south sub-county and KALRO Embu horticultural field in Manyatta sub-county, upper eastern Kenya. The crop was planted in one planting season in the two sites; December 2018 – March 2019. Meru south sub-county is found in Tharaka Nithi County on the eastern slopes of Mount Kenya. Chuka

University farm is located along the Nairobi – Meru highway approximately 186 kilometers from Nairobi city. The site lies at a latitude of 0.3229°S and longitude 37.6546°E. According to Jaetzold and Schmidt (1983), the area is in upper midlands 2 and 3 (UM2–UM3) agroecological zones with an average altitude of approximately 1,500 m above sea level, annual mean temperature of about 18° C and annual rainfall of about 1,500mm. The rainfall is bimodal, falling in two seasons, the long rains (LR) lasting from March through June and short rains (SR) from October to February. Soils are humic nitisols (Jaetzold and Schmidt 1983), which are extremely deep, well drained, dusky red to dark reddish brown, friable clay with acidic top soil and moderate to high inherent fertility. However, the soil is deficient in N, P and Zn (Ogolla *et al.*, 2019).

In Manyatta sub-county, the study was conducted at Kenya Agricultural and Livestock Research Organization station in Embu. The site lies at a latitude of 0.6762°S and longitude 37.4702°E. Manyatta sub-county is located on the eastern slope of Mount Kenya in Embu County. Embu lies in the lower midland 3, 4 and 5 (LM3, LM4 and LM5), upper midlands 1, 2, 3 and 4 (UM1, UM2, UM3 and UM4) and inner lowland 5 (IL 5) at an altitude of approximately 500 m to 1800 m above sea level (a.s.l.). It has annual mean temperature ranging from 17.4 to 24.5°C and average annual rainfall of 450 mm to 1400 mm. The rainfall is bimodal with long rains (LR) falling from around March to June and short rains (SR) from around October to December. It has *humic nitisols* soils and the prime cropping activity is maize intercropped with beans though livestock keeping is also dominant. Various agricultural activities have been carried out in the region hence the rationale behind its selection (Kisaka *et al.*, 2015).

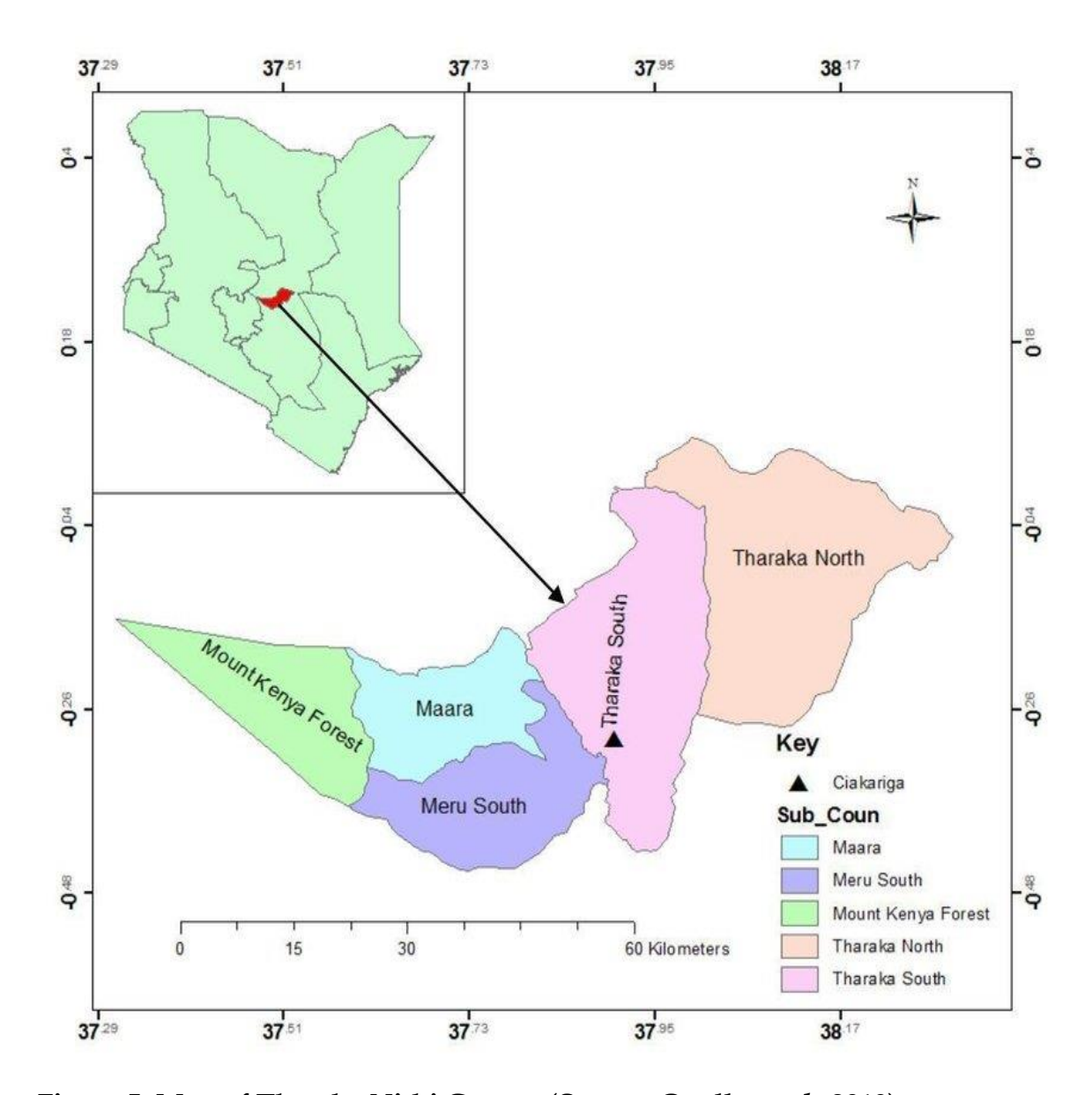


Figure 5: Map of Tharaka Nithi County (Source; Ogolla et al., 2019).

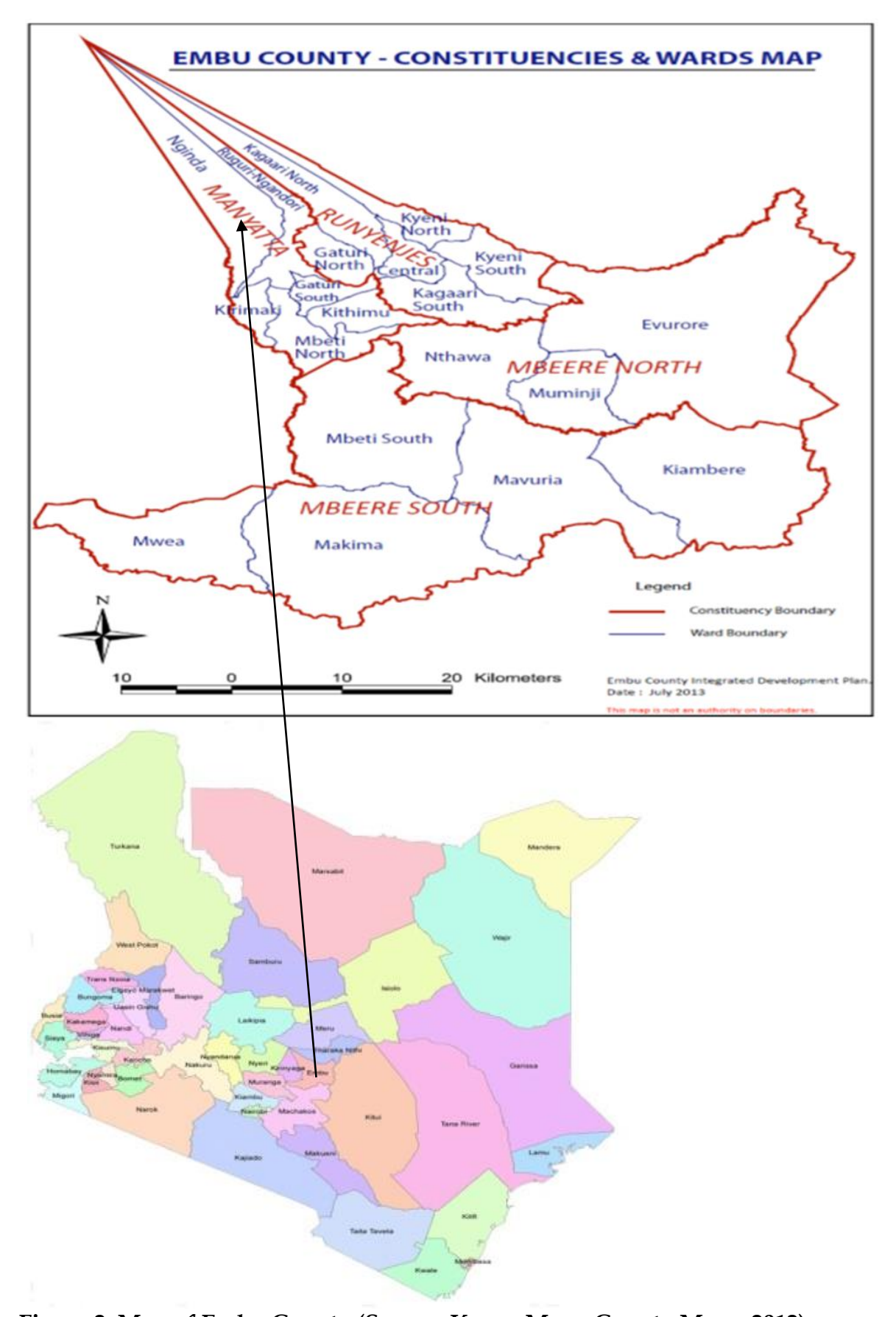


Figure 2: Map of Embu County (Source; Kenya Mpya County Maps, 2012).

Preparation of Goat Manure-Based Vermicompost

Goat manure was used as the main raw material to prepare vermicompost. A vermicompost bed was constructed using bricks and mortar on the walls. The bed measured 3 m long 1 m wide and 1 m high. A shed was erected above the vermicomposting bed to prevent direct sunlight and rain and also fenced round using wire chain link to keep away predators of earthworms like chicken and other birds.

A basal layer composed of broken bricks followed by a layer of coarse sand to a thickness of 7 cm was placed inside this bed to ensure proper drainage and restrict earthworm movement towards the soil layer. A 15 cm layer of loamy soil was placed at the top and moistened. Small lumps of fresh goat manure were scattered over the soil to form an active growing medium for earthworms then, 2,800 red wiggler earthworms (*Eisenia fetida*) species sourced from AAA growers in Naromoru, Laikipia County introduced to facilitate decomposition of the materials as described by Mbithi *et al.*, (2015). This was followed by 10 cm thick layer of dry grass, dry banana leaves and dry bean husks to act as bedding material for the worms. A 10cm thick dry goat manure weighing 100 kg was placed and spread on these materials. The same set of layering was continued till a height of 1 m followed by sprinkling uniformly 5 litres of water to the vermicompost bed to keep the worms moist and facilitate easy earthworm movement in these materials and gunny placed on top to cover the materials.

The vermicompost bed was kept moist by sprinkling 2 litres of water once a week and the process continued to the 7th week. Turning of these materials was gently done once after 15 days to avoid injuring earthworms. Goat manure-based vermicompost was harvested after 120 days when the earthworms were found sticking to the under surface of gunny bags indicating that composting process was complete and spread on a polythene sheet. Adult worms and young ones were handpicked from the manure dried for one day under a shed, screened and was filled into bags ready for organic growing of garlic.

A sample of goat manure-based vermicompost was analyzed for pH using a digital pH meter and total N estimated using kjeldahl method (Bremner and Mulvaney, 1982), available P using extraction with 0.5 M NaHCO₃ as described by Olsen *et al.* (1954) and exchangeable

K using Flame photometer (Jackson, 1967). Analysis was done at the University of Nairobi, upper kabete campus soil laboratories.

Experimental Design

The experiment was laid out in a Randomized Complete Block Design (RCBD) and replicated three times. Blocking of plots was done across the slope at the study sites. Treatments consisted of goat manure-based vermicompost applied at five amounts (0, 5, 10, 20 and 30 t ha⁻¹), inorganic fertilizer (NPK 17-17-17) applied at the recommended amounts of 200 Kg ha⁻¹ and goat manure (30 t ha¹). Treatments were randomly assigned to the various plots. Seven plots of equal measurements were used in each block giving a total 21 experimental plots. The distance between the blocks was 1m and distance between experimental plots 0.5 m. Experimental plots measured 2.60 m by 1.85 m giving a total area of 4.81 m⁻².

Plant Establishment and Agronomic Practices

Land was ploughed to a depth of 15 cm until a good tilth was obtained. Planting beds measuring 2.60 m by 1.85 m and raised 10 cm were prepared with paths of 50 cm apart and 1 m between blocks. Levelling of the beds was done using a rake. Planting cloves of a local garlic variety (moyale) were sourced from AAA growers, Naromoru. The planting beds were thoroughly soaked with water before planting. Goat manure-based vermicompost, NPK and goat manure applied on the experimental plots based on the assigned rates of application and well incorporated into soil in the entire experimental plots. Garlic cloves were planted with the base of the clove down and the tip in upright position and covered with soil. The recommended spacing adopted was 30 cm by 15 cm and a planting depth of 5 cm. Each experimental plot was having a total of 107 plants which translated to 222,453 garlic plants ha-1. Once established, all other necessary maintenance practices were carried out appropriately. Weeding was done through uprooting as weeds emerged. Pests were controlled through regular application of Duduthrin® at the rate of 15 ml 20 litres⁻¹ from the second week after garlic emergence at an interval of 14 days and stopped at 86 days after emergence. Diseases were controlled through regular application of Ridomil® fungicide at the rate of 40 gm 20 litres⁻¹ from the second week after garlic emergence at an interval of 21 days and stopped at 86 days after emergence. Sprinkler irrigation was done from morning to mid- afternoon after planting twice per week during growth of garlic crop and stopped two weeks to harvesting.



Figure 3: A view of experimental plots layout in Chuka

Data Collection Procedure on Soil Nutrients

Soil sampling was done before planting and after harvesting of garlic. Before planting, ten soil samples were taken randomly using a soil auger in a zigzag sampling design from the top to a depth of 20 cm of the soil profile from the entire experimental site, broken into small crumbs and thoroughly mixed. From this mixture, a composite sample weighing 1 kg was placed in aplastic bag, air-dried in the laboratory and crushed to pass through < 1mm sieve and chemically analysed. Soil samples were also taken from each polt at the end of the experiment in each growth season and analysed. To determine soil pH, H₂O, was added to soil sample at a ratio of 1:2.5 shaken for 30 min and pH determined using a digital pH meter fitted with a glass electrode. Total N was determined by sulphuric acid digestion using CuSO₄ and K₂SO₄ as catalyst. Total N in the digest was determined using kjeldahl distillation method (Bremner and Mulvaney, 1982). Available P was determined whereby 5cm³ soil was extracted for 30 min. with 100cm³ 0.5 NaHCO₃ solution (pH adjusted to 8.5). After filtration, phosphate concentration of solution was measured calorimetrically as described by Olsen *et al.* (1954). Exchangeable K was determined using flame photometer after K was extracted from air dried soil samples by shaking with 0.5M ammonium acetate

solution. Potassium content of the filtered extract was then determined as described by Jackson, (1967). Analysis was done at the University of Nairobi, Kabete campus soil laboratories. The soil chemical properties obtained were rated according to ranges given by Hazelton and Murphy, 2007 as shown in Table 1.

Table 1: Soil Chemical Properties Ratings according to Hazelton and Murphy, 2007

Parame	ter	Units	Values	Ratings
Soil	pH(soil:H ₂ O,	_	< 4.6	Extremely acidic
1:2.5)				
			4.6 - 5.5	Strongly acidic
			5.6 - 6.5	Moderately acidic
			6.6 - 6.9	Slightly acidic
			7.0	Neutral
			7.1 - 8.5	Moderately alkaline
			> 8.5	Strongly alkaline
N		%	< 0.05	Very low
			0.05 - 0.15	Low
			0.15 - 0.25	Medium
			0.25 - 0.50	High
			> 0.5	Very high
P		ppm	0 – 25	Low
			25 - 50	Medium
			> 50	High
K		Cmolkg-1	< 0.20	Very low
			0.21 - 0.30	Low
			0.31 - 0.60	Medium
			> 0.60	High

Statistical Analysis

Data on soil chemical properties obtained during the experimental duration were subjected to analysis of variance (ANOVA) to test the hypothesis of the study. Statistical analysis software (SAS, Version 2008) was used for data analysis. Significant means were separated using the Least Significance Difference test (LSD) at 5% probability level.

Results and Discussions

Soil Characteristics Before the Onset of the Experiment

Samples of each experimental site were analysed for soil chemical properties before planting and results are presented on Table 2.

Table 2: Soil Analysis Results of Experimental Sites Before Planting

Site	Soil chemical property	Units	Value	Ranges	*Ratings
Chuka	pH (soil:H ₂ O, 1:2.5)	_	6.64	6.6-6.9	Slightly acidic
	N	%	0.04	< 0.05	Very low
	P	ppm	4.66	0-25	Low
	K	Cmolkg-1	0.30	0.21-0.30	Low
Embu	pH (soil:H ₂ O, 1:2.5)	_	6.33	5.6-6.5	Moderately acidic
	N	%	0.03	< 0.05	Very low
	P	ppm	4.57	0-25	Low
	K	Cmolkg-1	0.26	0.21-0.30	Low

^{*}The ratings are based according to criteria described in Table 1.

Results showed that pH of the soil at Chuka is slightly acidic while that at Embu is moderately acidic based on the ranges by Hazelton and Murphy (2007). The total nitrogen content of the soils at Chuka and Embu were very low (Table 2). Tadesse (2015) reported that Nitrogen content of soil of less than 0.05% is very low, between 0.15 – 0.25% medium and greater than 0.25% is high. Available phosphorous in the two sites was low based on the ranges as described by Hazelton and Murphy (2007). Most vegetables benefit from P fertilization if the soil test is less than 35 – 40 ppm P using the Bray – Kurtz P₁ extraction method (Tadesse, 2015). Exchangeable potassium content of the soil of the two sites was low based on the ranges provided by Hazelton and Murphy (2007). According to Tadesse (2015) if the soil test is less than 85 ppm K, it is categorized as low potassium content. Garlic prefers a fairly neutral pH ranging 6.5 – 7.0. Thus, if the soil is too acidic or too alkalinic it causes slowed growth and late maturity of garlic. Moreover, N decreases as soil acidity increases while it becomes available as soil alkalinity increases (Tadesse, 2015).

Goat Manure-Based Vermicompost and Goat Manure Samples Analysis

A sample of goat manure-based vermicompost and goat manure used in the experiment were analysed for chemical properties and results presented on Table 3.

Table 3: Chemical analysis of goat manure-based vermicompost (GMBV) and goat manure (GM) samples used in the experiment

Type of	Chemical property	Units	Value	Ranges	*Ratings
manure					
GMBV	pH (soil:H ₂ O, 1:2.5)	_	7.73	7.1-8.5	Moderately alkaline
	N	%	1.79	> 0.5	Very high
	P	ppm	52	> 50	High
	K	Cmolkg-1	1.75	> 0.60	High
GM	pH (soil:H ₂ O, 1:2.5)	_	8.0	7.1-8.5	Moderately alkaline
	N	%	0.32	0.25-0.50	High
	P	ppm	24	0-25	Medium
	K	Cmolkg-1	0.59	0.31-0.60	Medium

^{*}The ratings are based according to criteria described in Table 1.

Chemical analysis of goat manure-based vermicompost used in the study showed very high total N, high available P and exchangeable K and it was moderately alkaline (Table 3) based on the ranges given by Hazelton and Murphy (2007). Goat manure used in the study had high total N, medium available P, medium exchangeable K and moderately alkalinic (Table 3). based on the ranges given by Hazelton and Murphy (2007).

Effect of Different Treatments on Soil Nutrients at Chuka and Embu

Results of mean separation on the soil nutrients (soil pH, total nitrogen, available phosphorous and exchangeable potassium) at the end of the experiment are presented in Table 4.

Table 4: Means of various soil nutrients under different treatments at Chuka and Embu at the end of experiment

0:4	TT	- C :1 II	TT (1 N T	A 11.1.D	T 1 11
Site	Treatment	Soil pH	Total N	Available P	Exchangeable
					K
Chuk	K ₆	7.336b	0.230bc	15.240bc	0.676bc
a					
	K ₅	6.650de	0.223c	13.380c	0.726ab
	K_4	8.000a	0.606a	21.933a	0.863a
	K_3	7.030c	0.286b	15.906b	0.743ab
	K_2	6.873cd	0.213c	6.920d	0.533cd
	K_1	6.806cde	0.090d	4.726e	0.503cd
	K_0	6.586e	0.043d	4.670e	0.456d
	Mean	7.040	0.241	11.825	0.643
	CV (%)	2.275	13.907	9.129	15.397
	LSD(0.05)	0.284	0.059	1.920	0.176
Emb	K_6	7.130b	0.200c	14.316bc	0.650a
u					
	K_5	6.620cd	0.203c	12.873c	0.630ab
	K_4	7.910a	0.563a	21.053a	0.710a
	K_3	6.860bc	0.273b	15.656b	0.683a
	K_2	6.813cd	0.183c	6.546d	0.496bc
	K_1	6.720cd	0.076d	4.700de	0.456cd
	K_0	6.543d	0.030e	4.596e	0.343d
	Mean	6.942	0.218	11.391	0.567
	CV (%)	2.539	11.721	9.432	14.119
	LSD(0.05)	0.313	0.045	1.911	1.142

^{*}Means followed by the same letter are not significantly different from each other at 5% level of significant. Where: K_0 is 0 t ha⁻¹, K_1 is 5 t ha⁻¹, K_2 is 10 t ha⁻¹, K_3 is 20 t ha⁻¹, K_4 is 30 t ha⁻¹, K_5 is NPK (17-17-17) and K_6 is goat manure (30 t ha⁻¹).

Soil pH

Soil pH was significantly (p \leq 0.05) affected by goat manure-based vermicompost treatments. Chuka recorded mean soil pH of 8.00 in K₄ treatment while the lowest mean soil

pH (6.58) was recorded in K₀ treatment. Similar to Chuka, at Embu, mean soil pH of 7.91 was recorded in K₄ treatment while the lowest mean soil pH of 6.54 was recorded in K₀ treatment (Table 4). Addition of goat manure-based vermicompost increased soil pH. Among the treatments, the soils blended with goat manure-based vermicompost at the rate of 30 t ha-1 had highest soil pH in comparison to the control treatment at the end of harvesting season. This is attributed to higher rates of application of goat manure-based vermicompost that supplied more organic compounds which are mineralized under aerobic conditions to produce ammonium that increases soil pH and reduces the potential of aluminium and manganese toxicity in soil. The increase in soil pH is also due to the fact that goat manurebased vermicompost had higher pH (7.73) when compared to Chuka soil pH (6.64) and Embu soil pH (6.33). This increase in soil pH (8.00) is not considered to have profound effect on the soil quality since it remains close to neutral. These results are consistent with those of Angelova et al. (2013) who reported that application of vermicompost increases soil pH. Contrary to these results, Atiyeh et al. (2002) reported decrease in soil pH as rates of application of vermicompost increased. This was attributed to production of NH⁺⁴, CO₂ and organic acids during microbial metabolism in vermicompost.

Total Nitrogen

Total N was significantly (p \leq 0.05) affected by goat manure-based vermicompost treatments with Chuka recording highest mean total N (0.606%) in K₄ treatment and the lowest mean total N (0.043%) in K₀ treatment. Similary. Embu, had the highest mean total N (0.563%) in K₄ treatment and the lowest mean total N (0.030%) was recorded in K₀ treatment (Table 4). Addition of goat manure-based vermicompost increased total N. Among the treatments, the soils blended with goat manure –based vermicompost at the rate of 30 t ha ⁻¹ had the highest total N in comparison to control treatment at the end of harvesting season. This is attributed to higher application of goat manure-based vermicompost that supplied more residual N in soil than the controls. These resuls are also similar to results of Angelova *et al.* (2013) who reported that total N concentration in soil was significantly affected by vermicompost treatments. The soils treated with vermicompost at the rate of 10 g kg⁻¹ had more total N compared to soils without vermicompost. This was attributed to organic matter, acidic pH and proper moisture in soil that avails N for plants. Azarmi *et al.* (2008) reported that a decrease in total N in soils without vermicompost application was due to larger amounts of

total C and N in vermicompost that could have provided a larger source of N for mineralization.

Available Phosphorous

This results showed that available P was significantly ($p \le 0.05$) affected by goat manurebased vermicompost treatments. Chuka recorded highest significant mean available P (21.933 ppm) in K₄ treatment while the lowest mean available P (4.670 ppm) was recorded in K₀ treatment. Similar to Chuka, at Embu, highest significant mean available P (21.053 ppm) was recorded in K₄ treatment while the lowest mean available P (4.596 ppm) was recorded in K₀ treatment (Table 4). The addition of goat manure-based vermicompost increased available P. Among the treatments, the soils amended with goat manure-based vermicompost at the rate of 30 t ha-1 had highest available P in comparison to the control treatment at the end of harvesting season. This is attributed to higher rates of application of goat manure-based vermicompost that gradually and continuously released more P into the soil even after garlic crop. Also release of P was due to the activity of microorganisms contained in vermicompost (Azarmi et al., 2008). Similar to these results, Angelova et al. (2013) reported that there was a significant increase in the soil extractable P with the increase of vermicompost doses applied. Soils treated with vermicompost at the rate of 10 g kg⁻¹ had significantly more P as compared to control plots. This was attributed to DTPA-extractable P with vermicompost thus release of humic acid during organic matter decomposition resulting in conversion of unavailable soil phosphate into available forms. Also, the enhancement of phosphatase activity and physical breakdown of material resulted in greater mineralization.

Exchangeable Potassium

This results showed that exchangeable potassium was significantly ($p \le 0.05$) affected by goat manure-based vermicompost treatments. Chuka recorded highest significant mean exchangeable K (0.863 Cmol Kg⁻¹) in K₄ treatment while the lowest mean exchangeable K (0.456 Cmol Kg⁻¹) was recorded in K₀ treatment. Similar to Chuka, at Embu, highest significant mean exchangeable K (0.710 Cmol Kg⁻¹) was recorded in K₄ treatment while the lowest mean exchangeable K (0.343 Cmol Kg⁻¹) was recorded in K₀ treatment (Table 4). This results showed that exchangeable potassium was significantly (p < 0.05) affected by goat manure-based vermicompost treatments. The addition of goat manure-based vermicompost increased exchangeable K. Among the treatments, the soils amended with goat manure-

based vermicompost at the rate of 30 t ha⁻¹ had highest exchangeable K in comparison to the control treatment at the end of harvesting season. This is attributed to higher rates of application of goat manure-based vermicompost that resulted in decreased K fixation and consequently increased K availability in the soils even at the end of harvesting season of garlic. Similar to the results obtained, Angelova *et al.* (2013) reported that significantly higher values of available K were obtained after the introduction of vermicompost compared to compost. The DTPA-extractable K were increased by the application of vermicompost. This was attributed to vermicompost which have high amounts of K in organic amendments that increases CEC thus the K amount raises in soil.

Conclusion and Recommendation

Amending soils with goat manure-based vermicompost enhances improved soil chemical properties. Among the different application rates used, the highest rate of 30 t ha⁻¹ proved the best in enhancing soil chemical properties in the study area. Even though chemical fertilizer quickly releases mineral elements, goat manure-based vermicompost stimulates microbial growth which promotes synthesis of phosphatase enzymes, it maintains and increases uptake of plant nutrients which leads to faster physiological development hence promotes growth and yield of garlic. Also, application of goat manure-based vermicompost does not result in the immobilization of plant available nutrients but instead it increases nutrient turnover through both increased microbial biomass and activity. Thus, goat manure-based vermicompost when applied in soil improves nutrient availability and also improves physical condition of soil. Hence, a shift to a more sustainable organically production systems that can significantly increase soil fertility and maintain garlic crop yield at levels comparable to those of chemically fertilized garlic. Thus, application of 30 t ha⁻¹ goat manure-based vermicompost is an efficient quality yield and economy enhancer in organic garlic production for sustainable agriculture.

References

Angelova, V. R., Akova, V. I., Artinova, N. S. and Ivanov, K. I. (2013). The Effect of Organic Amendments on Soil Chemical Characteristics. *Bulgarian Journal of Agricultural Science*, 19(5), 958-971.

- Atiyeh, R. M., Lee, S., Edwards, C. A., Arancon, N. Q. and Metzger J. D. (2002). The Influence of Humic Acids Derived from Earthworms-Processed Organic Wastes on Plant Growth. *Bioresource Technology*, 84, 7-14.
- Azarmi, R., Giglou, M. T. and Taleshmikail, R. D. (2008). Influence of Vermicompost on Soil Chemical and Physical Properties in Tomato (Lycopersicum esculentum) Field. *African Journal of Biotechnology*, 7(14), 2397-2401.
- Bhandari, S. A., Patel, K. S. and Nehete, D. S. (2012). Effect of Integrated Nutrient Management on Growth, Yield and Quality of Garlic (Allium sativum L.) cv. Gujarat Garlic-3. *The Asian J. Hort.*, 7, 48-51.
- Bhat, M. A., Singh, R. and Kohli, A. (2007). Effect Of Integrated Use of Farmyard Manure and Fertilizer Nitrogen with and Without Sulphur on Yield and Quality of Indian Mustard (Brassica Juncea L.). *Journal of Indian Society of Social Sciences*, 55(2), 224-226.
- Bremner, J. M. and Mulvaney C. S. (1982). *Nitrogen-Total. In: Methods of Soil Analysis, part 2, Chemical and Microbiological Properties*. American Society of Agronomy.
- Chaudhuri, P. S., Paul, T. K., Bhattacharjee, G. and Dey, S. K. (2000). Chemical Changes During Vermicomposting (Perionyx Excavatus) of Kitchen Waste. *Tropical Ecol*, 41, 107–110.
- Hazelton, P. and Murphy, B. (2007). *Interpreting Soil Test Results*. Collingwood VIC 3066: CSIRO.
- HCDA (2016). 2015-2016 Horticultural Validated Report. Nairobi: HCDA.
- Jackson, M. L. (1967). Soil Chemical Analysis. New Delhi: Prentice Hall of India.
- Jaetzold, R. and Schmidt, H. (1983). Farm Management Handbook of Kenya (Vol. II). Nairobi, Kenya: Ministry of Agriculture.

- Kioko, J. M. D., Kamau, P. A. and Mushimiyimana, D. (2017). Evaluation o the Effect of NPK Fertilizer and Spacing on Growth and Yield of Garlic (Allium Sativum) *In* Bomet County. *IJRDO-Journal of Educational Research*, 2(9), 85-108.
- Kisaka, O. M., Mucheru-Muna, M., Ngetich, F. K., Mugwe, J. N., Mugendi, D. and Mairura, F. (2015). Rainfall Variability, Drought Characterization, and Efficacy of Rainfall Data Reconstruction: Case of Eastern Kenya. *Advances in Meteorology*, 2015, 16 pages.
- Kokobe, W. Y., Derbew, B. and Adugna, D. (2013). Effect of Farmyard Manure and Nitrogen Fertilizer Rates on Growth, Yield and Yield Components of Onion (Allium Cepa L.) At Jimma, Southwest Ethiopia. *Asian J. Plant Sci.*, 12(6-8), 228-234.
- Lalitha, R., Fathima, K. and Ismail, S. A. (2000). The Impact of Bio-Pesticide and Microbial Fertilizers on Productivity and Growth of Abel-Moschus Esculentus. *Vasundhara: The Earth*, 1-2, 4-9.
- Lazcano, C. and Dominguez, J. (2010). Effects of Vermicompost as a Potting Amendment of Two Commercially-Grown Ornamental Plant Species. *Spanish J Agri Res*, 8(4), 1260–1270.
- Mbithi, M. A., Mwanarusi, S. and Mwangi, M. (2015). Effect of Different Rates of Vermicompost on Growth and Yield of Beetroot (Beta vulgaris L.). *Egerton J. Sci. and Technol.*, 15(ISSN No. 2073 8277), 30-43.
- Moghadam, A. L., Ardebill, Z. O. and Saidi, F. (2012). Vermicompost Induced Changes in Growth and Development of Lilium Asiatic Hybrid Var. Navona. *African Journal of Agricultural Research*, 7(17), 2609–2621.
- Mucheru-muna, M., Mugendi, D., Pypers, P., Kungu, J., Vanlauwe, B. and Merckx, R. (2013). Enhancing Maize Productivity and Profitability Using Organic Inputs and Mineral Fertilizers *In* Central Kenya Small-Hold Farms. *Cambridge Univ. Press, Exp. Agri*, 1-10.

- Nainwal, R. C., Singh, D., Katiyar, R. S., Sharma, L. and Tewari, S. K. (2014). Response of Garlic to Integrated Nutrient Management Practices *In* A Sodic Soil Of Uttar Pradesh, India. *Journal of Species and Aromatic Crops*, 24(1), 33-36.
- Ogolla, F. O., Muraya, M. M. and Onyango, B. O. (2019). Variation in Temperature and Nutrient Source Influence the Growth of Exserohilum Turcicum Mycelia Isolated from Sorghum. *Journal of Scientific and Engineering Research*, 6(2), 93-99.
- Okalebo, J. R., Othieno, C. O., Woomer, P. L., Karanja, N. K., Semoka, J. R. M., Bekunda, M. A., Mugendi, D. N., Muasya, R. M., Bationo, A. and Mukhwana, E. J. (2006). Available Technologies to Replenish Soil Fertility in East Africa. *Nutrient Cycling in Agroecosystems*, 76, 153-170.
- Olomilua, A. I., Akanbi, O. and Ojeniyi, S. O. (2007). Effects of Pig Manure on Nutrient Composition, Growth and Yield of Okra. *Nigerian Journal of Soil Science*, 17, 109-112.
- Olsen, S. R., Cole, C. V., Watanabe, F. S. and Dean, L. A. (1954). *Estimation of Available Phosphorus in Soils By Extraction with Sodium Bicarbonate*. USA: U.S. Dep. Agric. Circ.939, USA.
- Rop, K., Karuku, G. N., Mbui, D., Njomo, N. and Michira, I. (2019). Evaluating the Effects of Formulated Nano-NPK Slow Release Fertilizer Composite on the Performance and Yield of Maize, Kale and Capsicum. *Annals of Agricultural Sciences*, 1-11.
- Tadesse, A. A. (2015). Growth and Yield Response of Garlic (Allium Sativum L.) Varieties to Nitrogen Fertilizers Rates at Gantaafeshum, Northern Ethiopia. MSc Thesis, Haramaya University.
- Uwah, D. F. and Eyo, V. E. (2014). Effects of Number and Rate Of Goat Manure Application on Soil Properties, Growth and Yield of Sweet Maize (Zea Mays L. Saccharata Strut). Sustainable Agriculture Research, 3(4), 75-83.

Intelligent 2D Outdoor Location Tracking System

Gachoki, Nelson¹, Kamau, Stanley² & Ikua, Bernard²

¹Kirinyaga University, Kenya

²Jomo Kenyatta Universuity of Agriculture & Technology, Kenya

Correspondence: ngachoki@kyu.ac.ke

Abstract

This paper presents results of ongoing work on development of a real-time outdoor positioning system for an escaping target. The overall goal is determination of the location of the target relative to the pursuer in real time and determination of the speed and direction of escape of the target from a pursuer. This paper highlights on the location of a ground moving target confined in a two dimensional (2D) arena. The location parameters of the target are obtained by use of global positioning system (GPS) then transmitted to a central computer for analysis. Velocity of the target in the arena is obtained by use of haversine equation and direction of escape is determined from triangle's equations. From the data the system determines if the target is escaping and the direction of escape. The results obtained can be used to inform the development of a pursuit algorithm.

Keywords: Outdoor Tracking, Positioning, Real-time tracking

Introduction

Diverse applications of electronic based positioning systems have necessitated widespread research in hardware and software for localization and tracking. Such applications include traffic navigation, military asset monitoring and wildlife management. The setup usually consist of a mapped arena, a target and computation algorithm.

In literature, many approaches have been proposed such as GPS compressive sensing for location acquisition (Song 2018),hybrid systems (Jiang,et-al 2010) and smartphone based systems. These approaches present stand-alone systems that presents results to the end user but are not easy to integrate with other electronic systems such as pursuit systems. In this paper, a platform is presented for locating a target in a 2D arena and determining whether the target is escaping or not.

Platform Design

The platform as shown in Figure 1 consists of a portable electronic station that can be attached to the target and a central computer running a program designed to monitor a randomly moving ground target.

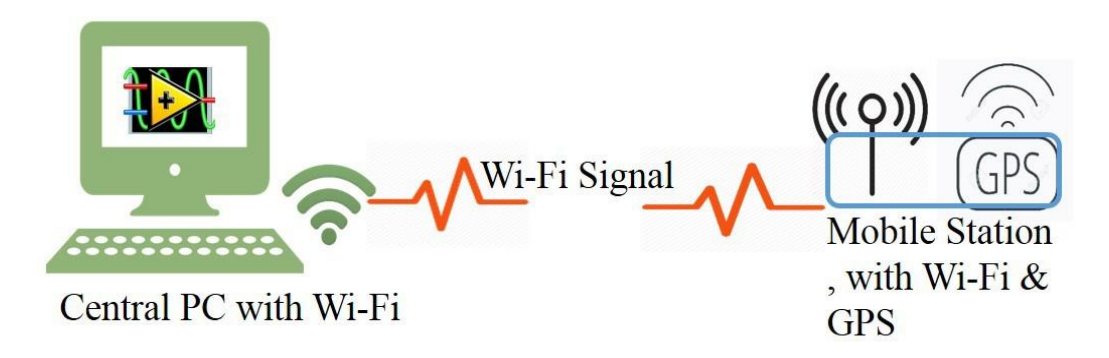


Figure 1: Platform

Communication between the central computer and mobile station is through Wireless fidelity (Wi-Fi). Wi-Fi is a wireless communication standard based on IEEE 802.11a with a range of about 100 metres (Lee& Shen 2007). The mobile station is equipped with GPS receiver and it receives the signals of several transmitters in known locations and computes its location based on the measured signals. The mobile GPS receiver is portable and with ability to endure outdoor environment for long. It should have a mobile power supply unit that could sustain it for a long time before recharging it.

The hardware for the system consist of Pmod GPS receiver, chipKIT WF32 both by Digilent and a rechargeable Li-ion 5V battery. The *PmodGPS* sensor uses UART interface for communication and was connected to WF32 TX (transfer data) and RX (receive data) pins. The chipKIT WF32 is a WiFi enabled Arduino based board with a PIC32 microcontroller (80 MHz). Detailed information of these boards are presented in their reference manuals (Micro, Czernek et-al 2016). The hardware also consists of a long range WiFi access point for connection of the mobile unit to the monitoring PC. The Station then uses triangulation in order to determine its location in latitudes and longitudes. This information is transmitted to the master station through a wireless data link.

The master station receives the data encoded in form of National Marine Electronics Association (NMEA) sentences. NMEA is a standard data format for GPS devices (Si 2011). NMEA data contains multiple data items in a single line separated by commas (Al-Taee et-al 2011). Each NMEA sentence begin with \$ and cannot be longer than 80 characters including line terminators

(Shoab 2013). In these sentences the data items are separated by commas. The main data items are Satellites in view, Longitude, Latitude, Altitude and Time. The sentences are then interpreted using a code in LabVIEW then distance and bearings are determined.

Once the coordinates are acquired, it is possible to determine the distance of the point of interest (say Q) from any other point on earth surface (say P) by use of haversine function (Winarno et-al 2017).

$$d = 2r\sin^{-1}\left(\sqrt{\sin^2\left(\frac{\phi_2 - \phi_1}{2}\right) + \cos(\phi_1)\cos\left(\phi_2\sin^2\left(\frac{\lambda_2 - \lambda_1}{2}\right)\right)}\right) \text{ where}$$

d is the space between two coordinates. *r* is the radius of the sphere

 Φ_1 , Φ_2 Longitude of position p and q.

 λ_1 , λ_2 Latitude of position p and q.

The function provides a means of determining the great circle distance which is the shortest distance between two points, measured along a sphere (Mishra 2016). See Figure 2.

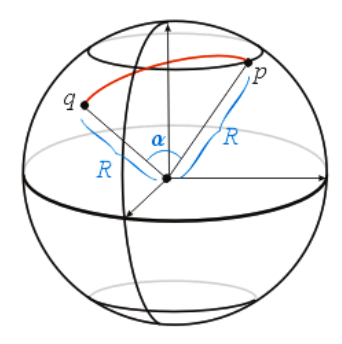


Figure 2: Great Circle Distance

In this case the sphere is the earth whose average radius at the equator is R. The equation determines the distance from point P to point Q along the indicated path as shown in the figure. The bearing is then computed from triangle geometry equations.

Test Setup and Results

Setup

The system was deployed for testing, where first the coordinates of a stationary pursuer were acquired and distance obtained against a stationary target as shown in Figure 3.

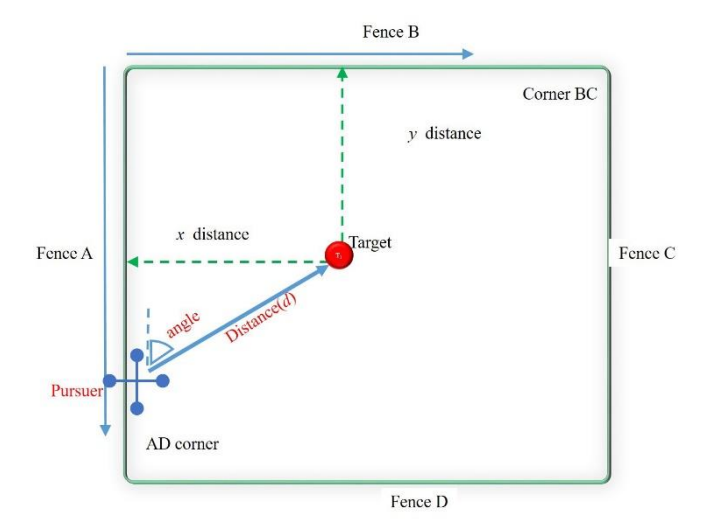


Figure 3: Target Distance

A program was developed in LabVIEW for acquisition of coordinates from microcontroller through WiFi as shown in Figure 4.

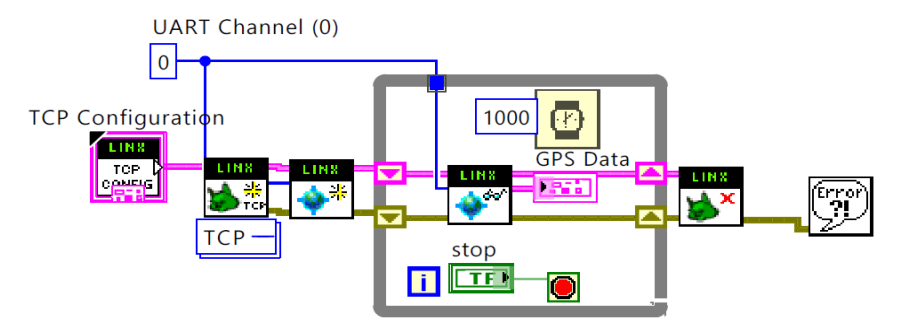


Figure 4: LabVIEW Screen-shot for Location Acquisition

The program acquires NMEA sentences from ChipKit WF32 through WiFi from UART channel 1. The sentences are then interpreted to give 11 parameters. These parameters include: -the Number of satellites in view, Time, Date, Longitude, Latitude, Altitude, Speed, Status and Fix type. The results obtained are represented in a graph and the distance of the target from reference points is obtained.

Experiments were carried out at the iPIC centre (JKUAT), sample was taken for the pursuer as shown in the screen-shot Figure 5.



Figure 5: GPS Parameters of Target

The device name box indicates the identity of the hardware used by the computer for data acquisition, Time provides the 24 hour clock data on the time of the experiment 10:23am, Date is the date when the data was taken (25th February).

Fix type (3) means that the data obtained is for three dimensional locations. The Status provides Navigation receiver warning status where A means OK and V indicates presence of a warning. Satellite in view gives the number of satellites available, the higher the number the better. The Latitude and Longitude data is given in decimal degrees while the altitude is in metres. Of these parameters, only the Latitude, the Longitude and Time are of interest to the research.

Results

The location of the target monitored and the motion pattern plotted as shown in Figure 6. The samples were taken at a constant time interval of 1 Second. The graph shows the Longitudes and Latitude location of the target.

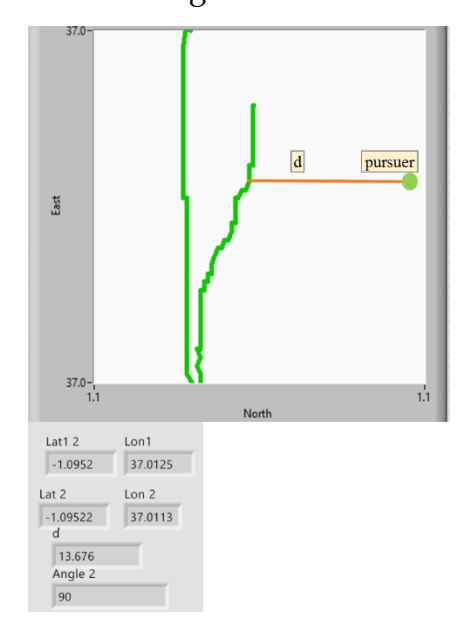


Figure 6: Target Map

The distance of the target from each wall was monitored and it was regarded as escaping when it was close to any of the walls and approaching it (speed is positive). This is shown in the screenshot of Figure 7. From the screenshot, the target state is "escaping" since it is close to wall C (0.9717m) hence the red dot on the screenshot and the speed of approach to wall C is positive (20.95m/s).

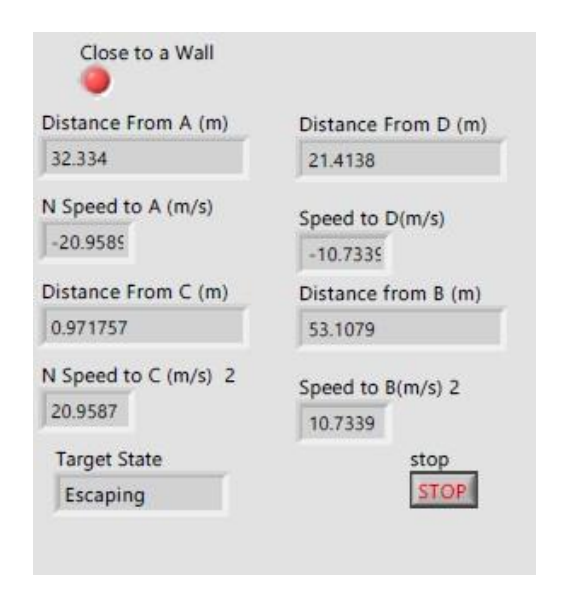


Figure 7: Target data

The distance from all other walls is above 5 metres (wall A=32.33m, wall B=53.1m and wall D=21.41m). The speed of approach to walls A and D is negative meaning it is moving far from the two walls. The speed of approach to wall B is positive (10.73m/s) but the target is not escaping through B since its far (53.1m) from wall B.

Conclusion

In this paper, partial results of development of a real-time outdoor positioning system for an escaping target are presented. Location parameters of the target in a two dimensional (2D) arena are obtained by use of global positioning system (GPS) then transmitted to a central computer for analysis. Velocity of the target in the arena is obtained by use of haversine equation and direction of escape is determined from triangle equations. From the data the system intelligently determines if the target is escaping. The results obtained can be used to inform the development of a pursuit algorithm.

References

Al-Taee, M. A. Khader, O. B. & Al-Saber N. A. (2007). Remote Monitoring of Vehicle Diagnostics and Location Using a Smart Box with Global Positioning System and General Packet Radio Service, In 2007 IEEE/ACS International Conference on Computer Systems and Applications, pp. 385–388, IEEE.

Czernek, W. Margas, W, Wyzgolik, R. Budzan, SZikebinski, A and R. Cupek, R (2016). Gps and Ultrasonic Distance Sensors for Autonomous Mobile Platform, *Studia Informatica*, Vol. 37, no. 4A, pp. 51–67

Jiang L, Hoe L. N., and Loon L. L., "Integrated uwb and gps location sensing system in hospital environment," in 2010 5th IEEE Conference on Industrial Electronics and Applications, pp. 286–289, IEEE, 2010.

Lee, J.S, Su, Y.W, Shen, C.C. (2007). A comparative Study of Wireless Protocols Bluetooth, UWB, Zigbee, and Wi-Fi, *Industrial Electronics Society*, Vol. 5, pp. 46–51.

Mishra, P.P. (2016). Deriving and Deducing the Equation of the Curve of Quickest Descent, *International Journal of Mathematics and its Applications*, Vol. 4, p. 7.

S. Micro, "Chipkit TM WF32 TM board reference manual,"

Shoab, M, Jain, K, Anulhaq, M & Shashi, M. (2013). *Development and Implementation of Nmea Interpreter for Real Time Gps Data Logging*, in 2013 3rd IEEE International Advance Computing Conference (IACC), pp. 143–146, IEEE.

Si, H& Aung, Z.M. (2011). Position Data Acquisition from Nmea Protocol of Global Positioning System. *International Journal of Computer and Electrical Engineering*, Vol. 3, no. 3, p. 353.

Song G. He, M., and Song P., "Gps signal acquisition based on compressive sensing," in 2018 *IEEE 18th International Conference on Communication Technology (ICCT)*, pp. 1013–1016, IEEE, 2018.

Winarno, W, Hadikurniawati, W & Rosso, R.N (2017). *Location based service for presence system using haver- sine method*, in 2017 International Conference on Innovative and Creative Information Technology (ICITech), pp. 1–4, IEEE,

Synthesis and Characterization of Nanoparticles from Extracts of Fruits of *Annona Muricata*: A Green Nanobiotechnology Approach

Gavamukulya, Y^{1,2,*}, Maina, E. N^{1,3}, El-Shemy, H. A^{1,4}, Wamunyokoli, F^{1,5}, & Magoma, G^1 .

¹PAUSTI, ²Busitema University, ³University of Nairobi, ⁴Cairo University, ⁵Jomo Kenyatta University of Agriculture and Technology

Correspondence: gavayahya@yahoo.com

Abstract

Green synthesis of nanoparticles from plant materials opens a new opportunity in nanobiotechnology and discourages use of expensive toxic chemicals. The aim of this study was to develop and optimise a method for synthesis of Silver Nanoparticles (AgNPs) from ethanolic extracts of fruits of Annona muricata as well as to characterise the green synthesized AgNPs. AgNPs were synthesized via AgNO₃ solution and characterized using spectroscopy and microscopy techniques. The formed AgNPs had an absorption maximum of 427 nm and were stable under different temperature, pH and storage conditions. Fourier Transform Infrared Resorption spectroscopy revealed the functional groups responsible for the synthesis and stabilization of the AgNPs. Scanning Electron Microscopy analysis revealed a spherical nature of the AgNPs while energy Dispersive X-Ray spectroscopy showed presence of Ag, Cl, Ca, and Si with Ag having the highest composition at 80%. X-Ray Diffraction and Dynamic Light Scattering revealed a crystalline nature of AgNPs with an average size of 60.12 nm and a polydispersity index of 0.1235 respectively. Transmission Electron Microscopy analysis further confirmed the crystalline and spherical nature of the AgNPs. This study reports an efficient, ecofriendly and low-cost method for synthesis and recovery of stable AgNPs using ethanolic extracts of Annona muricata fruits as both reducing and capping agents has been reported. The synthesized AgNPs could have many biomedical and clinical applications.

Keywords: Annona Muricata; Silver Nanoparticles (AgNPs); UV/VIS; FTIR; XRD; Fruit Extracts.

Introduction

Nanoparticles are materials that are small enough to fall within the nanometric range, with at least one of their dimensions being less than a few hundred nanometres. This reduction in size brings about significant changes in their physical properties with respect to those observed in bulk materials. A very interesting application of nanoparticles in the scope of life sciences is their use as 'smart' delivery systems where they are usually loaded with a drug or therapeutic agent (Gonzalez-Melendi et al., 2008). The various developed chemical and mechanical methods of producing nanoparticles include ball milling, thermal quenching, precipitation techniques, vapor deposition. However, these methods are often costly, and may result in toxic byproducts. Generally, nanoparticles are synthesized in three ways: physically by crushing larger particles, chemically by precipitation, and through gas condensation (Murphy et al., 2006; Wiley et al., 2007). The commercial significance of nanoparticles is limited by the nanoparticle synthesis process, which is generally energy intensive or requires toxic chemical solvents and is costly.

Annona muricata is known as Soursop (English), Graviola (Portuguese), Guanábana (Latin American Spanish), Omusitafeli / Ekitafeli (Uganda), and other local indigenous names as has been enlisted (Coria-Te´llez et al., 2018; Gavamukulya et al., 2017). The Annona muricata tree is about 5–10 m tall and 15–83 cm in diameter with low branches (Benavides et al., 2004; Orwa et al., 2009). It is widely distributed in the tropical regions of Central and South America, Western Africa, Central and Eastern Africa and Southeast Asia (Gavamukulya et al., 2015; Pinto et al., 2005) at altitudes below 1200 m above sea level, with temperatures between 25 and 28 °C, relative humidity between 60 and 80%, and annual rainfall above 1500 mm. The fruit is an edible collective ovoid berry, dark green in color.

The effectiveness of many species of medicinal plants depends on the supply of active compounds. It has therefore been widely proposed to combine herbal medicine with nanotechnology, because nanosystems can deliver the bioactive components at a sufficient concentration during the entire treatment period, directing them to the desired sites of action, and hence potentiating the action of the compounds, an aspect that conventional herbal treatments do not meet (Ansari et al., 2012; Bonifácio et al., 2014). Among several noble metal nanoparticles, silver nanoparticles have attained a special focus (Ahmed, Ahmad, et al., 2016a). Silver nanoparticles are of particular interest because of their antimicrobial, anticancer and cytotoxic activities. The aim of this study was therefore to develop and optimise a method for the synthesis of AgNPs from ethanolic extracts of fruits of *Annona muricata* as well as to characterise the green synthesized AgNPs.

Materials and Methods

Samples collection, authentication, preparation and extraction

Ripe fruits of *Annona muricata* were collected from the wild in Eastern Uganda in the districts of Kaliro, Iganga and Mbale during the month of January 2018. A sample of the plant was collected, pressed, dried and the plant was identified and authenticated in the Makerere University Botanical Herbarium (MHU) by Dr Namaganda Mary and a voucher specimen was deposited in the herbarium with the accession number MHU50860. The Fruits of *Annona muricata* were washed with clean water and then peeled to remove the fresh pulp. The pulp was then cut into small pieces and placed in a hot air oven to dry at 50°C for a week. The dried pulp was then milled into a powder using an electric grater. 50 g of powdered fruits were extracted using 250 ml of absolute ethanol for three days by the plant tissue homogenization method as previously described (Gavamukulya et al., 2014). The light brown Ethanolic Extracts of *Annona muricata* fruits was then filtered and kept at 4°C until use.

Synthesis of Silver Nanoparticles

AgNPs were synthesized by the following method. About 50 ml of the filtered fruits extract was mixed with about 450 ml of 1 mM AgNO₃ solution in a 500ml flask and mixed thoroughly, forming a uniform mixture. The mixture was then rested at room temperature in the dark storage cabinets for up to about 72 hours, with continuous monitoring. After about 3hours, the mixture was observed to start changing from light brown to yellowish brown. After about 72 hours, the mixture had completely changed colour to dark brown. This color change is visual evidence of formation of AgNPs or reduction of silver ions into AgNPs due to the excitation of surface plasmon vibration (Ezealisiji et al., 2017; P. & T., 2017; Santhosh et al., 2015).

Characterization of the AgNPs

The synthesis of AgNPs from the ethanolic extract of fruits of *Annona muricata* was further confirmed by ultraviolet - visible spectroscopy (UV/VIS) in the range of between 300nm to 650nm (Kumar et al., 2017; Santhosh et al., 2015) and ethanol was used as a blank.

About 10ml of the formed AgNPs suspension in boiling tubes were subjected to different temperature conditions by heating in a digital water bath for about 3 minutes each and measuring the absorbance spectra on the UV/VIS in a scan range of 350nm to 650nm (Ghoshal & Bhatnagar, 2017). The temperature tested included room temperature (25°C), 35°C, 45°C, 55°C, 65°C, 75°C, and 85°C.

About 15ml of the formed AgNPs suspension was aliquoted into 5 test tubes each containing about 3 ml of the AgNPs suspension. The suspensions in the test tubes were then adjusted to and subjected to different pH conditions ranging from about pH 2 to about pH 11. The suspension in each test tube was subjected to a different pH condition. The specific pH conditions tested were pH 2, 4, 7, 9, and 11. The pH were adjusted by either adding drops of 1N NaOH or 1N HCl until the desired pH was achieved as observed on the pH meter (Ghoshal & Bhatnagar, 2017; Verma & Mehata, 2016). The absorbance spectra of the suspensions were then measured on the UV/VIS in a scan range of 300nm to 650nm.

About 20ml of the formed AgNPs suspension was aliquoted into four 15ml universal tubes each containing about 5 ml of the AgNPs suspension. The suspensions in the tubes were then stored at different temperature conditions for a period of 3 months. The temperatures at which the storage was done included room temperature (which varied between at about 20°C to 30°C during the experimental period), 4°C, -20°C and -80°C. At the end of the 3 months, the samples were retrieved from the different storage facilities allowed to thaw at room temperature and then their absorbance spectra were measured on the UV/VIS in a scan range of 300nm to 650nm.

Recovery of the synthesized AgNPs and further characterizations

About 400 ml of the AgNPs suspension were transferred into different plastic bottles of about 250ml capacity each and frozen in freezer at -80°C for a period of about 12 hours. The frozen suspension was then removed from the freezer and allowed to completely thaw at room temperature. Upon thawing, the AgNPs were visibly observed spread throughout the now much clear suspension. The suspension with the dispersed AgNPs were then recovered by transferring them into 50ml universal centrifuge tubes and centrifuging them at and RCF of 4025 g for a period of between about 20 minutes to about 45 minutes. After

centrifugation, the supernatant in each of the tubes was poured off and the silver nanoparticles were retained as pellets at the bottom of the tubes. The pellets were then washed several times with distilled water (about 10ml of distilled water were added to each tube and then centrifuged afresh for about 5 minutes to wash and dissolve any water-soluble impurities). The now clean AgNPs were then lyophilized and kept in airtight tubes at 4°C until further use. A total of 1.2 g of AgNPs were recovered following lyophilization.

FTIR measurements were carried out to identify the promising biomolecules in the *Annona muricata* ethanolic extract accountable for the reduction of the silver ions and also the capping agents liable for the stability of the bio-reduced AgNPs as previously reported (Madivoli et al., 2018). The representative FTIR spectra of the recovered and dried AgNPs synthesized from ethanolic extracts of fruits of *Annona muricata* were recorded and the major and minor peaks were manifested and identified accordingly.

Scanning electron morphological analysis of Silver nanoparticles were performed using Scanning electron microscope FEI XL30 Sirion FEG (Oxford Instruments Plc, Abingdon, United Kingdom) operated at an accelerating voltage of 6 kV. The system was equipped with an Energy Dispersive X-ray Spectrometer (EDX) system from EDAX having a lithium doped silicon detector.

TEM was employed to characterize the size, shape and morphologies of formed biogenic synthesized AgNPs. A drop of AgNPs suspension was deposited on carbon coated copper grids and the film on grid was then dried. The TEM was operated and the measurements were performed at accelerating voltage of 100 KV.

XRD analysis was employed to determine the average crystalline size of the AgNPs formed. The XRD diffraction data was analyzed using the Match! Software (Crystal Impact, Bonn, Germany) and the average crystalline size of the AgNPs formed in the bio-reduction was determined using the Scherrer equation, with a constant of 0.94.

The hydrodynamic size distributions and polydispersity index (PDI) of the silver nanoparticles were analyzed by using dynamic light scattering (DLS) instrumentation. The average particle size, size distribution by intensity as well as PDI were determined by

injecting 1:20 dilution of silver nanoparticle resuspension into the U-shaped glass cuvette of the photon correlation microscope as previously reported (Danaei et al., 2018; Ezealisiji et al., 2017; Kumar et al., 2017).

Results

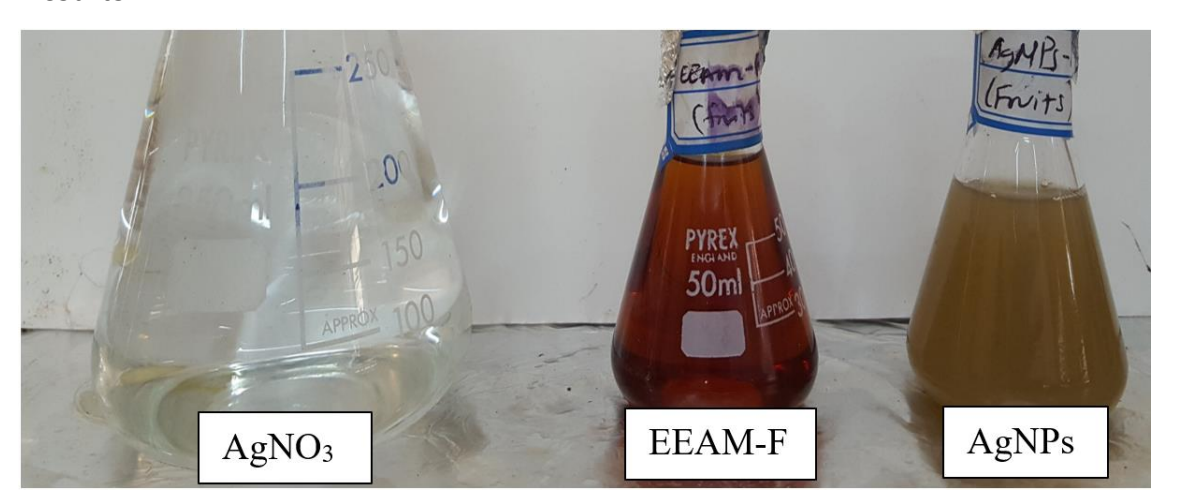


Figure 1: Photo showing colour of the green synthesized AgNPs relative to the Ethanolic extract of *Annona muricata* fruits (EEAM-F) and Silver Nitrate solution (AgNO₃).

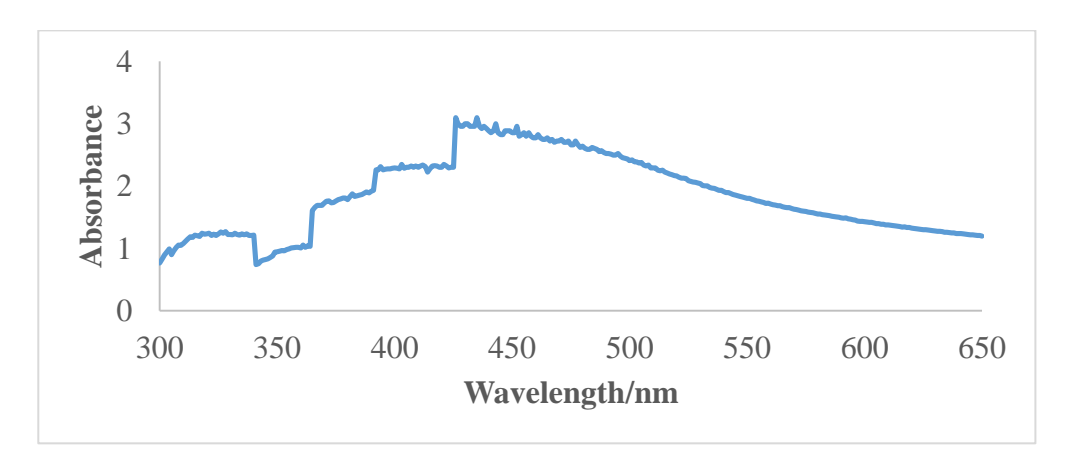


Figure 2: UV/VIS spectrum of fruits derived AgNPs at 72 hours of incubation.

The spectrum shown in figure 3 above has a maximum absorption peak at a wavelength of about 427 nm, which is in the range of the surface plasmon resonance for AgNPs which is reported to have an absorption maximum of between about 400nm to about 450nn.

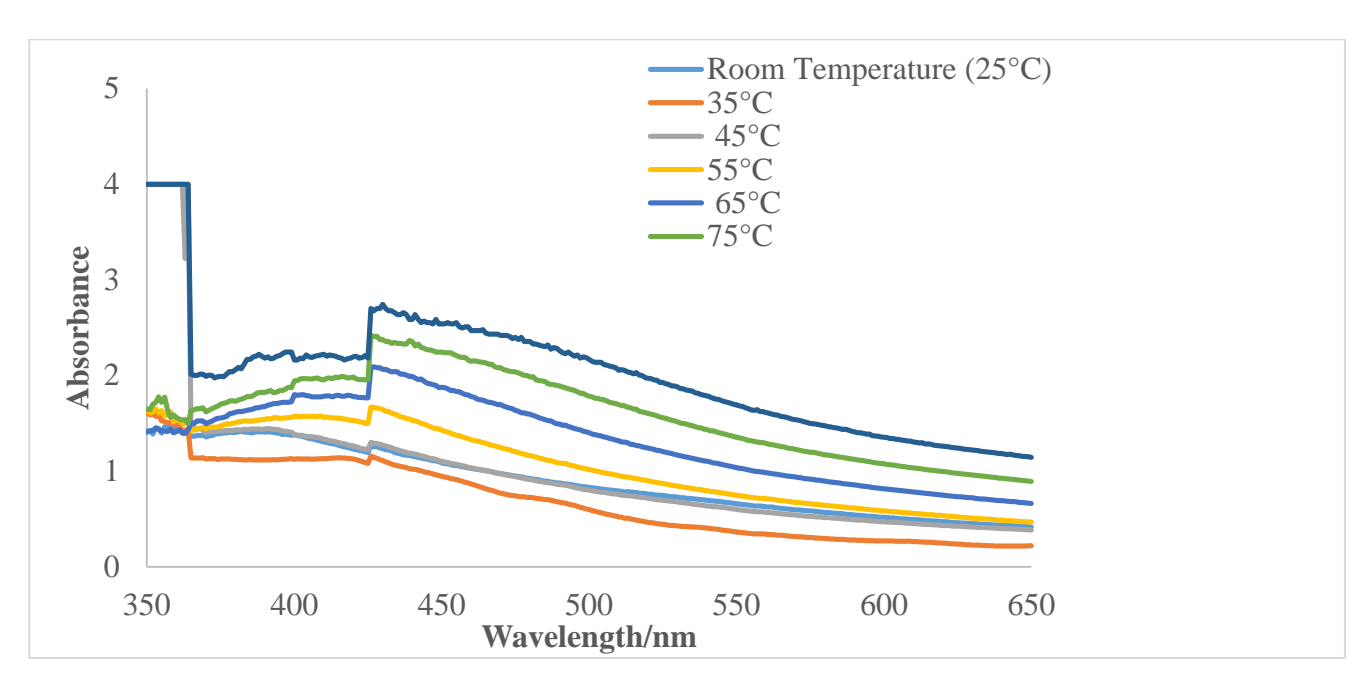


Figure 3: UV/VIS spectra showing temperature stability of AgNPs synthesized from fruits extract

From Figure 3 above it is evident that at all temperatures tested, the AgNPs remained stable maintaining a characteristic absorption maximum of about between 420nm to about 430nm which is within the AgNPs range.

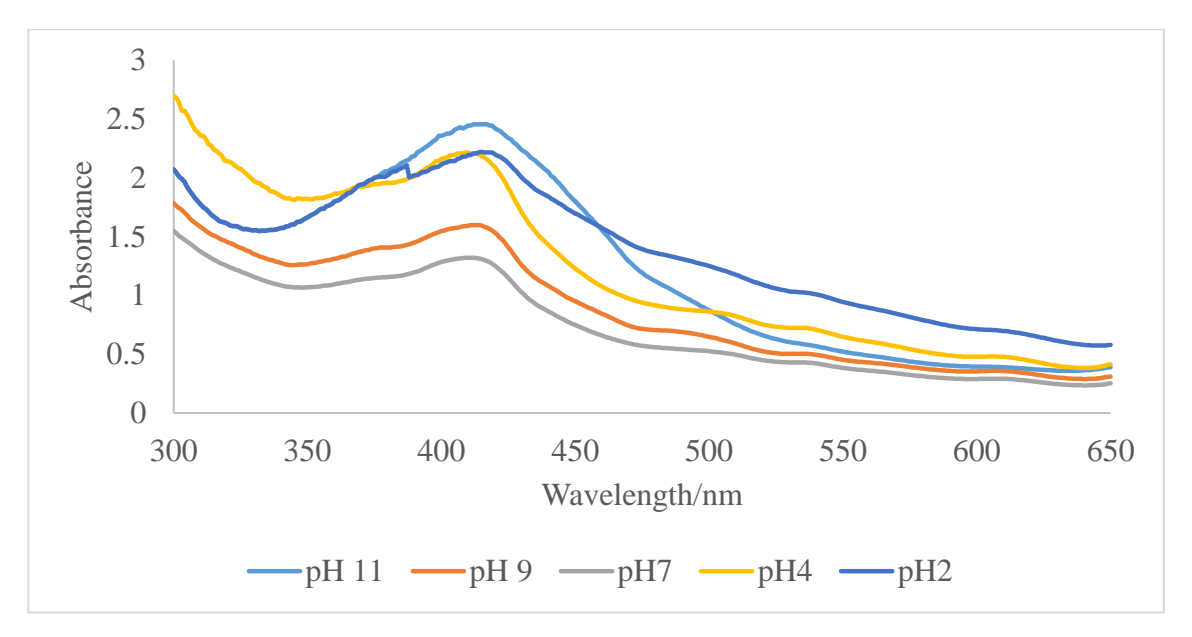


Figure 4: UV/VIS spectra showing pH stability of AgNPs synthesized from fruits extract From Figure 4 above, it is evident that at all pH conditions tested, the AgNPs remained stable maintaining a characteristic absorption maximum of about between 410nm to about

420nm which is within the AgNPs range. There was a notable and strong relationship between AgNPs absorption spectra at extreme acidic and alkaline pH conditions of 2 and 11.

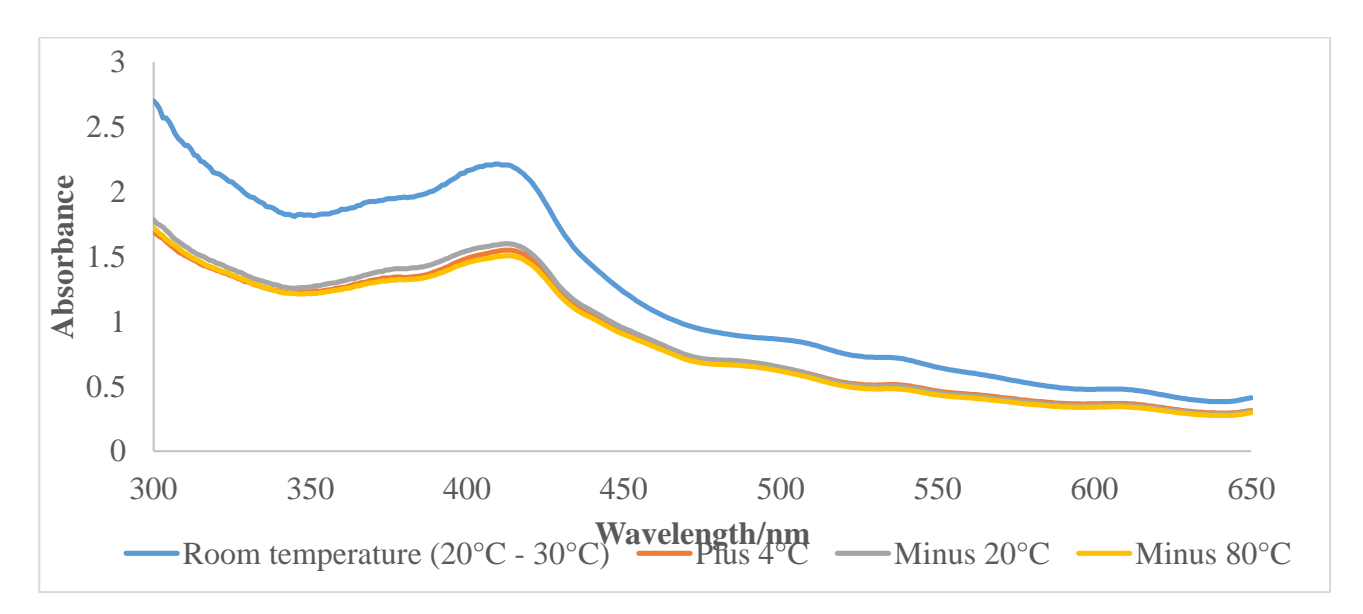


Figure 5: UV/VIS spectra showing storage stability of AgNPs synthesized from fruits extract From Figure 5 above, it is evident that at all storage temperatures tested for the 3 months, the AgNPs remained stable maintaining a characteristic absorption maximum of about between 410nm to about 430nm which is within the AgNPs range. There was a notable increase in the absorption of the AgNPs at room temperature compared to other storage conditions, nevertheless, the absorption maximum was maintained in the AgNPs range.

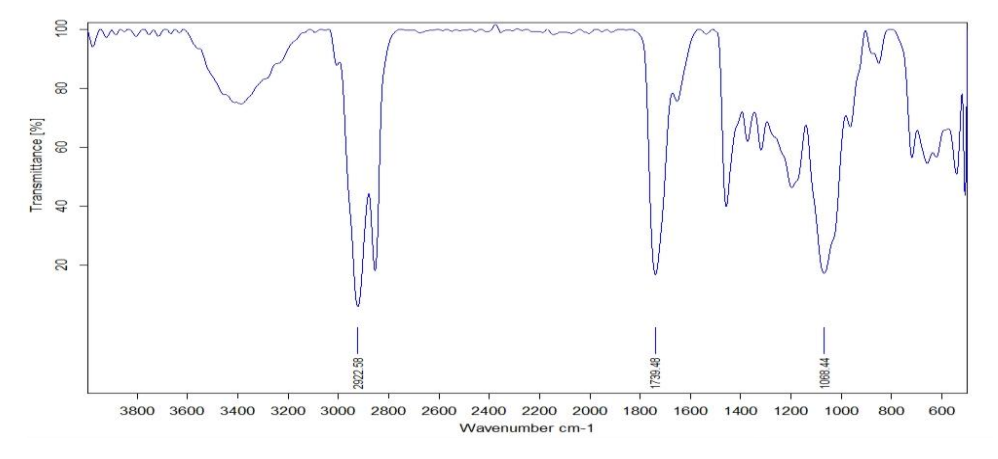


Figure 6: FTIR spectra of functional groups from the AgNPs synthesized from fruits extract

Table 1: FTIR functional group analysis of biosynthesized AgNPs from ethanolic extracts of Fruits of *Annona muricata*

Type of Peak	Frequency (cm-1)	Bond	Functional groups	
Major	2922.58	C-H stretch	Alkanes and alkyls	
	2850	C-H stretch	Alkanes and alkyls	
	1739.48	C=O stretch	Aldehyde and	
			Esters	
	1500	N-O Stretch	Nitro group	
	1068.44	C-O stretch	Alcohol group	
Minor	3400	O-H Stretch	Carboxylic acids	
	1650	C=O stretch	Amide	
	1400	-C-H Bend	Alkane	
	1200	C-O stretch	Acid	
	900	=C-H bend	Alkenes	
	700	C-Cl Stretch	Alkyl halide	
	550	C-Br Stretch	Alkyl halide	

As shown in Figure 6 and Table 1 above the functional groups responsible for the formation of the AgNPs included; Alkanes and alkyls, aldehydes and esters, nitro groups, alcohol groups, carboxylic acids, amides, alkenes, acids and alkyl halides.

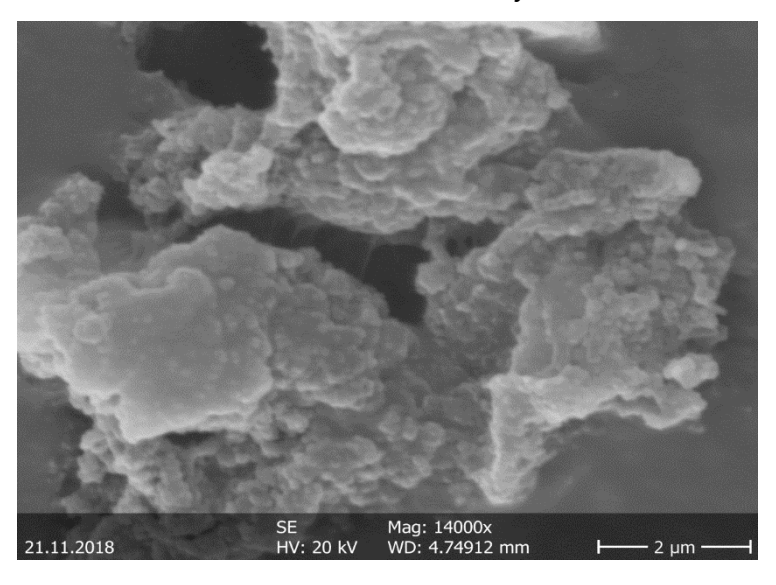


Figure 7: SEM micrograph showing the shape of AgNPs synthesized from fruits extract

As shown in Figure 7 above, the AgNPs were approximately spherical in shape with smooth surface. These results are in agreement with the shape of SPR band recognized from the UV-visible spectrum with absorption maximum at 427nm

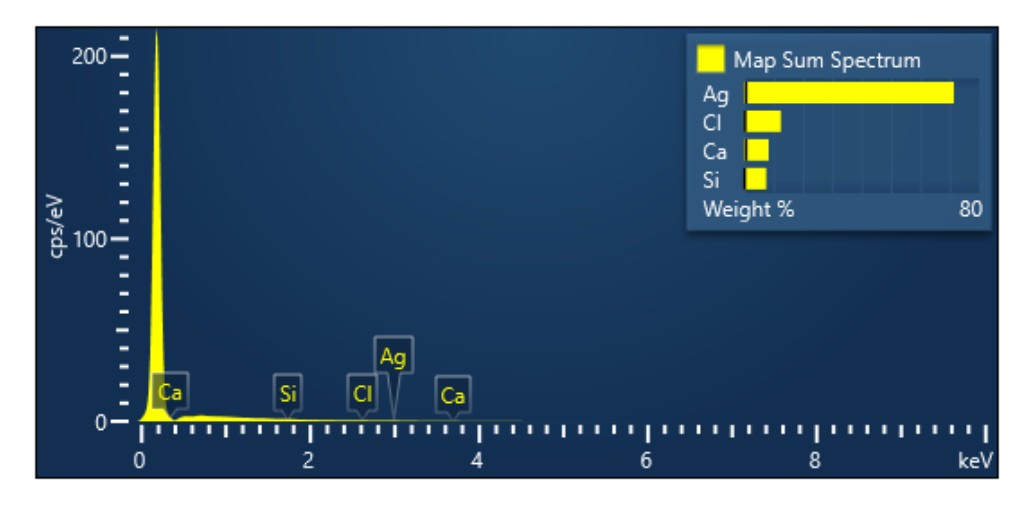


Figure 8: Energy Dispersive X-ray Spectrometer (EDX) spectra demonstrating the quantitative amounts of different elements present in the AgNPs synthesized from the fruits extract.

From Figure 8 above, the EDX spectra showed the presence of elements such as Ag, Cl, Ca, and Si. EDX quantitative analysis demonstrated that the highest concentration of a single element in the *Annona muricata* derived AgNPs was silver (Ag), at about 80%.

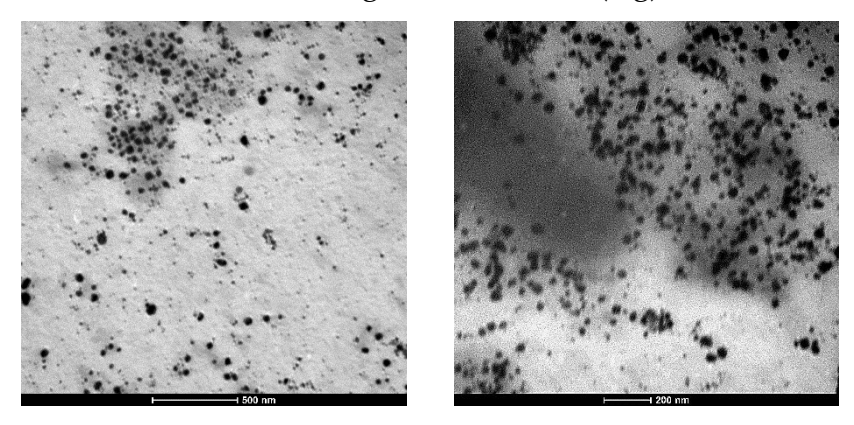


Figure 9: TEM Micrographs of the AgNPs at different resolutions

Figure 9 above shows the TEM micrographs of the AgNPs at different resolutions. The Micrographs reveal a spherical nature of the monodispersed AgNPs as well as a crystalline structure. Particle size analysis using the Image-J software further revealed the AgNPs having an average particle size of about 51 nm.

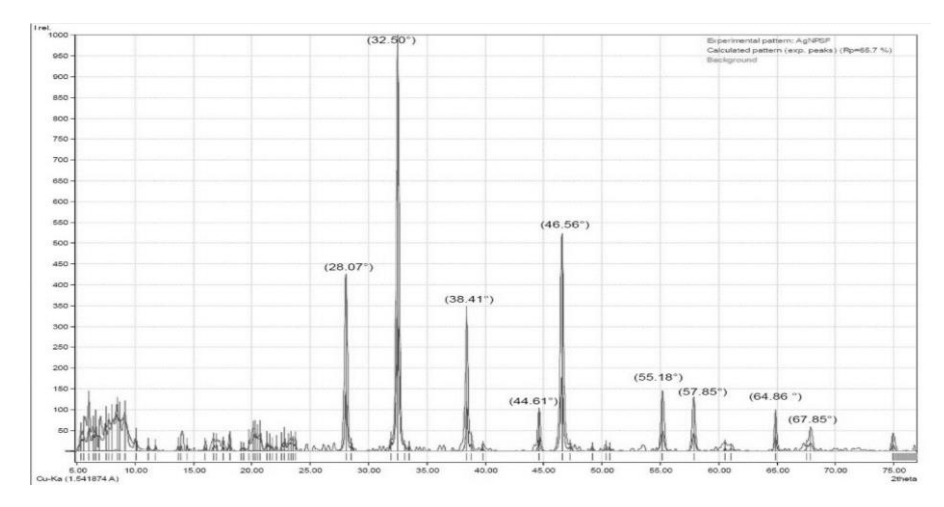


Figure 10: XRD diffraction pattern spectra of AgNPs synthesized from fruits extract

Figure 10 above shows the typical XRD pattern of biosynthesized AgNPs derived from ethanolic extracts of fruits of *Annona muricata*. Nine prominent diffraction peaks were observed at 28.07°, 32.50°, 38.41°, 44.61°, 46.56°, 55.18°, 57.85°, 64.86°, and 67.85°. The average size of the AgNPs formed in the bio-reduction was determined using the Scherrer equation and is estimated as 60.12 nm.

Table 2: DLS Analysis results

Counts	Intensity (kCnt/s)	Attenuation Level (%)	Diameter	PD Index
			(nm)	
1	1361	95.1	103.3	1.268e-01
2	1331	95.1	103.9	1.047e-01
3	1378	95.1	103.7	1.105e-01
4	1360	95.1	103.3	1.349e-01
5	1321	95.1	103.1	1.406e-01
Mean	1350	95.1	103.5	1.235e-01

Table 2 above shows the DLS analysis revealing the average particle size for the AgNPs as 103.5 nm with a polydispersity index of 0.1235.

Discussions and Conclusion

It has been known for a long time that silver nanoparticles exhibit a yellowish/ dark brown color in solution due to excitation of surface plasmon vibrations in AgNPs, and therefore reduction of the silver ion to AgNPs during exposure to the plant extracts could be followed by color change and thus UV/VIS spectroscopy (Ahmed, Saifullah, et al., 2016; Song & Beom, 2009). In the current study, the AgNPs formation was confirmed by the change in colour of the mixture from light brown to dark brown indicating the successful green synthesis process. The UV/VIS maximum absorption spectra of the synthesized AgNPs was recorded at 427nm which is in range with previously reported studies on synthesis on AgNPs from plant extracts. Various studies have reported synthesis of AgNPs with UV/VIS absorption maxima at 435nm(Kumar et al., 2017), 430nm (Song & Beom, 2009), 420nm (Ezealisiji et al., 2017; S. B. Santhosh et al., 2015), 410nm (Otari et al., 2017) among others. The current results further provide, for the first time, a confirmation on the use of the *Annona muricata* fruits extracts in the green synthesis of AgNPs as a cheap and eco-friendly approach.

The importance and use of any substances greatly depend on its stability under different conditions. In the current study, the temperature and heat stability, pH and storage stability of the biosynthesized AgNPs was studied and results have been presented. From the results on temperature stability, it is evident that at all temperatures tested, the AgNPs remained stable maintaining a characteristic absorption maximum of about between 420nm to about 430nm which is within the AgNPs range (Kumar et al., 2017; Shah et al., 2015). This is very important implying that the AgNPs can be stable under various temperature/ heating conditions without losing their effectiveness.

In relation to pH stability, it is evident that at all pH conditions tested, the AgNPs remained stable maintaining a characteristic absorption maximum of about between 410nm to about 420nm which is within the AgNPs range (Malik et al., 2014). This is very important implying that the AgNPs can be stable under various pH conditions without losing their effectiveness. This property is very important especially of the AgNPs are going to be delivered via the gastrointestinal tract which has gradients of pH conditions. The reported

stability plays a critical role in ensuring maintenance of effectiveness of the AgNPs and thus helps overcome one of the obstacles encountered by many conventional crude extracts from plants which lose effectiveness *in vivo* due to the changing pH gradients as previously reported (Bonifácio et al., 2014).

Storage stability is very important implying that the AgNPs can be stable under different storage temperature conditions without losing their effectiveness for long periods of time. The notable increase in the absorption of the AgNPs at room temperature compared to other storage conditions, could probably be attributed to the continuous exposure to the same conditions as those used in the synthesis process thereby allowing the process of formation of the AgNPs to continue throughout the storage period, albeit at very low rates.

Recovery of the biosynthesized AgNPs is of critical importance in the synthetic process. Various methods have been reported about the recovery of AgNPs (Shah et al., 2015). In the current study, we developed a blended method for quick and fast recovery of the AgNPs. We introduced a step where the AgNPs suspension is frozen for a period of 12-48 Hrs followed by thawing, centrifugation, washing and then drying. The freezing step allows for the particles to aggregate and thus easy sedimentation when the centrifugation step is conducted. This is the first study to report on such an optimization in the recovery of AgNPs.

FTIR results showed that the functional groups responsible for the formation of the AgNPs from ethanolic extracts of fruits of *Annona muricata* included; Alkanes and alkyls, aldehydes and esters, nitro groups, alcohol groups, carboxylic acids, amides, alkenes, acids and alkyl halides. These are probably due to the presence of most of the secondary metabolites reported much earlier in the plant (Ezealisiji et al., 2017; Gavamukulya et al., 2014, 2017). The AgNPs were approximately spherical in shape with smooth surface. These results are in agreement with the shape of SPR band recognized from the UV- visible spectrum with absorption maximum at 427nm. Many previous studies reported different shapes of AgNPs including spherical, conical, cuboidal, hexagonal, pentagonal among others (Ahmed, Ahmad, et al., 2016b; Malik et al., 2014). The spherical AgNPs synthesized in the current study are therefore in line with the expected shapes for AgNPs. Similarly, EDX elemental

analysis revealed that the AgNPs were composed of various elements as reported much earlier, with Ag taking the highest percentage composition at 80%. These results indicate the high purity of the AgNPs albeit with a few contaminants at the different subtle concentration which are probably due to the environmental conditions used during the synthesis process. Earlier studies on had also reported elemental compositions of AgNPs having Ag as the principle component (Nakkala et al., 2014; Otunola & Afolayan, 2018).

From the XRD diffraction patterns, the 2θ peaks observed at 38.41°, 44.61°, and 64.86° corresponds to (111), (200), and (220) reflection planes representing the face centered spherical structure of silver respectively (Kumar et al., 2016, 2017). The extra peaks near to 28.07°, 32.50°, 46.56°, 55.18°, 57.85°, and 67.85° are due to the presence of bio-organic phase on the surface of particles. Generally, the broadening of peaks in the XRD patterns of solids signifies smaller particle size and reflects the effects of the experimental conditions on the nucleation and growth of the crystal nuclei (Kumar et al., 2017; Otunola & Afolayan, 2018; Umadevi et al., 2012). The average size of the AgNPs formed in the bio-reduction was estimated as 60.12 nm. TEM analysis further confirmed the crystalline and spherical nature of the monodispersed AgNPs. The average particle size as determined by TEM analysis was on average 51 nm, which is within range with that calculated using XRD.

Dynamic light scattering is a method that depends on the interaction of light with particles and the method can be used for measurements of narrow particle size distributions especially in the range of 2–500 nm (Tomaszewska et al., 2013). The AgNPs size was larger as presented by DLS (103.5 nm) as compared to XRD (60.12 nm) and TEM (51 nm). This difference could be explained by the fact that the size measured by DLS is based on a combination of the particles as well as the hydrodynamic radius which is not a true size of the AgNPs due to the hydration layer around the particles as well as the presence of capping and stabilizing agents as previously explained (Danaei et al., 2018; Ezealisiji et al., 2017).

Polydispersity Index measures the homogeneous nature of nanoparticles, the smaller the PDI the more homogeneous nanoparticles. It is basically a representation of the distribution of size populations within a given sample. The numerical value of PDI ranges from 0.0 (for a perfectly uniform sample with respect to the particle size) to 1.0 (for a highly polydisperse sample with multiple particle size populations). Values of 0.2 and below are most commonly

deemed acceptable in practice for polymer-based nanoparticle materials, while nanoparticles with PDI smaller than 0.3 is considered acceptable for drug delivery (Clarke, 2013; Danaei et al., 2018). The synthesized AgNPs had an average PDI of 0.1235, which is a great indication that they are highly homogenous and would be effectively used in various applications.

In conclusion, we have reported and optimized for the first time an efficient, eco-friendly and low-cost method for the synthesis and recovery of AgNPs using ethanolic extracts of fruits of *Annona muricata*. The synthesized AgNPs are stable under different temperature, pH and storage conditions. The method used resulted into formation and recovery of spherical crystalline monodispersed AgNPs with an average size of about 60.12 nm and a polydispersity index of 0.1235. With the successful synthesis of AgNPs in the current study, we do recommend further studies aimed at testing the synthesized AgNPs from this method for different biomedical and clinical bioactivities such as Antimicrobial, Anticancer, Anti-inflammatory, Antimalarial, Antidiabetic, Toxicities among others as a step towards the pharmaceutical utilization of these green synthesized AgNPs.

References

- Ahmed, S., Ahmad, M., Swami, B. L., & Ikram, S. (2016a). A review on plants extract mediated synthesis of silver nanoparticles for antimicrobial applications: A green expertise. *Journal of Advanced Research Cairo University Journal of Advanced Research*, 7, 17–28. https://doi.org/10.1016/j.jare.2015.02.007
- Ahmed, S., Ahmad, M., Swami, B. L., & Ikram, S. (2016b). A review on plants extract mediated synthesis of silver nanoparticles for antimicrobial applications: A green expertise. *Journal of Advanced Research*, 7(1), 17–28. https://doi.org/10.1016/j.jare.2015.02.007
- Ahmed, S., Saifullah, Ahmad, M., Swami, B. L., & Ikram, S. (2016). Green synthesis of silver nanoparticles using Azadirachta indica aqueous leaf extract. *Journal of Radiation Research and Applied Sciences*, 9(1), 1–7. https://doi.org/10.1016/j.jrras.2015.06.006
- Ansari, S. H., Islam, F., & Sameem, M. (2012). Influence of nanotechnology on herbal drugs:

 A Review. *Journal of Advanced Pharmaceutical Technology & Research*, 3(3), 142–146. https://doi.org/10.4103/2231-4040.101006
- Benavides, A., González, A., & Cisne Contreras, J. (2004). Numerical characterization of African Journal of Science, Technology and Engineering Vol. 1, 2020 Page **167** of **232**

- Guanabana (Annona muricata L.) germplasm Sampling in situ in the Pacific and northern Nicaragua. *La Calera*, 10(15), 46–52.
- Bonifácio, B. V., Silva, P. B. da, Ramos, M. A. D. S., Negri, K. M. S., Bauab, T. M., & Chorilli, M. (2014). Nanotechnology-based drug delivery systems and herbal medicines: a review. *International Journal of Nanomedicine*, 9, 1-15. https://doi.org/10.2147/IJN.S52634
- Clarke, S. P. (2013). *Development of Hierarchical Magnetic Nanocomposite Materials for Biomedical Applications*. Ph.D. Thesis, Dublin City University, Northside, Dublin.
- Coria-Te´llez, A. V., Montalvo-Gonzalez, E., Yahia, E. ., & Obledo-Va´Zquez, E. N. (2018). Annona muricata: A comprehensive review on its traditional medicinal uses , phytochemicals, pharmacological activities, mechanisms of action and toxicity. *Arabian Journal of Chemistry*, 11(5), 662–691. https://doi.org/10.1016/j.arabjc.2016.01.004
- Danaei, M., Dehghankhold, M., Ataei, S., Hasanzadeh Davarani, F., Javanmard, R., Dokhani, A., ... Mozafari, M. R. (2018). Impact of particle size and polydispersity index on the clinical applications of lipidic nanocarrier systems. *Pharmaceutics*, 10(2), 1–17. https://doi.org/10.3390/pharmaceutics10020057
- Ezealisiji, K. M., Noundou, X. S., & Ukwueze, S. E. (2017). Green synthesis and characterization of monodispersed silver nanoparticles using root bark aqueous extract of Annona muricata Linn and their antimicrobial activity. *Appl Nanosci*, *7*, 905–911. https://doi.org/10.1007/s13204-017-0632-5
- Gavamukulya, Y., Abou-Elella, F., Wamunyokoli, F., & El-Shemy, H. A. (2014). Phytochemical screening, anti-oxidant activity and in vitro anticancer potential of ethanolic and water leaves extracts of Annona muricata (Graviola). *Asian Pacific Journal of Tropical Medicine*, 7(Suppl 1), S355–S363. https://doi.org/10.1016/S1995-7645(14)60258-3
- Gavamukulya, Y., Abou-Elella, F., Wamunyokoli, F., & El-Shemy, H. A. (2015). GC-MS Analysis of Bioactive Phytochemicals Present in Ethanolic Extracts of Leaves of Annona muricata: A Further Evidence for Its Medicinal Diversity. *Pharmacogn. J*, 7(5), 300–304. https://doi.org/10.5530/pj.2015.5.9
- Gavamukulya, Y., Wamunyokoli, F., & El-Shemy, H. A. (2017). Annona muricata: Is the natural therapy to most disease conditions including cancer growing in our backyard?

 African Journal of Science, Technology and Engineering Vol. 1, 2020 Page 168 of 232

- A systematic review of its research history and future prospects. *Asian Pacific Journal of Tropical Medicine*, 10(9), 835–848. https://doi.org/10.1016/J.APJTM.2017.08.009
- Ghoshal, G., & Bhatnagar, S. (2017). Rapid Green Synthesis of Silver Nanoparticles (AgNPs)

 Using (Prunus persica) Plants extract: Exploring its Antimicrobial and Catalytic Activities. *J Nanomed Nanotechnol*, 84172(8), 4522157–4527439. https://doi.org/10.4172/2157-7439.1000452
- Gonzalez-Melendi, P., Fernandez-Pacheco, R., Coronado, M. J., Corredor, E., Testillano, P. S., Risueo, M. C., ... Perez-de-Luque, A. (2008). Nanoparticles as Smart Treatment-delivery Systems in Plants: Assessment of Different Techniques of Microscopy for their Visualization in Plant Tissues. *Annals of Botany*, 101(1), 187–195. https://doi.org/10.1093/aob/mcm283
- Kumar, B., Angulo, Y., Smita, K., Cumbal, L., & Debut, A. (2016). Capuli cherry-mediated green synthesis of silver nanoparticles under white solar and blue LED light. *Particuology*, 24, 123–128. https://doi.org/10.1016/j.partic.2015.05.005
- Kumar, B., Smita, K., Cumbal, L., & Debut, A. (2017). Green synthesis of silver nanoparticles using Andean blackberry fruit extract. *Saudi Journal of Biological Sciences*, 24(1), 45–50. https://doi.org/10.1016/J.SJBS.2015.09.006
- Madivoli, E. S., Maina, E. G., Kairigo, P. K., Murigi, M. K., Ogilo, J. K., Nyangau, J. O., ... Kipyegon, C. (2018). In vitro antioxidant and antimicrobial activity of Prunus africana (Hook. f.) Kalkman (bark extracts) and Harrisonia abyssinica Oliv. extracts (bark extracts): A comparative study. *Journal of Medicinal Plants for Economic Development*, 2(2), 1–9. https://doi.org/10.4102/jomped.v2i1.39
- Malik, P., Shankar, R., Malik, V., Sharma, N., & Mukherjee, T. K. (2014). Green Chemistry Based Benign Routes for Nanoparticle Synthesis. *Journal of Nanoparticles*, 2014, 1–14. https://doi.org/10.1155/2014/302429
- Murphy, C. J., Gole, A. M., Hunyadi, S. E., & Orendorff, C. J. (2006). One-Dimensional Colloidal Gold and Silver Nanostructures. *Inorganic Chemistry*, 45(19), 7544–7554. https://doi.org/10.1021/ic0519382
- Nakkala, J. R., Mata, R., Gupta, A. K., & Sadras, S. R. (2014). Biological activities of green silver nanoparticles synthesized with Acorous calamus rhizome extract. *European Journal of Medicinal Chemistry*, 85, 784–794. https://doi.org/10.1016/j.ejmech.2014.08.024

- Orwa, C., Mutua, A., & Kindt, R. (2009). Agroforestree database: a tree species reference and selection guide version 4.0. *ICRAF*, *Nairobi*, *KE*.
- Otari, S. V., Pawar, S. H., Patel, S. K. S., Singh, R. K., Kim, S. Y., Lee, J. H., ... Lee, J. K. (2017). Canna edulis leaf extract-mediated preparation of stabilized silver nanoparticles: Characterization, antimicrobial activity, and toxicity studies. *Journal of Microbiology and Biotechnology*, 27(4), 731–738. https://doi.org/10.4014/jmb.1610.10019
- Otunola, G. A., & Afolayan, A. J. (2018). In vitro antibacterial, antioxidant and toxicity profile of silver nanoparticles green-synthesized and characterized from aqueous extract of a spice blend formulation. *Biotechnology and Biotechnological Equipment*, 32(3), 724–733. https://doi.org/10.1080/13102818.2018.1448301
- P., P. S., & T., K. S. (2017). Antioxidant, antibacterial and cytotoxic potential of silver nanoparticles synthesized using terpenes rich extract of Lantana camara L. leaves. Biochemistry and Biophysics Reports, 10(March), 76–81. https://doi.org/10.1016/j.bbrep.2017.03.002
- Pinto, A., De, Q., Cordeiro, M., De Andrade, SRM Ferreira, F., Filgueiras, H., De, C., ... Kinpara, D. (2005). Annona muricata. In J. T. Williams (Ed.), *Annona Species, Taxonomy and Botany Inter-national Centre Underutilised Crops.* (pp. 3–16). Southampton, UK: University of Southampton.
- Santhosh, S. B., Yuvarajan, R., & Natarajan, D. (2015). Annona muricata leaf extract-mediated silver nanoparticles synthesis and its larvicidal potential against dengue, malaria and filariasis vector. *Parasitology Research*, 114(8), 3087–3096. https://doi.org/10.1007/s00436-015-4511-2
- Santhosh, Shanthi Bhupathi, Ragavendran, C., & Natarajan, D. (2015). Spectral and HRTEM analyses of Annona muricata leaf extract mediated silver nanoparticles and its Larvicidal efficacy against three mosquito vectors Anopheles stephensi, Culex quinquefasciatus, and Aedes aegypti. *Journal of Photochemistry and Photobiology B: Biology*, 153, 184–190. https://doi.org/10.1016/j.jphotobiol.2015.09.018
- Shah, M., Fawcett, D., Sharma, S., Tripathy, S., & Poinern, G. (2015). Green Synthesis of Metallic Nanoparticles via Biological Entities. *Materials*, 8(11), 7278–7308. https://doi.org/10.3390/MA8115377

- Song, J. Y., & Beom, S. K. (2009). Rapid biological synthesis of silver nanoparticles using plant leaf extracts. *Bioprocess Biosyst Eng*, 32, 79–84. https://doi.org/10.1007/s00449-008-0224-6
- Tomaszewska, E., Soliwoda, K., Kadziola, K., Tkacz-Szczesna, B., Celichowski, G., Cichomski, M., ... Grobelny, J. (2013). Detection limits of DLS and UV-Vis spectroscopy in characterization of polydisperse nanoparticles colloids. *Journal of Nanomaterials*, 2013(February 2014). https://doi.org/10.1155/2013/313081
- Umadevi, M., Shalini, S., & Bindhu, M. R. (2012). Synthesis of silver nanoparticle using D. carota extract. *Advances in Natural Sciences: Nanoscience and Nanotechnology*, *3*(2), 025008. https://doi.org/10.1088/2043-6262/3/2/025008
- Verma, A., & Mehata, M. S. (2016). Controllable synthesis of silver nanoparticles using Neem leaves and their antimicrobial activity. *Journal of Radiation Research and Applied Sciences*, 9, 109–115. https://doi.org/http://dx.doi.org/10.1016/j.jrras.2015.11.001
- Wiley, B. J., Chen, Y., McLellan, J. M., Xiong, Y., Li, Z.-Y., Ginger, D., & Xia, Y. (2007). Synthesis and Optical Properties of Silver Nanobars and Nanorice. *Nano Letters*, 7(4), 1032–1036. https://doi.org/10.1021/nl070214f

Precision of 3-Configurations with Respective Sub-Configurations of 2-Ring Concentric Planar Array in Direction Finding

Kinyili, M. & Kitavi, D. M.

University of Embu, Kenya.

Correspondence: davismusyooo@gmail.com

Abstract

Direction finding is a key area of sensor array processing which is encountered in a broad range of important engineering applications. These applications include wireless communication, rada and sonar, among others. This work compares estimation accuracy of 3-configurations (based on the inner radius variation and constant outer radius) of a uniform 2-ring concentric planar array in direction finding via the Cramer-Rao bound derivation and analysis. The 3-configurations' estimation accuracy is articulated to their respective sub-configurations based on the sensors distribution in each ring. The sub-configurations use equal overall number of sensors (multiple of 4) but with 60% - 40% distribution, 50% - 50% distribution and 40% - 60% distribution on the inner-outer rings respectively. It is found that the estimation accuracy increases as the inner radius approaches the outer radius and thus configuration three (where the inner radius equals three-quarters of the outer radius) has the best precision in direction finding compared to configuration two (where the inner radius equals half of the outer radius) and configuration one (where the inner radius equals onequarter of the outer radius). Furthermore, based on the sub-configurations (where there is varying sensor distribution along the two rings), sub-configuration three (where 40% of the sensors are distributed along the inner radius and 60% of the sensors are distributed along the outer radius) is found to have the best estimation accuracy compared to the other two sub-configurations (50% - 50% and 60% - 40% distributions, respectively). It is observed that the closer the inner radius approaches the outer radius and/or the lower the inner-outer radius' sensor ratio, the better the estimation accuracy. It is thus recommended that all sensors should be distributed along the outer radius for better estimation accuracy. These findings would help direction finders such as engineers to economically utilize a given number of sensors.

Key terms: Array Signal Processing, Direction Finding, Planar Concentric Arrays, Circular Arrays, Estimation Accuracy, Parameter Estimation, Cramer-Rao Bound.

Introduction

Direction finding (DF) is also termed as direction-of-arrival (DoA) estimation problem. It basically refers to the problem of estimating angles-of-arrival (AoA) of an incident signal from an emitter (for instance plane wave or multiple plane waves) [1]. DF is a crucial technique in array signal processing following its wide-spread fields of applications especially in engineering. Some application areas include: radar, sonar, wireless communication, medical diagnosis and treatment, electronic surveillance, radio astrology [2]–[4], position location and tracing systems [5]. This is simply because it is a major method of location determination, in security services especially by reconnaissance of radio communications of criminal organization and in military intelligence by detecting activities of potential enemies and gaining information on enemy's communication order. Due to its diverse applications and difficulty in obtaining optimum estimator, the topic has attracted significant attention over the last several decades.

DF problem has so far been solved by employing various methods for both near-field and far-field sources emitting signal which is received by an array of sensors [6]. The methods aim to estimate the azimuth-polar angles-of-arrival. Some of the methods which have been employed in DF are: Maximum likelihood (ML) method [7], MUSIC (MUltiple SIgnal Classification) [8], ESPRIT (Estimation of Signal Parameters via Rotational Invariance Technique) [9], Cram´er-Rao Bound (CRB) [4], among other techniques. The Cram´er-Rao Bound which is utilized in this work has been found to be the most accurate technique in DF for it is the lowest error bound that any unbiased estimator can achieve and the simplest due to its simplicity in computations.

The aforementioned algorithms solve DF problem based on sensors either randomly distributed or arranged in a desired geometric pattern. The advantage of adopting any sensor-array geometry is mainly to improve the estimation performance. Among the many geometries that have been used in DF, circular and concentric circular geometries have a little bit more unique advantages which include: offering full rotational symmetry about the origin, flexibility in array pattern synthesis and design both in narrow band and broad band beam-forming applications, provision of almost invariant azimuth angle coverage and they can also yield invariant array pattern over a certain frequency band for beam-forming in 3-

dimensions [17]–[21]. Concentric circular array geometries alone offer less mutual coupling effect due to their significant structure of the ring array [23], they yield smaller side lobes in beam-forming [22]–[26], provide higher angle resolution compared to uniform circular array geometries and requires less area for the same number of sensor elements [27] and they increase array's spatial aperture [17]–[21], [28], [29].

Despite the fact that the concentric circular arrays increase array's spatial aperture, the strategy in which the aperture is widened is a great concern as well as the number and the distribution of the sensors along the aperture. This now raises an important question that, how would the proportional variation of the inner radius while the outer radius is held constant affect the estimation accuracy of a 2-ring concentric planar array in direction finding? and how would varying the inner radius alone translate to sensors distribution on the inner-outer rings for the precision in direction finding? This work now proposed 3configurations and their respective sub-configurations of a 2-ring concentric planar array which maintains all the advantages of concentric circular arrays and uses minimal number of sensors with an inter-spacing not exceeding half a wavelength. The three configurations are based on the proportional variation of the inner ring's radius as the outer ring's radius is held constant while the respective sub-configurations are based on the distribution of sensors on the inner-outer rings in which the distributions are in 60%-40%, 50%-50% and 40%-60%. For the configuration one, the inner radius is a quarter of the outer radius, configuration two's radius is ahalf of the outer radius and configuration three's radius is three quarters of the outer radius. The sub-configurations use equal overall number of sensors (multiple of 4) but with 60% – 40% distribution, 50% – 50% distribution and 40% – 60% distribution on the inner-outer rings respectively. The paper compares the estimation accuracy among the three configuration and their respective sub-configurations in DF via the derivation and analysis of their Cram´er-Rao bounds.

Finally, the paper consists of five sections in which Section I is the introduction, Section II presents the array response vector, Section III gives the Cram´er-Rao bound review and derivation, Section IV presents the Cram´er-Rao bound analysis for the 3-sub-configuration based on the sensors distribution, and Section V gives the conclusion.

II Array Response Vector (ARV)

II-A. Review Basics of ARV Using the General 2-Ring Concentric Planar array of Isotropic Sensors

Consider two concentric circles of radii R_{int} and R_{ext} sharing a common center at the Cartesian origin and lying on the x-y plane. See Figure 1.

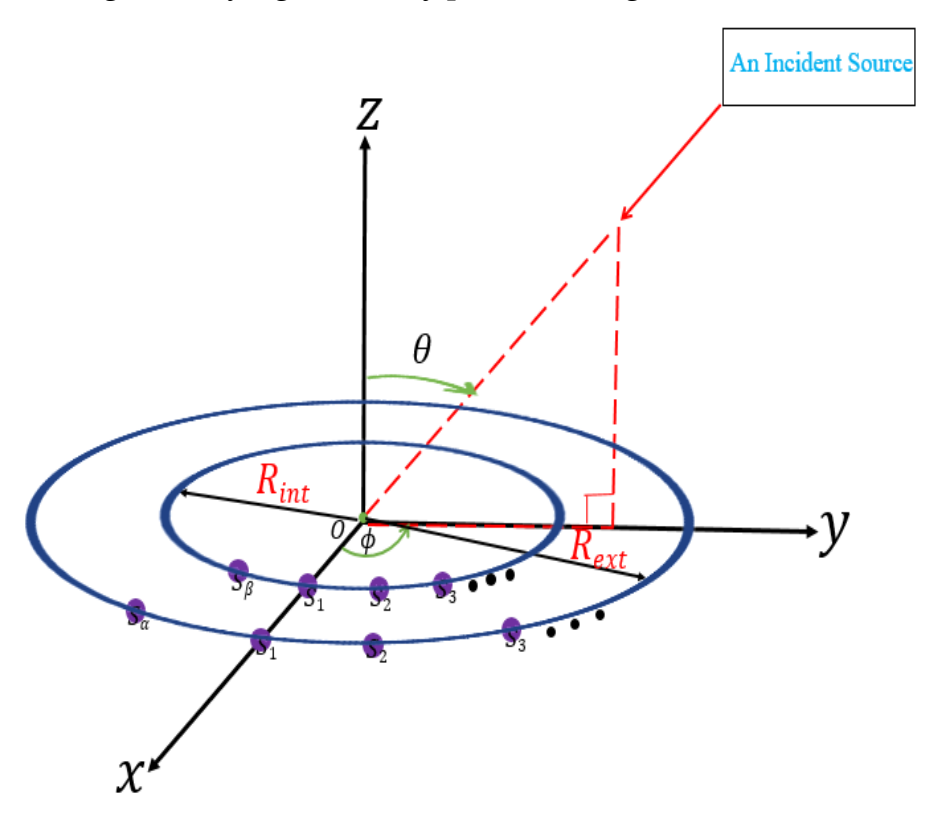


Figure 1: A general two-ring concentric planar array of isotropic sensors lying on the horizontal *x-y* plane and centered at the Cartesian origin.

The inner and the outer rings have L_{int} and L_{ext} number of isotropic sensors arranged on the rings' circumference respectively with equal inter-sensor spacing between any two adjacent sensors. The location of the ℓ -th sensor in terms of the Cartesian coordinates equals

$$\boldsymbol{p}_{\ell} = \begin{cases} \left[R_{int} cos \frac{2\pi(\ell_{int}-1)}{L_{int}}, R_{int} sin \frac{2\pi(\ell_{int}-1)}{L_{int}}, 0 \right]^{T}, & 1 \leq \ell_{int} \leq L_{int} \\ \left[R_{ext} cos \frac{2\pi(\ell_{ext}-1)}{L_{ext}}, R_{int} sin \frac{2\pi(\ell_{ext}-1)}{L_{ext}}, 0 \right]^{T}, & 1 \leq \ell_{ext} \leq L_{ext} \end{cases}$$

$$(1)$$

where ^T denotes the transposition.

Consider an incident signal from a far-field emitter impinging on the origin at a polar-azimuth angles-of-arrival of $\theta - \phi$ where $\theta \in (0,\pi)$ and $\phi \in (0,2\pi)$. Then, the 2-ring's array response vector equals

$$a(\theta, \phi) = \begin{bmatrix} a_{int}(\theta, \phi) \\ a_{ext}(\theta, \phi) \end{bmatrix}, \tag{2}$$

where the ℓ -th entries for a_{int} and a_{ext} are respectively given as:

$$[\mathbf{a}_{int}(\theta,\phi)]_{\ell} = exp\left\{j\frac{2\pi R_{int}}{\lambda}sin(\theta)cos\left(\phi - \frac{2\pi(\ell_{int}-1)}{L_{int}}\right)\right\}$$
(3)

For $\ell_{int} = 1, 2, \cdots L_{int}$ and

$$[\mathbf{a}_{ext}(\theta,\phi)]_{\ell} = exp\left\{j\frac{2\pi R_{ext}}{\lambda}sin(\theta)cos\left(\phi - \frac{2\pi(\ell_{ext}-1)}{L_{ext}}\right)\right\} \tag{4}$$

for $\ell_{ext} = 1, 2, \dots L_{ext}$. In the above entries, λ is the wavelength of the incident signal.

II-B. ARV of the Proposed 3-Configurations of the 2-Ring Concentric Planar Array

The 3-configurations of the 2-ring concentric planar array proposed in this work is based on the variation of the inner ring's radius in relation to the outer ring's radius while holding the latter radius constant. In all the configurations, the outer radius is hereby taken as 8λ . Consider the illustration of the configurations as follows:

II-B.1. **Configuration One (C-1):** This configuration has the following properties. See fig 2.

i.
$$R_{ext} = 8\lambda$$

ii.
$$R_{int} = \frac{1}{4}(R_{ext}) = 2\lambda$$

With reference to Eq.(3)- Eq.(4) in Eq.(2), the array response vector for the C-1 is given as

$$\boldsymbol{a}_{C-1}(\theta,\phi) = \begin{bmatrix} exp\left\{j4\pi sin(\theta)cos\left(\phi - \frac{2\pi(\ell_{int}-1)}{L_{int}}\right)\right\}, & 1 \leq \ell_{int} \leq L_{int} \\ exp\left\{j16\pi sin(\theta)cos\left(\phi - \frac{2\pi(\ell_{ext}-1)}{L_{ext}}\right)\right\}, & 1 \leq \ell_{ext} \leq L_{ext} \end{bmatrix}$$
 (5)

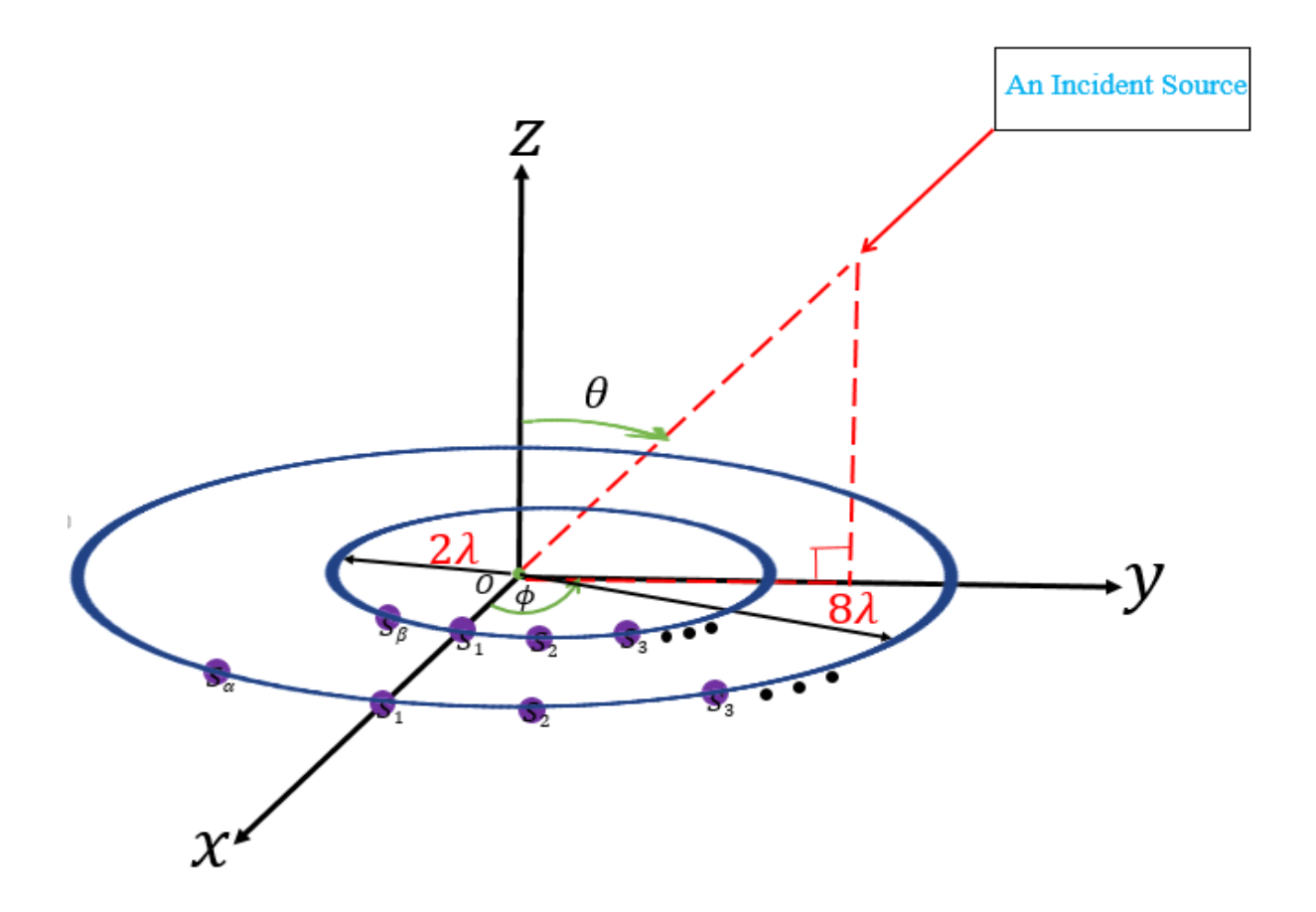


Figure 2: The proposed configuration one. β and α symbolizes L_{int} and L_{ext} respectively.

II-B.2. Configuration Two (C-2): This configuration has the following properties.

i.
$$R_{ext} = 8\lambda$$

ii.
$$R_{int} = \frac{1}{2}(R_{ext}) = 4\lambda$$

Referring to Eq.(3)-Eq.(4) in Eq.(2), the array response vector for the C-2 equals

$$\boldsymbol{a}_{C-2}(\theta,\phi) = \begin{bmatrix} exp\left\{j8\pi sin(\theta)cos\left(\phi - \frac{2\pi(\ell_{int}-1)}{L_{int}}\right)\right\}, \ 1 \leq \ell_{int} \leq L_{int} \\ exp\left\{j16\pi sin(\theta)cos\left(\phi - \frac{2\pi(\ell_{ext}-1)}{L_{ext}}\right)\right\}, \ 1 \leq \ell_{ext} \leq L_{ext} \end{bmatrix}$$
(6)

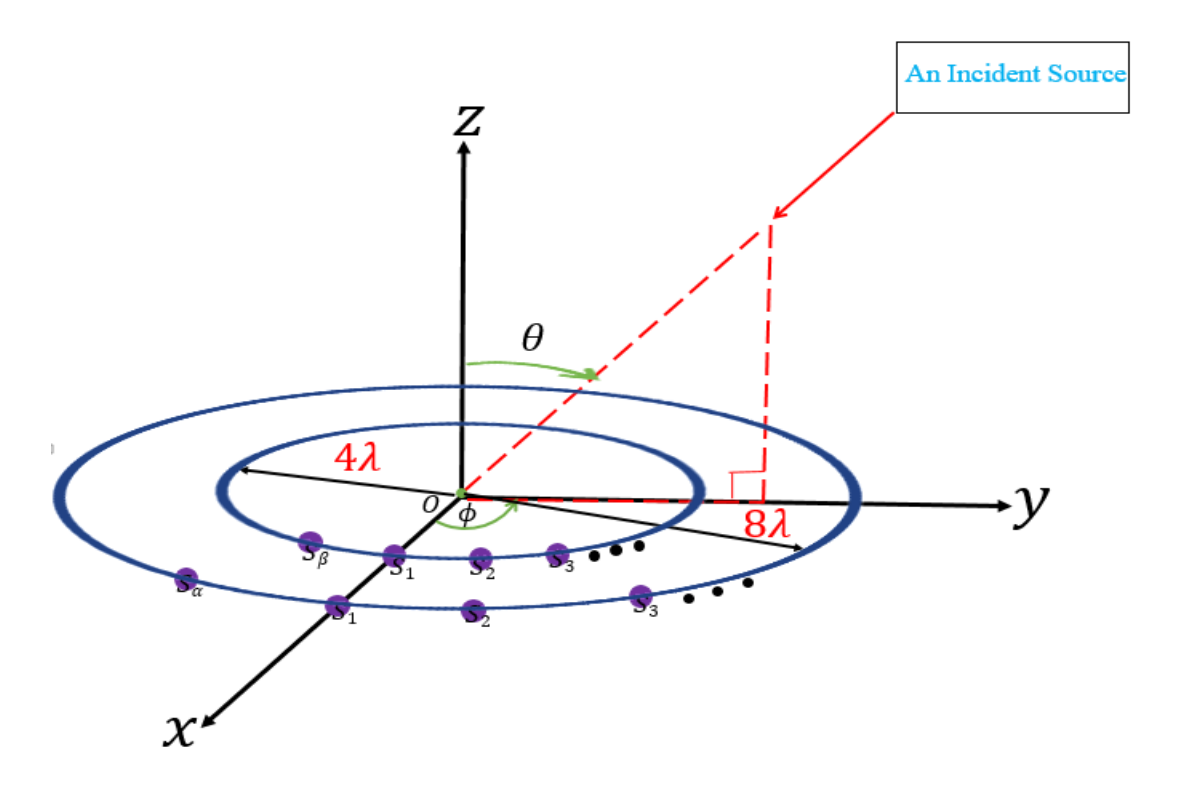


Figure 3: The proposed configuration two. β and α symbolizes L_{int} and L_{ext} respectively

II-B.3. Configuration Three (C-3): This configuration has the following properties. See fig. 4.

i.
$$R_{ext} = 8\lambda$$

ii.
$$R_{int} = \frac{1}{2}(R_{ext}) = 6\lambda$$

With reference to Eq.(3)-Eq.(4) in Eq.(2), the array response vector for the C-3 equals

$$\boldsymbol{a}_{C-3}(\theta,\phi) = \begin{bmatrix} exp\left\{j12\pi sin(\theta)cos\left(\phi - \frac{2\pi(\ell_{int}-1)}{L_{int}}\right)\right\}, \ 1 \leq \ell_{int} \leq L_{int} \\ exp\left\{j16\pi sin(\theta)cos\left(\phi - \frac{2\pi(\ell_{ext}-1)}{L_{ext}}\right)\right\}, \ 1 \leq \ell_{ext} \leq L_{ext} \end{bmatrix}$$
(7)

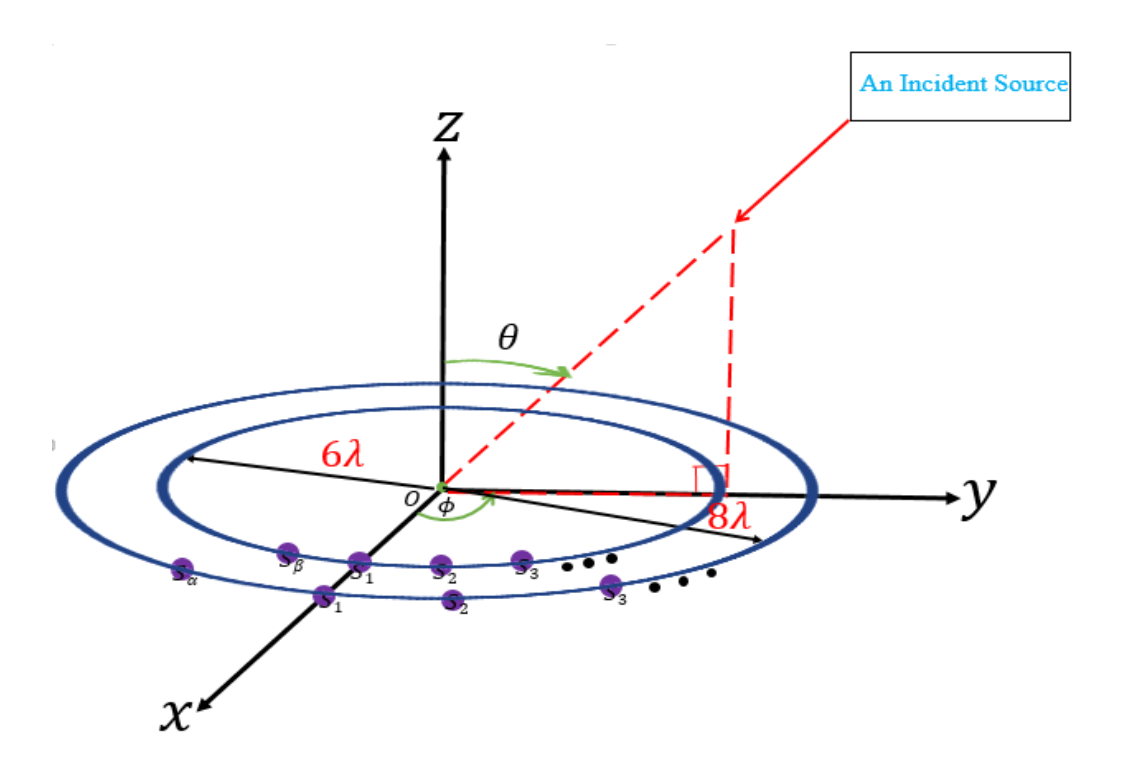


Figure 4: The proposed configuration three. β and α symbolizes L_{int} and L_{ext} respectively.

III The Cram'er-Rao Bound Review and Derivation

III-A. The Statistical Data Model

Let's consider a simple noise-corrupted replica of collected dataset at time instant *m* given by

$$\mathbf{z}(m) = \mathbf{a}(\theta, \phi)s(m) + \mathbf{n}(m) \tag{8}$$

where $\mathbf{n}(m)$ is modeled as a complex-valued zero-mean additive white Gaussian noise (AWGN) with a prior known variance of σ_n^2 , and s(m) is a scalar incident signal modeled as a white Gaussian complex-valued with a prior known variance of σ_s^2 [1], [6], [10], [12]–[16], [18]. Then, for multiple-discrete-time instances M, the dataset is represented as

$$\check{\mathbf{z}} := [\{\mathbf{z}(1)\}^T, \{\mathbf{z}(2)\}^T, \cdots, \{\mathbf{z}(M)\}^T]^T = \mathbf{s} \otimes \mathbf{a}(\theta, \phi) + \widecheck{\mathbf{n}}$$
(9)

where superscript ^T denotes transposition, ⊗ denotes the Kronecker product [12], [15] and

$$s := [s(1), s(2), \cdots, s(M)]^T$$

$$\check{\boldsymbol{n}} := [\{\boldsymbol{n}(1)\}^T, \{\boldsymbol{n}(2)\}^T, \cdots, \{\boldsymbol{n}(M)\}^T]^T.$$

III-B. The Fisher Information Matrix

The Fisher information matrix measures the amount of information that an observable random variable carries about an unknown parameter [31], [32]. Suppose the two parameters to-be-estimated are collected as entries of the 2×1 vector $\xi \in [\theta, \phi]$. Then the Fisher information matrix (FIM) $\mathbf{F}(\xi)$ has a (k,r)th entry equal to (see (3.8) on page 72 of [30])

$$[\mathbf{F}(\boldsymbol{\xi})]_{k,r} = 2Re\left\{ \left[\frac{\partial \mu}{\partial \xi_k} \right]^H \mathbf{\Gamma}^{-1} \frac{\partial \mu}{\partial \xi_r} \right\} + Tr\left\{ \mathbf{\Gamma}^{-1} \left[\frac{\partial \Gamma}{\partial \xi_k} \right]^H \mathbf{\Gamma}^{-1} \frac{\partial \Gamma}{\partial \xi_r} \right\}$$
(10)

where Re $\{\cdot\}$ signifies the real-value part of the entity inside the curly brackets, Tr $\{\cdot\}$ denotes the trace of the entity inside the curly brackets, the superscript H indicates conjugate transposition.

In equation (10),

$$\boldsymbol{\mu} \coloneqq E[\check{\mathbf{z}}] = \mathbf{s} \otimes \boldsymbol{a}(\theta, \phi) \tag{11}$$

$$\Gamma := E[(\check{\mathbf{z}} - \boldsymbol{\mu})(\check{\mathbf{z}} - \boldsymbol{\mu})^H] = \sigma_n^2 I_{(L_{int} + L_{ext})M}$$
(12)

are the mean and the covariance matrix of the data model where $E[\cdot]$ represents the statistical expectation of the entity inside the square brackets and $I_{(L_{int}+L_{ext})M}$ symbolizes an identity matrix of size $(L_{int} + L_{ext})M$. Clearly, Γ in Eq.(12) is functionally *in*dependent of both θ and ϕ , and thus the second term of (10) equals zero. Hence Eq.(10) reduces to

$$[F(\xi)]_{k,r} = \frac{2}{\sigma_s^2} Re \left\{ \left[\frac{\partial \mu}{\partial \xi_k} \right]^H \frac{\partial \mu}{\partial \xi_r} \right\}$$

Where

$$\begin{bmatrix} \frac{\partial \boldsymbol{\mu}}{\partial \boldsymbol{\xi}_{k}} \end{bmatrix}^{H} \frac{\partial \boldsymbol{\mu}}{\partial \boldsymbol{\xi}_{r}} = \left[\boldsymbol{s} \otimes \frac{\partial \boldsymbol{a}(\theta, \phi)}{\partial \boldsymbol{\xi}_{k}} \right]^{H} \left[\boldsymbol{s} \otimes \frac{\partial \boldsymbol{a}(\theta, \phi)}{\partial \boldsymbol{\xi}_{r}} \right] \\
= \underbrace{\boldsymbol{s}^{H} \boldsymbol{s}}_{:=M\sigma_{s}^{2}} \otimes \left\{ \left[\frac{\partial \boldsymbol{a}(\theta, \phi)}{\partial \boldsymbol{\xi}_{k}} \right]^{H} \left[\frac{\partial \boldsymbol{a}(\theta, \phi)}{\partial \boldsymbol{\xi}_{r}} \right] \right\} \\
= M\sigma_{s}^{2} \left[\frac{\partial \boldsymbol{a}(\theta, \phi)}{\partial \boldsymbol{\xi}_{k}} \right]^{H} \left[\frac{\partial \boldsymbol{a}(\theta, \phi)}{\partial \boldsymbol{\xi}_{r}} \right].$$

Hence,

$$[\mathbf{F}(\boldsymbol{\xi})]_{k,r} = 2\mathbf{M} \frac{\sigma_s^2}{\sigma_n^2} Re \left\{ \left[\frac{\partial a(\theta,\phi)}{\partial \boldsymbol{\xi}_k} \right]^H \left[\frac{\partial a(\theta,\phi)}{\partial \boldsymbol{\xi}_r} \right] \right\}. \tag{13}$$

The Fisher information matrix equals

$$F(\xi) = \begin{bmatrix} F_{\theta,\theta} & F_{\theta,\phi} \\ F_{\phi,\theta} & F_{\phi,\phi} \end{bmatrix},$$

the inverse of which gives Cram´er-Rao bound of θ and

$$\begin{bmatrix} CRB(\theta) & * \\ * & CRB(\phi) \end{bmatrix} = \begin{bmatrix} F_{\theta,\theta} & F_{\theta,\phi} \\ F_{\phi,\theta} & F_{\phi,\phi} \end{bmatrix}^{-1}$$

Iii-C. The Cram'Er-Rao Bound Derivation

Here we first derive the Cram´er-Rao bound for the general 2-ring concentric planar array then use the consequent results to give the Cram´er-Rao bounds for the 3-configurations. From Eq.(2), we have

$$\frac{\partial a(\theta,\phi)}{\partial \xi_k} = \left[\left[\frac{\partial a_{int}(\theta,\phi)}{\partial \xi_k} \right]^H, \left[\frac{\partial a_{ext}(\theta,\phi)}{\partial \xi_k} \right]^H \right]^T, \tag{15}$$

where the ℓ -th entries of $\frac{\partial a_{int}(\theta,\phi)}{\partial \theta}$ and $\frac{\partial a_{ext}(\theta,\phi)}{\partial \theta}$ for $\ell_{int}=1,2,\cdots L_{int}$ and $\ell_{ext}=1,2,\cdots L_{ext}$, are respectively given by

$$\left[\frac{\partial a_{int}(\theta,\phi)}{\partial \theta}\right]_{\ell} = j2\pi \frac{R_{int}}{\lambda} cos(\theta) cos\left(\phi - 2\pi \frac{\ell_{int}-1}{L_{int}}\right) \times \boldsymbol{a}(\theta,\phi)$$
 (16)

and

$$\left[\frac{\partial a_{ext}(\theta,\phi)}{\partial \theta}\right]_{\ell} = j2\pi \frac{R_{ext}}{\lambda} cos(\theta) cos\left(\phi - 2\pi \frac{\ell_{ext}-1}{L_{ext}}\right) \times \boldsymbol{a}(\theta,\phi)$$
 (17)

Similarly, the respective ℓ -th entries of $\frac{\partial a_{int}(\theta,\phi)}{\partial \phi}$ and $\frac{\partial a_{ext}(\theta,\phi)}{\partial \phi}$ equals

$$\left[\frac{\partial a_{int}(\theta,\phi)}{\partial \phi}\right]_{\ell} = j2\pi \frac{R_{int}}{\lambda} cos(\theta) cos\left(\phi - 2\pi \frac{\ell_{int}-1}{L_{int}}\right) \times \boldsymbol{a}(\theta,\phi)$$
(18)

and

$$\left[\frac{\partial a_{ext}(\theta,\phi)}{\partial \phi}\right]_{\rho} = j2\pi \frac{R_{ext}}{\lambda} cos(\theta) cos\left(\phi - 2\pi \frac{\ell_{ext}-1}{L_{ext}}\right) \times \boldsymbol{a}(\theta,\phi)$$
 (19)

From Eq.(16)-Eq.(17),

$$\left[\frac{\partial \boldsymbol{a}(\theta,\phi)}{\partial \theta}\right]^{H} \frac{\partial \boldsymbol{a}(\theta,\phi)}{\partial \theta} \\
= \left(2\pi \frac{R_{int}}{\lambda} \cos(\theta)\right)^{2} \underbrace{\sum_{\ell_{int}=1}^{L_{int}} \cos^{2}\left(\phi - 2\pi \frac{\ell_{int}-1}{L_{int}}\right)}_{L_{int}/2} \\
+ \left(2\pi \frac{R_{ext}}{\lambda} \cos(\theta)\right)^{2} \underbrace{\sum_{\ell_{ext}=1}^{L_{ext}} \cos^{2}\left(\phi - 2\pi \frac{\ell_{ext}-1}{L_{ext}}\right)}_{L_{ext}/2} \\
= \left(2\pi \frac{R_{int}}{\lambda} \cos(\theta)\right)^{2} \underbrace{L_{int}}_{2} + \left(2\pi \frac{R_{ext}}{\lambda} \cos(\theta)\right)^{2} \underbrace{L_{ext}}_{2} (20)$$

African Journal of Science, Technology and Engineering Vol. 1, 2020

From Eq. (18)-Eq. (19),

$$\left[\frac{\partial \boldsymbol{a}(\theta,\phi)}{\partial \phi}\right]^{H} \frac{\partial \boldsymbol{a}(\theta,\phi)}{\partial \phi} \\
= \left(2\pi \frac{R_{int}}{\lambda} \sin(\theta)\right)^{2} \underbrace{\sum_{\ell_{int}=1}^{L_{int}} \sin^{2}\left(\phi - 2\pi \frac{\ell_{int}-1}{L_{int}}\right)}_{L_{int}/2} \\
+ \left(2\pi \frac{R_{ext}}{\lambda} \sin(\theta)\right)^{2} \underbrace{\sum_{\ell_{ext}=1}^{L_{ext}} \sin^{2}\left(\phi - 2\pi \frac{\ell_{ext}-1}{L_{ext}}\right)}_{L_{ext}/2} \\
= \left(2\pi \frac{R_{int}}{\lambda} \sin(\theta)\right)^{2} \underbrace{\frac{L_{int}}{2} + \left(2\pi \frac{R_{ext}}{\lambda} \sin(\theta)\right)^{2} \frac{L_{ext}}{2}}_{L_{ext}} (21)$$

From Eq. (16) and Eq.(19),

$$\left[\frac{\partial a(\theta,\phi)}{\partial \theta}\right]^{H} \frac{\partial a(\theta,\phi)}{\partial \phi} = \left(2\pi \frac{R_{int}}{\lambda}\right)^{2} \frac{\sin(2\theta)}{4} \underbrace{\sum_{\ell int=1}^{L_{int}} \sin\left(2\phi - 2\pi \frac{\ell_{int}-1}{L_{int}}\right)}_{0} + \left(2\pi \frac{R_{ext}}{\lambda}\right)^{2} \frac{\sin(2\theta)}{4} \underbrace{\sum_{\ell ext=1}^{L_{ext}} \sin\left(2\phi - 2\pi \frac{\ell_{ext}-1}{L_{ext}}\right)}_{0} = 0 \quad (22)$$

using Eq.(20)-Eq.(22) in Eq.(13), we have

$$F_{\theta,\theta} = 4M \left(\frac{\pi}{\lambda} \frac{\sigma_s}{\sigma_n}\right)^2 \left(R_{int}^2 L_{int} + R_{ext}^2 L_{ext}\right) \cos^2(\theta)$$

$$F_{\theta,\phi}=0$$
,

$$F_{\phi,\phi} = 4M \left(\frac{\pi}{\lambda} \frac{\sigma_s}{\sigma_n}\right)^2 \left(R_{int}^2 L_{int} + R_{ext}^2 L_{ext}\right) \sin^2(\theta).$$

Using Eq.(23)-Eq.(24) in Eq.(14), we have

$$CRB(\theta) = F_{\theta,\phi}^{-1} = \frac{1}{M} sec^{2}(\theta) \left[\left(2\pi \frac{R_{int}}{\lambda} \right)^{2} L_{int} + \left(2\pi \frac{R_{ext}}{\lambda} \right)^{2} L_{ext} \right]^{-1} (26)$$

and

$$CRB(\phi) = F_{\phi,\phi}^{-1} = \frac{1}{M}csc^{2}(\theta) \left[\left(2\pi \frac{R_{int}}{\lambda} \right)^{2} L_{int} + \left(2\pi \frac{R_{ext}}{\lambda} \right)^{2} L_{ext} \right]^{-1} (27)$$

Consequently, the Cram´Er-Rao Bounds for the 3-Configurations are Given as Follows:

For the configuration one

$$CRB_{c-1}(\theta) = \frac{1}{M} \frac{1}{4\pi^2} sec^2(\theta) [4L_{int} + 64L_{ext}]^{-1} \left(\frac{\sigma_n}{\sigma_s}\right)^2$$
 (28)

and

$$CRB_{c-1}(\phi) = \frac{1}{M} \frac{1}{4\pi^2} csc^2(\theta) [4L_{int} + 64L_{ext}]^{-1} \left(\frac{\sigma_n}{\sigma_s}\right)^2$$
 (29)

For the configuration two

$$CRB_{c-2}(\theta) = \frac{1}{M} \frac{1}{4\pi^2} sec^2(\theta) [16L_{int} + 64L_{ext}]^{-1} \left(\frac{\sigma_n}{\sigma_s}\right)^2$$
 (30)

and

$$CRB_{c-2}(\phi) = \frac{1}{M} \frac{1}{4\pi^2} csc^2(\theta) [16L_{int} + 64L_{ext}]^{-1} \left(\frac{\sigma_n}{\sigma_s}\right)^2$$
(31)

For the configuration three

$$CRB_{c-3}(\theta) = \frac{1}{M} \frac{1}{4\pi^2} sec^2(\theta) [36L_{int} + 64L_{ext}]^{-1} \left(\frac{\sigma_n}{\sigma_s}\right)^2$$
 (32)

and

$$CRB_{c-3}(\phi) = \frac{1}{M} \frac{1}{4\pi^2} csc^2(\theta) [36L_{int} + 64L_{ext}]^{-1} \left(\frac{\sigma_n}{\sigma_c}\right)^2$$
 (33)

Observation: Comparing Eq.(28)-Eq.(33), it is clear that since $L_{int} < L_{ext}$, the Cram´er-Rao bounds decreases with increase in the inner radius implying that the estimation accuracy (precision) increases as the inner radius approaches the outer radius.

IV The Cram´er-Rao Bound Analysis for the 3-Sub-Configuration Based on the Sensors´ Distribution

These sub-configurations are based on the sensors distribution on the inner-outer rings while maintaining the overall number of sensors to be equal. The distributions are in 60% - 40%, 50% - 50% and 40%-60% of the overall number of sensors on the inner-outer rings respectively. For instance, consider the overall number of sensors to be 40.

IV-A. Sub-Configuration One

This sub-configuration adopts 60% - 40% sensors distribution implying that the inner ring has 24 sensors while the outer ring has 16 sensors. i.e $L_{int} = 24$ and $L_{ext} = 16$. Now inserting $L_{int} = 24$ and $L_{ext} = 16$ in Eq.(28)-Eq.(33), we have

$$(2\pi)^{2}M\left(\frac{\sigma_{s}}{\sigma_{n}}\right)^{2}\cos^{2}(\theta)CRB_{c-1}(\theta) \equiv (2\pi)^{2}M\left(\frac{\sigma_{s}}{\sigma_{n}}\right)^{2}\cos^{2}(\theta)CRB_{c-1}(\phi)$$

$$= [(4\times24) + (64\times16)]^{-1}$$

$$= [1120]^{-1} \tag{34}$$

$$(2\pi)^{2}M\left(\frac{\sigma_{s}}{\sigma_{n}}\right)^{2}\cos^{2}(\theta)CRB_{c-1}(\theta) \equiv (2\pi)^{2}M\left(\frac{\sigma_{s}}{\sigma_{n}}\right)^{2}\cos^{2}(\theta)CRB_{c-1}(\phi)$$

$$= [(16 \times 24) + (64 \times 16)]^{-1}$$

$$= [1408]^{-1} \qquad (35)$$

$$(2\pi)^{2}M\left(\frac{\sigma_{s}}{\sigma_{n}}\right)^{2}\cos^{2}(\theta)CRB_{c-1}(\theta) \equiv (2\pi)^{2}M\left(\frac{\sigma_{s}}{\sigma_{n}}\right)^{2}\cos^{2}(\theta)CRB_{c-1}(\phi)$$

$$= [(36 \times 24) + (64 \times 16)]^{-1}$$

$$= [1888]^{-1} \qquad (36)$$

IV-B. Sub-Configuration Two

This sub-configuration adopts 50% – 50% sensors distribution implying that both the inner ring and the outer ring have equal number of sensors. i.e $L_{int} = 20$ and $L_{ext} = 20$. Now inserting $L_{int} = 20$ and $L_{ext} = 20$ in Eq.(28)-Eq.(33), we have

$$(2\pi)^{2}M\left(\frac{\sigma_{s}}{\sigma_{n}}\right)^{2}\cos^{2}(\theta)CRB_{c-2}(\theta) \equiv (2\pi)^{2}M\left(\frac{\sigma_{s}}{\sigma_{n}}\right)^{2}\cos^{2}(\theta)CRB_{c-2}(\phi)$$

$$= [(4\times20) + (64\times20)]^{-1}$$

$$= [1360]^{-1} \qquad (37)$$

$$(2\pi)^{2}M\left(\frac{\sigma_{s}}{\sigma_{n}}\right)^{2}\cos^{2}(\theta)CRB_{c-2}(\theta) \equiv (2\pi)^{2}M\left(\frac{\sigma_{s}}{\sigma_{n}}\right)^{2}\cos^{2}(\theta)CRB_{c-2}(\phi)$$

$$= [(16\times20) + (64\times20)]^{-1}$$

$$= [1600]^{-1} \qquad (38)$$

$$(2\pi)^{2}M\left(\frac{\sigma_{s}}{\sigma_{n}}\right)^{2}\cos^{2}(\theta)CRB_{c-2}(\theta) \equiv (2\pi)^{2}M\left(\frac{\sigma_{s}}{\sigma_{n}}\right)^{2}\cos^{2}(\theta)CRB_{c-2}(\phi)$$

$$= [(36 \times 20) + (64 \times 20)]^{-1}$$

$$= [2000]^{-1}$$
(39)

IV-C. Sub-Configuration Three

This sub-configuration adopts 40% - 60% sensors distribution implying that the inner ring has 16 sensors while the outer ring has 24 sensors. i.e $L_{int} = 16$ and $L_{ext} = 24$. Now inserting $L_{int} = 16$ and $L_{ext} = 24$ in Eq.(28)-Eq.(33), we have

$$(2\pi)^{2}M\left(\frac{\sigma_{s}}{\sigma_{n}}\right)^{2}\cos^{2}(\theta)CRB_{c-3}(\theta) \equiv (2\pi)^{2}M\left(\frac{\sigma_{s}}{\sigma_{n}}\right)^{2}\cos^{2}(\theta)CRB_{c-3}(\phi)$$

$$= [(4\times16) + (64\times24)]^{-1}$$

$$= [1600]^{-1} \qquad (40)$$

$$(2\pi)^{2}M\left(\frac{\sigma_{s}}{\sigma_{n}}\right)^{2}\cos^{2}(\theta)CRB_{c-3}(\theta) \equiv (2\pi)^{2}M\left(\frac{\sigma_{s}}{\sigma_{n}}\right)^{2}\cos^{2}(\theta)CRB_{c-3}(\phi)$$

$$= [(16\times16) + (64\times24)]^{-1}$$

$$= [1792]^{-1} \qquad (41)$$

$$(2\pi)^{2}M\left(\frac{\sigma_{s}}{\sigma_{n}}\right)^{2}\cos^{2}(\theta)CRB_{c-3}(\theta) \equiv (2\pi)^{2}M\left(\frac{\sigma_{s}}{\sigma_{n}}\right)^{2}\cos^{2}(\theta)CRB_{c-3}(\phi)$$

$$= [(36 \times 16) + (64 \times 24)]^{-1}$$

$$= [2112]^{-1} \tag{42}$$

Observation: From Eq.(34)-Eq.(42), it is clear that, the Cram´ er-Rao bounds decreases as the inner radius approaches the outer radius across all the sub-configurations. However, configuration three has the lowest Cram´ er-Rao bounds in all the sub-configurations and hence has the best estimation accuracy among the proposed configurations of the 2-ring concentric planar array.

Conclusion

Three configurations of a 2-ring concentric planar array with their respective subconfigurations are proposed. The configurations are based on the variation of the inner ring's radius as the outer ring's radius is held constant while the respective subconfigurations are based on the distribution of sensors on the inner-outer rings in which the distributions are in 60% – 40%, 50% – 50% and 40% – 60%. The comparison of the estimation accuracy for the aforementioned configurations and their respective sub-configurations in direction finding is verified via the Cram´ er-Rao bound derivation and analysis. It has been observed that the Cram´ er-Rao bound decreases as the inner radius approaches the outer radius and the configuration three has the lowest Cram´ er-Rao bound across all the sub-configurations. Thus among the proposed configurations of the 2-ring concentric planar array, configuration three has the best estimation accuracy (precision) in direction finding. Observations from this study would greatly help engineers to economically utilize a given number of sensors and hence minimizing hardware cost.

References

Abedin. M.J & Mohan, A.S. (2010). Maximum Likelihood Near Field Localisation Using Concentric Circular Ring Array. *IEEE International Conference on in Electromagnetics in Advanced Applications*, pp. 533-536.

Albagory, Y.A M. Dessouky, M & Sharshar, H (2007). An Approach for Low Sidelobe Beamforming in Uniform Concentric Circular Arrays, *Wireless Personal Communications*, vol. 43, no. 4, pp. 1363-1368.

Ata, S.O & Isik, C. (2013). High-Resolution Direction-of-Arrival Estimation via Concentric Circular Arrays, *ISRN Signal Processing*, March, 2013.

Castanie, F. (2011). *Digital spectral analysis: Parametric, non-parametric and advanced methods,* New York, New York, U.S.A.: John Wiley and Sons.

Das, R (1966). Concentric ring array," *IEEE Transactions on Antennas and Propagation*, vol. 14, no. 3, pp. 398-400.

Delmas, J.P, M. Korso, M.N., Gazzah, H & Castella, M. (2016). CRB Analysis of Planar Antenna Arrays for Optimizing Near-Field Source Localization, *Signal Processing*, Vol. 127, pp. 117-134.

Delmas, J.P. & Gazzah, H (2013). CRB Analysis of Near-Field Source Localization Using Uniform Circular Arrays, *IEEE International Conference on Acoustics, Speech and Signal Processing*, pp. 3996-4000.

Devendra, M & Manjunathachari, K (2015). Solar DC Microgrid for Rural Electrification: A Case Study," *International Advanced Research Journal in Science, Engineering and Technology* (*IARJSET*), Vol. 2, No. 1, pp. 1-5.

Friedlander, B (2009). Wireless direction-finding fundamentals in classical and modern direction-of-arrival estimation, pp. 1-51, Elsevier

Haupt, R.L. (2008). Optimized element spacing for low sidelobe concentric ring arrays, *IEEE Transactions on Antennas and Propagation*, vol. 56, no. 1, pp. 266-268.

Jiang, Y. & Zhang, S. (2013). An Innovative Strategy for Synthesis of Uniformly Weighted Circular Aperture Antenna Array Based on the Weighting Density Method, *IEEE Antennas and Wireless Propagation Letters*, vol. 12, pp. 725-728, May 2013.

Kajaree, D & Behera, R (2017). A Survey on Web Crawler Approaches, *International Journal of Innovative Research in Computer and Communication Engineering*, vol. 5, no. 2, pp. 1302-1309. Kay, S.M (1993). *Fundamental of Statistical Signal Processing: Estimation Theory*, Upper Saddle River, New Jersey, USA: Prentice Hall.

Kitavi, D.M (2016). Direction finding with the sensors' gains suffering Bayesian uncertainty - hybrid CRB and MAP estimation," *IEEE Transactions on Aerospace and Electronic Systems*, vol. 52, no. 4, pp. 2038-2044.

Kitavi, D.M. (2016). Direction Finding with The Sensors' Gains Suffering Bayesian Uncertainty - Hybrid CRB and MAP Estimation," *IEEE Transactions on Aerospace and Electronic Systems*, Vol. 52, No. 4, pp. 2038-2044.

Kitavi, D.M. Wong, K. T & Hung, C (2017). An L-shaped array with nonorthogonal axes-its 2 Cramer-Rao bound for direction finding," *IEEE Transactions on Aerospace and Electronic Systems*, vol. 54, no. 1, pp. 486-492.

Kitavi, T. C (2016). A Tetrahedral Array of Isotropic Sensors, Each Suffering a Random Complex Gain -The Resulting Hybrid Cramr-Rao Bound for Direction Finding," *Proceedings of the IEEE National Aerospace Electronics Conference*, NAECON, pp. 412-415.

Krishnaveni, V & T. Kesavamurthy, T (2013). Beamforming for Direction-of-Arrival (DOA) estimation-A survey," *International Journal of Computer Applications*, vo. 61, no. 11, pp. 975-8887.

Mendez, R.A, Silva, J.F, Orsotica, R R. & Lobos, R. (2014). Analysis of the Cramer-Rao Lower Uncertainty Bound *In* the Joint Estimation Of Astrometry and Photometry," *Publications of the Astronomical Society of the Pacific*, vol. 126, no. 942, pp. 798-810, 2014.

Ram, G. Mandal, D., Kar, R & Ghoshal, S.P. (2015). Circular and Concentric Circular Antenna Array Synthesis Using Cat Swarm Optimization," *IETE Technical Review*, Vol. 32, no. 3, pp. 204-217.

Sasaki, Y. Tamai, S. Kagami, S. & Mizoguchi, H. (2005). 2D Sound Source Localization on a Mobile Robot with a Concentric Microphone Array, *IEEE International Conference on Systems, Man and Cybernetics*, vol. 4, pp. 3528-3533.

Shavit, R. Pazin, L, Israeli, Y. Sigalov, M & Leviatan, Y. (2005). Dual Frequency and Dual Circular Polarization Microstrip Nonresonant Array Pin-Fed from a Radial Line, *IEEE Transactions on Antennas and Propagation*, Vol. 53, no. 12, pp. 38973905.

Tayem, N& Kwon, H.M (2005). L-Shape 2-Dimensional Arrival Angle Estimation with Propagator Method," *IEEE Transactions on Antennas and Propagation*, Vol. 53, no. 5, pp. 1622-1630.

Van Trees, H.L (2002). *Detection, Estimation and Modulation Theory, Part IV: Optimum Array Processing*. New York: John Wiley and Sons.

Vorobyov, S. A. Gershman, B & Wong, K.M (2005). Maximum Likelihood Direction-of-Arrival Estimation *In* Unknown Noise Fields Using Sparse Sensor Arrays," *IEEE Transactions on Signal Processing*, vol. 53, no. 1, pp. 34-43.

Vu, D. T, Renaux, A. Boyer, R & Marcos, S. (2013). A Cramr Rao Bounds Based Analysis of 3D Antenna Array Geometries Made from ULA Branches," *Multidimensional Systems and Signal Processing*, Vol. 24, no. 1, pp. 121-155.

Wang, L. Wang, G & Chen, Z. (2013). Joint DOA-Polarization Estimation based on Uniform Concentric Circular Array, *Journal of Electromagnetic Waves and Applications*, vol. 27, no. 13, pp. 1702-1714.

Wong, K.T & Zoltowski, M.D. (2000). Self-Initiating MUSIC-based Direction Finding and Polarization Estimation *In Spatio-Polarizational Beamspace*, *IEEE Transactions on Antennas and Propagation*, vol. 48, no. 8, pp. 1235-1245.

Zhang, L. Jiao, Y.C, Chen, B & Weng, Z. B. (2012). Design of Wideband Concentric-Ring Arrays with Three-Dimensional Beam Scanning Based on the Optimization of Array Geometry, *Electromagnetics*, Vol. 32, no. 6, pp. 305-320.

Zhao, X, Yang, Q, & Zhang, Y. (2016). A Hybrid Method for the Optimal Synthesis of 3-D Patterns of Sparse Concentric Ring Arrays, *IEEE Transactions on Antennas and Propagation*, Vol. 64, no. 2, pp. 515-524.

Zhao, X, Zhang, Y & Yang, Q. (2017). Synthesis of Sparse Concentric Ring Arrays Based on Bessel Function, *IET Microwaves, Antennas and Propagation*, Vol. 11, no. 11, pp. 1651-1660.

Zoltowski, M. D & Wong, K.T. (2000). ESPRIT-Based 2-D Direction Finding with a Sparse Uniform Array of Electromagnetic Vector Sensors," *IEEE Transactions on Signal Processing*, vol. 48, no. 8, pp. 2195-2204, August 2000.

Socioeconomic Determinants of Adoption of Eco-Friendly Farming Practices in

Agroecosystems of Embu County, Kenya

Njeru, Moses Kathuri Chuka University

Correspondence: mnkathuri@gmail.com

Abstract

Agriculture is one of the economic activities that not only depends on and influences a number of environmental resources including water, land and biodiversity as well as production technologies and management skills. Given the vast global area under agriculture, the influence of agriculture on overall environmental sustainability cannot be overlooked. Environmental challenges such as pollution, soil erosion, soil acidification, low agricultural production and unsustainability of the agricultural ecosystems, have been associated with conventional farming practices. To address these environmental challenges, environmentalists have mooted Eco-friendly Farming Practices (EFFPs) as possible alternatives to the conventional farming approaches that have been greatly associated with the aforementioned challenges. This study was conducted among households of Embu County in Kenya to determine the socio-economic factors that influenced adoption of EFFPs. Earlier studies had indicated clearly that Embu County was experiencing soil erosion, pollution and soil acidification, yet EFFPs had been introduced to counter these environmental challenges. Therefore, the study sought to find out the influence of socioeconomic factors on adoption of the EFFPs. Ex post facto research design was used. Through multi-stage random sampling 402 household heads were selected and all the 32 extension officers in the area were interviewed. Average income from agriculture, gender, farming experience, level of education, size of the farm and age were statistically significant (at 5% significance levels) in influencing adoption of EFFPs among households of Embu County. The study concluded that the socioeconomic factors were significant in influencing adoption of EFFPs among households of Embu County. This implies that the household socioeconomic characteristics must be considered in designing effective environmental sustainability programmes in the County.

Keywords: Adoption, Eco-Friendly farming Practices, Socioeconomic factors, Households, Embe County

Introduction

The environment and its resources form the basis for human livelihood, sustenance of economies and agricultural development in the world (Mutuku, et al., 2017). Use of environmental resources for agriculture is central in the global economy accounting for over 24% of the global Gross Domestic Product (Smith, et al., 2007). One of the key roles of agriculture is food production. To meet the food requirements for the ever growing human global population (expected to rise to 11billion by 2100), ther is need to remodel conventional agriculture to keep up with the growing lobal food demands Conventional agriculture involves intensified mechanization, intensified use of pesticides and excess inorganic fertilizers, expansion of irrigated land, specialization and breeding of high yielding crops. Notably, conventional farming practices lead to a sudden increase in farm production. However, the increase in production is not sustainable. Additionally, the intensified conventional agriculture stretches environmental resources to limits thus weakening their natural processes (United Nations Environment Programme [UNEP], 2008). For instance, these conventional agricultural practices have been associated with acute soil degradation (Ngetich, et al., 2012), environmental pollution, soil acidification, biodiversity loss and salinization (Hurni, 2000; Rasul and Thapa, 2004; Roling, 2005).

To address the environmental challenges associated with agriculture, and simultaneously provide agroecosystem services, environmentalists have supported a paradigm shift in farming practices by encouraging adoption of Eco-Friendly Farming Practices (EFFPs). EFFPs constitute a set of farming practices that sustainably support provision of agroecosystem services and simultaneously, mitigate environmental challenges associated with agriculture Mozzato, *et al.*, (2018). These farming practices broadly consider tillage practices, cropping systems, choice of farm seeds, farms feeds, soil fertility practices, farm biodiversity; pests and diseases management, soil conservation, water conservation and marketing of the farm produce as well as cross cutting management practices. They are considered environmental friendly because these practices are based on similar tenets (tripod dimensions of ecological, social and economic aspects) as environmental sustainability. These practices are geared towards food production or meeting such other

market requirements, and are carried out without incurring any negative environmental impacts Mozzato, et al., 2018).

EFFPs through their multi-dimensional approach have been associated with benefits such as increased farm production, increased biodiversity, sustained soil fertility, reduced soil erosion, increased soil moisture, reduced environmental pollution improved food security and income stability to farming households (Njeru, 2015).

To realise the benefits of EFFPs including overall environmental sustainability, farmers have to accept and adopt these practices. Success stories and benefits of EFFPs have been recorded in South Africa, Zimbabwe and Zambia (Yadate, 2007). Despite the environmental benefits associated with EFFPs, their adoption rates in many African countries remain low (Giller, *et al.*, 2009; International Assessment of Agricultural Knowledge, Science and Technology for Development [IAASTD], 2009).

Agriculture being the backbone of Kenya's economy and a great user of environmental resources, adoption of EFFPs should be prioritised. In Kenya, very low (0-6%) adoption rates of EFFPs among farming households have been reported (Njeru, 2015; Chomba, 2016). However, despite the low adoption in some regions, some households have been reported to have high adoption intensity of EFFPs (Olwande et al 2009, Suri, 2011). This study sought to examine the influence of socioeconomic factors on adoption of EFFPs in Embu County. The socioeconomic determinants and their influence were examined against adoption of EFFPs covering soil fertility techniques, tillage practices, cropping systems, agroforestry, soil and water conservation practices.

Materials and Methods

The study was carried out in Embu County in Eastern part of Kenya. Embu County borders Kirinyaga County to the West, Kitui County to the east, Tharaka Nithi County to the North and Machakos County to the South. The County is located between 37°3′ and 37°9′ east. Embu County rises from about 515m above sea level at the Tana basin in the east to over 4870m on top of Mt. Kenya in the North West. The human settlement in the county is mainly rural. The County's agroecology has influenced the settlement pattern. The county lying averagely at an altitude of about 1,700m above sea level, experiences bimodal type of rainfall

with long rains falling from March to June while the short rains start at around October to February (Jaetzold, *et al.*, 2007a). A great majority of the farmers are small scale holders whose major cropping enterprises are coffee, tea, maize, beans, potatoes, macadamia. The households rear cattle, goats, sheep, poultry and bees. The combination and intensity of these enterprises vary across the upper midlands (UM1 and UM 2) and lower midlands (LM) of the County.

Ex post facto research design was used to determine the influence of socioeconomic factors on adoption of EFFPs among the farming households in Embu County. All the 80,138 farming households and the 32 agricultural extension officers in the Embu West, Embu East and Embu North sub-counties were targeted for the study. These extension officers represented the informed specialists, and the 80,138 farming household heads being the users of the EFFPs. The sample used in the study was selected through a multistage sampling technique. The first stage involved purposive selection of the block of the three sub-counties where EFFPs were intensively introduced. Twenty four out of the 70 sub-locations were a sample size of 402 household heads was proportionately and randomly chosen for the study.

The sampling unit was the household head because of their influence on decisions regarding farming practices. Questionnaires were administered on house to house basis. In cases where the household head was not present, a spouse was interviewed and if the spouse was absent any adult of the household was interviewed. Where none of these was present, the interview was postponed. Before the actual use of the questionnaire, it was pretested in a neighbouring county and its reliability established. An observation, schedule which is relatively free of bias, was also used to supplement information collected on various observable field practices.

Sixteen EFFPs that were relevant in the study area were considered in the study. These EFFPs considered specific attributes on cover cropping, weed management, cropping systems, soil fertility techniques, use of integrated pest management, minimum tillage,

retaining plant residues/mulching, use of inorganic pesticides, soil testing, soil fertility techniques and agroforestry.

The socioeconomic attributes examined were gender of the household head, level of income from agriculture, highest education level attained by the household head, household's farm size holding, farming experience and age of the household head. Data was cleaned and analysed using Statistical Package for Social Sciences (SPSS) version 22 for windows. The relationship between adoption of EFFPs and selected socioeconomic factors was determined using of chi-square statistics at 5% significance level. The computed p value was compared with 0.05 at 5% significance level. If the p value less than 0.05, signified a significant relationship between adoption of EFFPs and the socioeconomic attributes. A p value more than 0.05, sigified that a statistically significant relationship did not exist.

Results and Discussions

Influence of Socioeconomic Factors on Adoption of EFFPs

The p value obtained for the correlation between socioeconomic factors and adoption of EFFPs was less than 0.05 and therefore socioeconomic factors significantly influenced adoption of EFFPs among households in Embu County.

Table 1: Regression Coefficients for Socio-economic Factors influence on Adoption of Eco-Friendly Farming Practices

Independent Variables		Std.		Chi-	
	В		t	square	p value
		Error		value	
Constant	2.886				
Gender of Respondent	0.059	0.022	2.619	12.798	0.005
Age of Respondents	-0.109	0.025	-4.437	15.798	0.0001
Farming Experience	0.136	0.021	-6.575	34.064	0.0001
Size of Farm	0.070	0.023	-3.008	35.459	0.0001
Highest Level of Education Attained	n 0.214	0.016	-13.349	62.060	0.0001
Annual income from Agriculture	0.092	0.014	6.430	73.692	0.0001

Gender of the Respondents

A chi-square test on the relationship between gender of the respondents and the adoption of EFFPs yielded a p value of 0.005 which is less than 0.05. This implied a significant relationship between the gender and adoption of EFFPs (Table 1). Women were more likely to adopt EFFPs than men. This observation is in tandem with the findings of (Njeru, 2015). However, this finding contradicts the observations by Akama, *et al*, 1995, Fiallo and Jacobson 1995, De Boer and Baquete 1998, and Infield (1998); reported that gender had no influence towards adoption of environmental conservation practices.

Level of Income from Agriculture

Less than 1% of the respondents earned either Kshs 20,000 or less from agriculture, while 2.7% earned between Kshs 21,000 to Kshs 40,000; 11.7% earned between Kshs 41,000 to Kshs 60,000, and more than half (57%) of the respondents earned above Kshs 80,000 in a year (Table 2).

Table 2: Household's Annual Income from Agricultural Activities

Range of income (Kshs)	Frequency	Percent
1-20,000	2	0.5
21,000-40,000	11	2.7
41,000-60,000	47	11.7
61,000-80,000	113	28.1
Over 80,000	229	57.0
Total	402	100.0

Further tests on relationship between annual income and adoption of EFFPs using chisquare was carried out. A chi square value of 73.692 was obtained with a corresponding p
value of 0.0001 at 5% significance level (Table 1). The obtained p value of 0.0001 was less
than 0.05; thus there was a statistically significant and positive relationship between
households' levels of income from agriculture and adoption of EFFPs. This implies that
those who earned more from agriculture adopted more of EFFPs while those who earned
little from agricultural activities adopted less of the EFFPs. This positive relationship
between farm income and adoption of EFFPs is in agreement with the findings reported

elsewhere of Shields et al (1993) who averred that high income levels positively influences adoption of technologies while low farm income inhibits adoption of EFFPs. Higher levels of income from whichever source to the farm widen the financial base of a farmer and this hastens the adoption of technologies. However, the study's finding on the positive influence of income on adoption contradicts the opinion of Mengstie (2009) who reported that income levels do not influence adoption of EFFPs.

Where households realised more income from agriculture, then there was a high likelihood that they ploughed back part of the income into improving the agricultural enterprises. This included adopting more EFFPs because they support the production that gives higher income. With higher levels of income from agriculture, putting up structures like gabions, terraces (for soil and water conservation measures), engaging hired labour for the more labour-engaging EFFPS (composting and mulching) is made easier if households have more income. Lower income levels mean that more competing needs will be addressed before addressing farm related expenses. This low income is bound to be lower in the next season because fewer inputs (investment) went into the EFFPs. This lack of investment in EFFPs leads to low production and then less income. That sets in motion the cycle of less investment and low production and subsequently low income.

Educational Level of the Household Head

Slightly more than half (54%) of respondents had a minimum of secondary level of education, a third (33.8%) had attained up to primary level of education while 11.9% had no formal education (Table 3). The results were further tested to establish if a significant relationship exists between the highest level of formal education attained by the household head and adoption of EFFPs using the chi-square statistic. A chi square value of 62.060 with a corresponding p value of (0.0001) was obtained (Table 3). The p value obtained is less than 0.05 which implied a significant relationship between the highest level of formal education attained by the household and the adoption of EFFPs.

Table 3: Highest Educational Level Attained by the Household Head

Educational Level	Frequency	Percent
Post-secondary	84	20.9
Secondary	134	33.3
Primary	136	33.8
No formal education	48	11.9
Total	402	100.0

This finding is consistent with observations by Asrat, et al., (2004, Tenge, et al., 2004, Bodnár, et al., 2006, and Anley, et al., 2007) who associated higher level of education with higher adoption rates. This positive relation can be attributed to the fact that higher education levels do infer a greater capacity for adopters to learn and decide about new technologies. This implies that environmental education and higher conservation efforts would be successful among highly educated people because they are more open to new ideas. Higher education levels also increases famers' creative and innovative capacity. With higher levels of education, a farmer is expected to appreciate and understand the influences and relationship between environment and agricultural practices and thereof adopt more of the EFFPs. This findin however contradicts earlier observations by other studies (Tesfaye, 2003; Rahmeto, 2007; Tigist, 2010. In his study on soil and water conservation measures in Konso Wolaita and Wello, areas of Ethiopia; Tesfaye (2003) observed that no significant relationship existed between higher adoption rates of soil and water conservation measures and higher education levels. This study acknowledges the importance of formal education in enhancing environmental conservation. The higher the advancement in education level, the higher the likelihood that they are exposed to the intricate interactions of the environment and agriculture. Some of the household heads could have been trained in agriculture or even related disciplines.

Household's Farm Size

Four fifths of the respondents had their farm's sizes ranging between one to five acres, 12.4% of the households had land sizes between six to ten acres while 7.5% of the respondents

owned over 10 acres of land (Table 4). Essentially majority of the households in the study area are small holder farmers.

Table 4: Farm Size Holdings by Households

Farm Size (Acres)	Frequency	Percent
1-5	322	80.1
6-10	50	12.4
Over 10	30	7.5
Total	402	100.0

Chi square test was conducted to test the relationship between farm size holding by households and adoption of EFFPs. A chi square value of 35.459 with a corresponding p value of 0.0001 was realised. Since the obtained p value was less than 0.05 (Table 1), a statistically significant relationship was deemed to exist between farm size and adoption of EFFPs. This indicated a tendency of households on relatively bigger farm sizes to adopt more EFFPs than households on smaller farm sizes. These findings are consistent with earlier observations by Kasenge (1998, Uaiene, et al., 2009) and Mignouna, et al, (2011. Melesse 2018) too, avers that adoption of new agricultural technologies correlates positively with land size. Those in support of the positive relationship between farm size and adoption advance two reasons: first, return on investment is faster and stable in larger farm sizes. Second, is that larger farm sizes have the advantage of more land to carry out more trials (Carlisle, 2016).

Other scholars however have differed with the positive relationship between farm size and adoption of agricultural technologies. Carlisle (2016) argues that small holder farmers can identify a problem of soil degradation faster than large holder farmers, therefore small holder farmers adopt more than farmers with large sizes of land.

Age of the Household Heads

About half (51%) of the respondents were aged between 41-50 years. Forty percent of the respondents were over 50 years of age while the youthful and energetic segment (31-40

years) constituted a paltry 8% of the respondents. A negligible 1% of the respondents were the youngest respondents aged between 20-30 years (Figure 1). These were the youthful farmers who had ventured into farming.

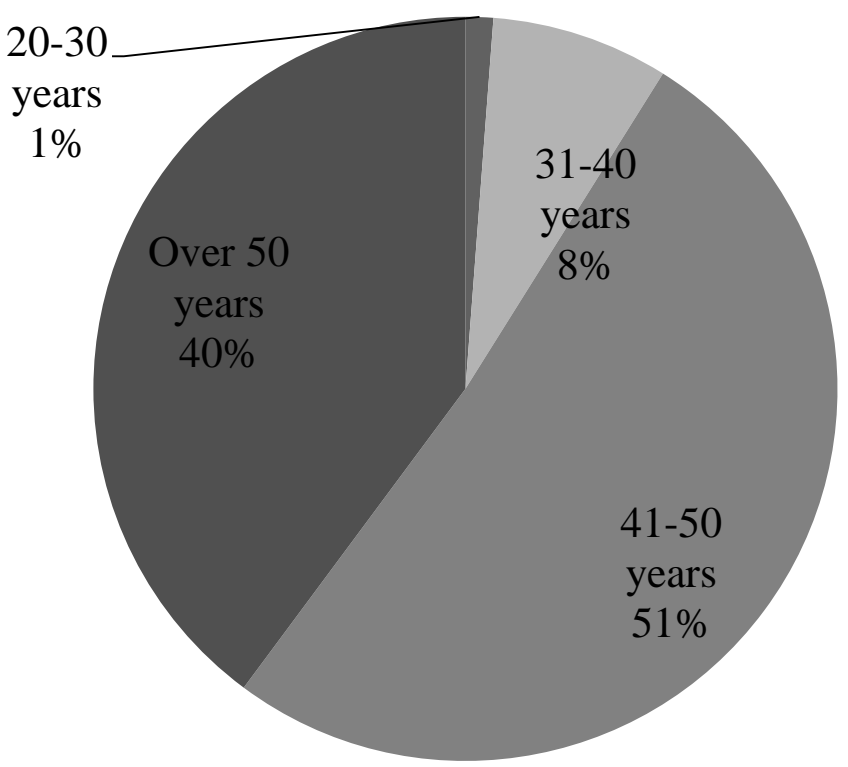


Figure 1. Age of the Household Heads

The age of the household heads was examined against the adoption status of EFFPs (adopted once, adopted more than once and those who have never). The greatest proportion of the adopters as found among household heads aged between 41-50 years. The least of the adopters were aged over 50 years (Table 5).

Table 5: Adoption Status of Eco-Friendly Farming Practices by Age

Age	of	the N	Status of adoption (%)		
Respond	ents		Never	Adopted once	More than once
20-30 Yea	ars	5	0 (0)	1 (20%)	4 (80%)
31- 40 Ye	ears	31	0 (0)	4 (13.0%)	27 (87.0%)
41-50 Yea	ars	206	0(0)	18 (8.7%)	188 (91.3%)
Over 50	Years	160	7 (4.4%)	94 (58.8%)	59 (36.9%)
Total		402	7		

To test on the relationship between the age of the household head and adoption of EFFPs, chi square test was run. A chi square value of 15.798 with a corresponding value of 0.0001 was obtained.

The p value obtained was less than 0.05 (Table 1), therefore a statistically significant but negative relationship exists between age of the household head and adoption of EFFPs in Embu County.

This corroborates observations by Bijesh, *et al.*, (2018) who found out that age of the farmer had a significant, but negative, effect on conservation practices. However, the findings contrast the findings by Tigist (2010) who found a positive relationship between age of the farmer and adoption of conservation practices. The study avers that more adoption of EFFPs is likely to be found among younger and energetic household heads while the elderly were not likely to adopt more EFFPs. The younger household heads (also likely to be educated) were more receptive to new technologies hence their higher adoption of EFFPs.

Farming Experience of the Household Head

A fifth (20.6%) of the respondents had a farming experience spanning between one to 10 years; slightly more than half (51.7%) of the respondents had between 11 to 20 years of farming experience. More than a quarter (27.6%) had over 20 years of farming experience (Table 6). Therefore, more than three quarters (79.3%) of the households had over ten years in farming. This is substantially a long period of time for a household to have learnt and evaluated new technologies. Farming experience is a household characteristic representing the time spent in undertaking farming activities. The household heads over time can evaluate the success and failure in crop production.

Table 6: Farming Experience of the Household Head

Farming experience (Years)	Frequency	Percent
1-10	83	20.6
11-20	208	51.7
Over 20	111	27.6
Total	402	100.0

To test whether a significant relationship existed between farming experience and adoption of EFFPs, chi-square test was carried out. A chi square value of 34.064 with a corresponding p value of 0.0001 was realised (Table 1). Since the p value obtained was less than 0.05 at 5% significance level, the study showed a statistically significant but negative relationship between adoption rates and farming experience

This contrasts what Kidane (2001), Melaku (2005, Yishak 2005) had earlier observed that households with longer farming experience had accumulated knowledge and skills in farming which enabled them to adopt EFFPs faster. Similarly, Mahdi (2005) observed a statistically significant mean difference in the farming experience between adopters and non-adopters of improved sorghum varieties in Ethiopia.

The study found out that the more experienced households adopted more EFFPs than households with fewer years of farming experience. The length of time a household is involved in farming activities serves as a learning forum. The more experienced households over time can evaluate success and failures of technologies and practices. This made the more experienced households to adopt more. For example, a household that has long adopted composting, in realising the high yields might be willing to adopt other EFFPs.

References

Mutuku, M. M., Nguluu, S.N., Akuja, T., Lutta, M. and Benard, P (2017). Factors that Influence Adoption of Integrated Soil Fertility and Water Management Practices by Smallholder Farmers *In* The Semi-Arid Areas of Eastern Kenya. *Tropical and Subtropical Agroecosystems*, 20 (2017): 141 – 153.

Smith, P., Martino, D., Cai, Z., Gwary, D., Janzen, H., Kumar, P., McCarl, B., Ogle, S., O'Mara, F., Rice, C., Scholes, B., Sirotenko, O., Howden, M., McAllister, T., Pan, G., Romanennkov, V., Schneider, U. and Towprayoon, S. (2007). Policy and Technological Constraints to Implementation of Greenhouse Gas Mitigation Options in Agriculture. Agricultural Economics and Environment, 118: 6-28

- United Nations Environmental Programme (2008). *Agriculture: The Need for Change-Press Releases April* 2008. *In UNEP-United Nations Environmental Programme Washington/London/Nairobi/Delhi,* 2008 Available from http://www.unep.org/Documents.Multilingual/Default.asp?DocumentID=531and Article ID=5769andl=en
- Ngetich, F. K., Shisanya, C. A., Mugwe, J. N., Mucheru-Muna, M. and Mugendi, D. N. (2012).

 The Potential of Organic and Inorganic Nutrient Sources in Sub-Saharan African Crop
 Farming Systems, Soil Fertility Improvement and Integrated Nutrient Management: A Global
 Perspective.
- Hurni, H. (2000). Soil Conservation Policies and Sustainable Land Management: A Global Overview. In: Napier, T. Napier, S.M., Tvrdon, J. (eds) Soil and Water Conservation Policies and Programmes: Successes and Failures. CRC Press, Boca Raton, Florida.
- Rasul, G. and Thapa, G. B. (2004). Sustainability of Ecological and Conventional Agricultural Systems in Bangladesh: An Assessment Based on Environment, Economic and Social Perspectives. *Agricultural Systems*. 79:327-351.
- Roling, N. (2005). *Gateway to the Global Garden: Beta/Gamma Science for Dealing with Ecological Rationality. In* Pretty, J. (eds). The Earth Scan Reader in Sustainable agriculture, Earth Scan, London.
- Mozato et al (2018), Drivers of Farmers Adoption and Contunation of Climate Smart Agriculutla

 Priactices: A study from NorthEastern Italy
- Njeru, M. K. (2015). The Practices, Challenges and Benefits of Organic Farming in Nembure Division, Embu County, Kenya. *International Journal of Humanities and Social Science, Vol* 5. No.12.

- Yadate, D. M. (2007). Evaluating Agricultural Sustainability and Adoption/ Diffusion of Conservation Tillage in Sub-Sahara Africa/ (Ethiopia in Some Selected Potential Areas).

 Retrieved from: http://www.sustainability.k.utokyo.ac.jp/members/documents/13-Yadete.pdf
- Giller, K. E, Witter, E., Corbeels, M. and Tittonel, P (2009). Conservation Agriculture and Small Holder Farming in Africa: The Heretics view. *Filed Crops Research* 114 (1) 23-34.
- International Assessment of Agricultural Knowledge, Science and Technology for Development (2009). Executive Summary of the Synthesis Report. International Assessment of Agricultural Knowledge, Science and Technology for development, Washington DC.
- Olwande, J., Sikei, G., and Mathenge, M. (2009). *Agricultural Technology Adoption: A Panel Analysis of Smallholder Farmers' Fertilizer Use in Kenya. CEGA Working Paper Series No. AfD-0908. Centre of Evaluation for Global Action.* University of California, Berkeley.
- Suri, T. (2011). Selection and Comparative Advantage in Technology Adoption. *Econometrica* 79(1): 159–209.
- Jaetzold R., Schmidt H., Hornet Z. B. and Shisanya, C. A. (2007a). Farm Management Handbook of Kenya. Natural Conditions and Farm Information. 2nd Edition. Vol.11/ C. Eastern Province. Ministry of Agriculture/GTZ, Nairobi, Kenya.
- Akama, J., Lant, C. and Burnet, D. (1995). Conflicting Attitudes Towards Wildlife Conservation Programme in Kenya. *Society and Natural Resources* 8: 133-144.
- Fiallo, E. and Jacobson, S. (1995). Local Communities and Protected Areas: Attitudes of Rural Residents Towards Conservation and Machililla National Park, Ecuador. *Environmental Conservation*, 26 (3): 241-249.

- De Boer, W. and Baquete, D. (1998). Natural Resource Use, Crop Damage and Attitudes of Rural People in the Vicinity of the Maputo Elephant Reserve, Mozambique. *Environmental Conservation*, 5 (3): 208-218.
- Infield, M. (1998). Attitudes of Rural Communities Towards Conservation and a Local Conservation Area in Natal, South Africa. *Biological Conservation*, 45: 211-46.
- Shields, M. L., Ganesh P. R., and Goode, F. M. (1993). A Longitudinal Analysis of Factors Influencing Increased Technology Adoption in Swaziland, 1985-1991. *The Journal of Developing Areas* 27 (July): 469-484.
- Mengstie, F. A, (2009). Assessment of Adoption Behavior of Soil and Water Conservation Practices in the Koga Watershed, Highlands of Ethiopia, Ph. D Thesis, Cornell University. Ethiopia.
- Asrat P, Belay K, and Hamito, D. (2004). Determinants of Farmers' Willingness to Pay for Soil Conservation Practices in the Southeastern Highlands of Ethiopia. *Land Degradation and Development* 15: 423-438.
- Anley Y, Bogale A and Haile-Gabriel A. (2007). Adoption Decision and Use Intensity of Soil and Water Conservation Measures by Smallholder Subsistence Farmers in Dedo District, Western Ethiopia. *Land Degradation and Development* 18(3): 289-302.
- Tesfaye, B. (2003). *Understanding Farmers: Explaining Soil and Water conservation in Konso, Wolaita and Wello, Ethiopia*. Ph. D Thesis, Wageningen University and Research Centre. Ethiopia
- Rahmeto, N. (2007). Determinants of Adoption of Improved Haricot Bean Production Package in Alaba Special Woreda, Southern Ethiopia. (Unpublished M. Sc Thesis) Haramaya University, Ethiopia.
- Tigist, P. (2010). Adoption of Conservation Tillage Technologies in Metema Woreda, North Gondar Zone, Ethiopia. (Unpublished M. Sc Thesis). Haramaya University, Ethiopia.

- Kasenge, V. (1998). Socio-economic Factors Influencing the Level of Soil Management Practices on Fragile Land In Proceedings of the 16th Conference of Soil Science Society of East Africa (Eds.: Shayo Ngowi, A.J., G. Ley and F.B.R Rwehumbiza), 13th-19th, December 1998, Tanga, Tanzania pp.102, 112,199
- Uaiene, R., Arndt, C., and Masters, W. (2009). Determinants of Agricultural Technology Adoption in Mozambique. *Discussion Papers* No. 67.
- Mignouna, B., Manyong, M., Rusike, J., Mutabazi, S., and Senkondo, M. (2011). Determinants of Adopting Imazapyr-Resistant Maize Technology and its Impact on Household Income in Western Kenya: *AgBioforum*, 14(3), 158-163. Hall, B. and Khan, B. (2002) Adoption of new technology. New Economy Handbook.
- Melesse, B. (2018). A Review on Factors Affecting Adoption of Agricultural New Technologies in Ethiopia. *Journal of Agricultural Science and Food Research*. 9 (3).
- Carlisle, L. (2016). Factors Influencing Farmer Adoption of Soil Health Practices in the United States: A Narrative review. *Agroecol Sustain Food Syst* 40(6):583–613.
- Bodnár, F., Schrader, T. and Van Campen, W. (2006). How Project Approach Influences Adoption of Soil and Water Conservation by Farmers; Examples from Southern Mali. *Land Degradation and Development* 17: 479-494.
- Kidane, G., (2001). Factors Influencing the Adoption of New Wheat and Maize Varieties in Tigray, Ethiopia: *The Case of Hawzien Woreda*. (Unpublished M.Sc. Thesis) Haramaya University.
- Melaku, G. (2005). Adoption and Profitability of Kenyan Top Bar Hive Beekeeping Technology.

 Study in Ambasal District of Ethiopia. (Unpublished M.Sc. Thesis) Haramaya

 University. Ethiopia

- Yishak, G. (2005). Determinants of Adoption of Improved Maize Technology in Damot Woreda, wolaita Zone, Ethiopia. (Unpublished M. Sc Thesis). Alemaya University of Agriculture, Ethiopia.
- Mahdi, E. (2005). Farmers' Evaluation, Adoption and Sustainable Use of Improved Sorghum Varieties in Jijiga Woreda, Ethiopia. (Unpublished M.Sc Thesis). Haramaya University, Ethiopia.

Soil Concentration of Selected Heavy Metals in Chuka, Nakuru and Thika Municipal Dumpsites

Kariuki, Joseph Maina ¹, Bates, Margaret², Magana, Adiel¹
Chuka University, Kenya and University of Northampton, United Kingdom
Correspondence: makgarix@yahoo.com

Abstract

Dumpsite waste pickers face numerous health and safety risk factors one of which is elevated concentration of heavy metals in the soil that could be a source of exposure through dusts. The purpose of this study was to determine the concentration of selected heavy metals (lead, cadmium, chromium and copper) in the top 15 cm of soil in the largest dumpsites in Tharaka Nithi, Nakuru and Kiambu counties namely; Chuka, Nakuru and Thika towns, respectively. The study was nonexperimental cross-sectional ecological survey, the sampling design a herringbone pattern with 96 soil samples collected with a stainless-steel auger. Laboratory analysis was done by USEPA Method 3050B and the concentration determined by Atomic Absorption Spectrophotometer at the Department of Mines and Geology Laboratory in Nairobi. F-test was done for differences between dumpsites at a=.05 and comparison made to WHO guidance values. Significant differences between the dumpsites were detected for lead (F=44.555, p=<.001), copper (F=5.897, p=<.01), cadmium (F=4.739, p=.016) and chromium (F=6.223, p=<.01). The largest percentage of samples with concentrations above the WHO guidelines were Kiambu (97%) for lead and Nakuru with 26.7% for chromium, 66.7% for cadmium and 56.7% for copper. Chuka dumpsite had the highest proportion of samples with the lowest concentration of lead and chromium and with the lowest proportion of samples where cadmium was detected. In conclusion, Nakuru and Kiambu dumpsite were highly polluted and were a huge risk factor to the waste pickers. In the short-term, it was recommended that waste pickers should wear adequate health and safety protective equipment while on site and possibly reduce the time at the dumpsite to minimise exposure. In the long-term, waste separation should be done to ensure that heavy metal containing waste do not get to the dumpsites, waste recovery facilities adopted to minimise waste picking at dumpsites and improve recycling, and the dumpsites upgraded to sanitary landfill status.

Keywords: Heavy Metals, Waste Pickers, Waste Management, Dumpsite, Electronic Waste, Klambu, Nakuru, Tharaka Nithi

Introduction

Waste picking is prevalent in the dumpsites in many of the developing in Asia, middle east; African countries and South American Countries. It has been noted that where dumpsites are in use, source waste separation is hardly practiced and for this reason all manner of hazardous waste finds their way into the dumpsite. Consequently, waste pickers in the dumpsites are faced with many health and safety hazards among which is exposure to heavy metals due to the presence of materials such as electronic waste.

Heavy metals are known to be persistent, bioaccumulative and toxic substance present in electronic waste (Lundgren, 2012; Hassan et al., 2016) and hence are a health risk factor upon exposure to living organisms. Especially, children being particularly vulnerable to toxins because they ingest more water, food, and air per unit of body weight; their metabolic pathways are less developed to detoxify and excrete toxins; and any disruption during their growth years can easily disrupt development of their organ, nervous, immune, endocrine and reproductive systems (Cointreau, 2006).

According to Song and Li (2014) the disposal of e-waste is a major environmental problem due to the presence of heavy metal like lead and cadmium that are used in electronic devices batteries, copper in wiring and chromium as an anti-corrosion agent in circuits. In Kenya, there is limited waste separation and e-waste is a common problem in the dumpsites (NEMA, 2014). Consequently, pollution by heavy metals in the dumpsite is a matter of concern not only because of environmental pollution but also due to the fact that waste pickers operate on the dumpsite where exposure to the heavy metals by dust or fumes is likely to be higher than for the general population.

Heavy metals are common in electronic waste for instance copper is said to make up 19% of a mobile phone (Peace, 2009) while between 1994 and 2003 computers containing approximately 718,000 tonnes of lead and 1,363 tonnes of cadmium were at their end of life (Lundgren, 2012). Further, Lundgren states that a Cathode Ray Tube in older computers and television sets contain 2–3 kilograms of lead and about 1kg in newer models. Human exposure to these heavy metals is through inhalation, dust ingestion, dermal exposure and

oral intake (Lundgren, 2012). In Africa, the number of lead-based batteries continue to go up as they are relied on in imported used vehicles, off-grid solar installation, uninterrupted power supply systems among others and hence the risk of the heavy metal getting to the environment will continue to increase (Gottesfeld et al, 2018).

Copper is described as a hazardous substance upon ingestion, inhalation or eye contact and in mammals its toxicity can result to inhibition of intracellular enzymes, oxidative stress and mitochondrial swelling. Whereas chromium (III) is recognised as an essential trace element Chromium (VI) compounds are toxic and carcinogenic. The carcinogenic effect is expressed in the respiratory system with the bronchial tree being the major target organ (WHO, 2000). Exposure to Cadmium has been associated with kidney and bone damage with the metal being also identified as a potential human carcinogen, causing lung cancer. (WHO, 2007)

Lead (Pb) has been reported as the number two most hazardous substance after arsenic, based on the frequency of occurrence, toxicity and the potential for human exposure in the United States with long-term exposure leading to memory deterioration, prolonged reaction times and reduced ability to understand (Ding et al., 2013). Lead poisoning has also been reported to cause anaemia, encephalopathy, arthritis, and muscular depression (Kondo et al., 2013). WHO (2007), identifies lead as a well-known neurotoxin with exposure resulting to neuro-behavioural effects on foetuses, infants and children, and elevated blood pressure in adults.

The USEPA hazard concentration level for lead in the soil for residential use is 400 mg/kg (Gottesfeld et al, 2018). In Finland, the health risk level for soil lead concentration is 200 mg/kg (Tóth et al 2016) which is the same for Tanzania (Kibassa et al, 2013). The WHO safe soil concentration limit for lead is 100 mg/kg whereas the limit by Canadian Environmental Quality Guidelines (CEQG) for both agricultural and residential uses is 70 mg/kg for agricultural and 140 mg/kg for residential land (Bongoua-Devisme *et al*, 2018). The United States Centre for Disease Control and Prevention reports that an increase of 1000 mg/kg of soil concentration of lead would result to a rise of 3-7 µg/dL in blood lead concentration (Gottesfeld et al, 2018).

USEPA requires clean-up of soils with chromium concentration of at least 230mg/kg while limits considered safe for various uses is 100mg/kg in Tanzania (Kibassa et al., 2013), 70mg/kg by WHO and 64mg/kg by CEQG for both agricultural and residential uses (Bongoua-Devisme et al, 2018). Concerning copper, the safe soil limit in Tanzania is 200mg/kg, the WHO limit 100mg/kg and is 63mg/kg by CEQG for both agricultural and residential uses (Bongoua-Devisme, 2018). The USEPA guidance level for sites polluted Cadmium and requiring clean-up is 70mg/kg soil. On the other hand, the lower guideline value for ecological risk in Finland is 10mg/kg (Tóth et al., 2016) and in Tanzania (Kibassa et al., 2013) the safe soil concentration is 1 mg/kg. WHO guideline for cadmium is 0.35mg/kg and by CEQG it is 1.4 mg/kg and 10mg/kg for agricultural and residential land, respectively (Bongoua-Devisme, 2018).

In this regard, the purpose of the present study was to determine the concentration of lead, copper, cadmium and chromium in the top 15 cm of soil which could easily become airborne and a health risk factor to the waste pickers in the named dumpsites.

Materials and Methods

The Physical Location, Climate and Economic Activities of the Study Area

The study area comprised the counties of Nakuru, Kiambu and Tharaka Nithi (Figure 1). The largest dumpsite in each of the three counties was selected for the study and were located in Chuka, Thika and Nakuru Towns respectively.



Figure 6: Position of Nakuru, Kiambu and Tharaka Nithi counties in Kenya Source: Maps of Kenya (2018)

Nakuru County covers an area of 7,495.1 km² and lies within longitude 35° 28′ and 35° 36′ East and latitude 0° 13′ and 1° 10′ South (RoK, 2013a). The temperatures range between 10°C during the cold months (July and August) to 20°C during the hot months (January to March) and receives between 700mm and 1200mm pa. The county's population is about 1.6 million with agriculture and tourism being major economic activities (County Government of Nakuru, 2014). Nakuru town, with a population of 307, 990, is the largest town in the county and fourth largest in Kenya. It is located 165 km northwest of Nairobi, the capital city of Kenya (County Government of Nakuru, 2014; KNBS, 2009). The main dumpsite, commonly known as Gioto and established in 1975 is situated about 3km to the northwest of Nakuru town, along Nakuru-Kabarak road on the slopes of Menengai crater and on a higher elevation than Nakuru town. Administratively it is located on London ward in Nakuru subcounty, about 25 acres (10ha)

Tharaka Nithi County has a total area of 2661.1 km² and a population of 365,330. It lies within latitude 00° 07′ and 00° 26′ South and longitudes 37° 19′ and 37° 46′ East and the altitude ranges from 5200m on top of Mt Kenya to 500m in the lowlands. The high-altitude areas experience reliable rainfall while middle and lower regions receive medium and unreliable rainfall, respectively. The key economic activities revolve around crop farming (Tharaka Nithi County Strategic Plan 2012-2017, RoK, 2013b). Chuka dumpsite is located less than 2km from Chuka town in Karingani ward in Meru South subcounty. It is quite small, occupying about one acre (0.41ha) for the main dumpsite area and a peripheral area of 0.71 acres where waste could overflow to but no vehicle could access. It is along the highway of Chuka-Meru and was accessed through a murram road that branched off from the highway. The dumpsite is located on a steep ground that was elongated along the murram road.

Kiambu County is located in the central region of Kenya and covers a total area of 2,543.5 Km². It lies between latitudes 0° 25′ and 0° 20′ South of the Equator and Longitude 36° 31′ and 37° 15′ East (County Government of Kiambu, 2013). The county population according to the 2009 census was 1,673,785 which was highly urbanised with 61% of the population being urban and 39% being rural. Thika town is the largest town in Kiambu county with a population of 139,853 (KNBS, 2009). The town is about 40km away from Nairobi city. It is one of the major industrial towns in Kenya (County Government of Kiambu, 2013). Kiambu municipal dumpsite, commonly called Kangʻoki is located on the lower side of Thika town about 7 km from the central business district. It is administratively in the Kamenu ward in Thika subcounty. Of the three dumpsites, it is the most extensive occupying an area of about 192 acres (78 hectares).

Study Design

The study was non-experimental and the design a cross-sectional ecological survey. A key concept of cross-sectional survey is that data is collected once from the subject/area which is what was done in the present study.

Sample Size

Nathanail et al, (2002) formula for calculating the number of sampling points was used. According to this formula:

N = kA/a

Where:

k= shape constant, whereby: k = 1.08 (for circular hotspot), 1.25 (plume shaped), 1.8 (Elliptical) and 1.5 where there is no information on hotspot shape.

In this study, k = 1.5 as there is no information on hotspot shape.

N=is the number of sampling points,

A=total dumpsite area,

a = hotspot area

The study was based on assumption of one hotspot of 5% of the total dumpsite area. This is based on the fact that the distribution of the pollutants within the sampling area was assumed to be generally uniform due to limited or no source separation of waste in most of Kenya (NEMA, 2014). Consequently, in this study each dumpsite was regarded as one continuous hotspot and hence an area of 5% within the dumpsite is not likely to be missed. According to this formula, with a 5% hotspot area and with the shape constant (k) taken as 1.5, a total of 30 sampling points was sufficient for each dumpsite, irrespective of the differences in dumpsite area of the three sites. This gave the total sampling points of all the dumpsites to 90.

Sampling Procedure

Sampling was a non-targeted approach which is non-biased and able to eliminate hotspots of a given size at a given confidence level (95% in this study), allow for determination of mean concentration and standard deviation and the determination of spatial distribution of the pollutants (Nathanail et al, 2002). Within this approach, the herringbone sampling pattern was used, which is systematic, stratified, unaligned and easy to set out on site. In this pattern, a square grid is drawn and in the first line, every other point is offset by a quarter of a unit, in the second line every point is offset by a quarter of a unit with regard to the first, and the third and fourth line mirror the first and second lines and subsequent lines follow the same pattern (Figure 2). According to the Department of Environment (DOE) a good spatial sampling design should meet four conditions: stratified, each stratum to carry one sampling point, systematic and sampling points not to be aligned. DOE further observes that herringbone approach satisfies all these conditions while simple random sampling satisfies

only one condition (nonalignment of sampling points) whereas grid sampling does not satisfy the condition on nonalignment of sampling points.

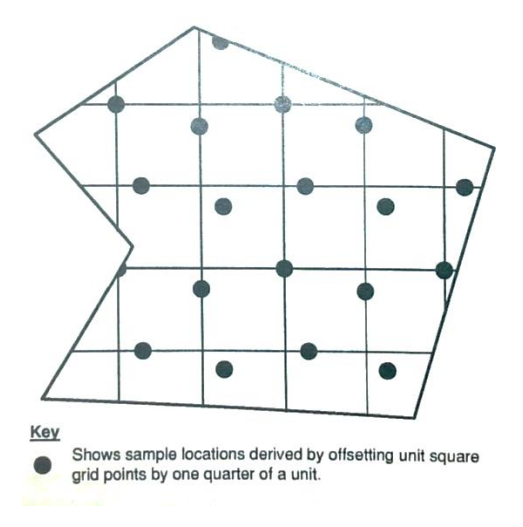


Figure 7: Setting Out a Herringbone Design (Nathanial et al., 2002)

Field Data Collection

Before data collection an application was made to the National Commission for Science and Technology and a permit was given. The permit was presented to the director of environment in each of the three counties before proceeding to the field for data collection. Field collection of samples involved some activities done before going to the field for instance labelling of collection containers. The soil samples were collected at 0-15 cm depth by use of a stainless-steel soil auger. This depth is deemed appropriate where the focus is to human health with regard to direct ingestion and inhalation (Nathanial et al., 2002). The container for soil collection was sturdy polythene bags which was used for transportation and storage. After collection from one sampling point, the soil attached to the surface of the auger was carefully scraped with a wooden device to avoid contaminating the soil from the next sampling point. The coordinates of each sampling site were recorded during collection.

Laboratory Analysis for Heavy Metals

Laboratory analysis for heavy metals was carried out in Department of Mines and Geology Laboratory in Nairobi and concentration determined by Atomic Absorption Spectrophotometer (AAS). Determination of heavy metals was carried out as per United States Environmental Protection Agency Method 3050B (USEPA, 1996; Dean, 2007). In the

laboratory, the soil samples were air dried by opening up the polythene bag and allowing it to dry to constant weight under the ambient room temperature. Each sample was homogenised using a mortar and pestle after which a 5mm sieve was used to get the fine soil appropriate for analysis. The soils were then digested with strong Nitric Acids. According to USEPA (1996) strong acids dissolve almost all elements that could become biologically available. After digestion and cooling, filtering was done and digestate transferred into 100ml volumetric flasks where dilution is done to 100ml for the analysis. The concentrations were then determined as described by Dean 2007.

Data Analysis

Statistical Package for Social Science (SPSS version 20) was used for data analysis. Concentration of heavy metal from the study was compared across the three dumpsites by F-test whereas qualitative comparison was done with secondary sources and reference values from WHO.

Results and Discussions

Lead was detected in all the samples tested (Table 1). Most of the samples from Chuka (72.7%) had concentrations less than 70ppm, 97% had concentrations below 200ppm and 3% had concentrations higher than 400ppm. The mean concentration in Chuka was 89.27±35.77ppm with a minimum of 7.43 and a maximum of 1214.91ppm. In Kiambu, only 3% of the samples had less than 70ppm concentration, 54.5% had concentrations of 200-400 and 42.4% had concentrations above 400ppm. The mean concentration in Kiambu was 397.80±22.47ppm with a minimum of 50.76 and a maximum of 680.67ppm. In Nakuru, 36.7% of the samples had less than 70ppm of concentration, 23.3% with a concentration of 100-400 and 23.3% with greater than 400ppm. The mean concentration in Nakuru was 292.33±66.51ppm with a minimum of 27.34 and a maximum of 1479.3 ppm. Significant differences were determined between all sites.

Table 1: Concentration of Lead in the Dumpsites

		Frequen	ncy	Description								
Site	Concentration distribution				Descriptive							
	(PPM)*	F	%	N	Min	Max	Mean	Std	Std.			
				1N		Max		Error	Dev.			
Chuka	≤ 70	24	72.7									
	70 - 100	4	12.1	33	7.43	1214.91	89.27a	35.77	205.47			
	100 - 200	4	12.1									
	>400	1	3.0									
	Total	33	100.0									
	≤ 70	1	3.0									
Kiambu	200-400	18	54.5	33	50.76	680.67	397.80 ^b	22.47	129.10			
Kiaiiibu	>400	14	42.4									
	Total	33	100.0									
	≤ 70	11	36.7									
	70 - 100	5	16.7									
Nakuru	100 - 200	1	3.3	30	27.34	1479.30	292.33c	66.51	364.26			
	200-400	6	20.0									
	>400	7	23.3									
	Total	30	100.0									

^{*}categories based on maximum allowed limits by various authorities; a,b,c means with different superscripts are significantly different (F-test).

The USEPA hazard concentration level for lead in the soil for residential use is 400ppm (Gottesfeld et al 2018) with sites above this concentration requiring clean up. From the result, each of the dumpsite had samples that had exceeded this level which were > 20% in Nakuru, > 40% in Kiambu and 3% in Chuka. In Finland, the health risk level for soil lead concentration is 200mg/kg Tóth et al., 2016) which is the same for Tanzania (Kibassa et al., 2013). The WHO safe soil concentration limit for lead is 100ppm whereas the limit by CEQG for both agricultural and residential uses is 70ppm for agricultural and 140ppm residential Page 217 of 232 land (Bongoua-Devisme et al, 2018). Ninety-seven percent of samples from Kiambu, 46.6% in Nakuru, 15.1% in Chuka and had exceeded the WHO guideline.

Results from a study of lead concentrations in areas around lead recycling plants in Kenya Gottesfel et al, (2018) indicated that out of 10 samples four had concentration between 400-600ppm, three samples between 600 and 1000ppm, two samples between 1000 and 2600 and two samples less than 50ppm. The mean concentration of lead in municipal dumpsite in Calabar Metropolis, Nigeria was reported to be 1489.1mg/kg (Ediene and Umoetok, 2017) which is 3.5 times the concentration in Kiambu dumpsite. In Manila dumpsite, Philippines the mean lead concentration was reported as 15.47ppm whereas in Uyo, Nigeria it was 43.28ppm for the municipal dumpsite and 18.57ppm for a rural dumpsite (Ebong et al, 2008). In Bonoua Dumpsite, Ivory Coast the concentration was 118ppm (Bongoua-Devisme et al, 2018).

This shows that the levels of lead are very high and it is a real hazard in the dumpsites. This especially so in Kiambu where almost all samples were above the WHO limit. On the basis of these results alone, the dumpsites are very unsafe for the waste pickers to work in. This might necessitate the use of breathing masks at all times to minimise the risk.

Copper was detected in all samples from Kiambu, Nakuru dumpsites and in most samples from Chuka at 81.8% (Table 2). Most of the samples in Chuka (63.6%) and Kiambu (87.9%) had concentrations of up to 100ppm whereas in Nakuru most of the samples had more than 100ppm. The highest mean concentration of copper was recorded in Nakuru (227.86±52.12) followed by Chuka (193.37±110.91) and Kiambu (113.23±52.31). there were significant differences between Chuka and Nakuru and between Nakuru and Kiambu but none between Chuka and Kiambu.

Table 2: Copper Concentration in the Dumpsites

		Free	quency			D						
Site	Concentration	n dist	ribution		Descriptive							
	$(mg/kg)^*$	F	F %		Min	Max	Mean	Std	Std.			
				N Mir	171111	IVIUX	Mean	Error	Dev.			
	≤ 100	21	63.6									
	100-200	2	6.1									
Chuka	>200	4	12.1	27	1.40	3032.66	193.37 a	110.91	576.28			
	Not detected	6	18.2									
	Total	33	100.0									
	≤ 100	29	87.9									
Kiambu	100-200	2	6.1	33	5.93	1279.34	113.23 a	52.31	300.52			
Kiaiiibu	>200	2	6.1									
	Total	33	100.0									
Nakuru	≤ 100	13	43.3									
	100-200	8	26.7	30	2.07	1245.83	227.86 b	52.12	285.48			
	>200	9	30.0									
	Total	30	100.0									

^{*}categories based on maximum allowed limits; a,b,c means with different superscripts are significantly different (F-test).

With regard to copper the maximum soil concentration deemed safe in Tanzania is 200mg/kg. The allowed soil concentration limit of copper by WHO is 100ppm and 63ppm by CEQG for both agricultural and residential uses (Bongoua-Devisme et al, 2018). The percentage of samples that had exceeded 200ppm was 12.1% in Chuka, 6.1% in Kiambu and 30% in Nakuru. Further, the percentage of samples that exceeded the WHO guidelines was 57% in Nakuru, 3% in Chuka and 12% in Kiambu. In Uyu, Nigeria copper concentration were reported as 33.7ppm for the municipal dumpsite and 56.33ppm for a rural dumpsite (Ebong et al, 2008). In Bonoua dumpsite, Ivory Coast copper concentration were reported as 9.5ppm (Bongoua-Devisme et al 2018) and 26.08ppm while in Calabar Metropolis, Nigeria municipal dumpsite (Ediene and Umoetok, 2017).

Copper pollution appear to be quite widespread in Nakuru as compared to the other two sites and is also quite high in comparison to the studies elsewhere. Exposure to Copper is upon ingestion, inhalation or eye contact. In this regard, use of protective equipment would be necessary to minimise risk.

In a majority of samples from Chuka (91%) and Kiambu (66.7%) cadmium was not detected whereas in Nakuru it was detected for a majority (66.7%) of the samples (Table 9; Appendix 3). In all the samples where detection was positive, the concentration was above 1mg/kg. The highest concentration was recorded for Nakuru (4.77±.48ppm) with a minimum of 1.67 and a maximum of 9.06 ppm. Chuka had the lowest mean concentration of (3.41±0.87ppm) with a minimum of 1.73 and a maximum of 4.62ppm. Significant differences were detected only between Nakuru and Kiambu only.

Table 3: Cadmium Concentration

	Concentration	Frequ	iency			Descriptive					
Site	(PPM)*	distri	bution		Descriptive						
		F	%	N	Min	Max	Mean	Std Error	Std. Dev.		
	1-5	3	9.1								
Chuka	Undetected	30	90.9	3	1.73	4.62	3.41 ^{ab}	.87	1.50		
	Total	33	100.0								
Kiambu	1-5	10	30.3								
	10-15	1	3.0	11	1.08	12.20	2.99 a	.97	3.21		
	Undetected	22	66.7								
	Total	33	100.0								
	1-5	11	36.7								
Nakuru	5-10	9	30.0	20	1.67	9.06	4.77 b	.48	2.13		
	Undetected	10	33.3								
	Total	30	100.0								

^{*}categories based on maximum allowed limits; a,b,c means with different superscripts are significantly different.

The guidance level for Cadmium is 70mg/kg soil concentration by USEPA for sites requiring clean up. On the other hand, the lower guideline value for ecological risk in Finland is 10mg/kg (Tóth et al., 2016) whereas in Tanzania (Kibassa et al., 2013) the safe soil concentration is 1 mg/kg. WHO guideline is 0.35ppm and by CEQG it is 1.4 ppm and 10ppm for agricultural and residential land, respectively (Bongoua-Devisme et al, 2018). Compared to the WHO maximum allowed limit, all samples in the study that tested positive had a higher concentration. However, all the samples had concentrations that were lower than the minimum required by USEPA for clean-up.

In Uyo Nigeria, the soil concentration in the municipal dumpsite was 9.25 and 14.1 for the rural dumpsite (Ebong *et al* 2008). Bongoua-Devisme *et al* (2018) reported quite a high concentration of 81ppm in Bonoua Dumpsite, Ivory coast and 1.04ppm was reported for Calabar Metropolis, Nigeria (Ediene and Umoetok, 2017).

Cadmium is a pollutant of concern in Nakuru having been detected in two thirds of the samples. Since cadmium is highly toxic being associate with kidney ad bone damage and a potential carcinogen (WHO, 2007) this implies that the waste pickers in Nakuru are highly exposed this pollutant. This might call for efforts to minimise exposure through dust ingestion.

Chromium was detected in 100% of all samples except for Kiambu where it was detected for 63.6% of the samples (Table 5). Most of the samples had concentration of up to 70ppm. The highest mean concentration was recorded in Nakuru of 87.65±23.12 with a minimum of 2.8 and a maximum of 573.47ppm followed by Kiambu (209.13±41.91ppm) and the lowest in Chuka (28.54±3.62ppm). Significant differences were determined between Chuka and Nakuru as well as between Nakuru and Kiambu.

Table 4: Chromium Concentration

	Concentration	5 Frequ	ency	Docarintivo							
Site	n (PPM)	distril	oution	Descriptive							
		F	%	N	Min	Max	Mean	Std	Std.		
				11	171111			Error	Dev.		
	≤ 70	31	93.9								
Chuka	70 - 100	1	3.0	33	7.69	112.47	28.54a	3.62	20.78		
Cituka	100 - 200	1	3.0								
	Total	33	100.0								
	≤ 70	17	51.5								
	70 - 100	1	3.0								
Kiambu	100 - 200	2	6.1	21	5.53	209.13	41.91a	12.24	56.11		
Klailibu	> 200	1	3.0								
	Undetected	12	36.4								
	Total	33	100.0								
	≤ 70	22	73.3								
Nakuru	70 - 100	2	6.7								
	100 - 200	3	10.0	30	2.80	573.47	87.65 ^b	23.12	126.62		
	> 200	3	10.0								
	Total	30	100.0								

^{a, b} Significant differences exist between means that do not share same superscript

Soil concentration of Chromium of 230ppm require clean up as per USEPA. In Nakuru 3 samples had more than this guideline level with concentrations of between 300 and 600ppm whereas in the other dumpsites the levels were less than 230ppm. Maximum soil concentration for chromium considered safe for various uses is 100ppm in Tanzania (Kibassa et al., 2013), 70ppm by WHO and 64ppm by CEQG for both agricultural and residential uses (Bongoua-Devisme et al 2018). The number of samples above the WHO guidelines were zero in Chuka, four in Kiambu (12.1%) and eight in Nakuru (26.7%). When compared to similar places, mean concentration of chromium in Bonoua dumpsite in Ivory Coast was 130.1ppm (Bongoua-Devisme et al, 2018). In Calabar Metropolis, Nigeria the mean concentration in the municipal dumpsite was reported as 120.28 ppm (Ediene and Umoetok, 2017).

Chromium pollution was less widespread than lead. Chromium toxicity depends on the presence of chromium VI whereas chromium III is not toxic. Due to this fact the overall risk may be less since the toxic chromium VI is only a portion of the total chromium in the soil. Nevertheless, chromium toxicity is associated with cancer of the respiratory system and as such exposure would need to be minimised.

Conclusion and Recommendation

In conclusion, Nakuru and Kiambu dumpsite were highly polluted and were a huge risk factor to the waste pickers. In the short-term, it is recommended that waste pickers should wear adequate health and safety protective equipment while on site and possibly reduce the time at the dumpsite to minimise exposure. In the long-term, waste separation should be done to ensure that heavy metal containing waste do not get to the dumpsites, waste recovery facilities adopted to minimise waste picking at dumpsites and improve recycling and, the dumpsites upgraded to sanitary landfill status.

References

Lundgren, K. (2012). The Global Impact of E-Waste: Addressing the Challenge. International Labour Office, Programme on Safety and Health at Work and the Environment (SafeWork), Sectoral Activities Department (SECTOR). – Geneva: ILO. Material Safety Data Sheet, (2013). Material Safety Data Sheet, Copper MSDS. Retrieved http://www.sciencelab.com/msds.php?msdsId=9923549

Hassaan, M. A., Nemr, A. E. and Madkour, F. F. (2016) Environmental Assessment of Heavy Metal Pollution and Human Health Risk. *American Journal of Water Science and Engineering*, 2 (3), 14-19.

http://www.euro.who.int/_data/assets/pdf_file/007/78649/e91044.pdf.

Cointreau-Levine, S. (2006). Occupational and Environmental Health Issues of Solid Waste Management Special Emphasis on Middle- and Lower-Income Countries. The International Bank for Reconstruction and Development/The World Bank. Accessed from http://siteresources.worldbank.org/INTUSolid Waste management/Resources/up-2.pdf.

- Song, Q. and Li, J. (2014). Environmental Effects of Heavy Metals Derived from the E-Waste Recycling Activities in China: A Systematic Review. *Waste Management* 34, 2587–2594.
- National Environment Management Authority, Kenya (NEMA) (2014). *The National Solid Waste Management Strategy*. Nairobi: NEMA.
- Green Peace (2009). *Where Does E-Waste End Up?* Retrieved from http://www.greenpeace.org/international/en/campaigns/detox/electronics/the-e-waste-problem/where-does-e-waste-end-up/
- Gottesfeld, P., Were, F. H., Adogame, L., Gharbi, S., Nota, M.M. and Kuepouo, G. (2018). Soil Contamination from Lead Battery Manufacturing and Recycling in Seven African Countries. *Environmental Research*, 161, 609–614.
- World Health Organisation, (2007). Health Risks of Heavy Metals from Long-Range Transboundary Air Pollution.
- Ding, C., Zhang, T., Wang, X., Zhou, F., Yang, Y., and Yin, Y. (2013). Effects of Soil Type and Genotype on Lead Concentration in Rootstalk Vegetables and the Selection of Cultivars for Food Safety. *Journal of Environmental Management*, 122, 8-14.
- Kondo, A., Yamamoto, M., Inoue, Y. and Ariyadasam, B. H. A. K. T. (2013). Evaluation of Lead Concentration by One-Box Type Multimedia Model in Lake Biwa-Yodo River Basin of Japan. *Chemosphere* 92, 497–503.
- Tóth, G., Hermann, T., Da Silva, M. R. and Montanarella, L. (2016). Heavy Metals in Agricultural Soils of the European Union with Implications for Food Safety. *Environment International 88*, 299–309.
- Kibassa, D., Kimaro, A. A. and Shemdoe, R. S. (2013). Heavy metals concentrations in selected areas used for urban agriculture in Dar es Salaam, Tanzania. *Academic journals*, 8 (27), 1296-1303.
- Bongoua-Devisme, A. J., Bolou Bi, B. E., Kassin K. E., Balland Bolou Bi, C., Gueable Y. K. D., Adiaffi B., Yao-Kouame, A. and Djagoua E. M. V., (2018). Assessment of Heavy Metal Contamination Degree of Municipal Open-Air Dumpsite on Surrounding Soils: Case of Dumpsite of Bonoua, Ivory Coast. *International Journal of Engineering Research and General Science*, 6 (5), 28-42.
- County Government of Nakuru, (2014). *Nakuru County*. Retrieved from http://www.nakuru.go.ke/about/

- Tharaka Nithi County Strategic Plan 2012-2017 (2012). Retrieved on 20.11.14 from http://chuka.ac.ke/Tharaka_Nithi_SP.pdf
- County Government of Kiambu, (2013). County Integrated Development Plan 2013 2017. Retrieved from http://www.kiambu.go.ke/wp-content/uploads/2015/03/20132017 20150303-Kiambu-CIDP.pdf.
- Kenya National Bureau of Statistics, (2009). Census Data of 2009 for Rural and Urban Population. Retrieved from https://www.opendata.go.ke/Population/2009-Census-Vol-1-Table-3-Rural-and-Urban-Populati/e7c7-w67t on 2nd February 2015.
- Nathanail, J., Bardos, P. and Nathanail, P. (2002). Contaminated Land Management Ready Reference. Update EPP Publications/ Land Quality Press. EPP Publications: Chiswick, London.
- Dean, J. R. (2007). *Bioavailability, Bioaccessibility and Mobility of Environmental Contaminants*. England: John Wiley and Sons Ltd
- Ediene, V. F. and Umoetok, S. B. A. (2017). Concentration of Heavy Metals in Soils at the Municipal Dumpsite in Calabar Metropolis. *Asian Journal of Environment and Ecology*, 3 (2), 1-11.
- Ebong, G. A., Akpan, M. M. and Mkpenie, V. N. (2008). Heavy Metal Contents of Municipal and Rural Dumpsite Soils and Rate of Accumulation by Carica papaya and Talinum triangulare in Uyo, Nigeria. *E-E-Journal of Chemistry*, 5 (2), 281-290.



KIRINYAGA UNIVERSITY

AFRICAN JOURNAL OF SCIENCE, TECHNOLOGY AND ENGINEERING (AJSTE)

Published by:

P.O BOX 143-10300, KERUGOYA, KENYA MOBILE +254709742000/+254729499650

Email: info@KyU.ac.ke
Website: www.KyU.ac.ke

KyU is ISO 9000: 2015 Certified